MINES AND MINERALS DIVISION

ONTARIO GEOLOGICAL SURVEY

Open File Report 5701

# Petrology and Geochemistry of the Duncan Lake, Beaton Bay, Milner Lake, and Miller Lake Nipissing Intrusions within the Gowganda Area

District of Timiskaming

by

D.M. Conrod

1989



Ontario Ministry of Northern Development and Mines

Ministère du Développement du Nord et des Mines

**Ontario Geological Survey**

**OPEN FILE REPORT**

Open File Reports are made available to the public subject to the following conditions:

This report is unedited. Discrepancies may occur for which the Ontario Geological Survey does not assume liability. Recommendations and statements of opinions expressed are those of the author or authors and are not to be construed as statements of government policy.

This Open File Report is available for viewing at the following locations:

(1) Mines Library
Ministry of Northern Development and Mines
8th floor, 77 Grenville Street
Toronto, Ontario M7A 1W4

(2) The office of the Regional or Resident Geologist in whose district the area covered by this report is located.

Copies of this report may be obtained at the user's expense from a commercial printing house. For the address and instructions to order, contact the appropriate Regional or Resident Geologist's office(s) or the Mines Library. Microfiche copies (42x reduction) of this report are available for $2.00 each plus provincial sales tax at the Mines Library or the Public Information Centre, Ministry of Natural Resources, W-1640, 99 Wellesley Street West, Toronto.

Handwritten notes and sketches may be made from this report. Check with the Mines Library or Regional/Resident Geologist's office whether there is a copy of this report that may be borrowed. A copy of this report is available for Inter-Library Loan.

This report is available for viewing at the following Regional or Resident Geologists' offices:

COBALT DISTRICT
Box 230, Presley St.
Cobalt, P0J 1C0

KIRKLAND LAKE DISTRICT
4 Government Rd. E.
Kirkland Lake, P2N 1A2

PORCUPINE DISTRICT
60 Wilson Ave.
Timmins, P4N 2S7

SUDBURY DISTRICT
200 Brady St.
Sudbury, P3E 5K3



V.G. Milne, Director
Ontario Geological Survey

CONTENTS

LIST OF PHOTOGRAPHS

LIST OF TABLES

## LIST OF FIGURES

Abstract

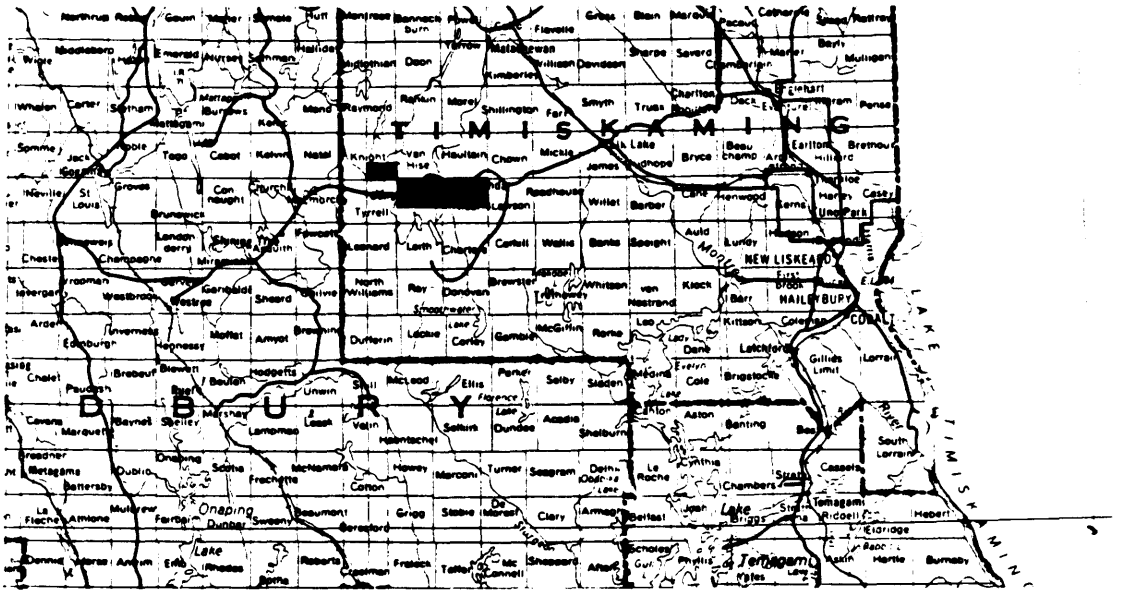


Figure 1: Key map showing the location of the study area

The Nipissing Intrusions of the Gowganda area (Figure 1) are interpreted to be the exposures of one or more three-dimensional, primary, undulating sheets, consisting of basins, arches and limbs that connect the basins with the arches. The lithologic stratigraphy, whole rock major and trace element distributions, as well as the trends defined by the mineral chemistry, all correlate well. These trends are related to be geometry of the intrusion, as was found for the Cobalt and Sudbury Nipissing Intrusions (Conrod 1988, Hriskevich 1968, Jambor 1971). Cummulate gabbronorite displaying a reverse differentiation trend is ubiquitous in basinal sections, while non-cummulate pegmatitic gabbro and granophyric and granitic differentiates are concentrated in the central portions of the arches and limbs.

A section taken across the Duncan Lake Intrusion indicates the presence of a reverse, followed by a normal,

differentiation trend. A section across the Milner Lake and Beaton Bay Intrusions indicates the presence of a normal differentiation trend expected of an intrusion cooling equally from both upper and lower contacts. Four reverse, followed by normal, differentiation trends were observed across the Miller Lake Intrusion. The repetition of these trends or "cycles" is anomalous and was not observed in previous studies of the Cobalt and Sudbury area intrusions (Hriskevich 1968, Conrod 1988). Cycles were described by Finn (1984) for the platinum-bearing Wanapitei Nipissing Intrusion located in the Sudbury area.

Although the source of the Nipissing magmas is unknown, the low Mg-number of the chill margins and the presence of partially resorbed olivine fractionation occurred prior to emplacement. The high Th/Yb ratio relative to Ta/Yb ratio of the Temagami, Cobalt and Sudbury chilled rocks indicate that the magma was most likely contaminated prior to emplacement. Limited contamination of the magma with partially melted country rock is expected to occur after emplacement.

A model involving the tapping of a progressively more primitive magma from an auxillary magma chamber beneath the unconformity, limited mixing with partial melts derived from the country rock, fractionation and slumping of a crystal mush from the floors of the arches into the basins, and finally the emplacement of a more fractionated magma which had a longer residence time in the auxillary chamber can best explain the cyclic nature of some of the basins as well as the lithologic distribution throughout the sheet. An updip migration of bouyant volatile material generated by filter pressing in the

cummulate pile within the basins is believed to have formed the varied textured gabbros above the gabbronorite in the basins and in the interiors of the limbs and arches.

Relative to rift-related continental flood basalt volcanism such as the Keweenawan basalts, the Nipissing suite, (including the chilled magma), is enriched in the large ion lithophile elements. Chondrite-normalized and M.O.R.B. - normalized spidergrams of the Nipissing suite show profiles very similar to calc-alkalic collision-type magmas. On a number of trace element and mineral chemistry tectonic setting discrimination diagrams, the Nipissing suite always plots within the calc-alkalic destructive plate margin setting. If the discrimination diagrams adequately distinguish tectonic setting, then the Nipissing suite provides a window into subvolcanic magmatic process at destructive plate margins.

A preliminary U-Pb age determined on zircon separates from the Bonanza Lake Nipissing Intrusion located in the Sudbury area, gives a minimum age of emplacement at 2210-2214 Ma ago. This age is very similar to the U-Pb age of 2219 ± 4 Ma determined by Corfu and Andrews (1986) for the Miller Lake Intrusion in the Gowganda area.

# PETROLOGY AND GEOCHEMISTRY OF THE DUNCAN LAKE, BEATON BAY, MILNER LAKE, AND MILLER LAKE NIPISSING INTRUSIONS WITHIN THE GOWGANDA AREA

D.M. Conrod [1]

[1]Geologist, Precambrian Geology Section, Ontario Geological Survey, Toronto.

Manuscript approved for publication by V.G. Milne, Director, Ontario Geological Survey, February 1989.

This report is published with the permission of V.G. Milne, Director, Ontario Geological Survey, Toronto.

# INTRODUCTION

## General Geology

The Nipissing Intrusions of northern Ontario comprise a suite of predominantly tholeiitic rocks with calc-alkalic affinities, ranging from chilled basaltic magma through gabbronorite, gabbro, pegmatitic gabbro, quartz diabase, and associated differentiated phases of granodiorite and granite. They extend from the Cobalt-Gowganda area to Sault Ste. Marie. The intrusions, ranging in thickness from a few hundred metres to over a thousand metres, outcrop at the present erosional level as solid mafic bodies, open ring structures, and long linear intrusions, which have been interpreted in the past to be the surface expression of cone sheets, ring dikes, dikes, and sills, but predominantly, primary, undulating sheets (Figure 1) (Card and Pattison 1973). The intrusions have generally been intruded along the Archean-Proterozoic unconformity or intruded into the overlying Huronian Supergroup.

A number of Rb/Sr and K/Ar age dates have been determined for the Nipissing Intrusions, (van Schmus 1965), (Fairbairn et al. 1969), (Lowdon et al. 1963); however, a very precise U-Pb age determination on baddeleyite on a Nipissing Intrusion in the Gowganda area, of 2219 ± 3.6 Ma has recently been published (Corfu and Andrews 1986).

The Nipissing intrusions in the Cobalt-Gowganda area are relatively undeformed and unmetamorphosed, whereas Nipissing intrusions in the Sudbury - Blind River area have undergone some deformation and regional metamorphism probably related to the Early Proterozoic Penokean Orogeny, ca. 1850 to 1900 Ma

(Card 1978). Buchan and Card (1985), suggest that the close spatial association between the Nipissing Intrusions and the Huronian metasedimentary rocks indicates a genetic relationship; whereby the major faults which created the basins for the deposition of the Huronian sediments later served as pathways for the mantle-derived mafic magas.

The Nipissing Intrusions have a distinct lithologic stratigraphy which is related to the geometry of the intrusion (Conrod 1988, Hriskevich 1968, Jambor 1971). The sheets can be described in term of a series of basins and arches with limbs connecting the basins and arches. The near-horizontal basinal portions of the undulating sheets are characterized by the presence of a basal and capping quartz diabase unit, a basal to central gabbronorite unit and an overlying variably-textured gabbro containing pegmatitic gabbro pods up to 3 metres in size, set within a finer grained gabbro to quartz diabase matrix. Differentiated phases of granodiorite and granite may occur near the roof. The steeply dipping limbs of the sheets are characterized by the presence of a border quartz diabase, near-border gabbro, and abundant pegmatitic gabbro, granodiorite and granitic differentiates, located in the central portion of the intrusion.

Chemically the intrusions are predominantly tholeiitic but they also show calc-alkalic affinities, which are interpreted by the author to be the result of: (1) a pre-emplacement enrichment of the large ion lithophile elements (LILEs) due to contamination and olivine fractionation and (2) simultaneous assimilation of the country rock and fractional crystallization after emplacement, (Lightfoot et al. 1987, and Conrod 1988).

A close spatial association between mineralization and the Nipissing Intrusions has long been recognized. Card and Pattison (1973) recognized that the associated mineralization varies in both type and style across the Nipissing Province; from predominantly Ag, Co and Ni as native metals, arsenides and sulfarsenides within quartz-carbonate veins in the eastern sector of the province; to Cu-Ni sulfides which occur as fine disseminations or as massive pods within the intrusions in the central sector; and finally to Cu-sulfides which occur as fine disseminations or in quartz carbonate veins in the western sector (Figure 2). According to Jambor (1971), mineralization within the Cobalt area occurs both within the Nipissing Intrusions and the country rock - (both Archean metavolcanic and Huronian metasedimentary rocks); but always within 213 m of the intrusion - country rock contact.

Recent paleomagnetic data (Buchan and Card 1985) suggests that the Nipissing Intrusive Suite carries one of two distinct directions of remnant magnetism and their relative age is however controversial. If the two directions are in fact primary, then these directions imply two distinct ages of emplacement of which only one has been dated by U-Pb methods (Corfu and Andrews 1986).

## Previous Geological Work

Previous work on the Nipissing Intrusions within the Gowganda area is extensive and varied and too numerous to be mentioned here. Some of the more recent work includes: fairly recent mapping projects at a scale of 1:15 860 (McIlwaine 1978, Carter 1983); age determinations (Corfu and Andrews 1986,

Fairbairn et al. 1969); paleomagnetic work (Buchan and Card 1985); chemical and petrological studies in the Gowganda and Cobalt areas (Hriskevich 1968, Jambor 1971, Conrod 1988, Lightfoot et al. 1987), studies of the ores associated with the intrusions (Petruk 1971) and extensive small scale detailed mapping and assay work undertaken by the various mining and exploration companies in the area (Ontario Geological Survey, Assessment Files Research Office, Toronto).

## Objective of the Present Study and Approach

The objective of the present project was to study the Nipissing Intrusions within the Gowganda area petrologically and chemically in an attempt to obtain a better understanding of which intrusions, or portions of intrusions, host the native silver and cobalt and nickel arsenide mineralization for which the area is famous.

The approach taken to meet the objective was to map and sample in detail one transect across the surface of each of four intrusions within the area. Two of the transects were across intrusions containing mineralization of economic significance and the other two were from intrusions containing no known economic deposits. Further, comparison of the Gowganda area intrusions with the Nipissing Intrusions of the Cobalt and Sudbury areas may aid in understanding the variation in type and style of mineralization associated with the intrusions across the Southern Province. A U-Pb age determination on zircon separates from the Bonanza Lake Nipissing Intrusion, within the Sudbury area, was undertaken by the author; and when compared to the U-Pb age determination

reported for the Gowganda area intrusions (Corfu and Andrews 1986), should aid in deciding whether the variation in type and style of mineralization across the Nipissing is age related.

Acknowledgments

The author wishes to thank M. Hackett of Agnico Eagle Mines for providing access to the Castle Mine and accompanying and aiding the author during the sample collection. The author also wishes to thank Dr. D. Davis from the Royal Ontario Museum for his guidance during the zircon separation procedures and for handling the chemical and mass spectrometer portions of the U-Pb age determination. Thanks are also due to M. Carter at the Ontario Geological Survey for his guidance in the use of the universal stage and finally to H. James for her assistance in the field.

Means of Access

The four intrusions chosen for this study and the location of the transects across each are shown in Figure 3. All are within the vicinity of the Town of Gowganda. The four intrusions are informally named by the author as the Duncan Lake Intrusion, Beaton Bay Intrusion, Milner Lake Intrusion and Miller Lake Intrusion.

The Castle Mine (number 3 shaft) is located four kilometres northeast of the village of Gowganda and immediately west of LeHeup Lake. The site is accessible by a dirt road leading north from Highway 560 which connects Gowganda to Elk Lake.

The Mann Mine site can be reached via a dirt road leading south from Highway 560, located 4.9 kilometres west of Gowganda.

The sample collection sites for the Duncan Lake and Beaton Bay Intrusions can be reached by boat. A boat launch onto the Montreal River from Highway 560 is located 16.2 kilometres west of Gowganda. There are many boat launch points on Gowganda Lake from which the Beaton Bay Intrusion can be reached.

## GEOLOGY OF THE GOWGANDA AREA NIPISSING INTRUSIONS

Within the Gowganda area, Nipissing Intrusions have penetrated Archean trondhjemite, intruded along the Archean-Proterozoic unconformity and cut Huronian Supergroup metasedimentary rocks. Emplacement of the magmas within the area, has been dated at 2116 ± 541 . (Fairbairn et al. 1969), on the basis of whole rock Rb/Sr methods. They have also been dated at 2,219 ± 3.6 Ma (Corfu and Andrews 1986), based on a U-Pb determination on baddeleyite separates. Northerly striking faults have, to some degree, controlled the emplacement of the intrusions. McIlwaine (1978) has interpreted the dominant northerly trending orientation of many of the Nipissing intrusions to be a result of this fault influenced emplacement. Local movement along such faults is believed to have continued after emplacement. The intrusions in the Gowganda area are cut by a number of later faults and quartz diabase dikes reported to be 1,230 Ma (Fahrig and Wanless 1963) - a K/Ar biotite age. The diabase dikes, however, have also been reported to be 2,180

---

1Rb-Sr ages in the report are corrected to the 1.42 X $10^{-10}$ de? constant

± 125 Ma (Gates and Hurley 1973) - a whole rock Rb/Sr determination. The disagreement in age may be the result of a resetting of the Ar clock during the Grenville Orogeny, or the presence of two distinct ages of dikes. The Nipissing Intrusions are also cut by northwesterly trending olivine diabase dikes. The olivine diabase dikes in the area are very similar petrologically to the northwesterly trending olivine diabase dikes cutting the Nipissing Intrusions within the Sudbury area, with K-Ar ages of 950 to 75 Ma, (Wanless et al. 1966).

The form of the intrusions, (irregularly shaped, solid bodies, open ring structures and dikes), are believed to be primary, and are not significantly modified by later folding and faulting.

The Nipissing Intrusions in the Gowganda area are the main host for the native silver and cobalt - nickel-arsenide deposits in the area.

## Geology and Geological Setting of the Four Intrusions Under Consideration

### Duncan Lake Intrusion

The Duncan Lake Intrusion is a long, gently-curving concave eastward body extending from the western edge of Leith Township to the eastern edge of Raymond Township. The intrusion dips concordantly with the Huronian Supergroup metasedimentary host rocks, approximately 25° to the east (Carter 1983).

Samples were collected along the shoreline as shown in Figure 4, and projected onto a plane perpendicular to the intrusion - host rock contact plane.

A lithologic transect across the present erosion surface is shown in Figure 5. The lithologic section which takes into account the dip of the intrusion is shown in Figure 6.

Beaton Bay Intrusion

The Beaton Bay Intrusion is a MNW - SSE trending linear intrusion located between Milner Bay and Gowganda Lake (Figure 3). Samples were collected along the traverse shown in Figure 7. Sample location was determined by pace and compass method and the use of 1:20 000 air photographs of flightlines flown in 1986.

The northeasterly dipping intrusion has penetrated the Huronian Supergroup metasedimentary rocks. The lithologic transect across the surface is shown in Figure 8. Assuming that the pods of granophyric and pegmatitic gabbro represent the upper contact of the intrusion, a reconstructed section was drawn (Figure 9), and samples collected along the surface were projected onto a plane oriented perpendicular to the contacts, to produce a true section (Figure 10). Diamond drilling carried out by Chimo Limited on the Northcliff Prospect, north of the sampling transect, indicates that the intrusion must dip less than 33 degrees to the east in that location (Figure 11). Diamond drilling carried out on a claim, held by D. Sutherland in 1969, located approximately 355 metres south of the sampling transect, indicates the presence of a contact breccia zone dipping approximately 22 degrees to the east in this location

(Figure 7). The author feels that a dip of approximately 20° in the location of the transect, correlates well with the lithologic distribution observed along the surface transect. This shallow dip to the east differs from the dip determination of Burrows (1922), who claimed that the intrusion-country rock contact along Milner Bay dipped steeply to the west (60°). This discrepency may be the result of local "rolls" in the intrusion surface; however, the presence of pegmatitic gabbro and pink graonphyre along the shoreline of Beaton Bay, and the diamond drilling of both Chimo Limited and on the Sutherland Property indicate to the author that the true dip is shallowly to the east.

Based on the reconstructed section shown in Figure 9, the Beaton Bay Intrusion is a 213 m thick intrusion consisting predominantly of quartz-rich gabbro and granophyric differentiated phases.

Milner Lake Intrusion at the Mann Mine Site

The Mann Mine transect is located across the eastern limb of a basin defined by an undulating Nipissing sheet (Figure 3). The intrusion has penetrated the Cobalt Group metasedimentary rocks belonging to the Huronian Supergroup. The intrusion dips 45° to the west at the Mann Mine site (Cunningham 1985).

Samples were collected across the "Mann Ridge" in an east to west direction (Figure 12). Sample location was determined using the pace and compass method aided with 1986 air photographs at a scale of 1:20 000. Figure 13 illustrates the section across the intrusion. Underground diamond drilling at the site (Figures 14a and 14b) (McIlwaine 1978) confirms the

dip of 45° and suggests a true thickness of approximately 213 m. Using the data collected in this study as well as the information provided by the drilling, a reconstruction of the Mann Ridge section was produced (Figure 15). Figure 14 indicates that the projection of the basal contact onto the surface plots 168 metres west of the Mann Fault. This correlates well with the observed lithologies in the area, although the chill margin is not exposed on the surface.

Three prominent north trending faults have been reported in the intrusion at the Mine: the Hangingstone Fault, the Mann Fault and the 89 Fault (Cunningham 1985). The direction of movement on the 89 Fault is suggested to be east side down (Cunningham 1985), however, the amount of displacement was not determined. The direction and amount of movement on the Mann and Hangingstone Faults either have not been determined or reported at this time.

The relationship of samples 87-DMC-0100, 101, 102, 103 and 104, on the cross-section (Figure 15), to the rest of the intrusion is uncertain and they have not been used in the construction of the stratigraphic sections or subsequent chemical studies. Figure 16 shows the true lithologic variation through the intrusion.

## Miller Lake Intrusion at the Castle Mine Site

The Castle Mine is located on the northwest limb of a basinal structure within the undulating Nipissing sheet (Figure 3). At this location the Nipissing Intrusion has intruded the Archean metavolcanic and the Huronian Supergroup

metasedimentary rocks. At the mine site both upper and lower bordering host rocks are Archean metavolcanics.

The surface plan and section of the workings are shown in Figure 17. As samples could not be obtained directly down the number three shaft, samples were collected at 15.2 metre intervals along a NNW-SSE trending drift on the sixth level, 145 metres below the surface and along a NW-SE trending drift on the tenth level, 236 meters below the surface (Figure 18a and 18b). When these sample sites are projected onto a plane perpendicular to the intrusion-host rock contact plane, and the dip of the intrusion (26°) is accounted for, a lithologic section through the 274 m thick intrusion was obtained with a sampling interval of 6.4 m (Figures 19a and 19b).

## ECONOMIC GEOLOGY OF THE MILNER LAKE MILLER LAKE, BEATON BAY, AND DUNCAN LAKE NIPISSING INTRUSIONS

### Introduction

The Gowganda region, from which 60,000,000 ounces of silver has been produced, is located within the Temiskaming silver area (Cunningham 1985). Ninety-five percent of the silver produced within the region was obtained from the basins within the Nipissing Sheet, predominantly the Miller Lake Basin (Cunningham 1985).

### Mann Mine (Milner Lake Intrusion)

Silver was first discovered at the Mann Mine site in 1908, in a 13 cm thick quartz-calcite vein trending approximately east to west, (McIlwaine 1978). From 1908 to 1984, 323,384 ounces of silver were produced from the Mann Mine (Cunningham

1985). Table 1 lists the production record for the mine. The high grade ore is predominantly native silver and smaltite in calcite. Gold may also be present (McIlwaine 1978).

Two major vein systems have been reported in the intrusion at the mine site: 1) an east-trending system perpendicular to the intrusion contacts and 2) a north-trending system parallel to the intrusion contacts, both of which are productive. The east-trending veins tend to be more productive than the north-trending veins.

According to Thompson (1968), the best silver deposits occurred near the central part of the intrusion within the quartz carbonate veins. Figure 12b, indicates however, that extensive workings are found in both the upper and central parts of the intrusion. According to Cunningham (1985), the intersection of veins adjacent to low angle faulting control to localization of the ore shoots. This geological feature has also been recognized in the Castle and Sisco Mines located on the rims of the Miller Lake Basin.

Castle Mine (Miller Lake Intrusion)

Ninety-five percent of the silver produced from the Gowganda area deposits have come from veins within the Miller Lake basin, (Drake 1976). The ore, which is predominantly silver and cobalt-iron-nickel arsenides, occurs as a variety of minerals, as listed in Table 2 (Drake 1976), in quartz-carbonate veins and in adjacent fractures. Along with these minerals, Burrows (1922) reported the presence of chalcopyrite and specularite in parts of veins. Generally the veins are steeply dipping (60° to 90°), although falt-lying veins have

also been reported. Mineralization that is found in faults is always in close proximity to the intersection of a fault with a well mineralized vein (Drake 1976).

Generally the ore is almost always found within the upper half of the Nipissing Intrusion, however small ore shoots have also been found in all pre-Nipissing lithologies located adjacent to the intrusion. Mineralization was found within the lower half of the intrusion at the Everett Mine and along the basal contact at the Lower Bonsall Mine both of which are located on the western limb of the Miller Lake Basin, (Figure 3).

Native silver in leaf form or in a dendritic habit is surrounded by cobalt-iron arsenides. In some of the best mineralized section of the veins the calcite is pink in colour (Drake 1976). The leaf silver occurs in calcite veins, in joints within the wall rock close to the veins, rarely in fault planes of the intrusion, and rarely in the quartz bearing sections of the veins (Drake 1976).

The average ore grade recovered from the mine site was between "20 and 40 ounces of silver per ton" (Drake 1976). Silver production from the mine between the years 1920 and 1931 totalled 6,461,021 ounces (Drake 1976) (Table 3). Work did not begin again until 1970. Between 1970 and 1979 there was no production from the mine. From 1979 to the present between 2.8 and 2.9 million ounces of silver were produced (personal communication, M. Hackett Geologist, Aginco Eagle Mines, Cobalt, Ontario) (Table 3). From 1979 to the present the cobalt was left in the concentrate and not recovered.

## Beaton Bay Intrusion

Minor mineralization (McIlwaine 1978) was reported from diamond drilling at a site on the southern part of Beaton Bay (Figure 7). The mineralization, determined in this study consists of galena and chalcopyrite in strained quartz and as reported by McIlwaine (1978) is of sub-economic grade. For a description of the occurrences elsewhere in this intrusion, the reader is referred to the assessment work data section in McIlwaine's report (1978).

## Duncan Lake Intrusion

Although a number of thick (up to 30 cm wide), quartz veins were observed near both upper and lower contacts of the Duncan Lake Intrusion, mineralization of economic interest has not been reported in the location of sample collection. Descriptions of occurrences elsewhere in this intrusion are documented by Carter (1983). These occurrences consist predominantly of chalcopyrite, erythrite, silver, and hematite.

## Lithologies of the Nipissing Intrusions within the Gowganda Area

### Introduction

The Nipissing Intrusions of the Gowganda area are composed of several lithologies. All lithologies may not be present in every intrusion, or in every part of a given intrusion. A relationship between the lithologic stratigraphy and the intrusion geometry exists within the Gowganda Nipissing Intrusions; as was found in previous studies of the Sudbury and Cobalt area intrusions (Conrod 1988, Hriskevich 1968, Jambor

1971). Basinal portions of undulating sheets typically, but not always contain a capping and basal border quartz diabase, a central, thick gabbronorite that is typically overlain by variably textured gabbro. The varied texture gabbro contains pegmatitic gabbro pods within a finer-grained gabbro matrix. The limbs of the sheet, which connect the arches with the basins, typically contain a border quartz diabase and a central zone of pegmatitic gabbro and granophyric differentiates. The arch areas are characterized by an abundance of very quartz-rich gabbros, varied texture gabbro containing the pegmatitic phase and granitic and granophyric phases located predominantly near the roof.

The following lithologies were observed in this study of the Gowganda intrusions: chilled magma, quartz diabase, gabbro, gabbronorite, pegmatitic gabbro and the pink granophyre. Transitional phases were also observed.

## Chilled Mafic Phase

The chilled phase of the Nipissing suite was observed in all four intrusions studied. It occurs as a very fine-grained flinty, massive black rock immediately adjacent to the intrusion - country rock contact. In all intrusions, this chilled phase grades into a fine grained quartz diabase within 25 cm of the contact. No plagioclase or olivine phenocrysts are recognizable in hand sample.

## Border Quartz Diabase

Border quartz diabase, in hand sample is dark green in colour and contains distinct grey quartz crystals. It

generally, but not in all places, occurs along both capping and basal borders throughout most parts of an intrusion. This lithology is uniformly textured, generally equigranular, and is fine to medium grained. The diabasic texture is not easily recognized in hand sample because of the fine grain size and extensive alteration. The overall colour of this lithology is pale green - a reflection of saussuritization of the plagioclase and the alteration of the clinopyroxene to uralite and chlorite.

Gabbro

The gabbro phase of the Nipissing Intrusive suite occurs as a fine-to medium-grained, equigranular, and generally uniformly textured rock. This lithology is coarser grained, less altered, and contains less quartz in comparison to the quartz diabase. Plagioclase and pyroxene are easily recognized in hand sample. A transitional phase from quartz diabase to the gabbro is recognized by the loss of quartz, the lesser amounts of alteration products, and the loss of the ophitic texture between the plagioclase and clinopyroxen.

Pegmatitic Gabbro

Pegmatitic gabbro was found to comprise part of the varied texture gabbro within the Gowganda area intrusions, where it occurs as distinct pods or schlieren containing both sharp and diffuse boundaries with the enclosing gabbro or quartz diabase (Photo 1). This phase consists predominantly of very coarse-grained plagioclase and uralitized clinopyroxene, and therefore weathers to a very rough and irregular surface. The pegmatite

is never chilled against its quartz diabase matrix. The plagioclase within the pegmatite is usually white in hand sample but may also be greenish due to the alteration to saussurite or may be pinkish due to hematitic dusting of the crystals.

### Gabbronorite

Gabbronorite was found to occupy the basal to central portion of the Duncan Lake Intrusion, and the capping and basal border zones, as well as the central portion of the Miller Lake Basin. In hand sample, this lithology is medium grained, equigranular, uniformly textured, and rather massive. It can easily be recognized by the presence of brown phenocrystic hypersthene along with dark green to black augite and white plagioclase (Photo 2). It is generally the least altered lithology of the Nipissing Intrusive Suite and therefore, relative to the gabbro and quartz diabase, has an overall lighter colour.

### Granophyric and Granodioritic Differentiates

The granophyre of the Gowganda area is locally known as "red rock". In hand sample the most distinctive features of this lithology are: the bright pink colour of the feldspar, the common clotty arrangement of the feldspar crystals (Photo 3), and the common occurrence of vugs (Photo 4).

The granophyre occurs in close spatial association with the varied textured gabbro as irregularly shaped patches ranging from less than a metre to several metres in size.

Altered clinopyroxene and hornblende are the main mafic minerals and are greenish-black in colour. Calcite may also occur as irregularly shaped crystals upto 2 mm in size.

Cobaltinitrite staining of the samples collected in this study a test sensitive to the presence of the K+ cation (Nold and Erickson 1967), indicated that most of the pink feldspar was hematized plagioclase, not potassium feldspar. Hematization of the feldspar probably occurred during late stage hydrothermal alteration.

Although much of this lithology is medium grained, a finer-grained, more felsic phase was observed within the central part of the Beaton Bay Intrusion (Photo 5). This finer-grained rock is a deep red-brown in colour and contains fewer mafic minerals relative to the typical medium-grained granophyre. White plagioclase crystals, generally 2 mm in length, are set in a deep red-brown matrix. Quartz occurs as greyish crystals up to 2 mm in size, and locally the rock is vuggy. Staining shows that much of the matrix is potassium feldspar.

Altered Gabbro

In hand sample the altered hornblende gabbro which occurs within the Miller Lake Basin is recognized by the presence of pale green rectangular shaped phenocrysts, up to 4 mm X 3 mm in size, set in a medium-to fine-grained dark grey matrix. The pale green phenocrysts are pyroxenes which have undergone alteration to actinolite-tremolite which is discussed in the petrology section.

## Lithologic Variation Across the Miller Lake Intrusion at the Castle Mine Site

Samples collected along drifts on the 6th and 10th levels of the Castle Mine number 3 shaft were projected onto planes oriented perpendicular to the intrusion-country rock contacts, to produce the lithologic section shown in Figure 19a, b. The dip of the 274 metre thick intrusion was determined from diamond drilling at the site, to be 26° to the southeast.

The intrusion is characterized by a basal and capping chilled phase, a very thin border quartz diabase transitional to gabbronorite, and a central core of gabbronorite that can be subdivided into four zones separated by rock typically found near intrusion - country rock border zones: (quartz diabase and gabbronorite - quartz diabase transition rocks). The interface rocks typically contain little to no orthopyroxene, but contain significant amounts of pigeonite and inverted pigeonite. The absence of well developed border quartz diabases is somewhat anomalous in the Miller Lake Intrusion, however, the gabbronorite of the Bonanza Lake Intrusion, located south of Lake Wanapitei and east of Sudbury, contains only a very thin to absent, basal quartz diabase, which rapidly gives way to gabbronorite. No differentiated phases of granite, granophyre, granodiorite or pegmatite were observed at the mine site.

## Lithologic Variation Across the Duncan Lake Intrusion

A lithologic section through the Duncan Lake Intrusion was constructed by projecting samples collected along the lakeshore, shown in Figure 4, onto a plane oriented

perpendicular to the intrusion - country rock contacts and taking into account the dip of the intrusion. The section (Figure 6) assumes a dip of 35° to the east, conformable with the dip of the Huronian Supergroup metasedimentary rocks.

The 274 metre thick intrusion is characterized by a capping and basal fine-grained border quartz diabase, a basal near border medium-grained gabbro - gabbronorite transition phase, and a thick central medium grained gabbronorite which is overlain by variable texture gabbro containing pods of pegmatitic gabbro. In hand sample phenocrystic hypersthene of the gabbronorite is not easily distinguished from clinopyroxene.

## Lithologic Variation across the Beaton Bay Intrusion

The distribution of lithologies throughout the Beaton Bay Intrusion was determined from the cross-section shown in Figure 9. This section (Figure 10) assumed a dip of approximately 20° to the east.

The 221 metre thick intrusion is characterized by a basal chill zone, a thick central zone of quartz-rich gabbro, pegmatitic gabbro and granophyre, and an upper near-roof zone consisting of pegmatitic gabbro and granophyric differentiates.

## Lithologic Variation across the Milner Lake Intrusion at the Mann Mine Site

The distribution of lithologies throughout the Milner Lake Intrusion was determined from the section reconstruction shown in Figure 15. An average dip of 45 degrees to the west was

determined for the intrusion, from diamond drilling by Manridge Explorations in 1967 at the mine site (Figure 14a, b).

The 213 m thick intrusion consists of a thin capping and basal border chill phase, a thin border quartz diabase, and central zone of quartz rich gabbro, varied texture gabbro and minor granodiorite. Aplitic dikes 1-3 cm wide occur near the top of the intrusion, (Figure 16). At the upper contact a near vertical, approximately 25 cm wide carbonate vein containing chalcopyrite and cobalt arsenides occurs.

### Lithologic Distribution and Geometry

The lithologic distribution across a typical Nipissing Intrusion depends on the part of the undulating sheet being examined. If the four transects considered in this study were placed on a hypothetical undulating sheet, then the transects would represent; (1) a section through the basin, (2) two sections through the limbs which connect the arches to the basins and (3) a section through an arch as shown in Figure 20.

## PETROLOGY OF THE GOWGANDA AREA NIPISSING LITHOLOGIES

### Chilled Phase

Chilled phases of most Nipissing Intrusions within the Gowganda area grade into the bordering quartz diabase less than 50 cm from the country rock contact. The changes in texture and grain size across this transition can be observed by examining the following sequence of samples in Table 4.

The chilled phase is characterized by the presence of quenched pyroxene and plagioclase crystals arranged in radiating fan-like clusters (Photo 6). Intergranular pyroxene

and magnetite are present between the radiating sheaths of these fans. All completely chilled samples observed in this study contained glomeroporphyritic plagioclase, occurring as crystals up to 0.6 mm X 0.1 mm in size, and in clusters up to 0.55 m in size (Photo 7). Intratelluric, partially resorbed, olivine phenocrysts, completely pseudomorphed by antigorite and talc (Photo 8) may be present in the chilled phases but clearly account for less than one volume percent. Hollow and forked-tailed crystals of plagioclase are generally not observed in these chilled samples.

An increase in grain size, quartz content, and diabasic texture; and a decrease in the quench texture, marks the transition from the chilled phase to the border quartz diabase.

Alteration within the chill involves the sericitization of plagioclase and the uralitization and chloritization of the pyroxene.

Bordering Quartz Diabase

The bordering quartz diabase typically contains plagioclase and pyroxene in a diabasic texture. The presence of independent interstitial quartz crystals and quartz in eutectoid, granophyric, intergrowth with feldspar along with significant amounts of inverted pigeonite, often molded onto augite, (Photo 9), is typical of this lithology in thin section. The inverted pigeonite is easily identified by the extensive exsolution of clinopyroxene as thin plates parallel to (101) of the orthorhombic crystal structure, (which is (001) of the original monoclinic crystal), and parallel to (100) of the orthorhombic crystal. Exsolution lamellae occurring

parallel to (001) of the clinopyroxene crystal produces a herringbone texture with the (100) twin plane (Photo 10). The molding of inverted pigeonite onto augite and augite onto inverted pigeonite indicates that pigeonite and augite crystallized from the melt simultaneously, however the predominance of inverted pigeonite molded onto augite indicates that the crystallization of augite slightly preceeded the pigeonite but continued after the pigeonite crystallized.

Although varied in size, the clinopyroxene of this lithology averages 0.44 mm X 1.65 mm. Plagioclase averaging 0.15 mm X 0.44 mm in size, is intergrown with pyroxene to form the diabasic texture. Intratelluric olivine generally is most abundant in this lithology occurring as phencrystic completely altered and rounded crystals averaging 0.7 mm X 1.0 mm in size. These commonly partially resorbed crystals in places are surrounded by inverted pigeonite (Photo 11).

A relatively thin transition zone between the border quartz diabase and the interior gabbronorite is charaacterized by a decrease in the amount of inverted pigeonite and an increase in the amount of hypersthene.

The border quartz diabase of Nipissing Intrusions in the Gowganda area and elsewhere is typically one of the most altered lithologies of the suite. Alteration includes uralitization and chloritization of the pyroxenes, sericitization and saussuritization of the feldspars, the alteration of magnetite - ilmenite to leucoxene, and phenocrystic olivine to antigorite and talc.

While most intrusions and parts of intrusions contain the bordering quartz diabase this zone is absent, to only very

weakly developed in the Castle Mine area of the Miller Lake Intrusion. In contrast to most Nipissing Intrusions, the Miller Lake Intrusion contains a capping and basal hypersthene to bronzite-bearing gabbronorite. Similarly, the eastern end of the basal quartz diabase in the Bonanza Lake Intrusion located on the south shore of Lake Wanapitei in the Sudbury area, is missing.

The capping quartz diabase of both the Beaton Bay and Milner lake Intrusions contains pods of pegmatitic gabbro and granophyre.

Gabbronorite

Gabbronorite is generally restricted to the basal and central portions of basins in undulating Nipissing sheets. In contrast, however, the Miller Lake Intrusion at the Castle Mine site contains a 73 metre thick basal gabbronorite, a 73 metre thick capping gabbronorite and two central gabbronorite zones, each approximately 63 metre thick. The transition from border zone quartz diabase to the central gabbronorite is observed by the change from a diabasic texture to a gabbroic texture, the loss of quartz, the loss of inverted pigeonite, and the presence of phenocrystic orthopyroxene. The orthopyroxene, the most distinctive feature of this lithology, undergoes continuous changes across a given zone. Early orthopyroxene, (that is those crystals found in close spatial relation to the bordering quartz diabase), show the most extensive clinopyroxene exsolution. These crystals are generally irregularly shaped and partially enclose plagioclase and less commonly clinopyroxene in their crystal rims. They

characteristically show exsolution of clinopyroxene as thin plates along two crystallographic directions: along (100) and (101), as well as irregularly shaped blebs generally occurring in the crystal rims or as patches throughout the hypersthene crystal (Photos 12 and 13). In some crystals the remnant herringbone exsolution texture of the monoclinic inverted pigeonite is retained in the orthohombic hypersthene (Photo 14). Toward the interior portion of a given gabbronorite zone, the orthopyroxene becomes rounded to subhedral in shape and shows higher birefringent rims. Areas in the section containing the most abundant orthopyroxene, contain the most euhedral and most exsolution-free cummulus orthopyroxene (Photos 15 and 16).

Augite is the predominant clinopyroxene within the gabbronorite averaging 1.3 mm X 0.44 mm. Occasionally long, curved, phenocrystic, augite occurs up to 3.3 mm X 0.33 mm (Photo 17). Plagioclase, averaging 0.33 mm X 1.5 mm, shows selective alteration of the cores in zoned crystals. Olivine is, for the most part, absent from the interior gabbronorite in the Gowganda area, however, a few altered phenocrysts were observed surrounded by orthopyroxene or inverted pigeonite, generally near the outer edges of both basal and capping border gabbronorite zones of the Miller Lake Intrusion.

The gabbronorite zones are less altered than other lithologies within the Nipissing Intrusions. Alteration commonly occurs in distinct zones within the gabbronorite. Within an alteration zone hypersthene and bronzite typically alter to actinolite and tremolite intergrowths, while the augite alters to uralite and the plagioclase alters to sericite

and saussurite. It is interesting to note that a zone of alteration occurs approximately 100 metres above the basal contact of the Miller Lake Intrusion and also occurs about 100 metres above the base of the Cross Lake Intrusion within the Cobalt Area.

Gabbro

The gabbro of the Nipissing Intrusions is found in close spatial association with the varied texture gabbro in the arches and limbs of undulating sheets. This gabbro generally contains augite as the predominant pyroxene along with very minor amounts of inverted pigeonite. The texture ranges from subophitic to gabbroic. In subophitic samples augite occurs as oikocrysts, upto 2 mm X 1 mm in size, partially enclosing plagioclase. Orthopyroxene is absent from this lithology and quartz varies from being relatively minor to occurring extensively as individual crystals or in eutectic intergrowth with feldspar.

Plagioclase, augite, very minor inverted pigeonite, quartz, and magnetite are the main minerals comprising this lithology. The spatial distribution, variation in quartz content, and variation in texture, has led the author to believe that this lithology represents a transition from the border quartz diabase to the pegmatite gabbro and also represents the more uniform medium-grained portions of the variable texture gabbro. Accessory minerals are zircon and apatite.

Alteration is extensive in this lithology. Plagioclase is extensively sericitized, pyroxene is altered to actinolite and tremolite, and biotite to chlorite.

Pegmatitic Gabbro

Pegmatitic gabbro was collected from the top of the Beaton Bay and Duncan Lake Intrusions and from the central portion of the Milner Lake Intrusion. In all three intrusions the pegmatite forms part of the varied texture gabbro. Pegmatite was not observed in the section across the Miller Lake Intrusion at the Castle Mine site.

The pegmatite consists of uralitized clinopyroxene, averaging 5 mm X 1.5 mm, sericitized feldspar (plagioclase and antiperthite), magnetite-ilmenite, 1.5 mm X 1.5 mm in size, and abundant eutectic intergrowth of quartz and feldspar. Abundant accessory minerals, including apatite, zircon and calcite, occur in close spatial association with the quartz-feldspar intergrowths.

The pegmatitic gabbro lacks the diabasic texture of the border quartz diabase, however, it can be better discribed as subophitic rather than granitic. Some samples show a weakly developed hornblende rim on a very altered pyroxene. The primary or secondary nature of this hornblende is difficult to determine in this case.

Alteration within the pegmatite is extensive. Plagioclase is completely sericitized and saussuritized. Pyroxene is altered to uralite and chlorite, and magnetite containing exsolution plates of ilmenite is altered to leucoxene.

Secondary biotite may occur in close spatial association to the chlorite or with the magnetite-ilmenite.

A narrow transition phase joins the pegmatite to the quartz diabase. Sample 0118 shows the characteristic irregularly shaped dots of coarser-grained magnetite, plagioclase and pyroxene within a finer-grained matrix.

Granophyre

The term granophyre has been applied to the pink rock found near the roof of the intrusions and in the interior of limbs connecting basins to arches. The pink coloration may be due to either the presence of potassic feldspar or a process resulting in hematite dusting of the plagioclase. The results of staining indicated that only two samples contained potassium feldspar. The petrologic analyses indicated that the potassium feldspar occurs predominantly as antiperthite in eutectoid intergrowth with quartz in this lithology. The antiperthite does not readily pick up the stain.

The granophyre is composed predominantly of sericitized feldspar and uralitized pyroxene along with extensive eutectoid intergrowth of feldspar and quartz (Photo 18). Abundant accessory minerals including zircon, calcite, titanite and apatite occurring as needles, or skeletal or resorbed crystals (Photo 19).

This petrologic study indicated that the finer-grained granophyre, represented by sample 0096, has considerably more potassium feldspar and accessory minerals than the medium-grained version found along the shoreline of Gowganda Lake. The only mafic phase left in this lithology is chlorite which

occurs as clusters of flakes, most likely replacing pyroxene. The feldspar within this fine grained lithology are strongly zoned.

Pink aplitic dikes observed as 2-3 cm wide dikelets in the upper portion of the Milner Lake Intrusion were not studied in this project, however, similar aplite from the Portage Bay Intrusion 80 km directly to the southeast have been documented by Hriskevich (1968), Jambor (1971), and Conrod (1988).

## Modal Analyses across the Beaton bay, Milner Lake, Duncan Lake, and Miller Lake Intrusions

The results of the modal analyses (about 750 counts per thin section) for each of the intrusions are listed in Tables 5 to 8, and are displayed in Figures 21 to 24.

The volume percent of minerals display trends which are related to the dip of the intrusion and the relative position from which the transect was taken within the undulating sheet (basin, limb, or arch).

The samples collected across the Milner Lake Limb, which dips 45° W, shows an increase in late-stage crystallizing minerals toward the center of the intrusion. This can be observed in the variation of abundance of quartz (Figure 21). A decrease in the clinopyroxene abundance accompanies this variation. The variation in potassium feldspar was difficult to evaluate due to the extreme alteration of the feldspars and thus "hidden" amounts of antiperthite which did not apparently stain.

Variation across the Duncan Lake Intrusion, which dips 35° E, shows a relative decrease in the abundance of quartz and

clinopyroxene toward the lower central portion of the intrusion. A corresponding increase in the abundance of bronzite accompanies this trend (Figure 22).

The modal analyses of quartz and clinopyroxene display "mirror-image" trends across the Beaton and a rapid increase in the late stage crystallizing phases such a quartz toward the center of the intrusion. The modal analyses of quartz, plagioclase, clinopyroxene, orthopyroxene and olivine across the Miller Lake Limb have defined four zones of reverse - followed - by - normal differentiation trends. These zones labelled A, B, C, and D are best defined by the variations in abundance of orthopyroxene. Each zone is an average thickness of 65 metres and shows a trend of decreasing quartz content and increasing orthopyroxene content toward the center of the zone. Olivine is present only near the upper and lower contacts of the intrusion. Clinopyroxene tracks in an opposite trend to the orthopyroxene. The fact that the olivine is most abundant in the near-contact zones, indicates that the olivine is most likely intratelluric in nature. Comparison of the modal analyses of selected minerals across these four Gowganda area intrusions define trends that are related to the geometry of the intrusion as was found in the previous studies by Hriskevich (1968), Jambor (1971) and Conrod (1988). The cyclic trends observed in the Miller Lake Intrusion, in this study, are somewhat anomalous and may be a key factor for why this particular intrusion is the major silver producer in the Gowganda area.

## Opaque Minerals

A complete study of the opaque minerals within the Gowganda area intrusion was not undertaken in this project, however, the distribution of the opaques, their crystal shapes, and textures appear to be identical to the opaque minerals within the Cobalt and Sudbury Nipissing Intrusions. Detailed studies of the opaque minerals within the Sudbury and Cobalt areas (Hriskevich 1968, Jambor 1971, and Conrod 1988) led to the conclusion that the dominant opaque mineral was magnetite with exsolved lamellae of ilmenite in various stages of alteration to leucoxene - an alteration product consisting of finely crystalline rutile or brookite. Very minor amounts of disseminated pyrite and chalcopyrite are generally present. The opaque minerals of the Gowganda area intrusions are expected to be the same as those of the Cobalt and Sudbury areas.

## Alteration within the Nipissing Lithologies

Most lithologies comprising the Nipissing Intrusive Suite are considerably altered, however, some lithologies are more suseptible to alteration than others. The border quartz diabase, pegmatitic gabbro, and granophyric rocks are more altered than the interior gabbro and gabbronorite. A detailed study of the alteration was beyond the scope of this project, however, the following alteration reactions were observed in the petrologic study:

plagioclase → sericite ± chlorite

plagioclase → saussurite (epidote + clinozoicite ) ± chlorite ± sericite

olivine → antigorite

olivine → talc

orthopyroxene → uralite (tremolite + actinolite) ± chlorite

orthopyroxene → talc

clinopyroxene → uralite (actinolite + tremolite) ± chlorite

The following reactions are believed to be applicable to what is observed in thin section. Although microprobe analyses of the alteration products or the original minerals were not undertaken, these reactions are expected to accurately represent what is observed in thin section.

Plagioclase to saussurite alteration

$2\ CaAl_2SiO_8 + H_2O - Ca_2(ALOH)\ Al_2Si_3O_{12} + HAISiO_4$

(anorthite) (zoisite) (base of mica)

(Shand, 1950,p.172)

$CaAl_2Si_2O_8 + KAISi_3O_8 + 2H_2O - > 2\ SiO_2 + KAI_2(AlSi_3)O_{10}(OH)_2$

(anorthite) (microcline) (muscovite)

$+ 2\ Ca_2Al_3Si_3O_{12}(OH)$

(epidote)

(Mueller and Saxena 1977,p.193)

Olivine to antigorite and talc alteration

$3\ Mg_2SiO_4 + 4\ H_2O + SiO_2\ 2\ Mg_3Si_2O_5(OH)_4$

(olivine) (serpentine)

$2\ Mg_3Si_2O_5(OH)_4 + 3CO_2 - Mg_3SiO_4O_{10}(OH)_2 + 3MgCO_3 + 3H_2O$

(serpentine) (talc) (magnesite)

(Deer et al. 1966,p.5)

Orthopyroxene to tremolite alteration

$3MgSiO_3 + 2CaMgSi_2O_6 + H_2O$ Â $Ca_2Mg_5Si_8O_{22}(OH)_2$

(enstatite) (diopside) (quartz) (tremolite)

(Deer et al. 1966,p.163)

Clinopyroxene to tremolite alteration

$5\ CaMgSi_2O_6 + 3CO_2 + H_2O - Ca_2MgSi_8O_{22}(OH)_2 + 3CaCo_3 + 2SiO_2$

(diopside) (tremolite) (calcite) (quartz)

(Deer et al. 1966, p.165)

Clinopyroxene + talc to tremolite alteration

$3CaMgSi_2O_6 + Mg_3Si_4O_{10}(OH)_2 + H_2O - Ca_2Mg_5Si_8O_{22}(OH)_2$

(clinopyroxene) (talc) (tremolite)

(Mueller and Saxena 1977, p.59)

Actinolite and clinozoisite to chlorite and calcite alteration

$3Ca_2(Mg,Fe)_5Si_8O_{22}(OH)_2 + 10CO_2 + 8H_2O + 2Ca_2Al_3Si_3O_{12}(OH) \rightarrow$

(actinolite) (clinozoisite)

$3(OH)_8(Mg,Fe)_5Al_2Si_3O_{10} + 10CaCO_3 + 21SiO_2$

(chlorite)

(Deer et al. 1966, p.67)

Orthopyroxene to talc alteration

$3\ MgSiO_3 + SiO_2 + H_2O - Mg_3Si_4O_{10}(OH)_2$

(orthopyroxene) (talc)

(Mueller and Saxena 1977, p.43)

## MINERAL CHEMISTRY

### Orthopyroxene Chemsitry Across the Miller Lake and Duncan Lake Intrusion

To help define differentiation trends across the Miller dLake Intrusion, the Mg-numbers of 48 crystals from 22 samples

across the intrusion were determined optically from their 2V angles. The $2V_X$ angles (Table 9) were determined on the universal stage using the orthoscopic method described by Phillips (1971) and the conoscopic method described by Hutchison (1974). The proofs for those analyses, determined by orthoscopic method, are displayed on the Wulff nets in Appendix 1. All proofs use a lower hemisphere plot.

The good correlation between the optical properties of orthopyroxene and its chemical composition indicate a direct relationship between the $2V_X$ angle and the Mg-number defined as: 100 Mg/(Mg + $Fe^{+2}$ + $Fe^{+3}$ + Mn). Figure 25 shows the samples and their 2V angles listed in Table 9, plotted onto the $2V_X$ - composition curve from Deer et al. (1980). The resulting Mg number for those samples are listed in Table 10.

The variation in Mg-number of the orthopyroxene across the Miller Lake Intrusion is shown in Figure 26. The plot indicates that the orthopyroxene is predominantly bronzite and hypersthene and that the mineral chemistry (Mg-number), tracks well with the trends determined by the modal analyses of orthopyroxene. The samples containing the most abundant orthopyroxene contain crystals with higher Mg-numbers, as seen when compared to the modal analyses plot, (Figure 24). Only samples that are spatially very close to the boundary between zones, show decreased Mg-numbers in the orthopyroxene.

The compositions determined in this study compare well with those determined by Hriskevich (1968) for the Colonial Mine and Shag Silver Mine within the Cobalt area.

Comparison of these results with the microprobe analyses of orthopyroxene from the Cross Lake Intrusion, Cobalt area and

the Bonanza Lake Intrusion in the Sudbury area (Conrod 1988) indicate that the crystals from the central portions of the cyclic zones within the Miller Lake Intrusion, are slightly more enstatitic than those of the central portions of the other two intrusions.

Only two samples from the central portion of the Duncan Lake Intrusion contained hypersthene. The 2V measurements are listed in Table 11 while the Mg-numbers are listed in Table 12. Although only three crystals were measured the Mg-number on average is less than those of the Miller Lake Intrusion and more comparable to those of the Cross Lake and Bonanza Lake Intrusions.

Core and rim measurements from selected grains across both intrusions indicate that normal zoning is present. Both normal and reverse zonation was observed for the Shag Silver and Colonial Mine Transects in the Cobalt area (Hriskevich 1968) and for the Cross Lake and Bonanza Lake Intrusions (Conrod 1988).

## WHOLE ROCK CHEMISTRY OF THE GOWGANDA NIPISSING INTRUSIONS

### Introduction

The distribution of major and trace element concentrations across the four intrusions was determined in order to better understand differentiation trends across various parts of an undulating Nipissing Sheet.

### Sample Preparation

All analyses were carried out at the Ontario Geological Survey Laboratories in Toronto.

Clean representative samples were crushed in a chrom-steel jaw crusher to a 7 mm chip size. This material was then pulverized to a - 50 mesh size powder with a ceramic plated Braun Pulverizer and then finely ground to a - 100 mesh powder in an alumina bowl using a Pulversette Planetary Mill.

The major element analyses were determined by conventional XRF technique on fused rock powders. The detection limits for these elements and the precision at the 95% confidence level are listed in Table 13a. The method of analyses, detection limits and precision at the 95% confidence level for the LOI, FeO, $Co_2$, S and $H_2O^+$ and $H_2O^-$ are listed in Table 13b.

The trace elements, Nb, Zr, Y, Rb, Sr, and Th were determined by XRF techniques on the fused powders. The detection limits and precision of these elements for this analytical method are listed in Table 14.

Major Element Variation within the Duncan Lake, Beaton Bay, Milner Lake and Miller Lake Intrusions

The concentration of major elements across the Duncan Lake, Beaton Bay, Milner and Miller Lake Intrusions are listed in Tables 15 to 18.

Trends correlative with those observed in the modal analyses across each intrusion can be recognized in the distribution of $SiO_2$, MgO, $TiO_2$, $P_2O_5$, and MnO. The $SiO_2$, content increases toward the contacts of the Duncan Lake Intrusion and the borders of each of the four zones delineated by the modal analyses in the Miller Lake Intrusion. In both the Milner Lake and Beaton Bay Intrusions the $SiO_2$ content increases toward the center of the intrusion. $TiO_2$, $P_2O_5$, and

MnO follow the same trend as $SiO_2$, while the variation in MgO is opposite to that of the $SiO_2$, as would be expected. The $SiO_2$, $TiO_2$, $P_2O_5$, and MnO are enriched in the late stage differentiates and the central portions of limbs, and depleted in the central portions of the basins which are rich in cummulate orthopyroxene. The differentiation trend across the four intrusions can best be displayed with the variation in whole-rock Mg-number defined as: (wt% MgO/mol. wt.)/[(wt% MgO/mol. wt) + (wt% $Fe_2O_3$/mol. wt)]. These trends are displayed in Figures 27-30.

A reverse differentiation trend is observed in the basal to central portion of the Duncan Lake Intrusion. This trend is followed by a normal differentiation trend extending from the central to upper parts of the intrusion, as was observed for the Cross Lake and Bonanza Lake Intrusions within the Cobalt and Sudbury areas, (Figures 31-33) (Conrod 1988). Four of these reverse, followed by normal, differentiation trends can be observed across the Miller Lake Intrusion; each correlating well with the modal analyses of orthopyroxene and the Mg-number of the orthopyroxene crystals. The Beaton Bay and Milner Lake Intrusion show a normal differentiation trend typical of that produced by a sill-like body cooling inward equally from both upper and lower contacts; very similar to that observed in the Portage Bay Intrusion from the Cobalt area (Figure 34). The concentration of late-stage differentiated material toward the centre of the intrusion, accompanied by the increase in $SiO_2$, $TiO_2$, $P_2O_5$, and MnO, correlates well with the decrease in Mg-number.

Reverse differentiation is not uncommon in many mafic intrusions and has been recognized in other Nipissing Intrusions (Finn 1984, Jambor 1971, Conrod 1988), as well as, in the Waterfall Gorge Section of the Insizwa Complex in the Karoo of South Africa (Lightfoot et al. 1984), the Fongen-Hilligen Complex in Norway (Wilson et al., 1981), the Stillwater Complex in Montana (Jackson 1961), and parts of the Bushveld Intrusion, South Africa (Cameron 1980). These trends are opposite to those of the Skaergaard Intrusion of Greenland (Wager and Borwn 1968), and those of the Palisade Sill of New Jersey (Walker 1969).

Although the precipitation of magnetite can affect the Mg-number; the trend of whole rock Mg-number variation across the Nipissing Intrusions appear to be unmodified; since the trends define by the whole rock Mg-number are reflected in other major elements ($SiO_2$, $P_2O_5$, $TiO_2$, MnO), the mineral chemistry, modal analyses of orthopyroxene, and in the trace element distributions which will be discussed in the next section.

The low whole rock Mg-number of all of the Nipissing chilled phases and the presence of olivine phenocrysts within the chilled phases suggests that significant amounts of olivine fractionated from the melt prior to emplacement. Although the source of the Nipissing magma is unknown and mantle heterogeneity can provide problems in estimating the chemical composition of the source magma, magmas derived by the partial melting of a mantle lherzolite with a $Mg/Mg + Fe^{2+}$ is approximately equal to 0.72 to 0.74 (Ringwood 1975, Hanson and Langmiur 1978). The low values observed in the chilled phases could be a reflection of a number of processes ranging from

various degrees of partial melting of the source, derivation from the source with a low Mg-number, significant amounts of oliving fractionation, or contamination by a number of lithologies moderately rich in $Fe^{2+}$ on the way to the surface. The presence of olivine within the chill zone strongly suggests that olivine fractionation prior to emplacement was involved.

A comparison of the Gowganda Nipissing chilled phases with those from Cobalt and Temagami, (Table 19) indicate that all chilled samples have an Mg-number significantly less than 0.72 - 0.74. The Mg-numbers of the Duncan Lake Intrusion are almost identical to those of the Portage Bay Intrusion. The Temagami area Nipissing intrusions are less primitive.

Although analyses for Ta and Yb were not done for the Gowganda Nipissing Intrusions the Th values proved to be in most cases less than the detection limits for the conventional XRF techniques, accurate instrumental neutron activation analyses of the Portage Bay chill margin (Conrod 1988) and chilled samples from the Temagami area (Lightfoot et al. 1987) plot in a location on the Th/Yb verses Ta/Yb plot of Pearce (1982) (Figure 35) where either subduction zone enrichment or crustal contamination appears to have accompanied olivine fractionation prior to emplacement.

## Trace Element Variation Within the Duncan Lake, Beaton Bay, Milner Lake and Miller Lake Intrusions

The trace element concentrations across the Gowganda Intrusions are listed in Tables 20 to 23. Except for the granophyre and highly differentiated samples, all other lithologies of the four intrusions contain concentrations of Nb

less than the detection limit of 5 ppm and concentrations of Th less than the dection limit of 10 ppm. The variation in Zr, Y, Sr, and Rb across the four intrusions are shown in Figures 36 to 39.

Due to the very low distribution coefficients of Y and Zr for the rock forming minerals, these elements are highly incompatible as well as relatively immobile in hydrothermal fluid devoid of complexing agents such as $F^-$. Because of these characteristics, these elements can be used to monitor chemical changes to the residual magma during cooling and crystallization.

Because of their similarly low distribution coefficients for the minerals crystallizing from the melt, Zr and Y are expected to track together across a given intrusion, which is the case for all of the intrusions except along the upper and lower boundaries of zone B in the Miller Lake Intrusion, where the Zr appears to be depleted relative to the Y. Samples from these zones are severely altered and it is expected that the Zr was affected in these two zones by the hydrothermal fluids, or that these particular analyses are suspect.

The erratic trends defined by the Rb and Sr across the intrusions strongly suggests that these elements (Rb and Sr) were mobile in the presence of deuteric or low grade metamorphic hydrothermal fluids.

The distribution of Y and for the most part Zr define the same trends defined by the variation in $SiO_2$, $P_2O_5$, $TiO_2$, and MnO, and trends opposite to that of the MgO content, the whold rock Mg-number, the modal analyses of orthopyroxene, and the Mg-number of the orthopyroxene.

Post-Emplacement Magmatic Processes

Quantitative modelling of the Cross Lake and Portage Bay Intrusion within the Cobalt area and the Bonanza Lake Intrusion within the Sudbury area Figures 40 - 42 (Conrod 1988); as well as selected intrusions within the Sault Ste. Marie and Temagami areas (Lightfoot et al. 1987) indicate that assimilation of Huronian Supergroup metasedimentary country rock accompanied fractional crystallization. A simultaneous assimilation - fractional crystallization (AFC) process described mathematically by DePaolo (1981) can best explain the chemistries of the various lithologies that comprise the Nipissing suite. From these studies however, it was found that the mass of the contaminant relative to the mass of material fractionated from the magma through crystallization and removal (Ma/Mf) was not constant throughout the cooling history; and that not all parts of the undulating sheet were affected by the contamination to the same degree. Campbell and Turner (1987) have proposed that melted roof rock may initially mix with some of the mafic magma within magma chambers, but because of the density differences, remains for the most part isolated from the rest of the magma. Lightfoot (in prep.) is currently testing this proposal on the Kerns intrusion in the Cobalt camp. The double-diffusive interface, proposed by Campbell and Turner (1987), that separates the melted country rock from the mafic magma, allows rapid thermal transport from the crystallizing pile across the interface to assimilate more roof rock but does not permit the transfer of significant amounts of melted roof rock into the underlying mafic magma. This could

explain why the Portage Bay Limb was best modelled by an AFC process while the Cross Lake Basin was best modelled by a Rayleigh Fractionation Crystallization process in the studies undertaken by Conrod (1988) (Figures 40 and 41). The initial assumption made in the modelling, carried out by Conrod (1988) and Lightfoot et al. (1987), is that the Nipissing Magma was emplaced by one large pulse. The assumption was made because the chemical trends observed across the intrusions were continuous and both capping and basal chilled magma were of the same chemistry.

The four reverse, followed by normal, differentiation trends found within the Miller Lake Basin indicate that multiple pulse emplacement is more appropriate for at least some of the Nipissing Intrusions.

A plot of whole-rock Y versus Zr for the four Gowganda Intrusions (Figure 43) shows that most samples fall on a LIL-enrichment trend with a bulk distribution coefficient for both Zr and Y approaching zero. Some the Beaton Bay, Milner, and Duncan Lake samples, however, deviate from the LIL-enrichment line and fall along a trajectory closer to the average composition of the Huronian Supergroup metasedimentary rocks. The granophyre with a Zr concentration of 159 ppm and an Y concentration of 25 ppm is an example of this deviation, and also indicates that the granophyre does not lie on a simple binary mixing line between the initial composition of the liquid at the time of emplacement and the Huronian rocks. The concentration of Y plotted against Zr, however, is not adequately sensitive to show contamination effects. Elements such as Th, La and Ce are much better for detecting

contamination; but their analyses could not be provided by the laboratories in the time frame of this project.

## A MODEL FOR THE EMPLACEMENT AND CRYSTALLIZATION OF THE GOWGANDA AREA NIPISSING MAGMAS

The recent petrochemical studies of Conrod (1988) and Lightfoot et al. (1987) show that the chemical distributions across a given part of a Nipissing Intrusion produce smooth continuous trends: a reverse differentiation pattern in the basal to central portion of basins followed by a normal differentiation trend; and a normal differentiation trend expected of dike-like bodies cooling equally from upper and lower contacts, in the arch portions. Similar trends were documented amongst others by Hriskevich (1968) for the Cobalt Intrusions and by Jambor (1971) for the Henwood Township Intrusion. In contrast to the trends in these cycles, the trends observed within the Miller Lake Intrusion show a basal reverse differentiation trend across each zone or cycle. The four zones of gradual reverse, followed by normal, differentiation trends are similar to the one overall trend observed for the Cross Lake and Bonanza Lake Intrusions, (Conrod 1988). The recognition of these trends and the determination of the process that formed them are of importance, since the Miller Lake Basin is the major Ag - producing intrusion in the Gowganda area.

Modelling of the Nipissing Intrusions must account for all of the lithologies observed, the distribution of lithologies - (gabbronorite cummulates in the basins and granophyric and granodioritic differentiates in the arches), and the reverse

differentiation in the basins and normal differentiation in the arches observed in both mineral and whole rock chemistries.

The reverse differentiation within the Lake Wanapitei Intrusion was proposed to be the result of the emplacement of multiple pulses into an auxilary magma chamber, (Finn 1981). The loosely packed cummulate crystals in the basins suggest that trapped interstitial liquid did not play a major role in the evoluation of the residual magma until late stage filter-pressing, which liberated volatile-rich material from the cummulate pile and formed the pegmatitic gabbros. The present geophysical data is generally not detailed enough to support or refute the proposal of feeders beneath the basins. For the Miller Lake Intrusion a multiple pulse model would require the emplacement of a progressively more primative magma in each cycle which is then allowed time to differentiate before the next pulse. It is interesting to note that the variation in Mg-number across the Miller Lake Intrusion (Figure 30) shows that each cycle "A" through to "C" has become more differentiated (i.e., have progressively less Mg-rich liquids near the top of each cycle). If such a model were operative then the replenishing primative magma would have to be restricted to the basins only, and the arches would represent the accumulation of differentiated material from the initial pulse of magma which formed the chill in both arches and basins is identical in chemical composition.

Because of the predominance of roof rock melting in the limb and arch areas, Conrod (1988) proposed that convection and perhaps the slumbing of crystal mushes form the arches into the basins has played a major role in the present distribution of

lithologies. This idea was suggested for the Henwood Intrusion by Jambor (1971). Such a model would not require the presence of a feeder under every basin but proposes the presence of one feeder for a group of arches and basins, (ie,.an undulating sheet rather than a cone sheet configuration). The periodic or continuous erosion of a crystal mush located on the floor of the arches and limbs and its subsequent gravity-driven slumping down into the basins could account for the reverse differentiation and presence of gabbronorite cummulates in the basins. Because of the convex surface of the arches, crystallization would have begun prior to that in the basins. Initially, the slumping of the crystal mush into the basins may have displaced hot magma upward along the roof of the limbs and into the arches, where localized melting of the country rock occurred. Because of the bouyant nature of the hybrid melt, (mafic + melted country rock), it remained within the arches and limbs (Conrod 1988).

The following model (Figures 44a-e), which attempts to combine these two proposals, seems the most appropriate for the data available at this time. Initially hot mafic magma was emplaced into an auxillary magma chamber beneath the Proterozoic-Archean unconformity. This initial magma assimilated some of the Archean rock during the formation of this auxilary magma chamber and is therefore contaminated with crustal material. Fractionation of olivine began within the auxiliary chamber. A pressure build up within the auxiliary magma chamber or a new influx of denser magma allows the initial magma to penetrate upward, (above the original feeder where it is hottest), and to move along the structurally

weakened zone of the unconformity, as a thin slightly undulating sheet coating both roof and basal contacts with differentiated, contaminated magma. In-situ crystallization of undifferentiated magma against the chills produced the border quartz diabases, found along both upper and lower contacts in both basins and arches. The draining of the auxiliary magma chamber allows a new influx of hot mafic magma into the auxiliary magma chamber. This magma is hotter and more primitive than the initial magma because the conduit and chamber had already been formed. The second pulse being more primitive undergoes limited mixing with the residual magma and spreads out laterally along the floor of the auxiliary chamber.

The second magma pulse has a lower residence time in the auxiliary chamber and becomes less fractionated than the initial one, before it moves up the conduit and along the unconformity. Because this magma is hotter it may even absorb some of the olivine precipitated from the initial magma as suggested by Finn (1984). This second magma is more primitive than the initial magma for two reasons: (1) it remains hotter longer and thus was less fractionated because the conduit was already formed by the penetration of the initial magma and (2) it may have absorbed olivine precipitated from the initial magma making it more Mg-rich. Because of the convex surface in the arches cooling is expected to proceed at a faster rate than in the basins. The crystal mush accumulating on the floor of the arches slumps downward into the basin under the influence of gravity and with the incoming denser pulse. Subsequent pulses proceed as did pulse number 2, with progressively shorter residence times in the auxillary chamber. The roof of

the unconformity sheet directly above the conduit becomes very hot and may be subjected to much melting as each new hot pulse enters the sheet. The hybrid mamga formed by the melting of tyhe country rock is not expected to undergo extensive mixing with the hot magma because of its bouyant nature and is expected to remain along the upper surface of the arch and limb sections. During the latest stages of magmatism the magma has a longer residence time in the auxiliary chamber and is allowed to fractionate to the point of producing a highly volatile granitic or granodioritic differentiate. This differentiate may be not only the product of fractionation, but also local melting of the wall rock. This magma makes its way up into the unconformity sheet and mixes with the local melts derived from melting of the roof rock in the arches and cools from both the upper and lower contact at an equal rate. Filter pressing of the crystal mush accumulated in the basins expells highly volatile material which produced the gabbor pegmatite veins which cut the gabbronorites and accumulated above the gabbronorites as the variable texture gabbros. The accummulation of these volatile phases above the gabbronorite cause their lateral migration up the limbs and toward the arches.

This model explains why most assimilation of country rock accurs in the arch areas and why the arch and limb areas can best be modelled quantitatively by an assimilation - fractional crystallization process and the basins by a Rayleigh Fractional Crystallization process (Conrod 1988). The reverse differentiation trend within the basins is the result of the emplacement of continuously more primative denser, but hotter

magma from the auxiliary chamber, with simultaneous slumping of any crystal mush accummulating on the floors of the arches. The most convincing evidence for the emplacement of a later granitic phase from the auxiliary chamber is seen in the chondrite normalized rare-earth element (REE) plot for the lithologies comprising the Portage Bay Intrusion within the Cobalt area, (Figure 45). The two features on the plot which indicate the presence of two magmas which have crystallized as distinct entities are: (1) a gap separating the chilled phase, quartz diabase, gabbro, and gabbro pegmatite from the granodiorite differentiates, and (2) the uniform value for the Eu for each group - a function of the absolute $K_D$ value for Eu into plagioclase being very close to the value of 1. Sample 12 (a granodiorite), however, appears to belong with the lower group indicating that some interaction occurred, between the fractionating magma and either partial melts of the country rock or the later emplaced granodioritic magma.

The determination of the correct genetic model is critical for understanding where and how the native Ag, the Co and Ni arsenide mineralization, as well as possible Pt concentrations may occur. The model proposed in this paper indicates that areas of intrusions high in heat, such as feeder zones as well as areas that have undergone multiple pulse emplacement and contamination by wholesale or partial melting of the country rock (Huronian Supergroup metasediments) are good exploration targets. Regardless of whether the Ag and Co-Ni arsenides were derrived by hydrothermal leaching of the adjacent country rock or fractionation and contamination processes within the magma, the hottest areas can set up the best convecting hydrothermal

systems and can assimilate the most country rock, which can play an important role in the precipitation of sulfides as seen for the Sudbury ores (Naldrett et al. 1986). This study provides good evidence for multiple pulse emplacement in the Miller Lake Basin - the largest Ag producing intrusion within the Gowganda area. This feature may prove to be a good indicator for areas of concentrated Ag and Co-Ni arsenide mineralization. Intrusions showing features of significant silica contamination may have undergone sulfide saturation and exsolution. If the exsolving sulfide phase is in contact with large volumes of the mafic magma, then, because of the very high distribution coefficient of the PGEs for the sulfide phase over the silicate magma, the seggregating sulfide may act as a scavenger and concentrator of the PGEs. Significant concentrations of PGEs in sulfides of the Nipissing suite have been documented for the Wanapitei Intrusion within the Sudbury area (Rowell 1984).

## TECTONIC SETTING OF THE NIPISSING INTRUSIONS

Little is known about the tectonic setting of the Nipissing Intrusions. They are commonly thought to represent the intrusive equivalents of an extensive eroded continental flood basalt plain extending across the Nipissing Province. Lovelle and Caine (1979) proposed that much of the Nipissing Magmas may have been fed from a rift located under Lake Timiskaming. Recent geochemical studies of the Sudbury and Cobalt area intrusions (Conrod 1988), however, indicate a moderately strong calc-alkalic character to the magmas.

Conrod (1988) and Lightfoot et al. (1987) indicated that all Nipissing lithologies, including the chilled phases are enriched in the large ion lithophile elements (LILs); a feature most likely a function of combined fractionation and contamination prior to emplacement and assimilation of country rock and fractionation after emplacement (Conrod 1988). Comparison of the Nipissing Intrusive suite to a representative of rift-related continental flood basalt volcanism, (the Keweenawan continental flood basalt reference suite), on a chondrite-normalized spidergram, shows the pronounced enrichment in the LILs in the Nipissing suite over the Keweenawan suite (Figures 46 and 47). The enrichment within the chill phases indicates that the enrichment process began prior to emplacement of the magma. While the source of the Nipissing magmas is unknown, chondrite-normalizing allows easy comparison between different suites of rocks. The profile of the Nipissing lithologies in Figure 45 very closely resembles the profile generated when dolerite sills have undergone pelite contamination (Figure 48) (Thompson et al. 1984). The strong Sr depression within the Nipissing granodiorite profile matches well with the contaminated dolerites.

Normalizing to mid-ocean-ridge basalt (M.O.R.B.) also allows comparisons to be made between suites of rocks, without invoking a specific tectonic environment. The MORB-normalized spidergram profiles of the Nipissing suite (Figure 49a and b) are very similar to that of a basaltic magma which has been contaminated by 20 percent of a quartz diorite which has undergone 50 percent partial melting, (Pearce 1984), (Figure 50). Both profiles show a similar enrichment in the LIL

elements on the left hand side of the diagram relative to those elements on the right, and similar Ta and Nb depressions. The pronounced depressions for P and Ti in the Nipissing suite, [erroneously recorded as $P_2O_5$ and $TiO_2$ in Conrod (1988)], are not observed in the contaminated M.O.R.B.

A similar enrichment in the LIls is observed in the calc-alkalic basalts from Central Chile (Figure 51) (Pearce 1984). Pronounced Ta and Nb depressions are observed in both profiles. Ti and P depressions are not as pronounced in the Chilean magmas as in the Nipissing lithologies.

The above data raises the question of whether spidergram profiles adequately discriminate between various tectonic settings, or whether similar enrichment processes in different tectonic settings could lead to a similar spider profiles. Thompson et al. (1984) compiled geochemical data on a number of representative continental flood basalts and hypabyssal intrusions and showed that different types of contamination led to different spidergram profiles.

To try to solve the above problem, the Nipissing lithologies were plotted on a number of tectonic discrimination plots. Figure 52 shows the position of the Nipissing suite on the Th-Hf-Ta discrimination plot of Wood (1980) (data from Conrod 1988). All lithologies including the chilled phases plot within the field designated by Wood (1980) as "destructive plate-magin calc-alkalic basalts and their differentiates".

The elements used in Wood's triangular plot are relatively immobile and incompatible. (The Nipissing samples from Conrod (1988) were crushed in an agate mill and therefore no contamination of Ta is expected).

The same data were plotted on the Zr-Ti-Y plot of Pearce and Cann (1973), (Figure 53). Again the data plots within the calc-alkalic basalt field and not the within-plate basalts. Ti, Zr and Y are all high field strength elements (HFSE), having a high charge to radius ratio, and are both fairly incompatible and immobile. Even though Ti can substitute into the ilmenite structure, the entire suite including the chilled phases falls outside of the within plate basalt field and within the calc-alkalic basalt field.

Samples of chilled Nipissing phases from the Temagami Lake, Cobalt and Gowganda aeas (Table 24) were plotted on a Zr/Y verses Zr discrimination plot of Pearce and Norry (1979) for non-cummulate basalts of three tectonic settings, (Figure 54). All but one of the samples lie outside of the three fields delineated in the plot, especially the within-plate basalts. The same samples plotted on the Ti versus Zr plot of Pearce (1980) also distinguishes the chilled Nipissing phases from within-plate basalts (Figure 55).

Beard (1986) proposed that the chemical composition of coexisting olivine and plagioclase in gabbro cummulates can be used to determine the tectonic setting of ancient volcanic complexes. Microprobe analyses of plagioclase and olivine from the Cross Lake Intrusion, Cobalt, (Conrod 1988), plot within the arc field on this discrimination plot and fall outside of the tholeiitic layered intrusion field, (Figure 56). Fresh olivine was not present in the Gowganda area intrusions.

Samples of Nipissing chilled margins from the Cobalt, Temagami and Sudbury Nipissing Intrusion as well as the Portage Bay, Cross Lake and Bonanza Lake Nipissing lithologies all plot

in the calc-alkalic field on the Th/Yb versus Ta/Yb plot of Pearce (1982) (Figure 35).

All of the Nipissing data from this study and that of Conrod (1988) plot outside of the within-plate basalt field and in the calc-alkalic field on the various discrimination diagrams. The spidergram profiles of the Nipissing lithologies are very similar to calc-alkalic basalts of Chile and different from the lithologies which make up the Keweenawan Reference Suite, however, they are also very similar to the profile generated by the contamination of MORB with partial melts of quartz diorite and similar to the profile of dolerite contaminated with pelite. If the discrimination diagrams adequately distinguish the tectonic settings, then the above data indicates that the Nipissing magmas may be genetically related to a plate-boundary collision type of tectonic setting. If this is the case, then the Nipissing Intrusions provide a window to processes within the magma chambers beneath arc type volcanos - that is enrichment processes such as fractionation, contamination or a combination of the two. If, however, the discrimination diagrams do not adequately distinguish one tectonic setting from another, then the above data indicates that similar processes of selective element enrichment can be operating in different tectonic settings and can produce very similar profiles on the spidergrams.

Hawkesworth et al. (1982) have proposed that the chemical variation observed within the Andean lavas from Chason to Purico are the result of a shift from subduction related magmas to magmas showing a greater crustal affinity; involving processes of bulk assimilation of crustal material, mixing

between mantle - and crustal-derived magmas, and partial melting of pre-existing crust. This could explain the chemical similarities observed between the Nipissing suite and the Chilean lavas, however, the chondrite normalized REE profiles of both Purico and Chason are considerably steeper than those observed within the Nipissing suite.

## A U-PB AGE DETERMINATION FOR THE BONANZA LAKE INTRUSION FROM THE SUDBURY AREA, AND COMPARISON WITH THE U-PB AGE OF THE GOWGANDA AREA NIPISSING INTRUSIONS

### Introduction

Hollow quenched zircon crystals (Photo 20) from two samples of the granodiorite phase within the Bonanza Lake Intrusion, located immediately south of Lake Wanapitei in the Sudbury area, were separated and used in a U-Pb age determination (Krogh 1982) at the Royal Ontario Museum in Toronto. The preliminary results are listed in Table 25, and represent a minimum age only. This age of 2210 Ma and 2214 Ma is in close agreement with the age of the Miller Lake Intrusion in Gowganda (2219 ± 3.6 m.y., Corfu and Andrews 1986); but is considerably older than the K/Ar age determination of 2109 ± 40 Ma documented for the Wanapitei Lake Intrusion on the northeastern shore of Lake Wanapitei (Rowell 1984).

### Implications for Age-related variation in the type and style of mineralization spatially associated with the Nipissing Intrusions

Card and Pattison (1973) recognized a change in the type and style of mineralization spatially associated with the Nipissing Intrusions from east to west across the Nipissing Province. Recent work by Buchan and Card (1985) on the paleomagnetic direction of samples of Nipissing Intrusions from across the province suggests that there may be two distinct stable paleomagnetic directions: $N_1$ which is north and up 40° or south and down 40° and $N_2$ which is steeply down to the west. Symons and Londry (1975) proposed that $N_1$ was primary and that $N_2$ was a secondary overprint. Ray and Lapointe (1976) proposed that $N_2$ was the primary direction and that $N_1$ was a metamorphic orverprint. Both directions have been observed in the contacting baked Huronian Supergroup metasedimentary rocks, (Symons 1967, Morris 1979, Roy and Lapointe 1976). Neither $N_1$ or $N_2$ can be exclusively associated with petrologically fresh or altered samples, however $N_1$ appears to be more prominent in the Cobalt - Sault Ste. Marie area while $N_2$ is more prominent in the Blind River - Sudbury area. Morris (1979) and Stupavsky and Symons (1982) have interpreted the above data to indicate the presence of two ages of intrusion for the Nipissing magmas, however, as Buchan and Card (1985) point out, if these two paleomagnetic directions, that are both found within fresh samples, are indeed primary, then two periods of magma emplacement is inevitable. If, however, some of the petrologically fresh samples have aquired a second magnetic direction resulting from a thermal overprinting without chemical alteration, then one or both directions may be secondary. If the first case is correct then the variability

in type and style of mineralization across the Nipissing Province may well be age related.

The minimum ages obtained for the Bonanza Lake Intrusion, located in the central sector of the Nipissing Province which is devoid of any known silver mineralization, are in close agreement with the U/Pb ages obtained by Corfu and Andrews (1986) for the Miller Lake Intrusion located in eastern sector of the Province which contains abundant silver mineralization. Even when the errors on the age determinations are considered, the age of the Bonanza Lake and Miller Lake Intrusions contrasts with the whole rock Rb/Sr age determined by Fairbairn et al. (1969) for a Gowganda area intrusion (2116 ± 54 Ma) and a K/Ar age determined for the Wanapitei Lake Intrusion located on the northeastern shore of Lake Wanapitei. The dates also contrast with the whole rock Rb/Sr age determined by van Schmus (1965), for the Nipissing Intrusions located along the north shore of Lake Huron between Bruce Mines and Blind River, (2109 ± 80 Ma). The data does, however, indicate that intrusion of at least some of the Nipissing magmas occurred in a moderately close time interval between the central and eastern sectors of the province and only the intrusions in the eastern region appear to contain the spatially associated silver mineralization. This data also indicates that the emplacement of the magma began in both the central and eastern sectors at approximately the same time. While there is no paleomagnetic data for the Bonanza Lake Intrusion, Buchan and Card (1985) have determined the Miller Lake Intrusion in Gowganda to have both $N_1$ and $N_2$ paleomagnetic directions. A number of other intrusion across the Nipissing Province also contain both

magnetic directions. Therefore, it appears that at least in some intrusions one of the directions is the result of thermal overprinting - either metamorphic, deuteric, or contact metamorphic through the emplacement of other intrusions. Since the Miller Lake Intrusion contains silver and the Bonanza Lake Intrusion does not; and both intrusions are of similar age, it appears that the variation in the type and style of mineralization across the Nipissing Province is probably not likely age-related.

References

Beard, J.S.

1986: Characteristic mineralogy of Arc-Related Cummulate Gabbros: Implications for the Tectonic Setting of Gabbroic Plutons and for Andesite Genesis; Geology, Volume 14, p. 848-851.

Buchan, K.L. and Card, K.D.

1985: Preliminary Comparison of Petrographic and Paleomagnetic characteristics of Nipissing Diabase Intrusions in Northeastern Ontario; in Current Research, Part A, Geological Survey of Canada Paper 85-1A, p. 131-140.

Burrows, A.G.

1922: Gowganda Silver Area (4th report), in Gowganda and Other Silver Areas; Ontario Department of Mines, Volume 30, part 3, 54 p.

Cameron, E.N.

1980: Evolution of the Lower Critical Zone, Central Sector Eastern Bushveld Complex and its Chromite Deposits; Economic Geology, Volume 75, p. 845-871.

Campbell, I.H. and Turner, J.S.

1987: A Laboratory Investigation of Assimilation at the Top of a Basaltic Magma Chamber; Journal of Geology, Volume 95, p. 155-172.

Card, K.D.

1978: Metamorphism of the Middle Precambrian (Aphebian) Rocks of the Eastern Southern Province, in Metamorphism in the Canadian Shield; Geological Association of Canada Paper 78-10, p. 269-282.

Card, K.D. and Pattison, E.F.

1973: Nipissing Diabase of the Southern Province, Ontario; Geological Association of Canada Special Paper, Number 12, p. 9-30.

Carter, M.W.

1983: Geology of the Natal and Knight Townships, District of Sudbury and Timiskaming; Ontario Geological Survey, Report 225, 74 p.

Chimo Gold Mines Limited

1960: Chimo (Northcliff) Property; Assessment Work Files, Ontario Department of Mines, Resident Geologist' Office, Cobalt, Ontario.

Conrod, D.M.

1988: Petrology, Geochemistry and Platinum Group Element Potential of the Portage Bay, Cross Lake, and Bonanza Lake Nipissing Intrusions of Northern Ontario; Unpublished M.Sc. Thesis, University of Toronto, Toronto, Ontario, 494 p.

Corfu, F. and Andrews, A.J.

1986: A U-Pb Age for mineralized Nipissing Diabase, Gowganda, Ontario; Canadian Journal of Earth Sciences, Volume 23, p. 107-109.

Cunningham, L.J.

1985: Report on Manridge Explorations Limited, Milner Township, Ontario; Assessment Work Files, Ontario Geological Survey, Toronto, Ontario, 33 p.

Deer, W.A., Howie, R.A., and Zussman, J.

1980: A Introduction to the Rock-Forming Minerals; Longmann Group Limited, London, England, p. 108-114.

DePaolo, D.J.

1981: Trace Element and Isotopic Effects of Combined Wallrock Assimilation and Fractional Crystallization; Earth and Planetary Science Letters, Volume 53, p. 189-202.

Drake, K.H.

1976: Geological Exploration Report on the Former Castle-Tretheway Mine (McIntyre) Properties, Haultain and Nicol Townships, Ontario, Larder Lake Mining Division, District of Timiskaming for Milne Consolidated Silver Mines Limited; Assessment Work Files, Ontario Geological Survey, Toronto, Ontario, 22 p.

Fahrig, W.F. and Wanless, R.K.

1963: Age and Significance of Diabase Dyke Swarms of the Canadian Shield; Nature, Volume 200, p. 934-937.

Fairbairn, H.W., Hurley, P.M., Card, K.D., and Knight, C.J.

1969: Correlation of Radiometric Ages of Nipissing Diabase and Huronian Metasediments with Proterozoic Orogenic Events in Ontario; Canadian Journal of Earth Sciences, Volume 6, p. 489-497.

Finn, G.C.

1984: Petrogenesis of the Wanapitei Gabbronorite Intrusion: a Nipissing-type Diabase from Northern Ontario; Unpublished M.Sc. Thesis, University of Western Ontario, 112 p.

Gates , T.M. and Hurley, P.M.

1973: Evaluation of Rb/Sr Dating Methods Applied to the Matachewan, Abitibi, MacKenzie, and Sudbury Dike Swarms in Canada; Canadian Journal of Earth Sciences, Volume 10, Number 6, p. 900-919.

Hanson, G.N. and Langmuir, C.H.

1978: Modelling of Major Elements in Mantle-Melt Systems using Trace Element approaches; Geochimica et Cosmochimica Acta, Volume 42, p. 725-742.

Hawkes, D.D.

1966: Differentiation of the Tumatumari-Kopinang Dolerite Intrusion, British Guiana; Geological Society of America Bulletin, Volume 77, p. 1131-1158.

Hawkesworth, C.J., Hammill, M., Gledhill, A.R., van Calsteren, P., and Rogers, G.

1982: Isotope and Trace Element Evidence for late stage intra-crustal melting in the High Andes; Earth and Planetary Science Letters, Volume 58, p. 240-254.

Hriskevich, M.E.

1968: Petrology of the Nipissing Diabase Sill of the cobalt Area, Ontario; Geological Society of America Bulletin, Volume 7, p. 1387-1404.

Hutchison, C.S.

1974: Laboratory Handbook of Petrographic Techniques; John Wiley and Sons Incorporated, New York, United States of America, p. 98-103.

Jackson, E.D.

1961: Preliminary Textures and Mineral Associations in the Ultramafic Zone of the Stillwater Complex, Montana, United States; Geological Survey Professional Paper 358, 106 p.

Jambor, J.L.

1971: The Nipissing Diabase, in The Silver Arsenide Deposits of the Cobalt-Gowganda Region, Ontario; Edited by L.G. Berry, Mineralogical Association of Canada, 429 p.

Krogh, T.E.

1982: Improved Accuracy of U-Pb Zircon Ages by the creation of more concordant systems using an Air-Abrasion Technique; Geochimica et Cosmochimica Acta, Volume 37, p. 485-494.

Lightfoot, P.C., Naldrett, A.J. and Hawkesworth, C.J.

1984: The Geology and Geochemistry of the Waterfall Gorge Section of the Insizwa Complex, with particular reference to the origin of the nickel sulfide deposits; Economic Geology, Volume 79-8, p. 1857-1879.

Lightfoot, P.C., Conrod, D.M., Naldrett, A.J. and Evensen, N.M.

1987: Petrologic, Chemical, Isotopic, and Economic Potential studies of the Nipissing Diabase; in Geoscience Research 1986-1987; Ontario Geological Survey, Miscellaneous Paper 136, p. 4-26.

Lovell, H.L. and Caine, T.W.

1970: Lake Timiskaming Rift Valley; Ontario Department of Mines, Miscellaneous Paper 39, 16 p.

Lowdon, J.A., Stockwell, C.H., Tipper, H.W., and Wanless, R.K.

1963: Age Determinations and Geological Studies; Geological Survey of Canada, Paper 62-17, 140 p.

McIlwaine, W.H.

1978: Geology of the Gowganda Lake - Miller Lake Silver Area, District of Timiskaming; Ontario Geological Survey, Report 175, 161 p.

Morris, W.A.

1979: A positive contact test between Nipissing Diabase and Gowganda Argillites; Canadian Journal of Earth Sciences, Volume 16, p. 607-611.

Mueller, R.F. and Saxena, S.K.

1977: Chemical Petrology with Applications to the Terrestrial Planets and Meteorites; Springer-Verlag, New York, 394 p.

Naldrett, A.J., Rao, B.V. and Evensen, N.M.

1986: Contamination of Sudbury and its role in Ore Formation; Institute of Mining and Metallurgy, extract from Metallogeny of basic and ultrabasic rocks, p. 75-91.

Nold, J.L. and Erickson, K.P.

1967: Changes in K-Feldspar staining methods and adaptions for field use; American mineralogist, Volume 52, p. 1575-1576.

Pearce, J.A.

1984: Role of the sub-continental lithosphere in magma genesis at active continental margins, in continental basalts and mantle xenoliths; editors C.J. Hawkesworth and M.J. Norry, Shiva Publishing Limited, Nantwich, Cheshire, United Kingdon, p. 230-249.

Pearce, J.A. and Cann, J.R.

1973: Tectonic Setting of Basaltic Volcanic Rocks determined using Trace Element Analyses; Earth and Planetary Science Letters, Volume 19, p. 290-300.

Pearce, J.A. and Norry, M.J.

1979: Ti, Zr, Y, and Nb Variations in volcanic rocks; contributions to Mineralogy and Petrology, Volume 69, p. 33-47.

Petruk, W.

1971: General characteristics of the deposits, in the Silver-Arsenide deposits of Cobalt-Gowganda Region, Ontario;

edited by L.G. Berry, Mineralogical Association of Canada, p. 76-107.

Phillips, R.W.

1971: Mineral Optics, principles and Techniques; W.H. Freeman and Company, San Francisco, United States of America, p. 205-207.

Ringwood, A.E.

1975: Composition and Petrology of the Earths Mantle; McGraw-Hill, New York, 618 p.

Rowell, W.F.

1984: Platinum Group Elements and Gold in the Wanapitei Nipissing-type Intrusion, Northeastern Ontario; Unpublished M.Sc. Thesis, University of Western Ontario, London, Ontario, 87 p.

Roy, J.L. and Lapointe, P.L.

1976: The Paleomagnetism of Huronian Redbeds and Nipissing Diabase, Post-Huronian Igneous Events and Apparent Polar Path for the Interval 2300 Ma to 1500 Ma for Laurentia; Canadian Journal of Earth Sciences, Volume 13, p. 749-773.

Stupavsky, M. and Symons, D.T.A.

1982: Extent of Grenvillian Remanence Components in Rocks of the Southern Province; Canadian Journal of Earth Sciences, Volume 13, p. 749-773.

Sutherland, D.

1971: Milner Township; Assessment Work Files, Ontario Department of Mines, Resident Geologist's Office, Cobalt, Ontario.

Symons, D.T.A.

1967: Paleomagnetism of Precambrian Rocks Near Cobalt, Ontario; Canadian Journal of Earth Sciences, Volume 4, p. 1161-1169.

Symons, D.T.A. and Londry, J.W.

1975: Tectonic Results from Paleomagnetism of the Aphebian Nipissing Diabase at Gowganda, Ontario; Canadian Journal of Earth Sciences, Volume 12, p. 940-948.

Thompson, R.

1968: Manridge Mines Limited, Milner Township, Ontario, Unpublished Report, as reference by McIlwaine, 1978: Ontario Geological Survey Report 175.

Thomspon, R.N., Morrison, M.A., Dickin, A.P. and Hendry, G.L.

1984: Continental Flood Basalts .... Arachnids Rule O.K.?, in Continental Basalts and Mantle Xenoliths; editors: C.J. Hawkesworth and M.J. Norry, Shiva Publishing Limited, Nantwich, Cheshire, United Kingdom, p. 158-185.

Wager, L.R. and Brown, G.M.

1968: Layered Igneous Rocks; Oliver and Boyd, Edinburgh, 588 p.

Walker, K.R.

1969: The Palisade Sill, New Jersey: A reinvestigation; Geological Society of America, Special Paper number 3, 178 p.

Wanless, R.K., Stevens, R.D., Luchance, G.R., and Rimvaite, R.Y.H.

1966: Age determinations and geological studies, K-Ar isotopic ages, report 6; Geological Survey of Canada, Paper 65-17, 101 p.

Wilson, R.J., Esbensen, K.H., and Thy, P.

1981: Igneous Petrology of the Synorogenic Fongen-Hilligen Layered Basic Complex, south central Scandinavian caledonides; Journal of Petrology, Volume 22, p. 584-627.

Wood, D.A.

1980: The Application of a Th-Hf-Ta Diagram to Problems of Tectonomagmatic Classification and to establishing to nature of crustal contamination of basaltic lavas of the British Tertiary Volcanic Province; Earth and Planetary Science Letters, Volume 50, p. 11-30.

Van Schmus, W.R.

1965: The Geochronology of the Blind-River Bruce Mines Area, Ontario, Canada; Journal of Geology, Volume 73, p. 774-780.

Appendix 1

Wulff Net Plots of the Orthopyroxene Optical Measurements and the 2V Determinations (all measurement are on a lower hemisphere plot)

1987 DMC 0202 1

grain 1

| | iv | arc | oad |
|---|---|---|---|
| Y = 192 | ; 38.3 | ↔ | ; ⊤ 40.5 |
| X = 277 | ; ↔ 5.5 | | |

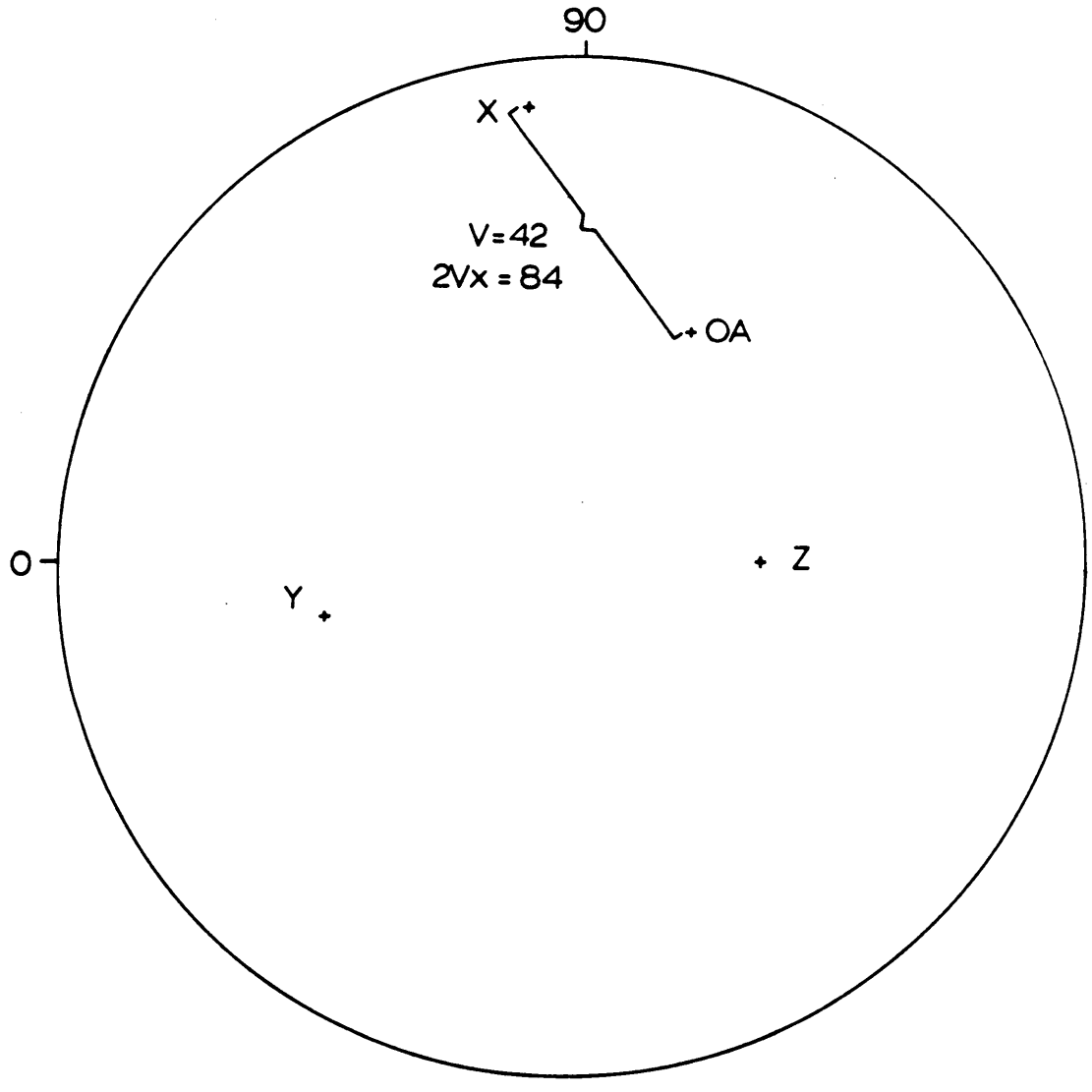

2

1987 DMC 0202

grain 2

| | iv | arc | oad |
|---|---|---|---|
| Y | 354.5 | 9 ↔ | ↑ 24.5 |
| Z | 086 | 17 ↔ | |

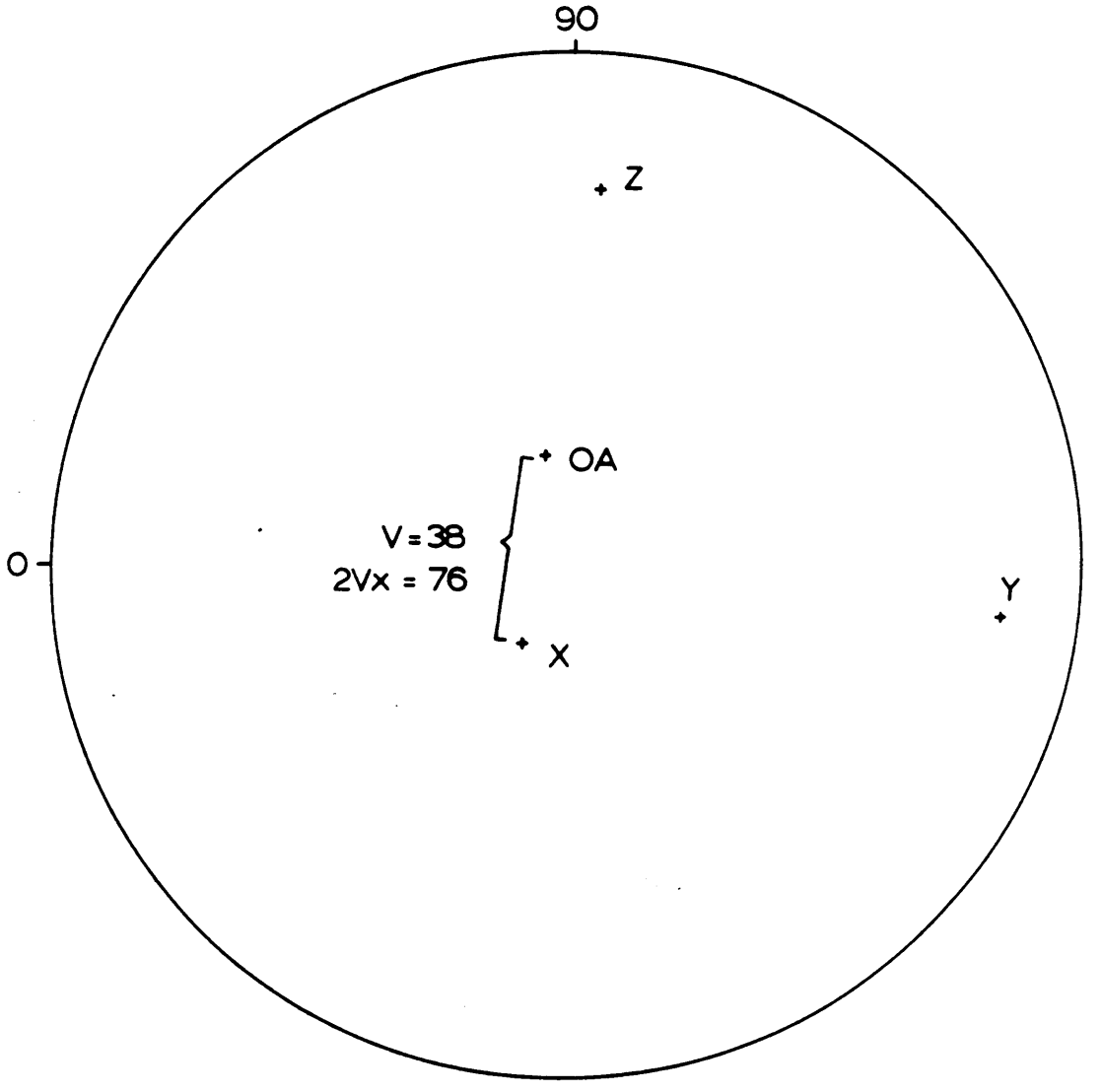

1987 DMC 0206

grain 1

3

| iv | arc | oad |
|---|---|---|

Y=296.5; ↦ 20.5; ↥ 21

Z=199.5; ↦ 20.5

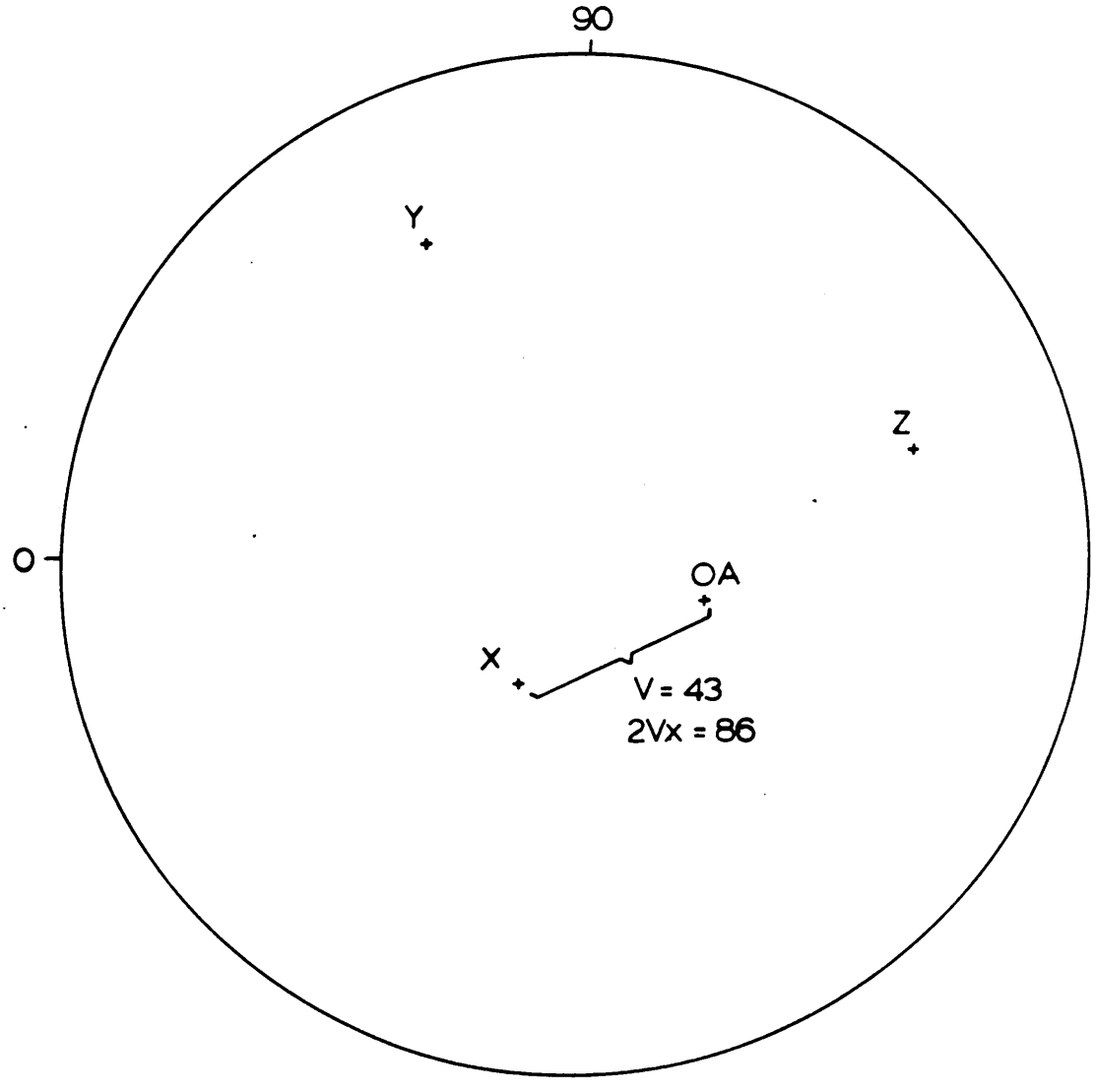

1987 DMC 0209 4

grain 1

| | iv | arc | oad |
|---|---|---|---|
| Y = 230 | ; ↦ 2 | ; ↧ 19.5 | |
| Z = 318 | ; ↦ 19.5 | | |

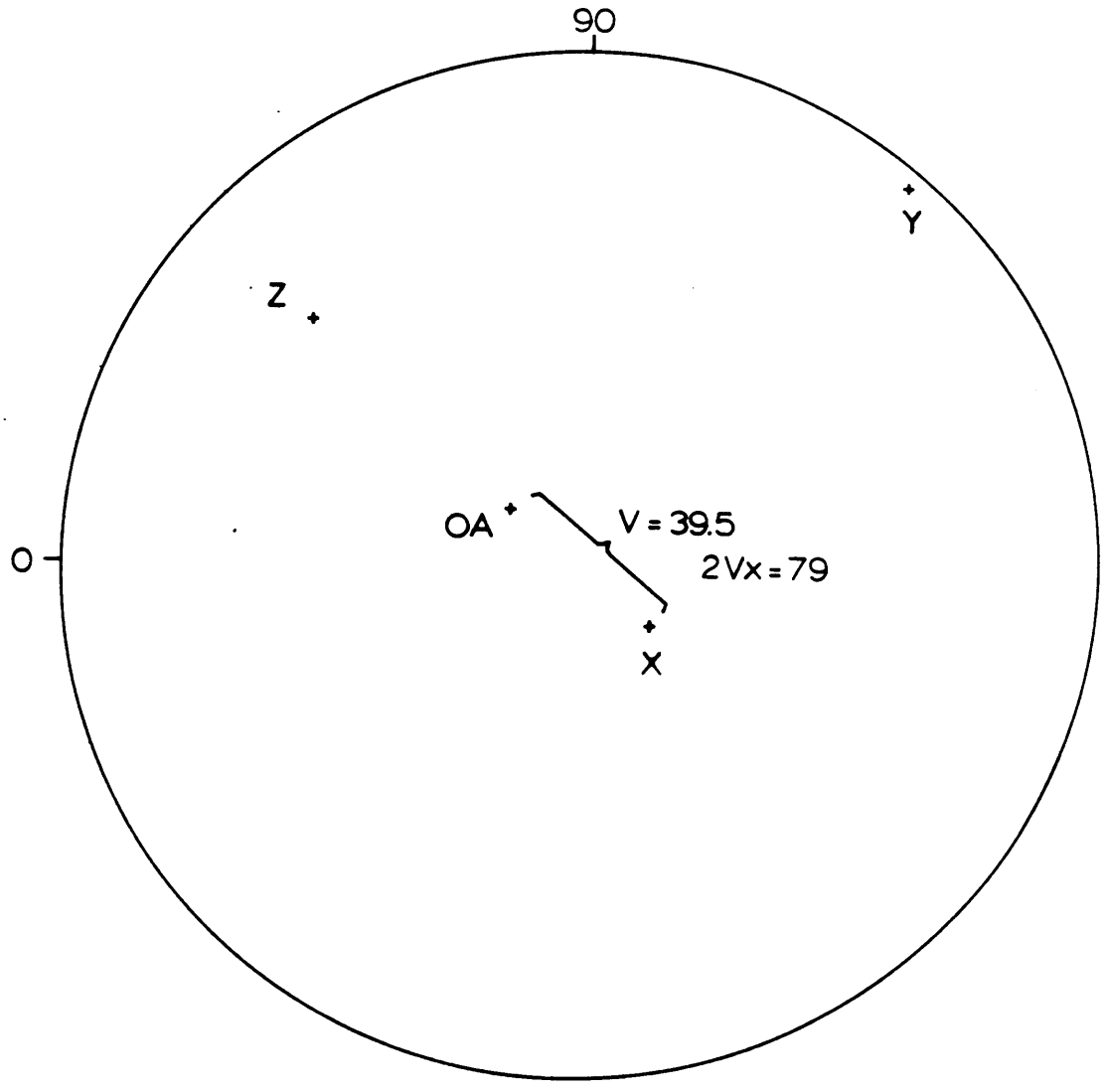

1987 DMC 0211

grain 1

5

| | iv | arc | oad |
|---|---|---|---|
| Y | 210 | 57 ← | ↓ 25 |
| Z | 299 | → 10.7 | |

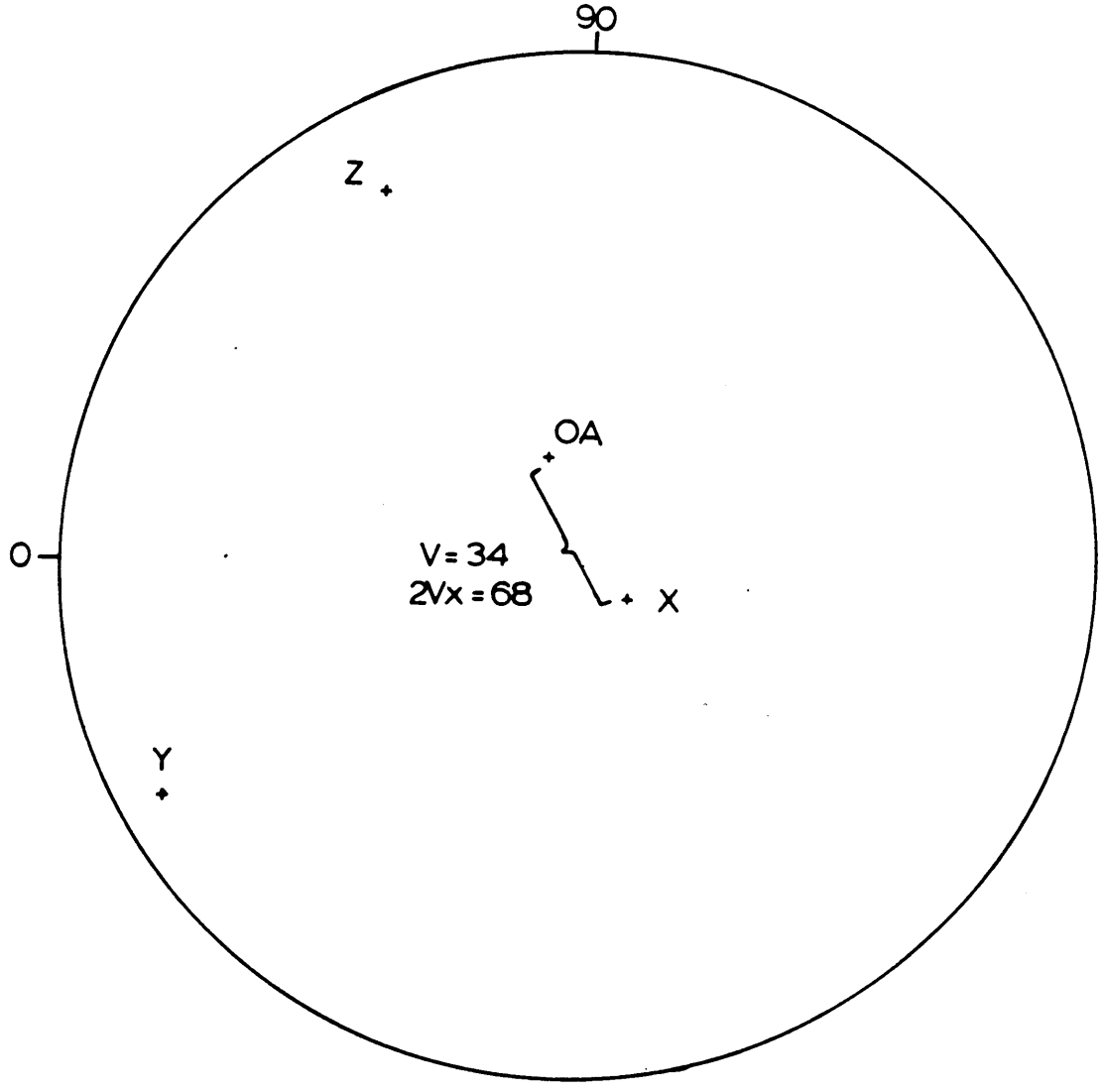

1987 DMC 0211 6

grain 2

| iv | arc | oad |
|---|---|---|

Y=232.5, 63 ↤ ; ↧ 24.5 and ↥ 50.5

Z=322 ; ↦ 12

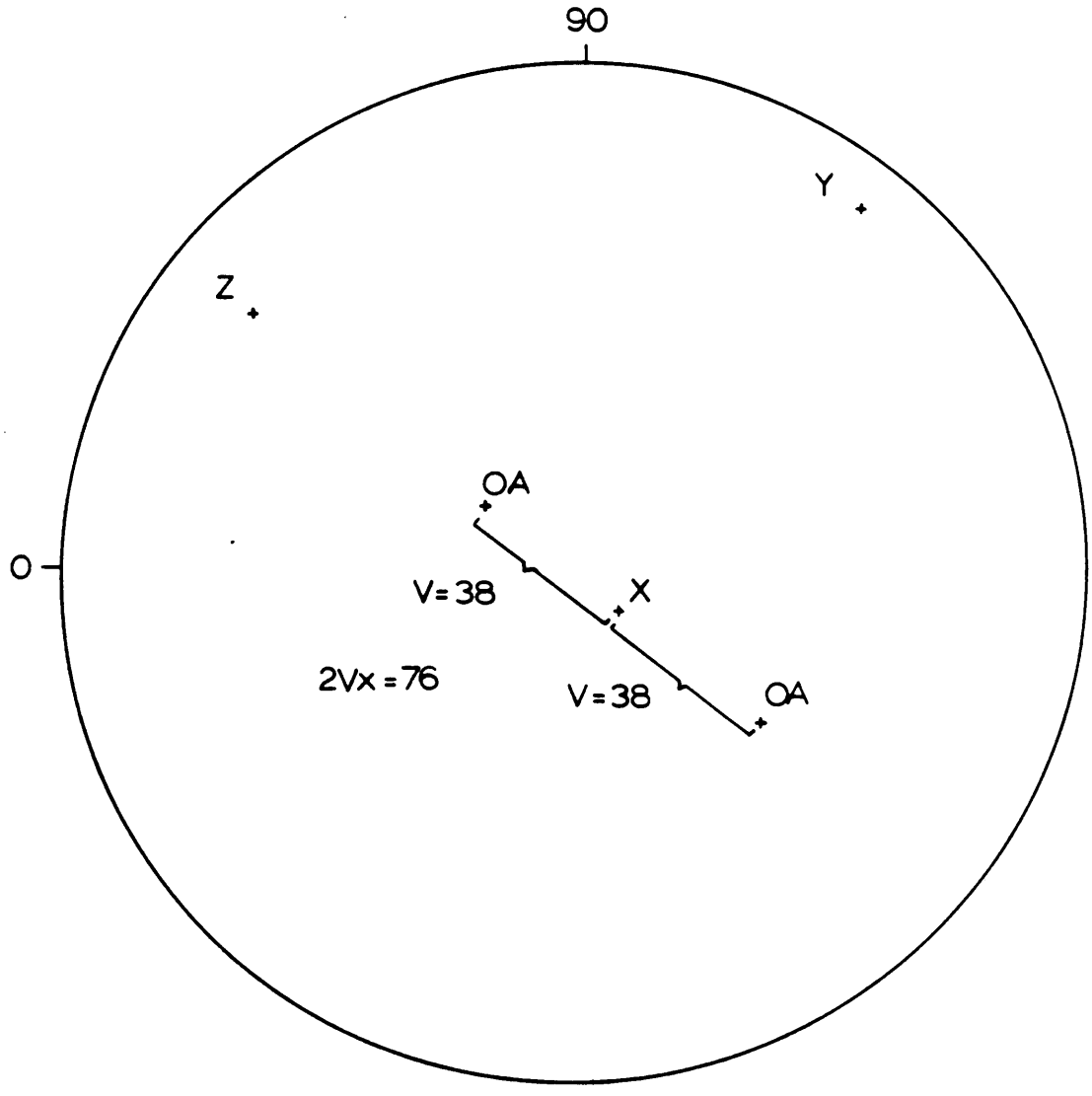

1987 DMC 0213

grain 1

7

IV arc oad

Y = 139.7 ; ⇢ 25.5 ; ↓ 30.5 and ↑ 48.5

Z = 054 ; 8 ↔

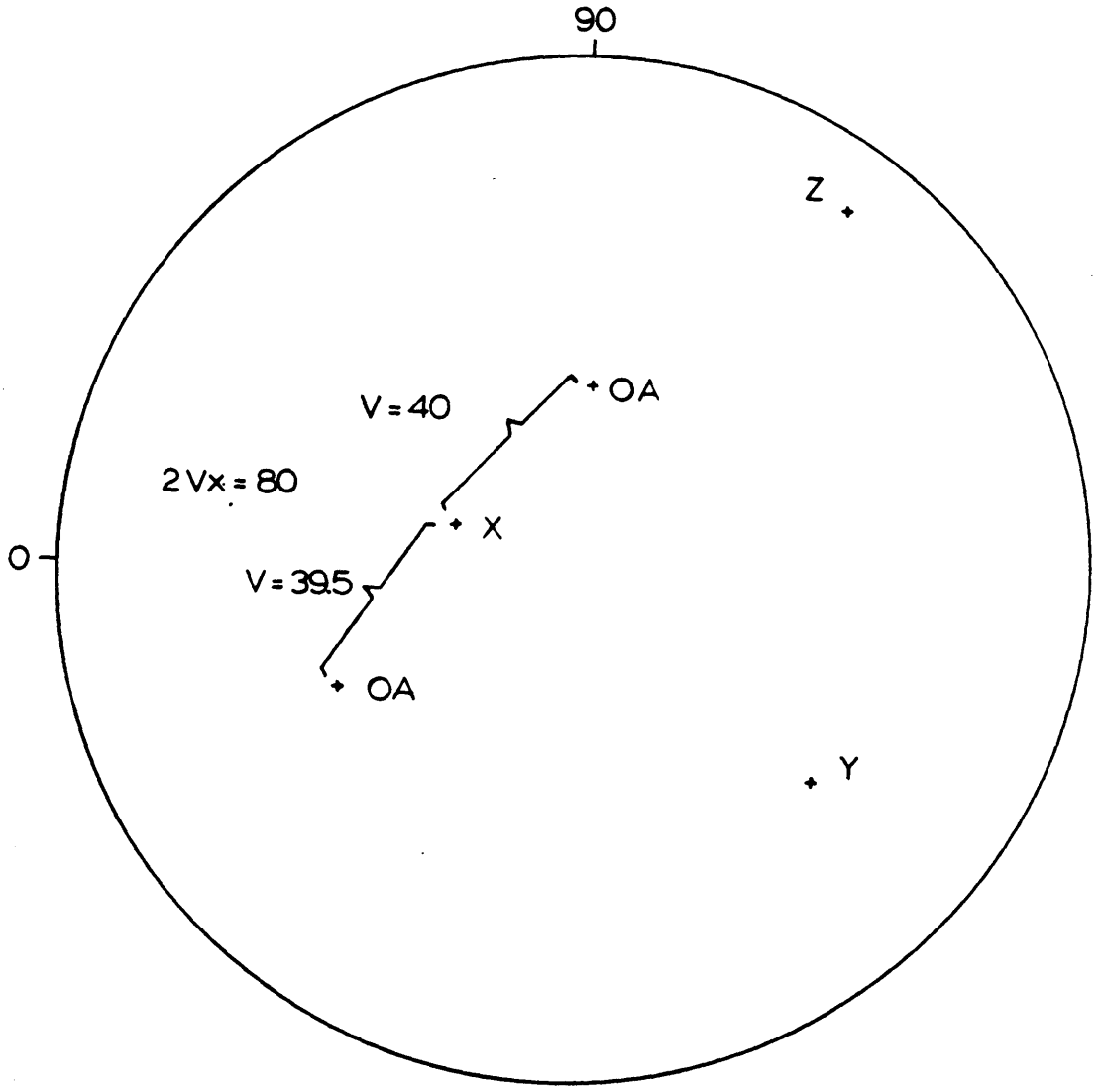

1987 DMC 0213

grain 2

8

| iv | arc | oad |
|---|---|---|

Y = 170 ; ↦ 26.5 ; ↥ 48.5

Z = 084.5 ; 4 ↤

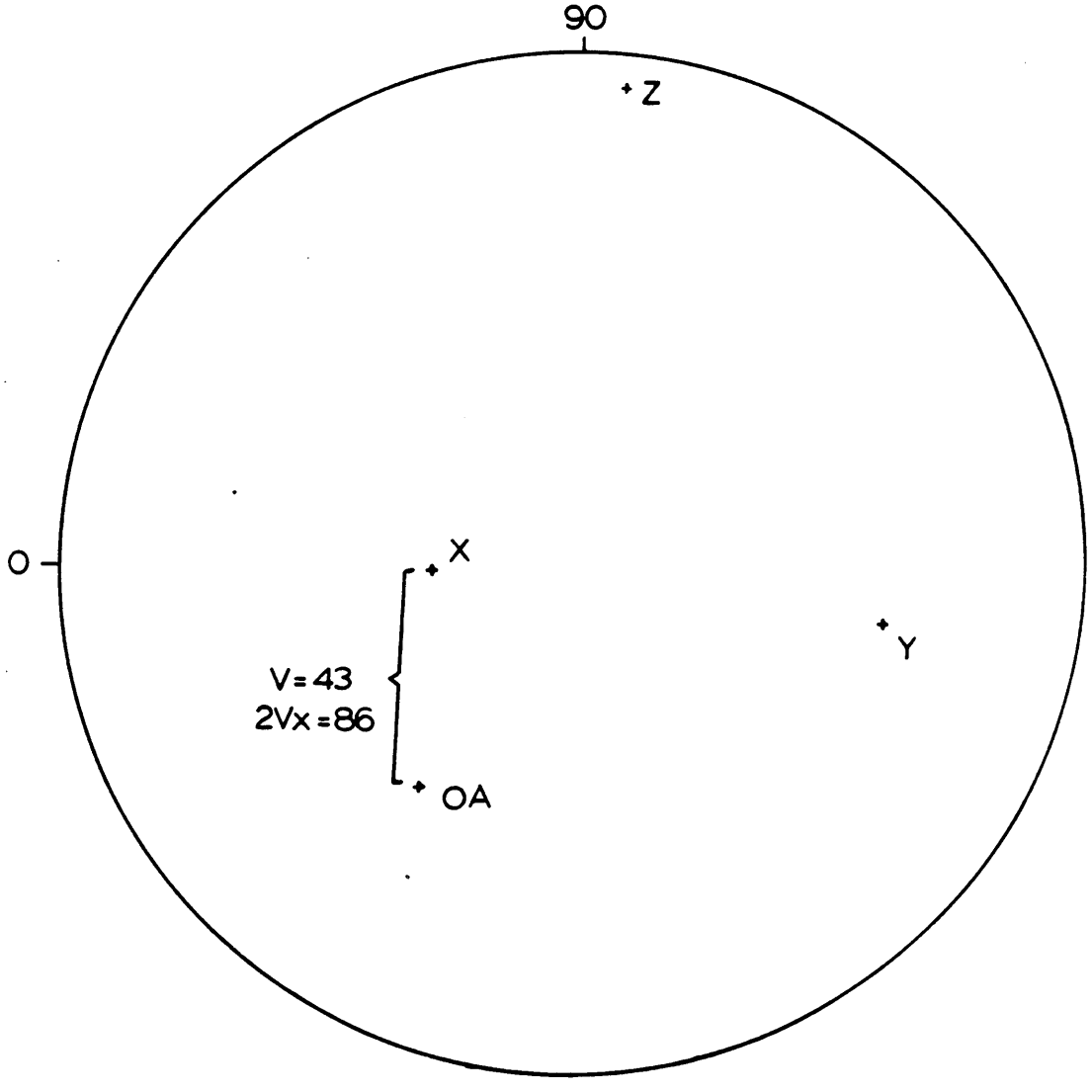

1987 DMC 021 3 9

grain 3

| iv | arc | oad |
|---|---|---|

Y=118.5; ↦ 30.6; ↥ 23.1

X=188 ; 26 ↤

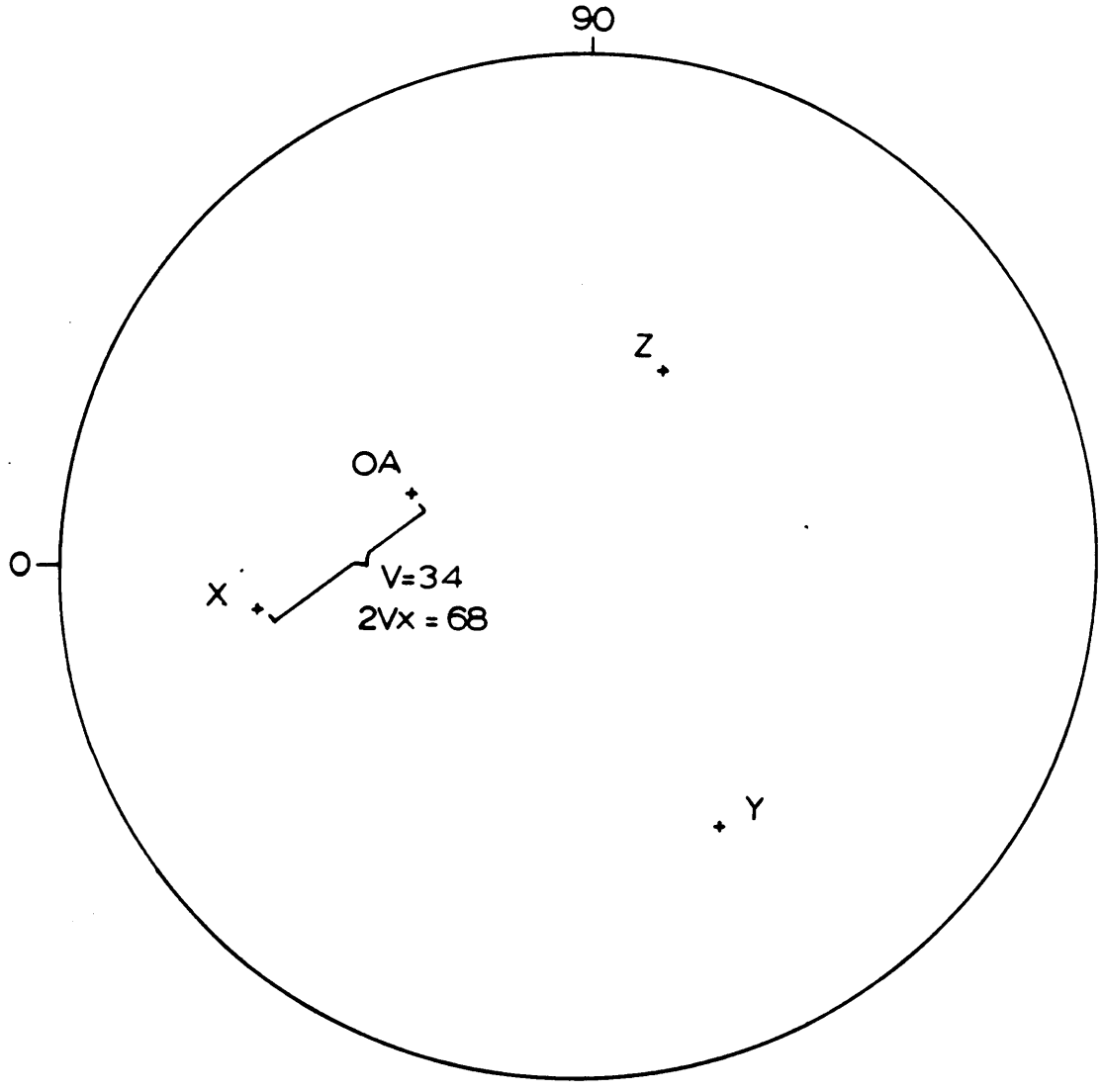

1987 DMC 0213 10

grain 4

| | iv | arc | oad |
|---|---|---|---|
| Y | 322.2 | ↦ 30.5 | ↥ 26.7 |
| X | 213 | ↦ 29.5 | |

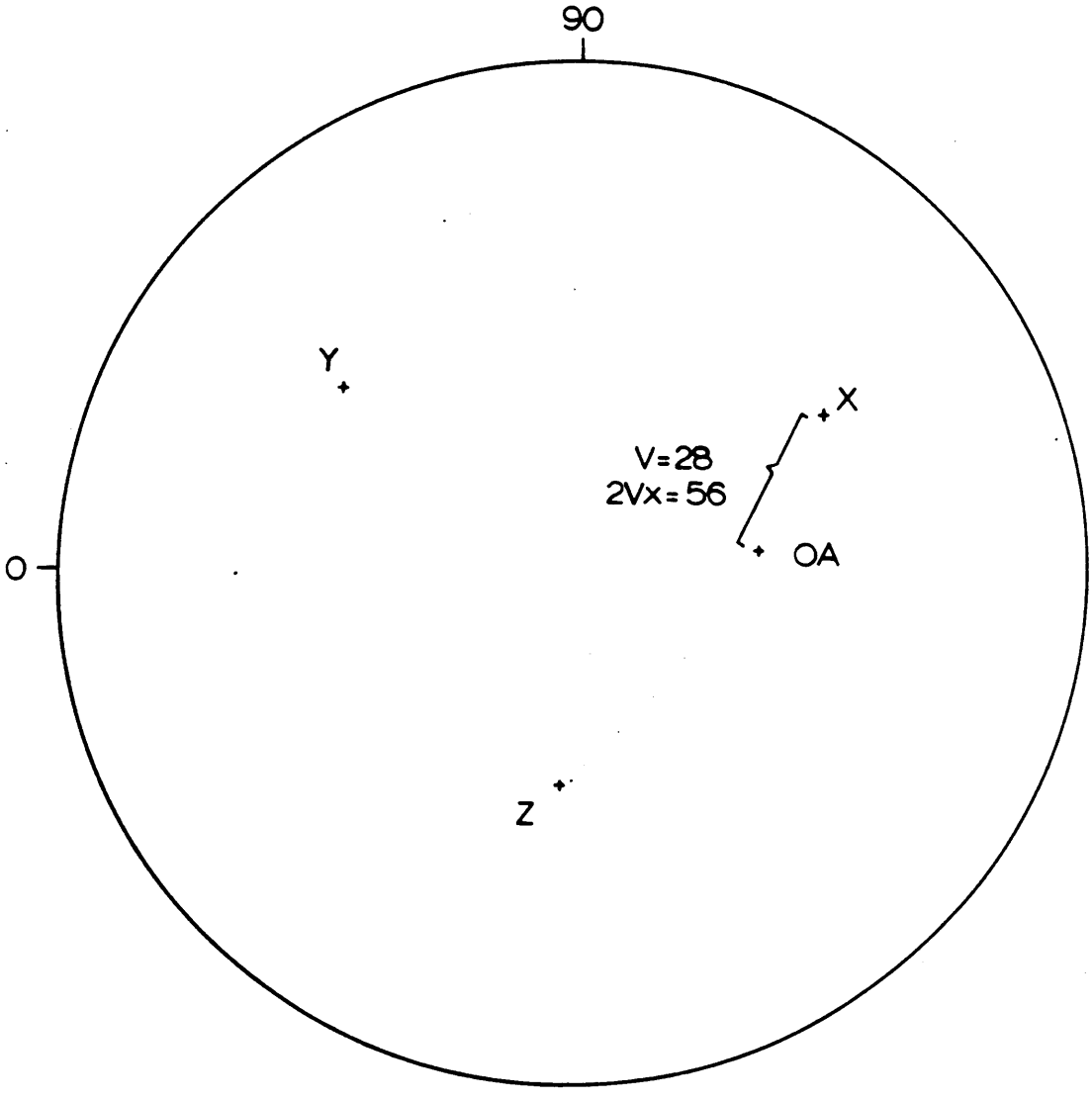

1987 DMC 0242

11

grain 1

iv arc oad

Y= 059.5 ; ⇻ 1.5 ; ↥35 core , ↥44 rim

X= 148.5 ; 21 ↜

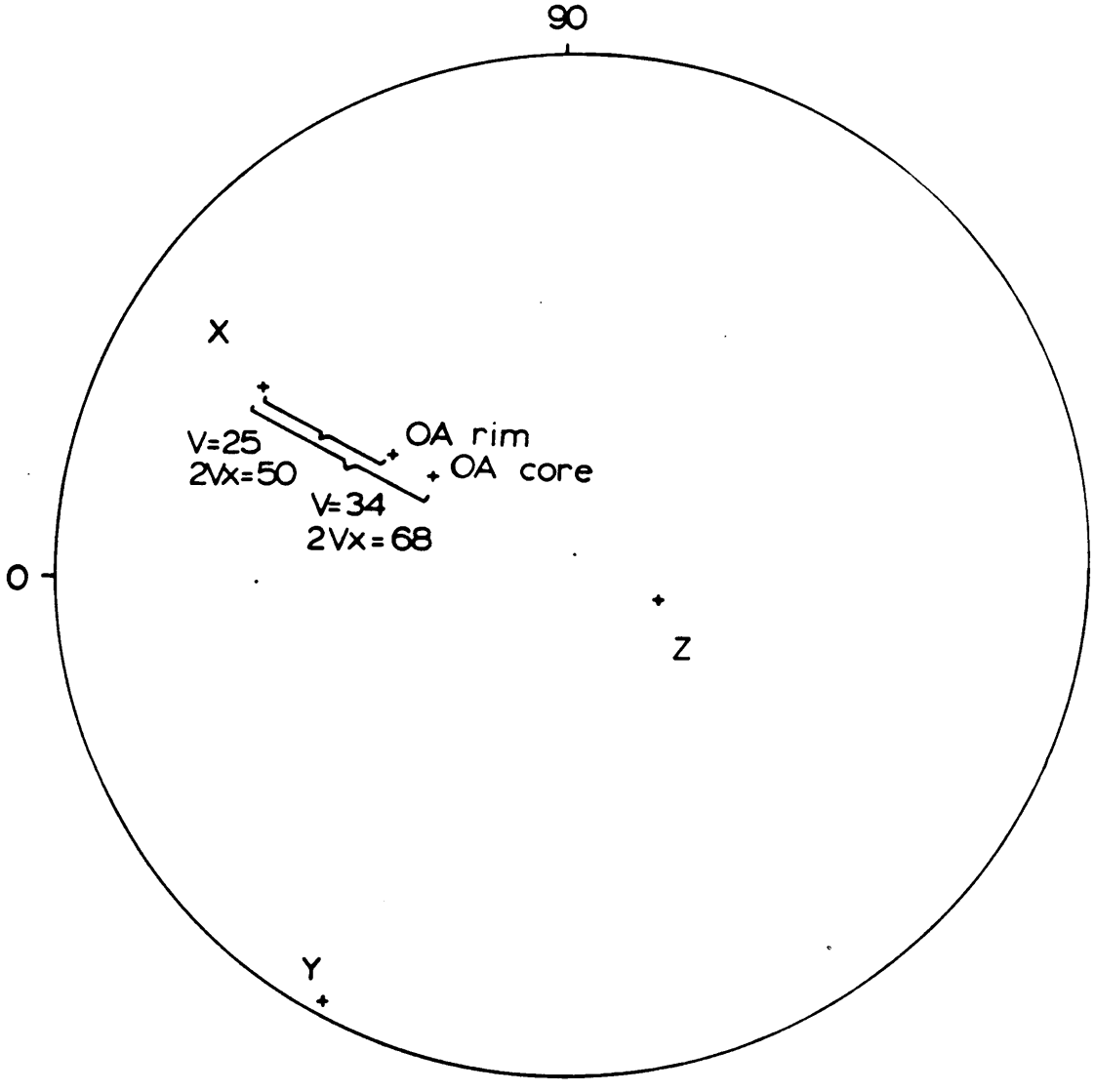

1987 DMC 0242

grain 2

12

| | iv | arc | oad |
|---|---|---|---|
| Y= | 066.5 | ↦ 17.5 | ⊽ 46 |
| X= | 157.5 | ↦ 35 | |

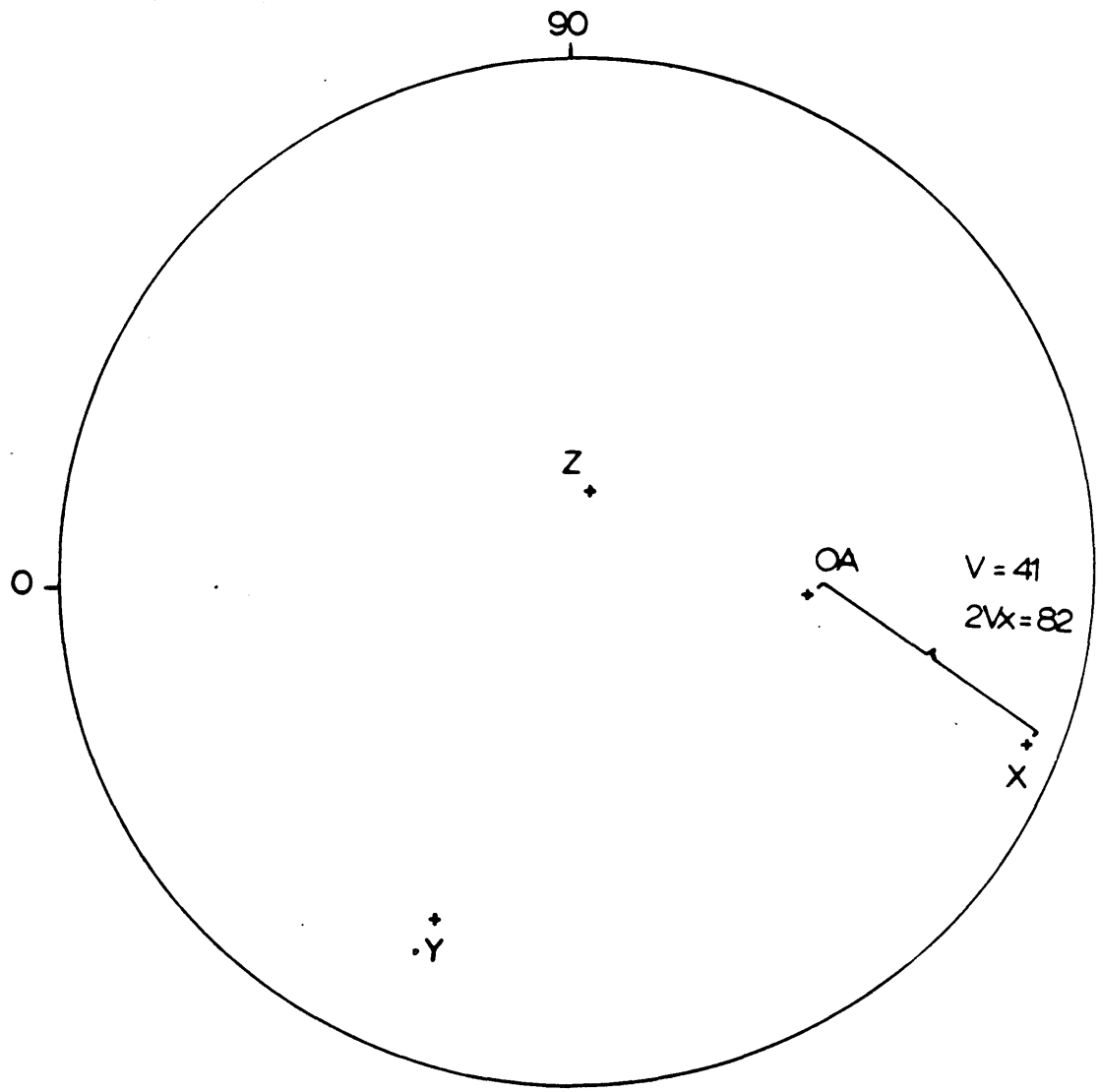

1987 DMC 0241
grain 1

13

| | iv | arc | oad |
|---|---|---|---|
| Y = | 292 ; | 0 ; | ⊤ 32.5 |
| X = | 021.3 ; | ↦10.7 | |

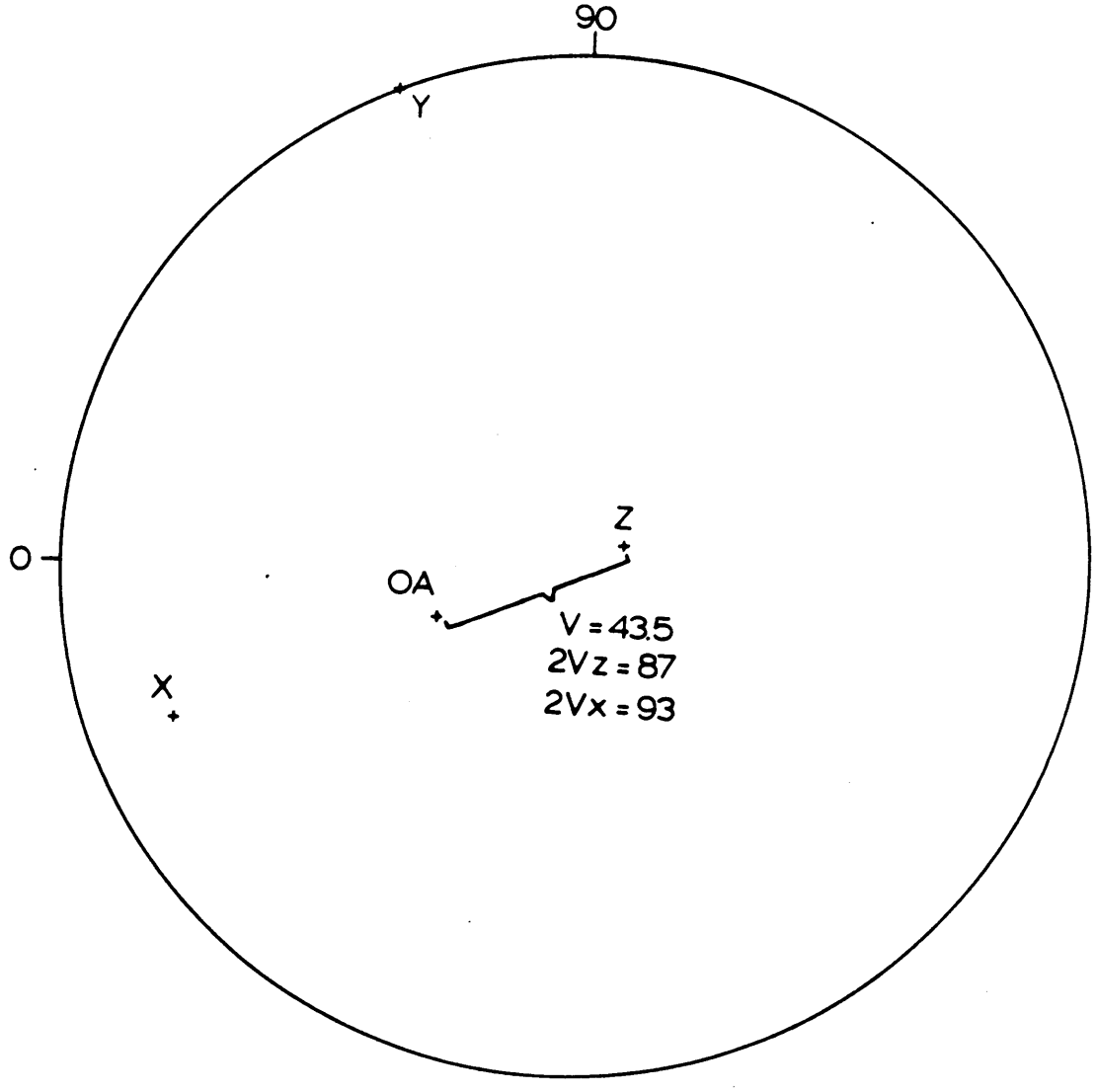

1987 DMC 0239

grain 1

14

| | iv | arc | oad |
|---|---|---|---|
| Y= | 260 | 1.3 ↔ | ↥ 40 |
| X= | 351 | 12 ↔ | |

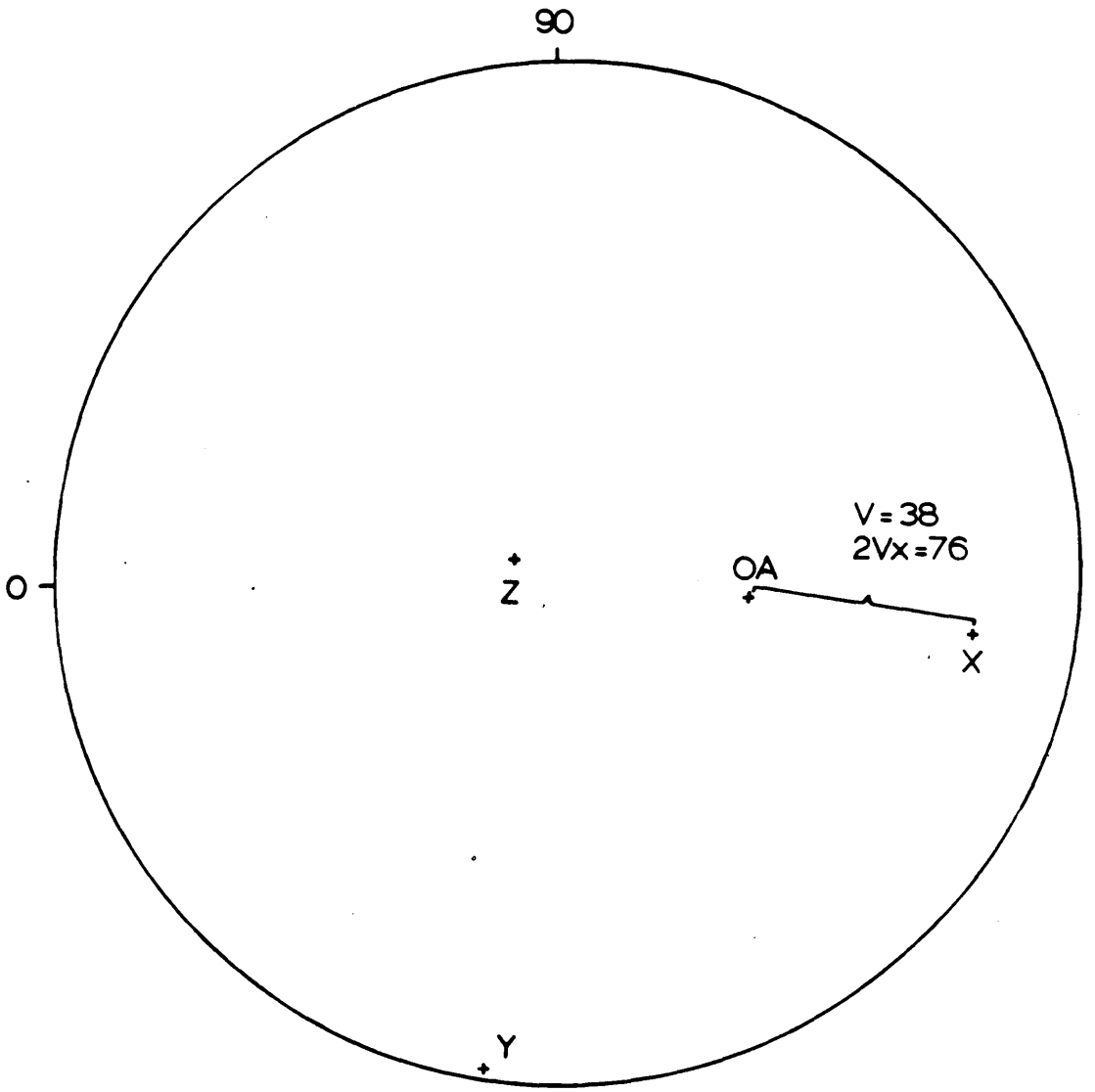

1987 DMC 0238

15

grain 1

| | iv | arc | oad |
|---|---|---|---|
| Y= | 016 ; | (→ 32 ; | ⊥ 31 |
| X= | 086.3 ; | 29 (←) | |

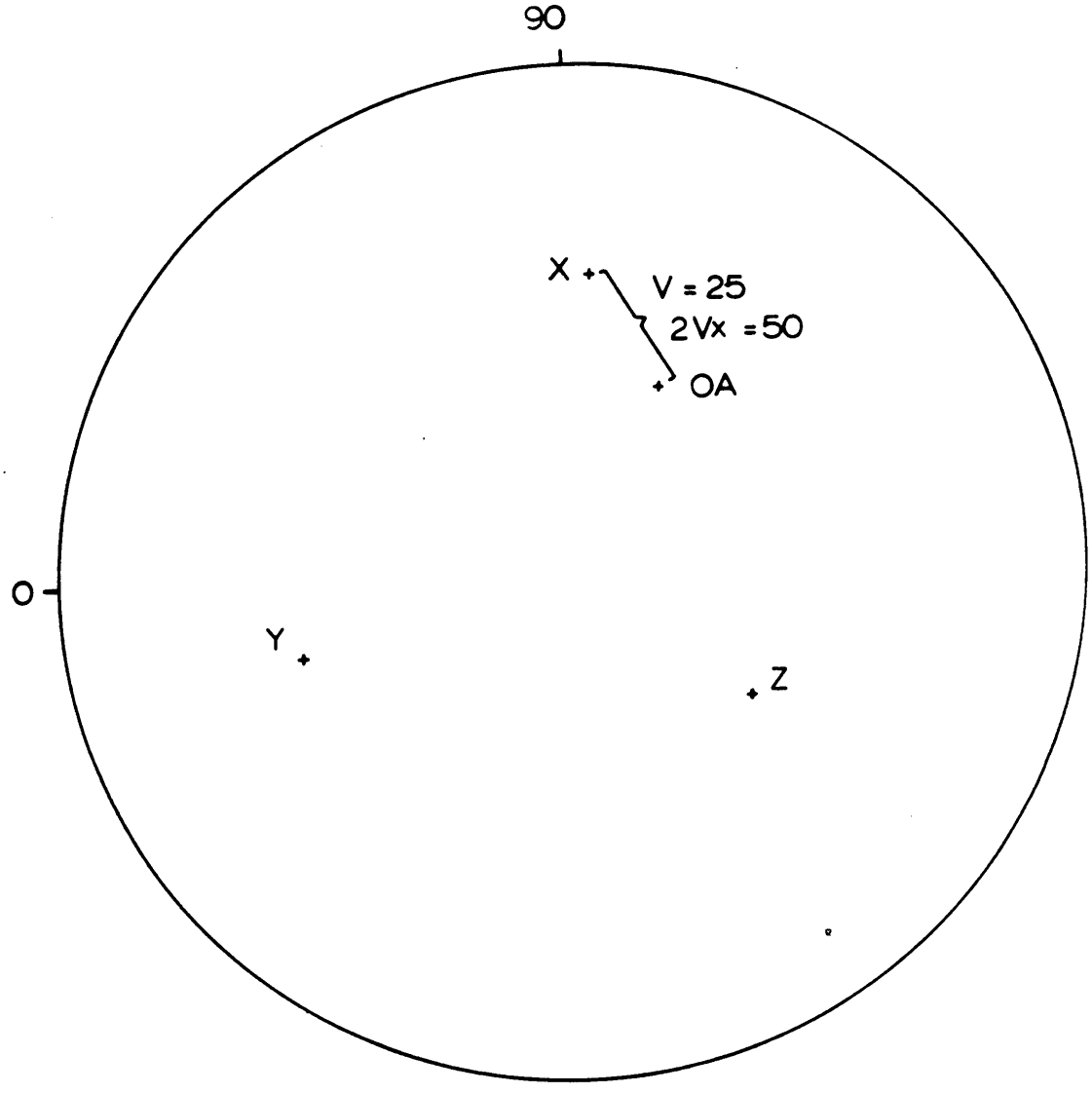

1987 DMC 0238

16

grain 2

| | iv | arc | oad |
|---|---|---|---|
| Y= | 061 ; | ⇢ 24.3 ; | ↥ 28 |
| X= | 136.3 ; | 29 ⇠ | |

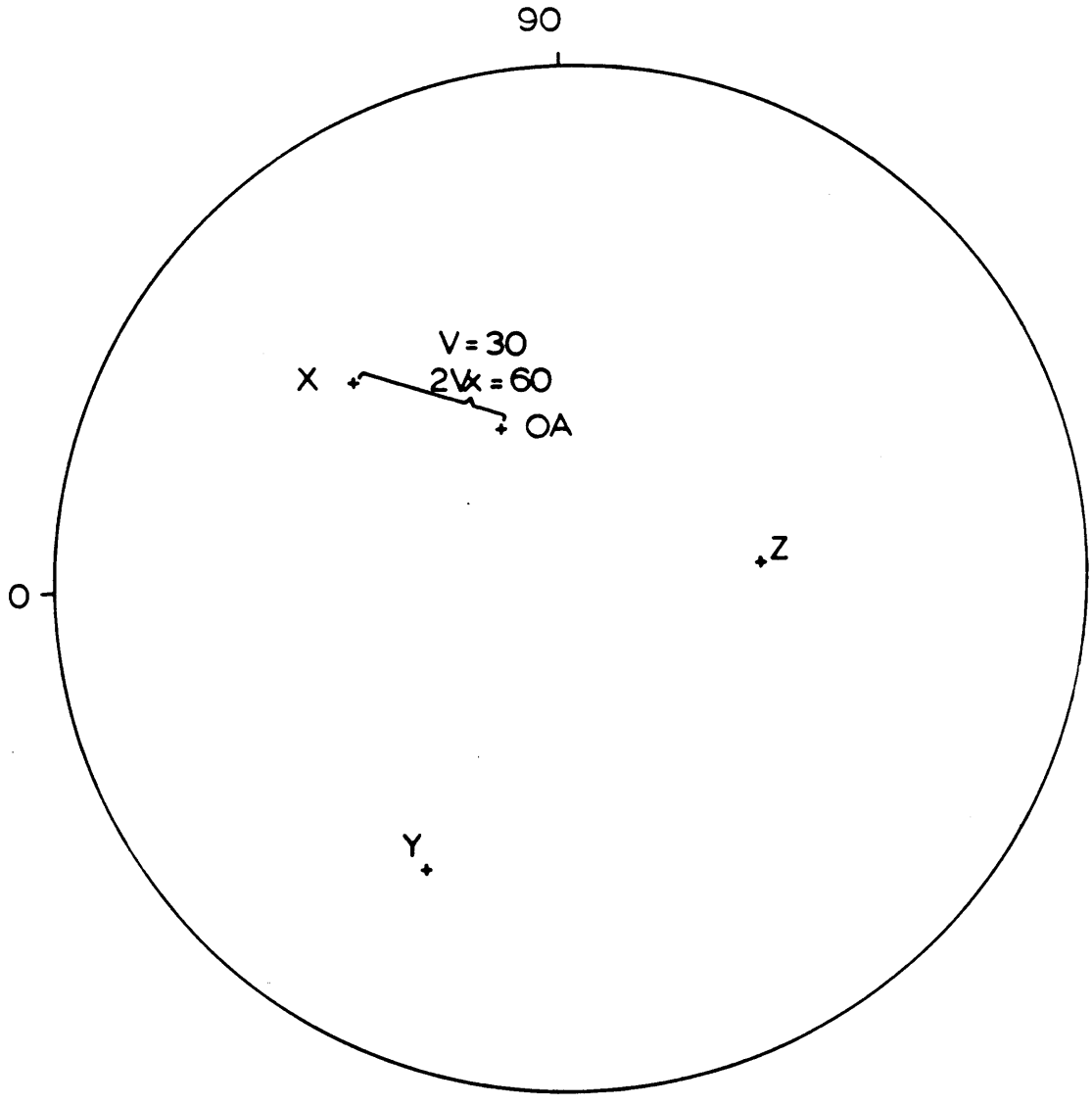

1987 DMC 0237 17

grain 2

| iv | arc | oad |
|---|---|---|

Y = 104 ; ↦ 18.5 ; ↥ 11

183 ; 24 ↤

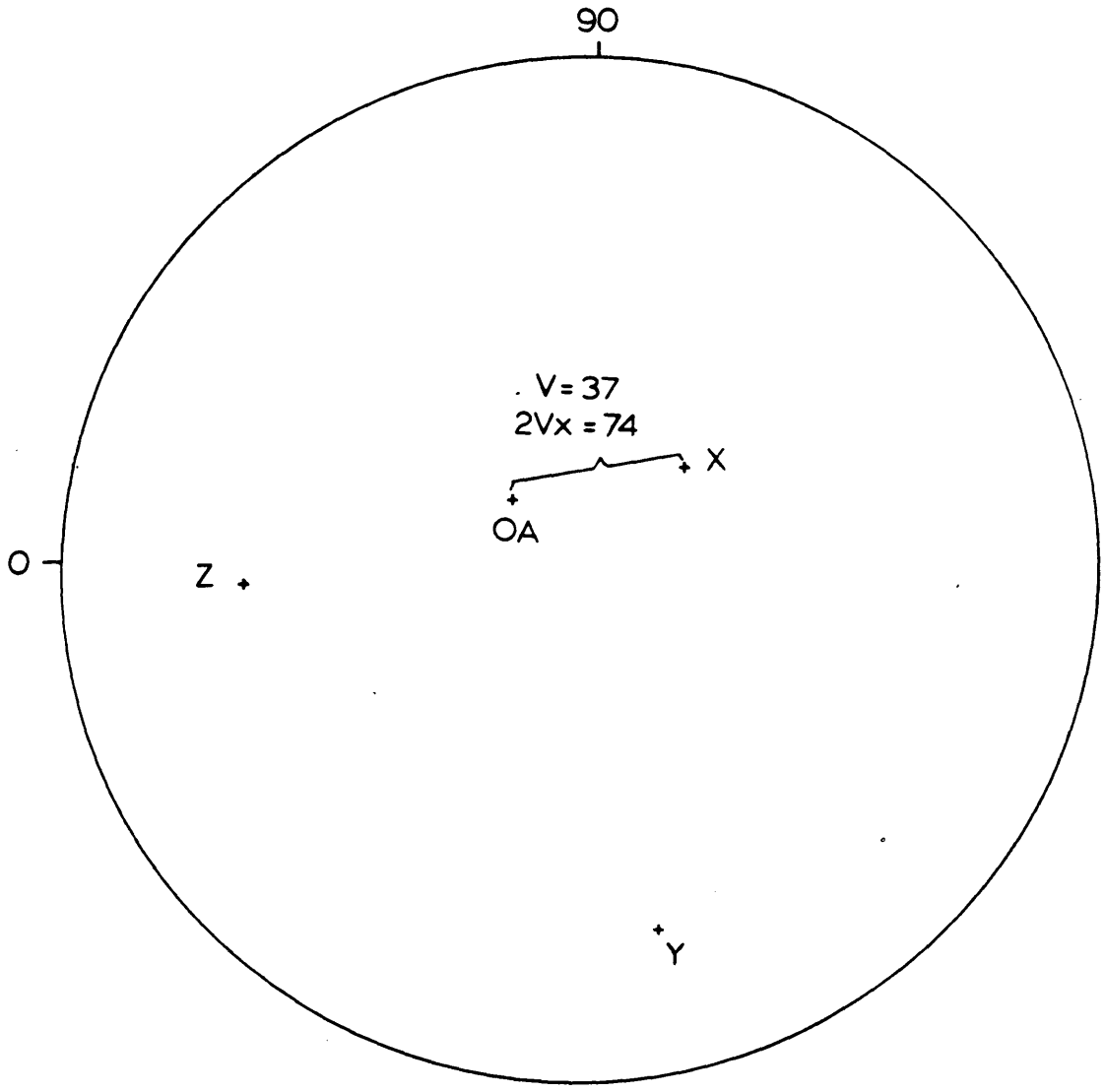

1987 DMC 0237 **18**

grain 3

| | iv | arc | oad |
|---|---|---|---|
| Y = | 297.5 ; | ↦ 44.5 ; | ↥ 26 |
| Z = | 188 ; | ↦ 18.2 | |

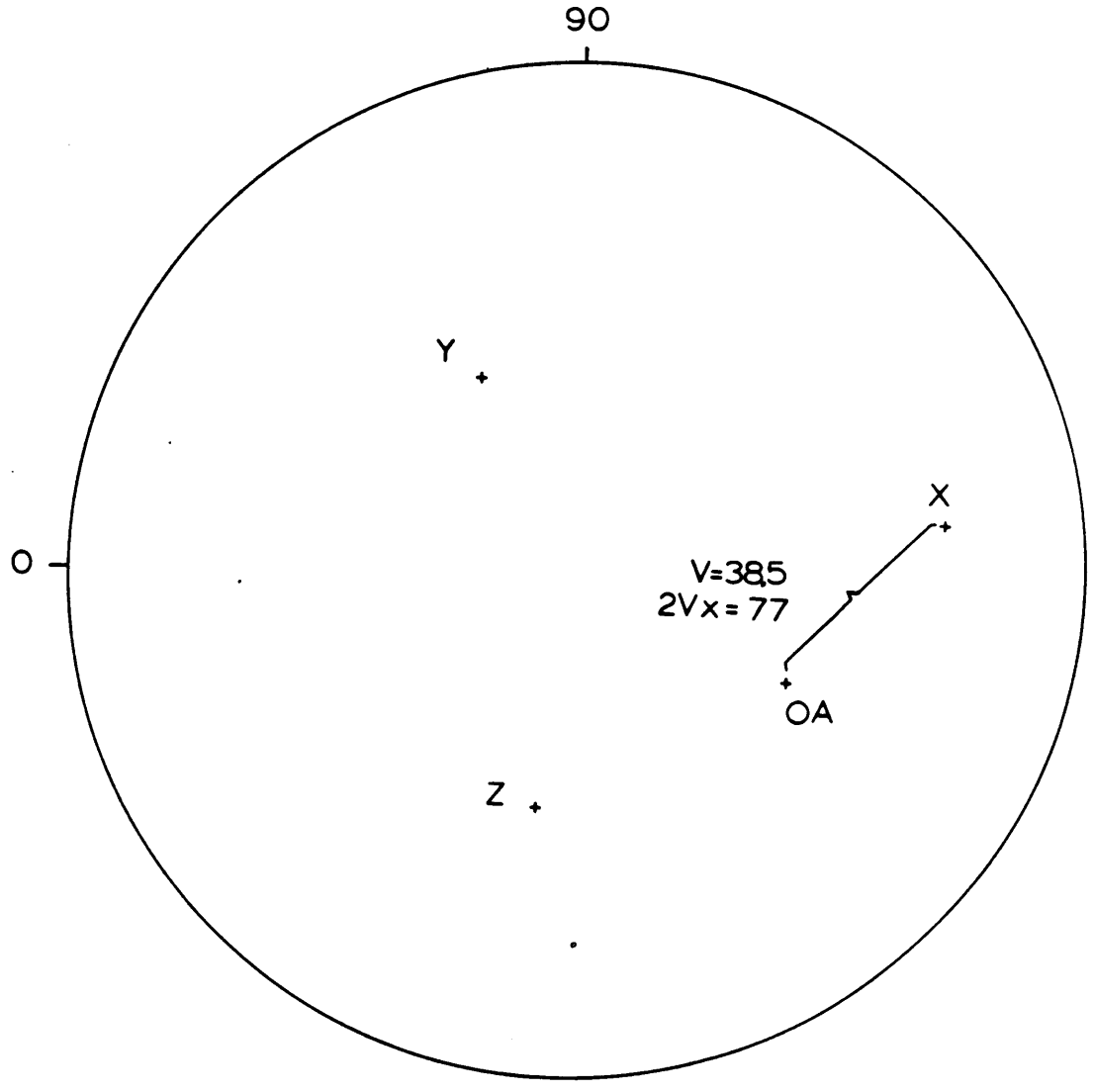

1987 DMC 0237

grain 4

19

| iv | arc | oad |
|---|---|---|
| Y = 099 ; | 27.2 ↔ ; | ↑ 9 |
| X = 036 ; | ↔ 41 | |

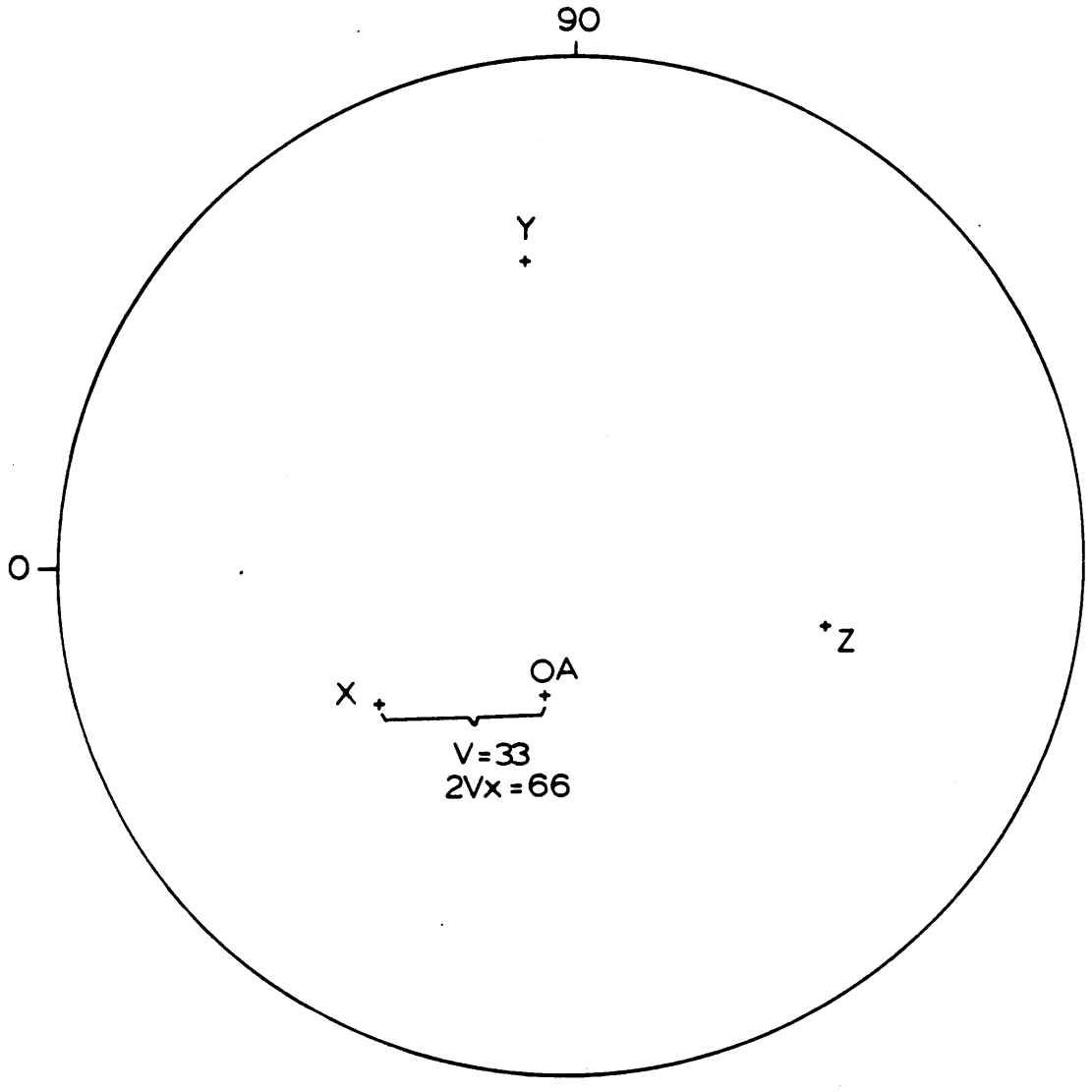

1987 DMC 0236

20

grain 1

| | iv | arc | oad |
|---|---|---|---|
| Y = | 096.5, | 31.5 ↔; | ↥ 6 |
| X = | 216.5 ; | 40.5 ↔ | |

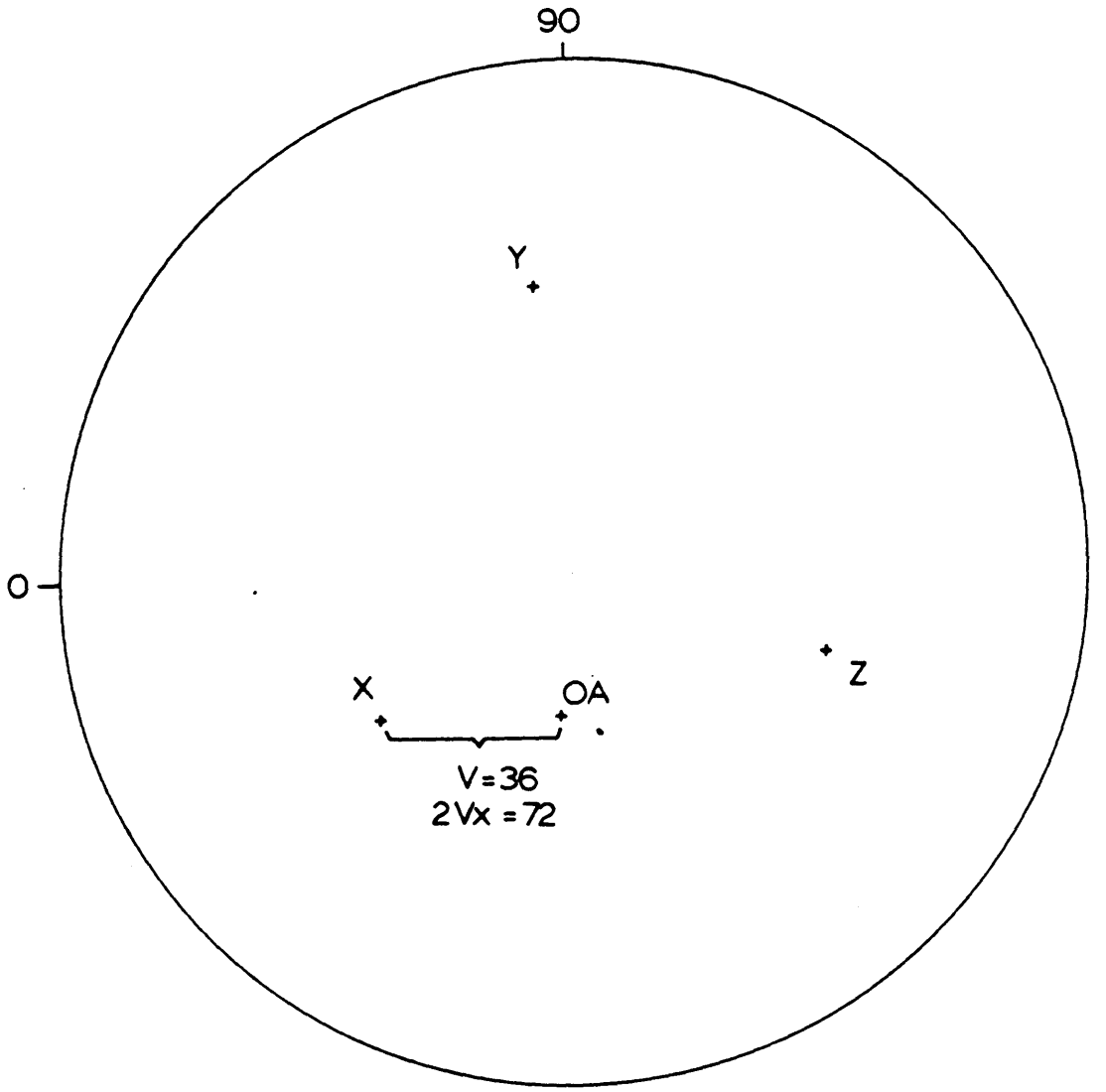

21

1987 DMC 0236

grain 2

iv arc oad

Y = 280 ; 3.5 ↔ ; ↑ 3.5 core , ↓ 11.5 rim

Z = 006 ; ↔ 38.5

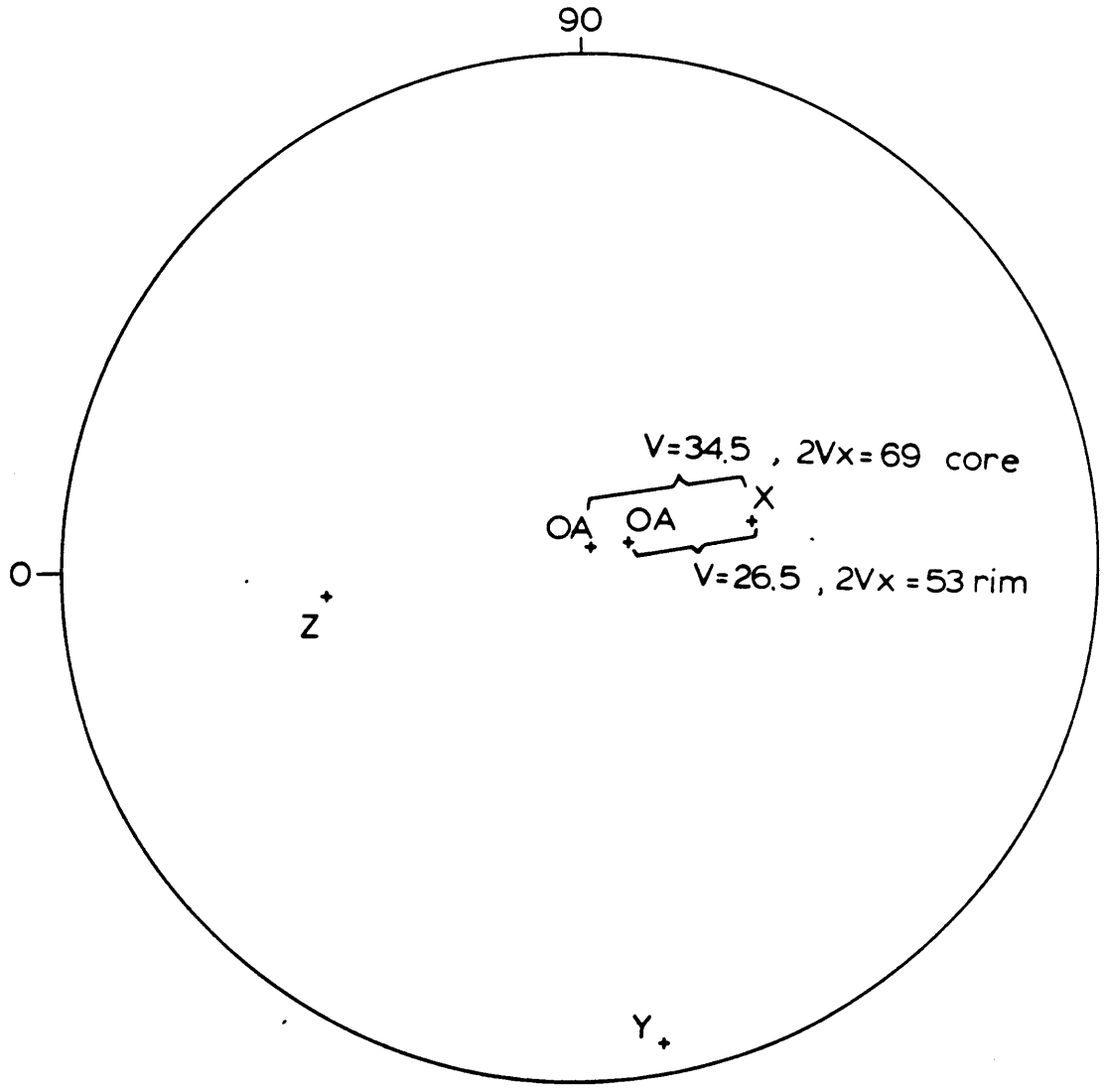

1987 DMC 0235

22

grain 1

| | iv | arc | oad |
|---|---|---|---|
| Y | 154.5 | 2 ↔ | ▽ 28.5 |
| X | 063 | 28 ↔ | |

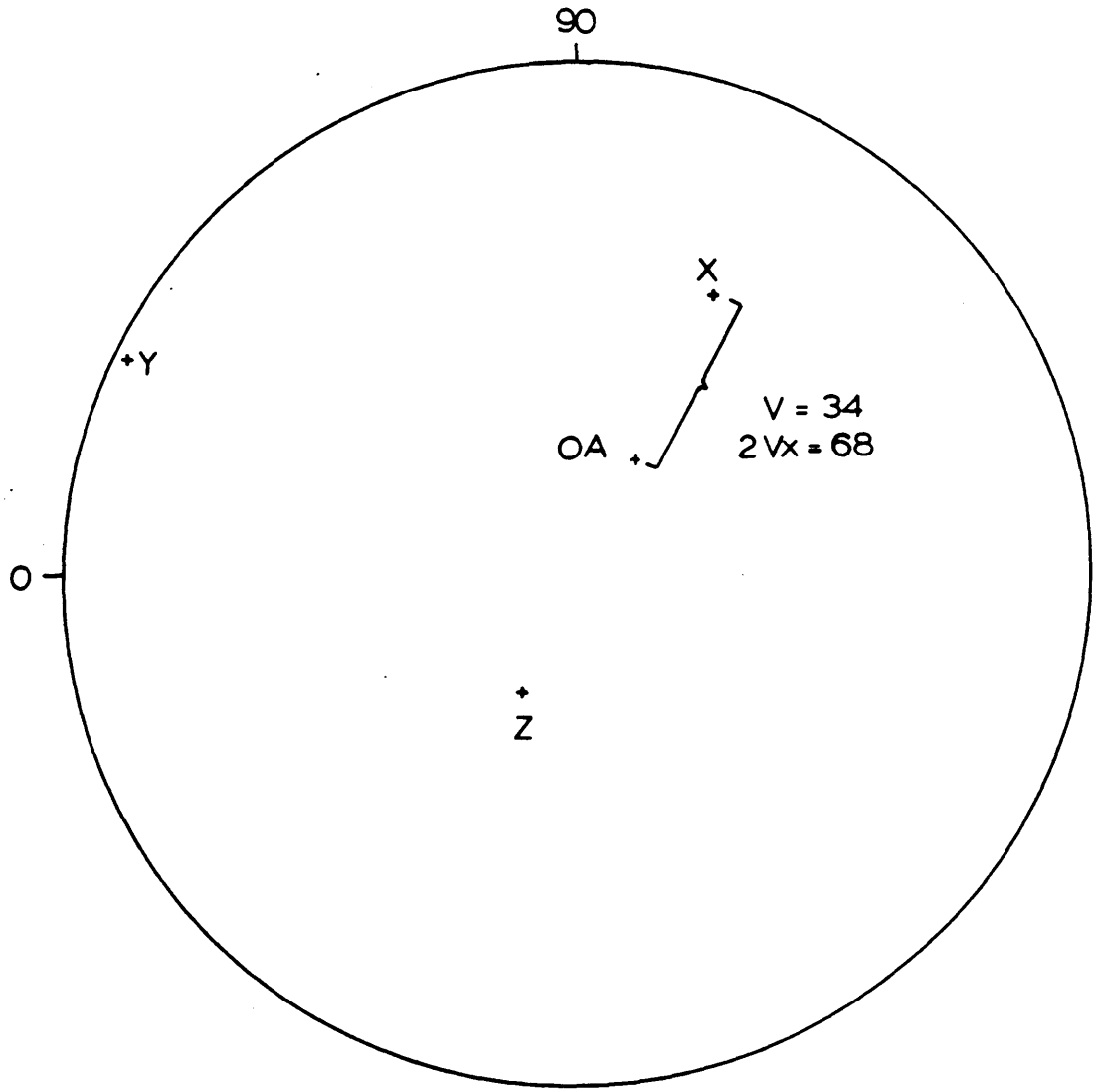

1987 DMC 0235

23

grain 2

| IV | arc | oad |
|---|---|---|

Y = 349 ; 1 ↔ ; ↓ 7.5 core , ↑ 2 rim

Z = 259.5 , 30 ↔

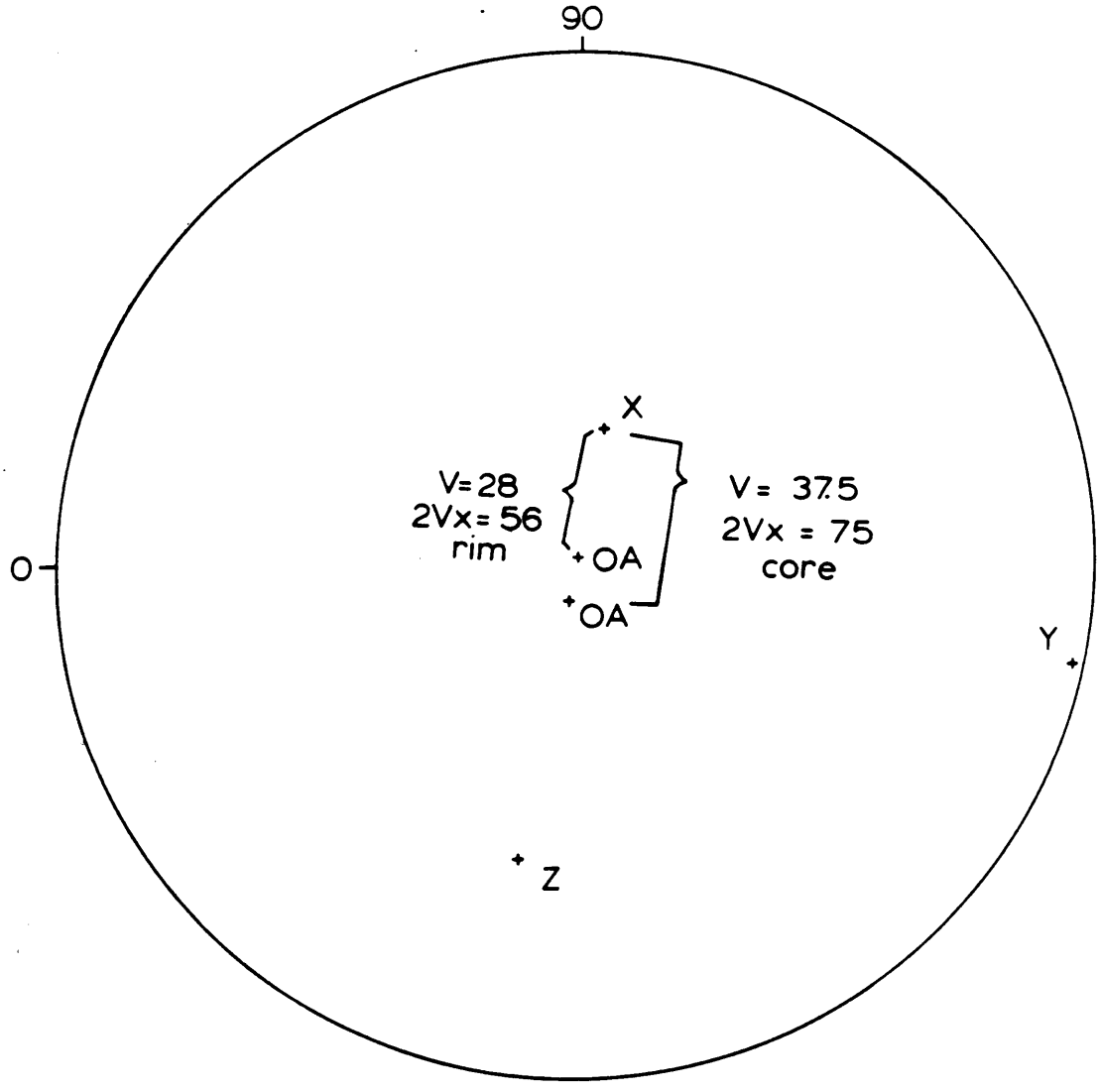

24

1987 DMC 0235

grain 3

| | iv | arc | oad |
|---|---|---|---|
| Y = 172.5, 13 | ↔ , | ↥ 19 | |
| X = 273 ; 36.5 | ↔ | | |

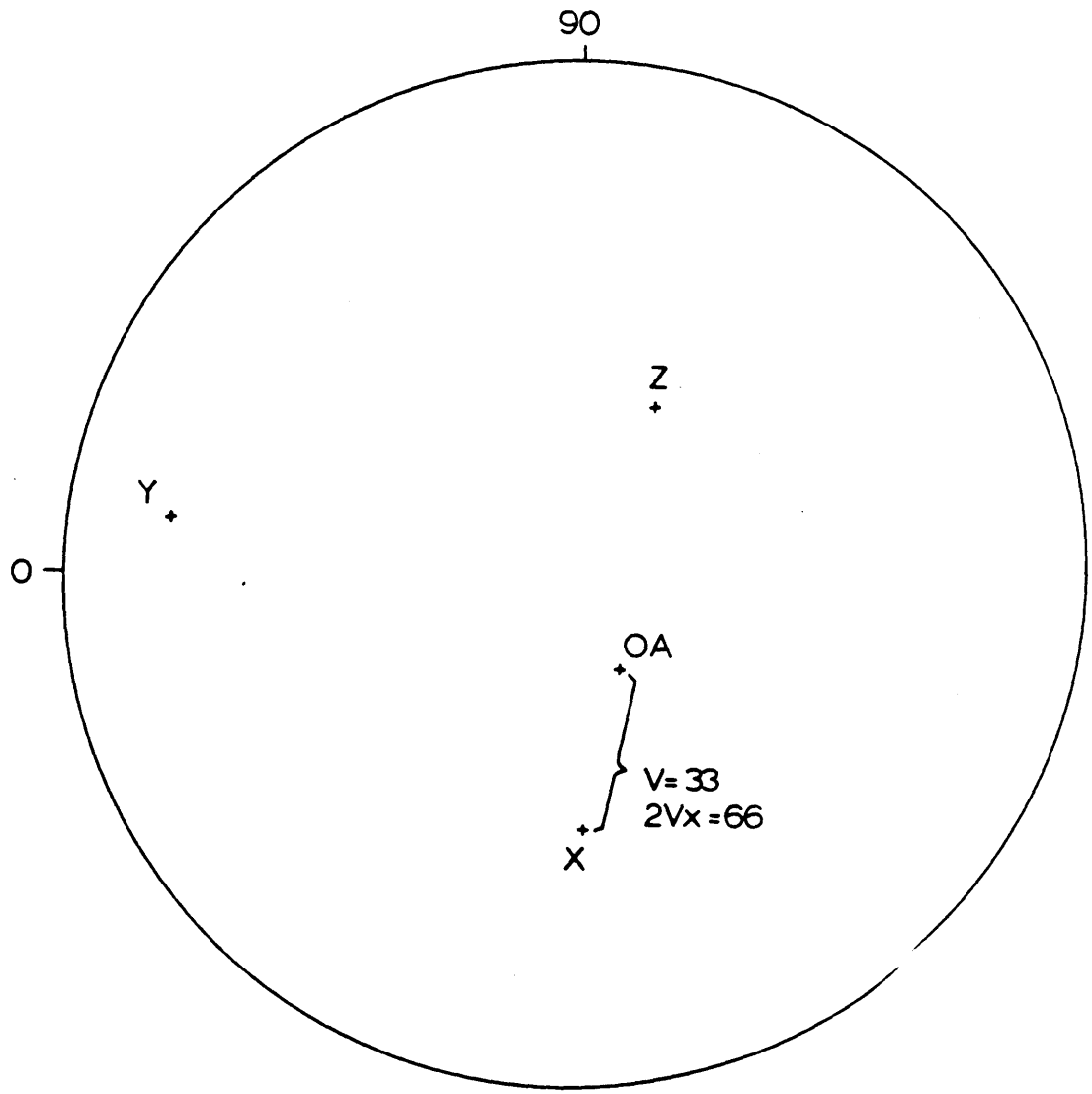

1987 DMC 0233

25

grain 1

| | iv | arc | oad |
|---|---|---|---|
| Y | 021.5 | 22 ↔ | ↥ 34 |
| Z | 292 | 2.2 ↔ | |

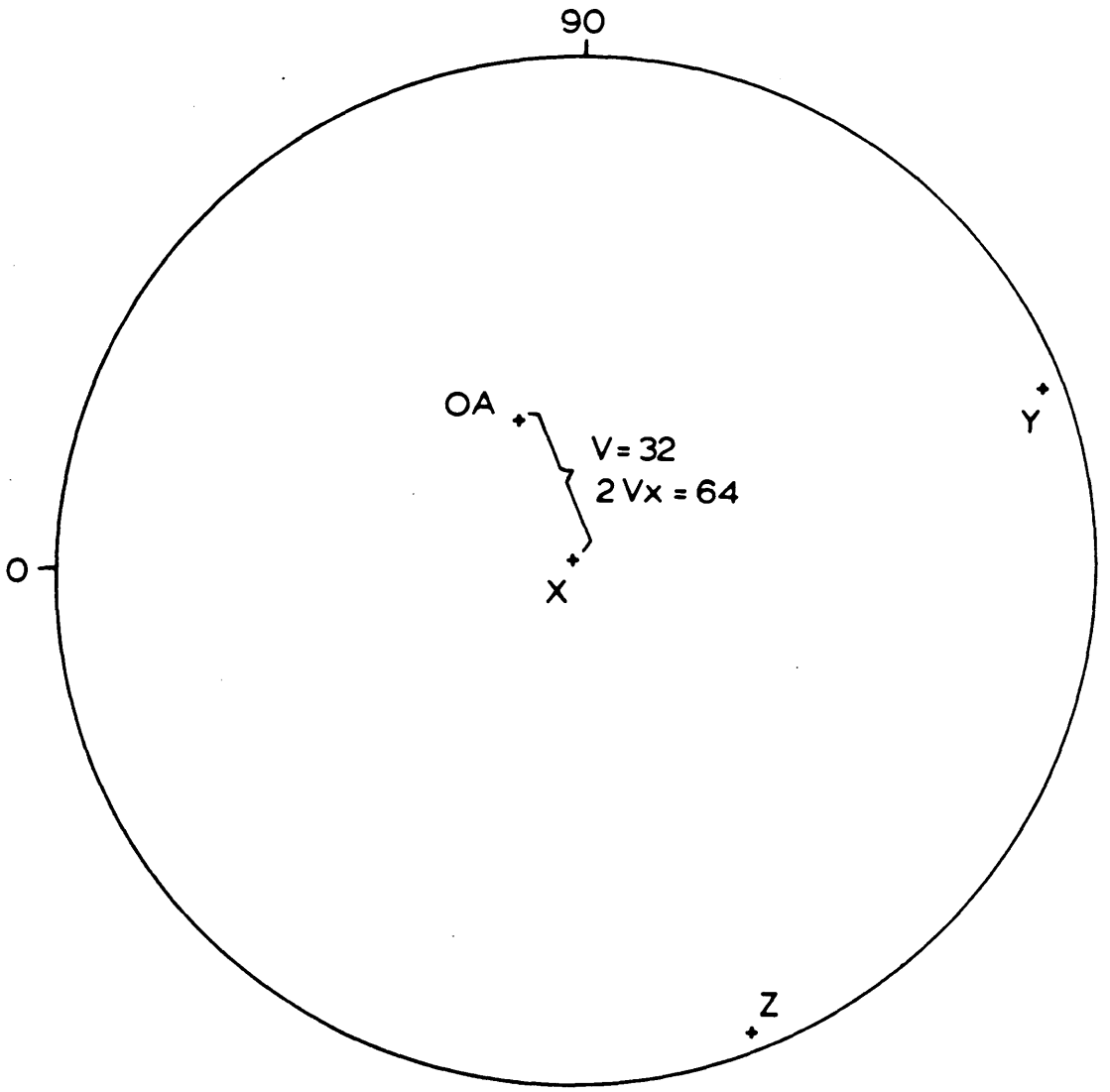

1987 DMC 0233

grain 2

26

| | iv | arc | oad |
|---|---|---|---|
| Y = | 283.5, | ↦ 22.5; | ↥ 2.5 |
| Z = | 025.5; | ↦ 28.5 | |

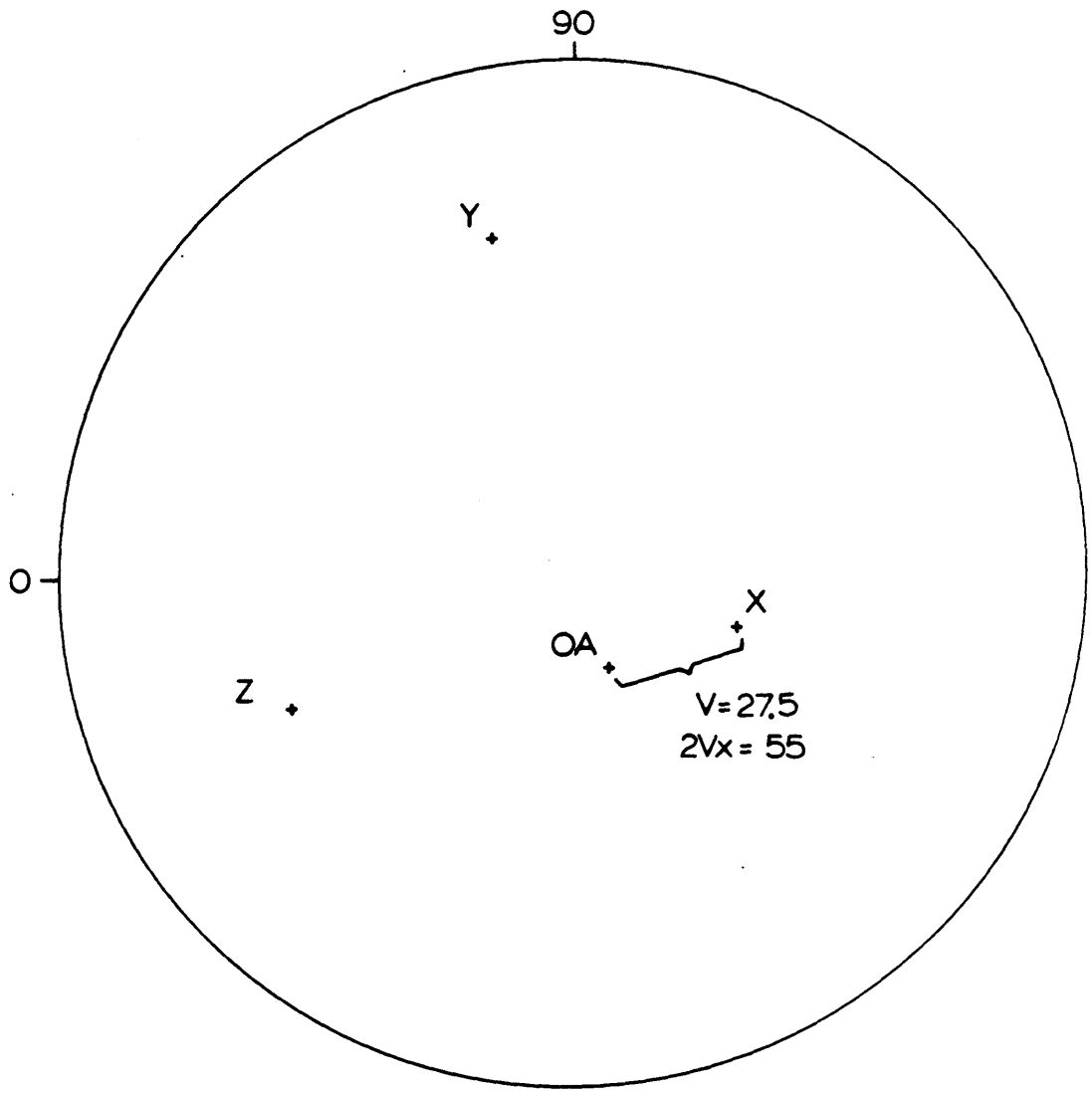

1987 DMC 0233

grain 3

27

| | iv | arc | oad |
|---|---|---|---|
| Y = | 358 ; | 17.5 ↔ ; | ↥ 31.5 |
| Z = | 268.5 ; | 4 ↔ | |

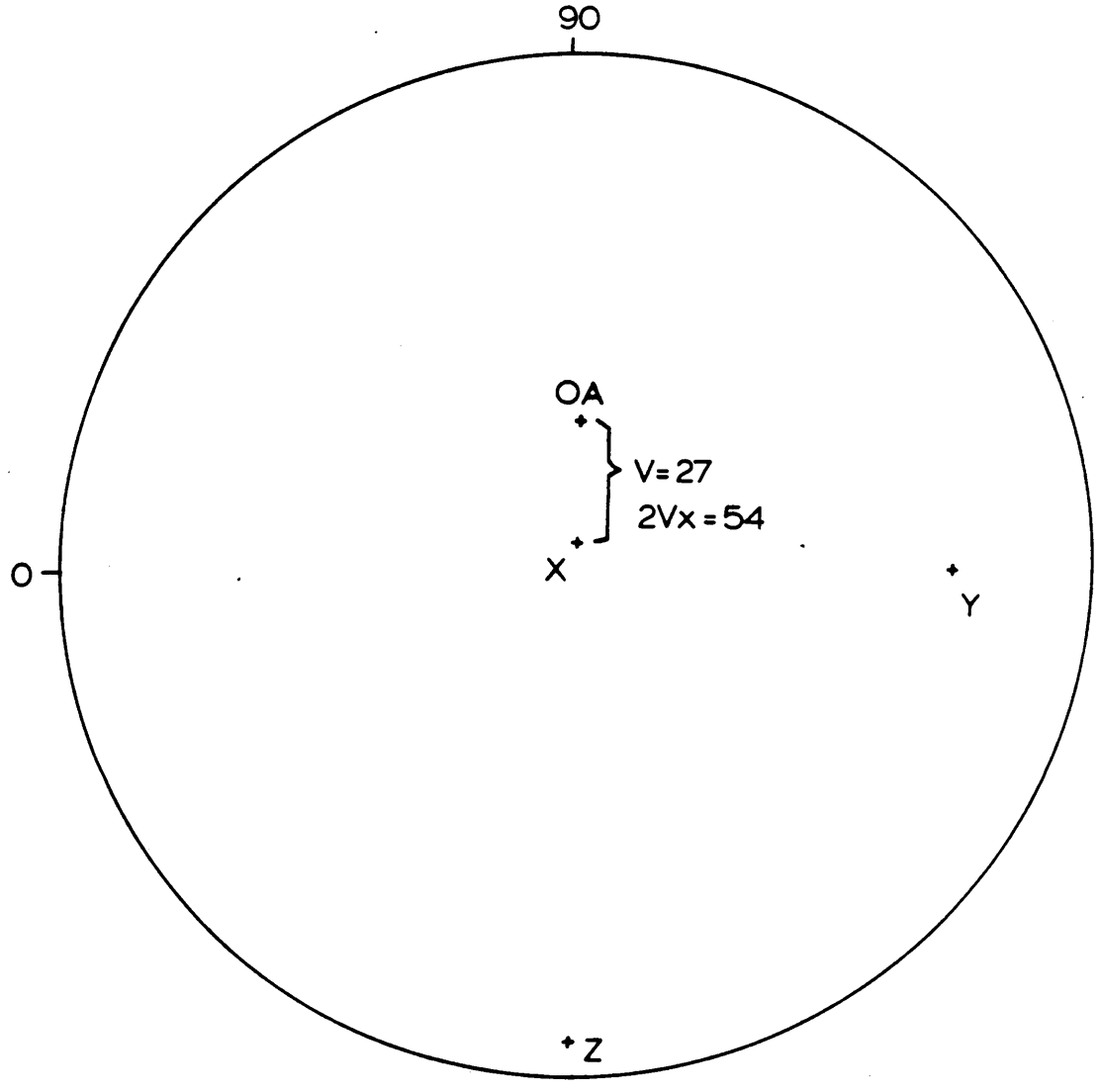

1987 DMC 0232

28

grain 1

| | iv | arc | oad |
|---|---|---|---|
| Y = 276 | ; 39 | ↔ | ; ↥ 2.5 |
| Z = 209.5 | ; ↔ 23 | | |

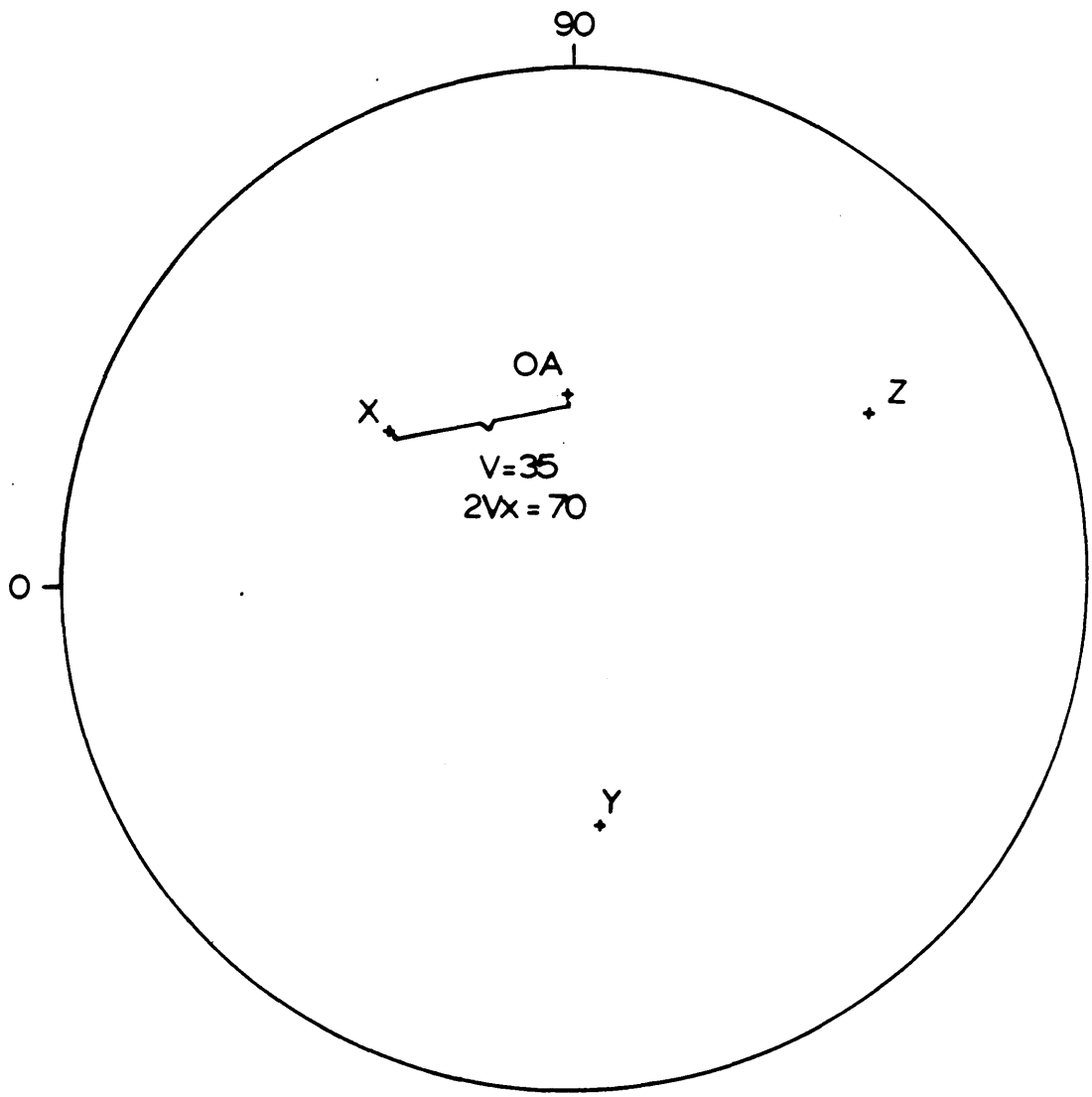

1987 DMC 0232

29

grain 2

| | iv | arc | oad |
|---|---|---|---|
| Y = | 318 ; | ↦ 22 ; | ↥ 30.5 |
| Z = | 227 ; | ↦ 2.5 | |

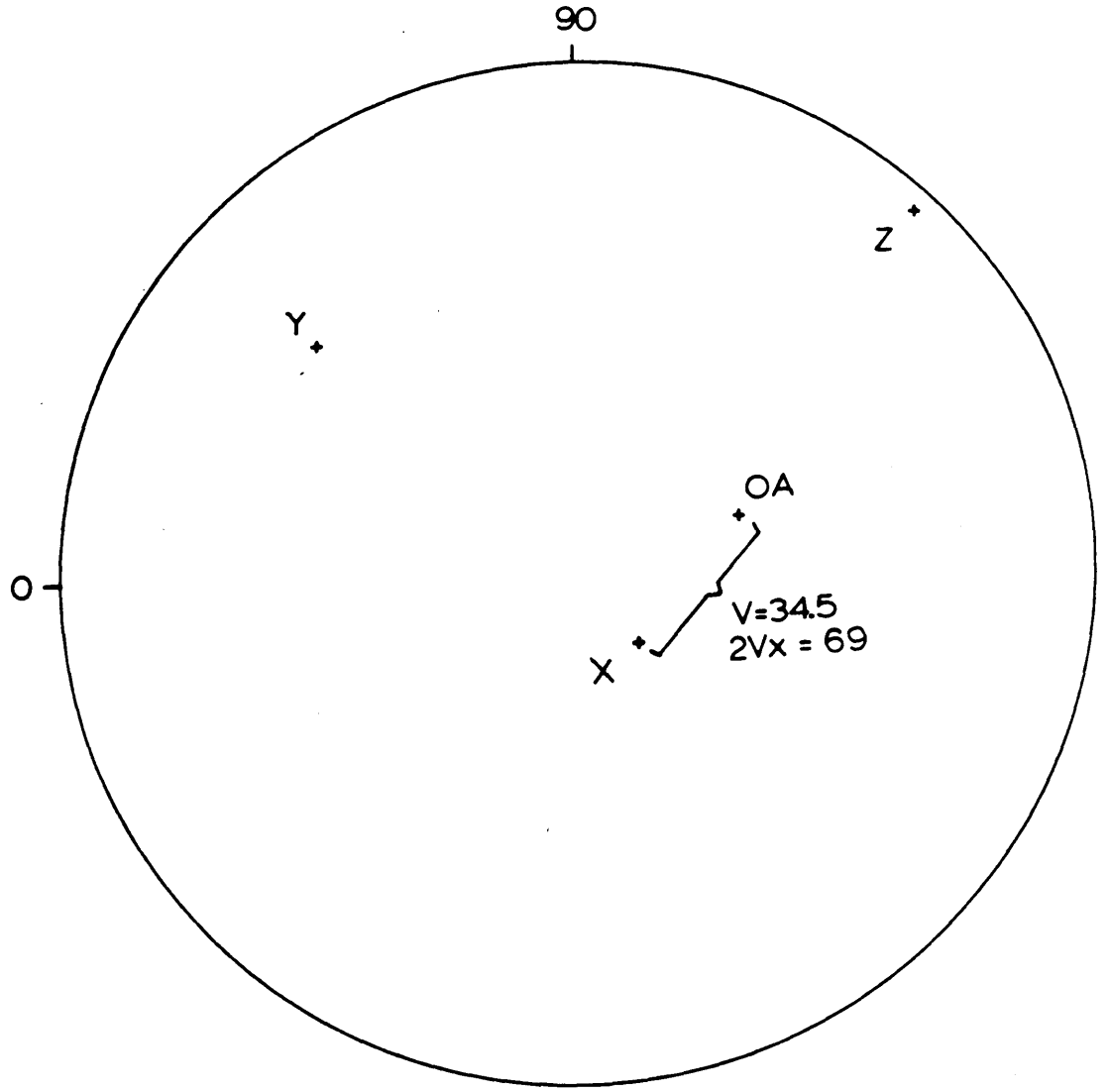

1987 DMC 0232

30

grain 3

| | iv | arc | oad |
|---|---|---|---|
| Y = 359.5 | 8 ↔ | ↑ 47 and ↓ 17 (core) | and ↑ 39 and ↓ 9 (rim) |
| Z = 268 | 14 ↔ | | |

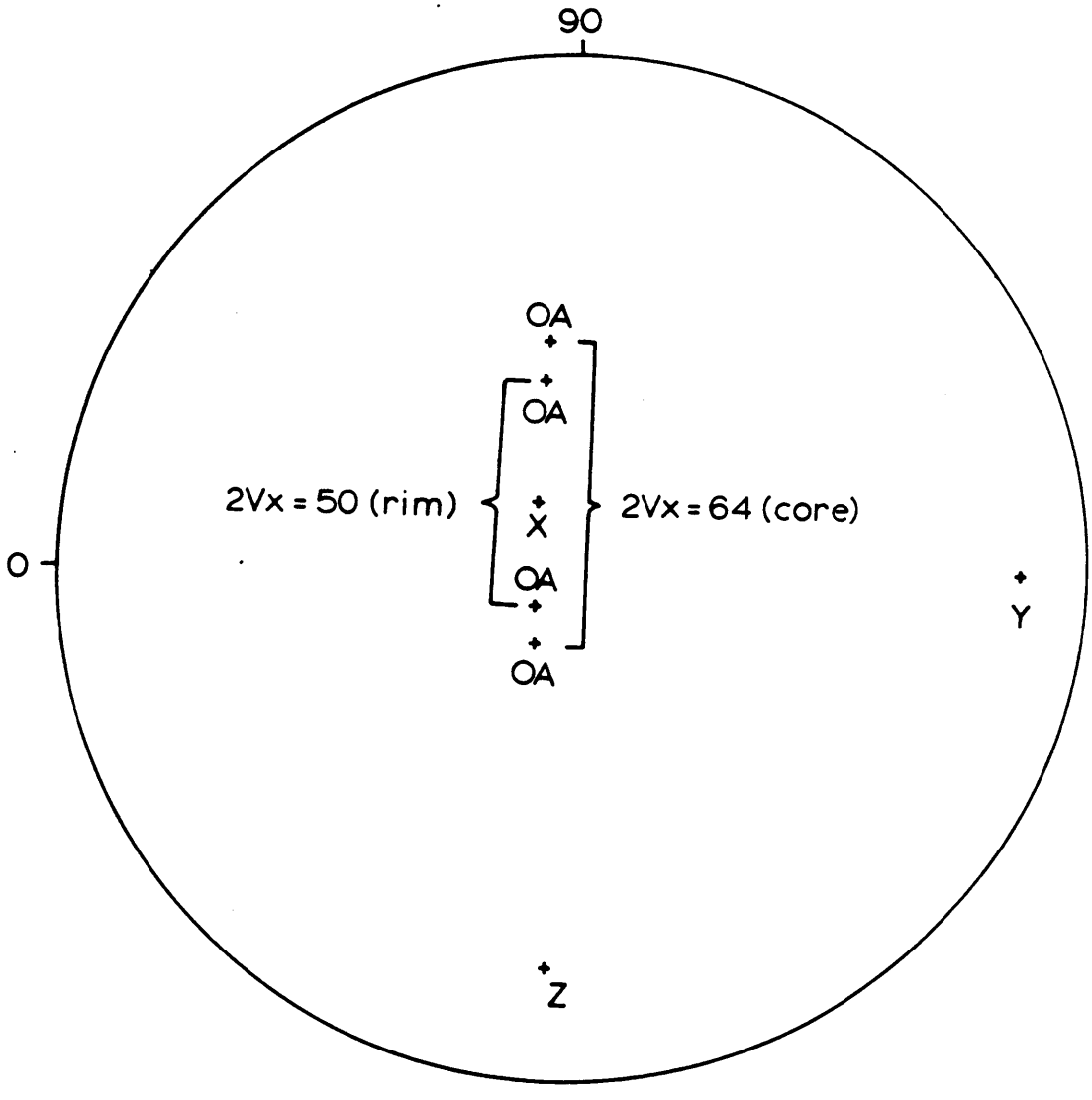

1987 DMC 0230
grain 1

31

| | iv | arc | oad |
|---|---|---|---|
| Y = | 098 ; | ↦ 10 ; | ↥ 155 |
| X = | 358 , | ↦ 39.5 | |

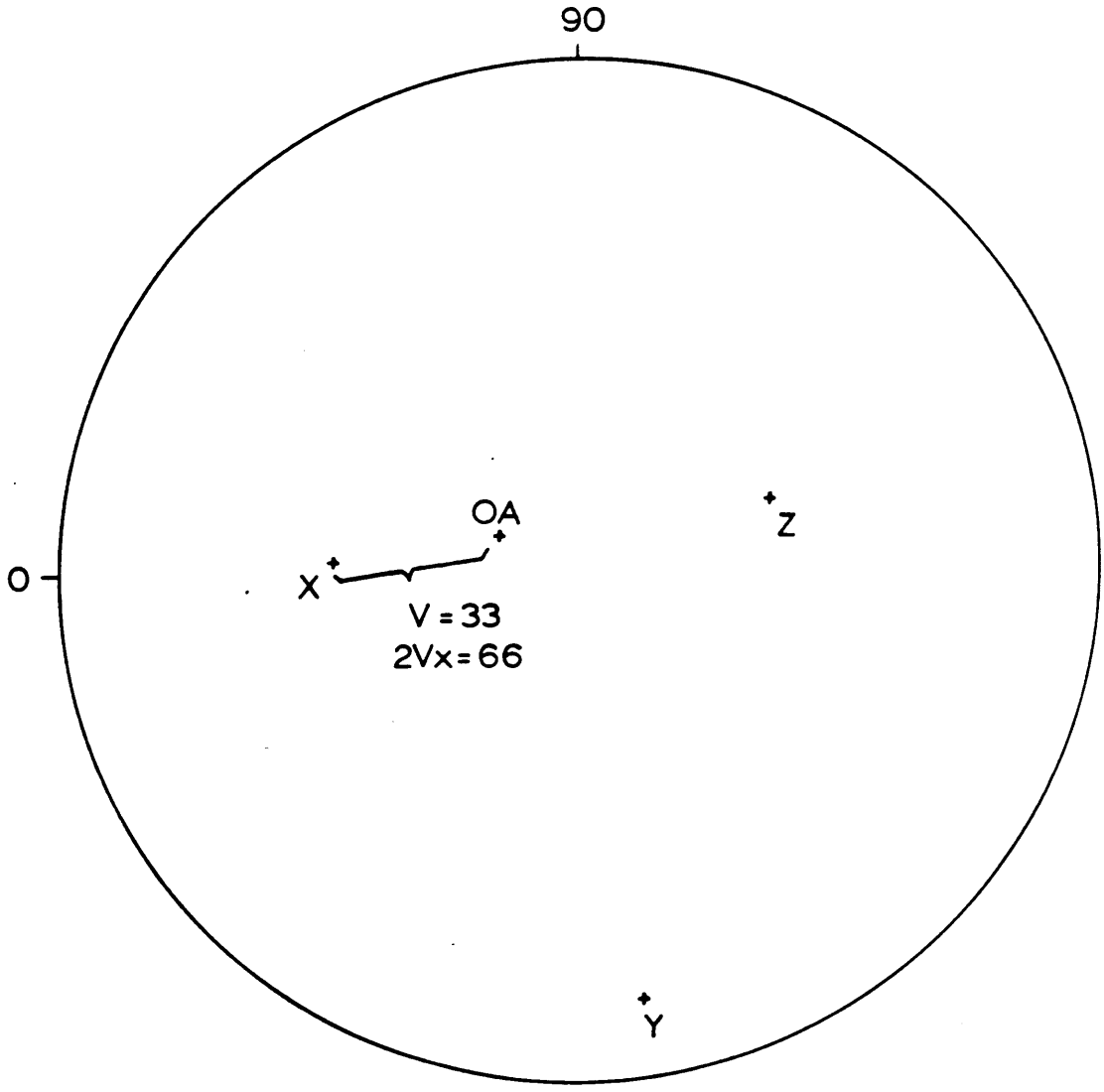

1987 DMC 0229 32

grain 1

| iv | arc | oad |
|---|---|---|

Y = 260 ; 28 ↔ ⊥ 39.2 and ⊤ 38

Z = 350 ; 0

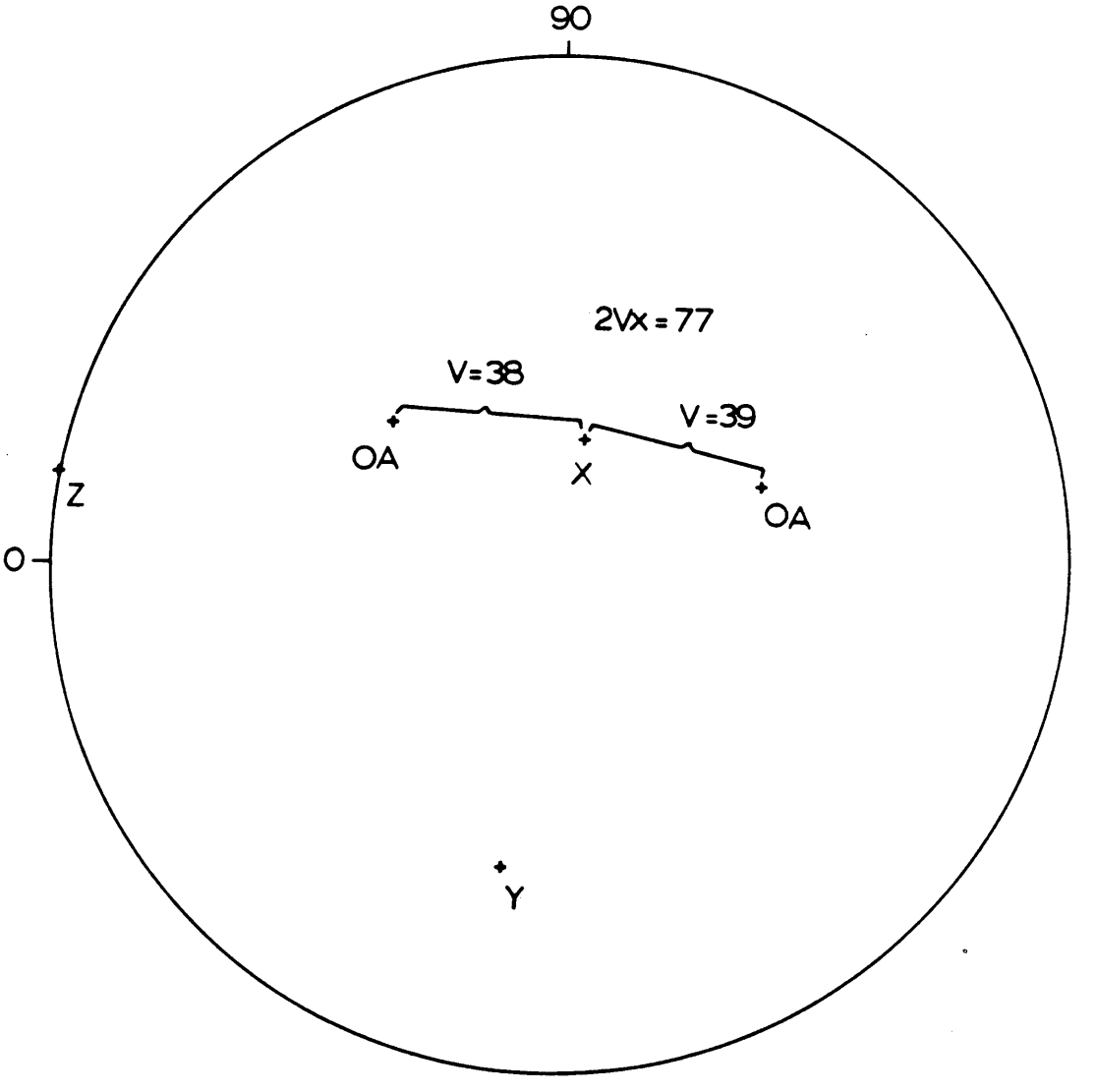

33

1987 DMC 0229

grain 2

iv arc oad

Y = 263.3; ⇾ 30.5; ↧ 38.5 and ↥ 40.5

Z = 354.5 ; 0

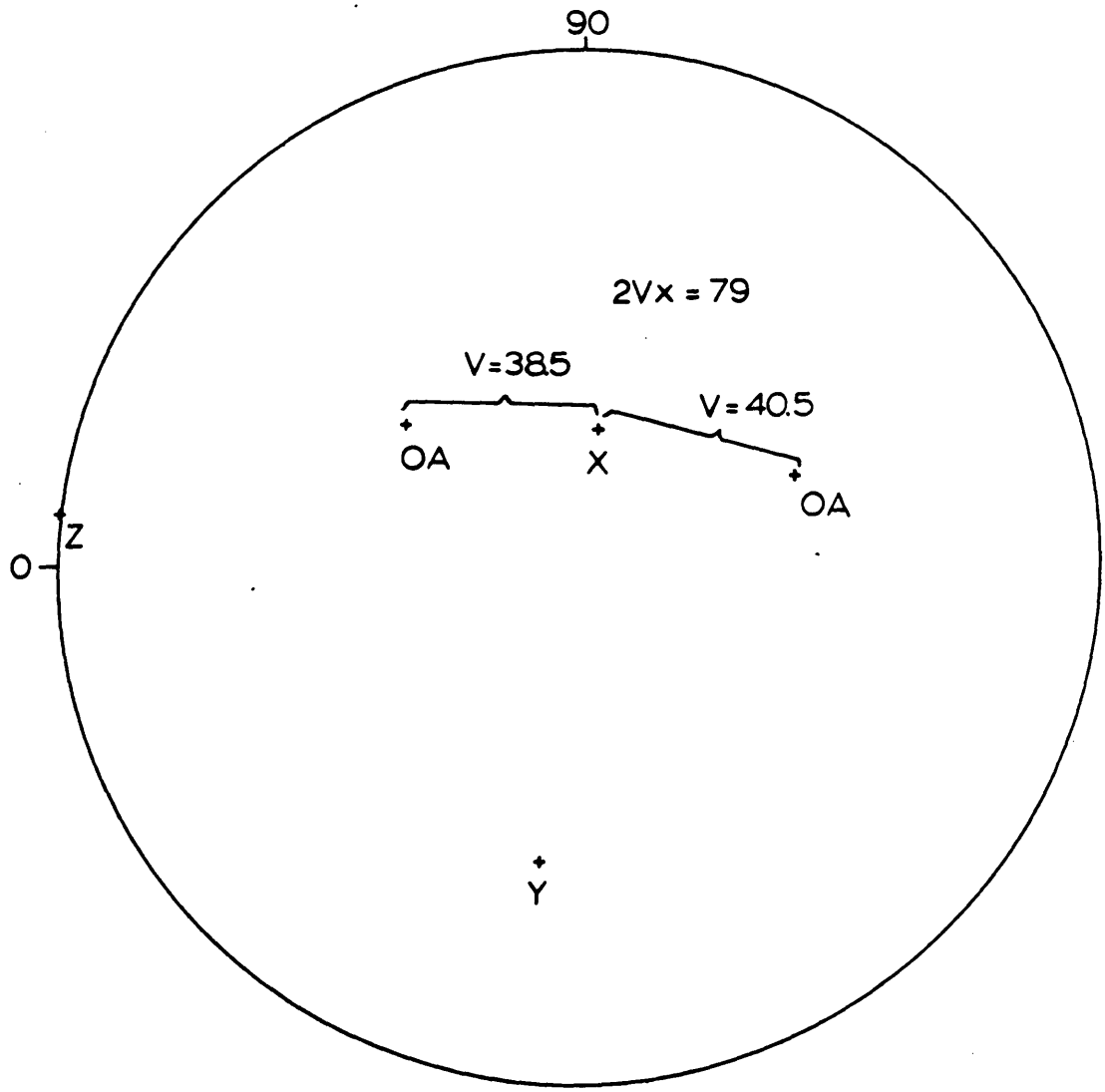

34

1987 DMC 0229

grain 3

| iv | arc | oad |
|---|---|---|

Y = 259.5 ; ↦ 30 , ↥ 40

Z = 170.5 ; 1 ↤

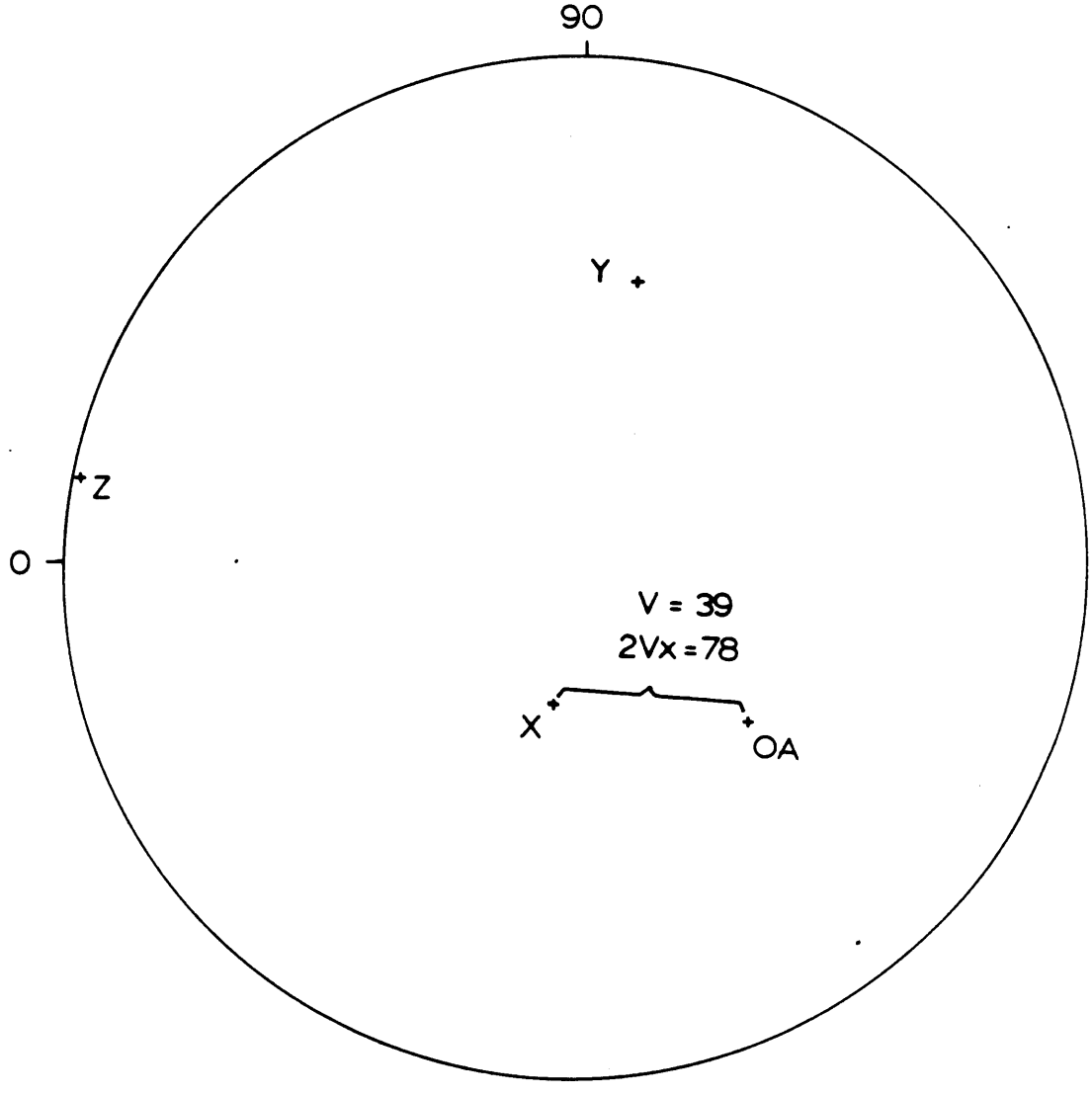

35

1987 DMC 0227

grain 1

| | iv | arc | oad |
|---|---|---|---|
| Y= | 166.5 | 16 ⇐ | ⇓ 8.5 |
| X= | 063.5 | 33.5 ⇐ | |

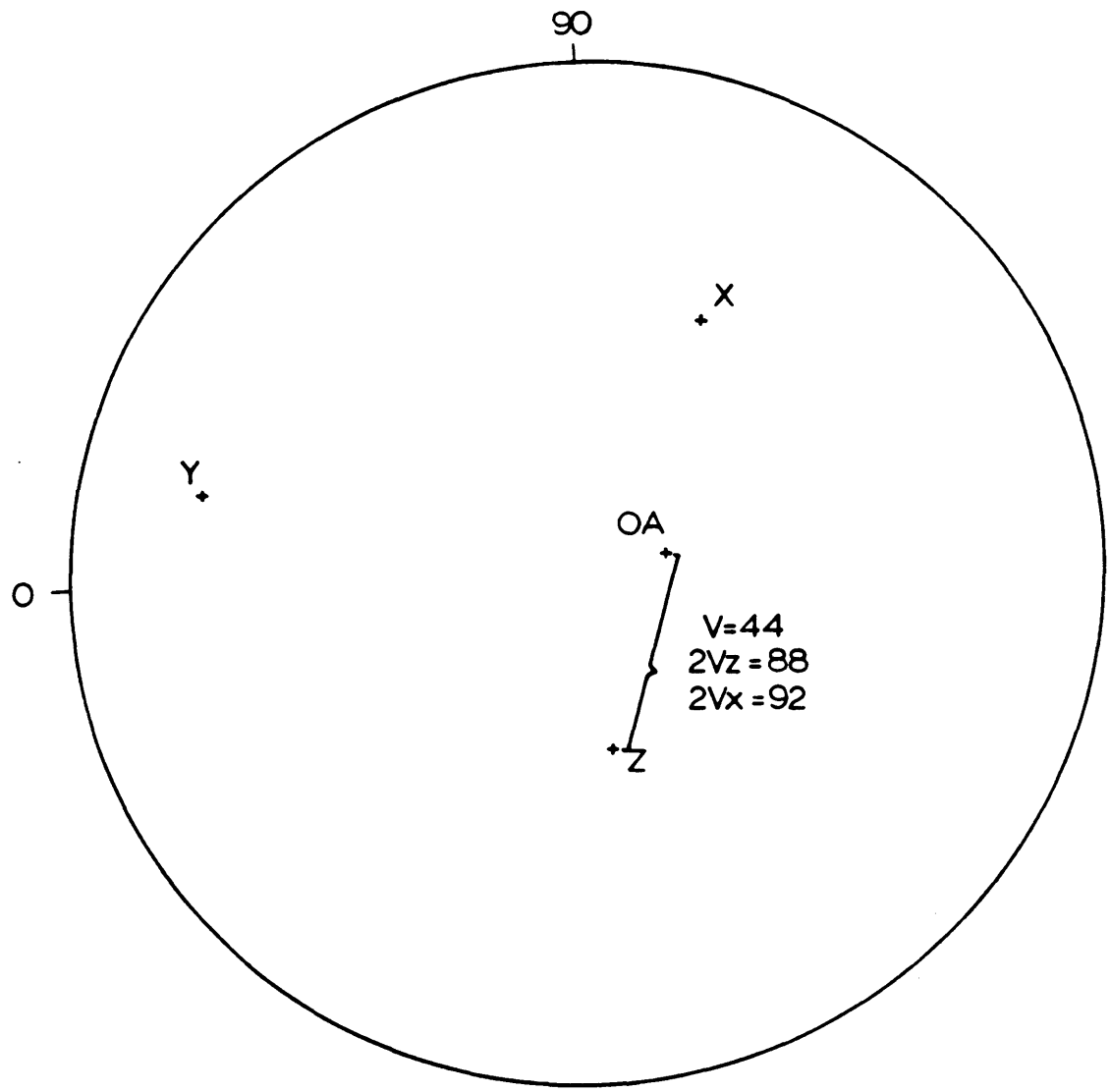

36

1987 DMC 0227

grain 2

| | iv | arc | oad |
|---|---|---|---|
| Y = 211 | ; 28 ↔ | ; ↓ 18 | and ↑ 36.5 |
| Z = 299.5 | ; ↔ 7 | | |

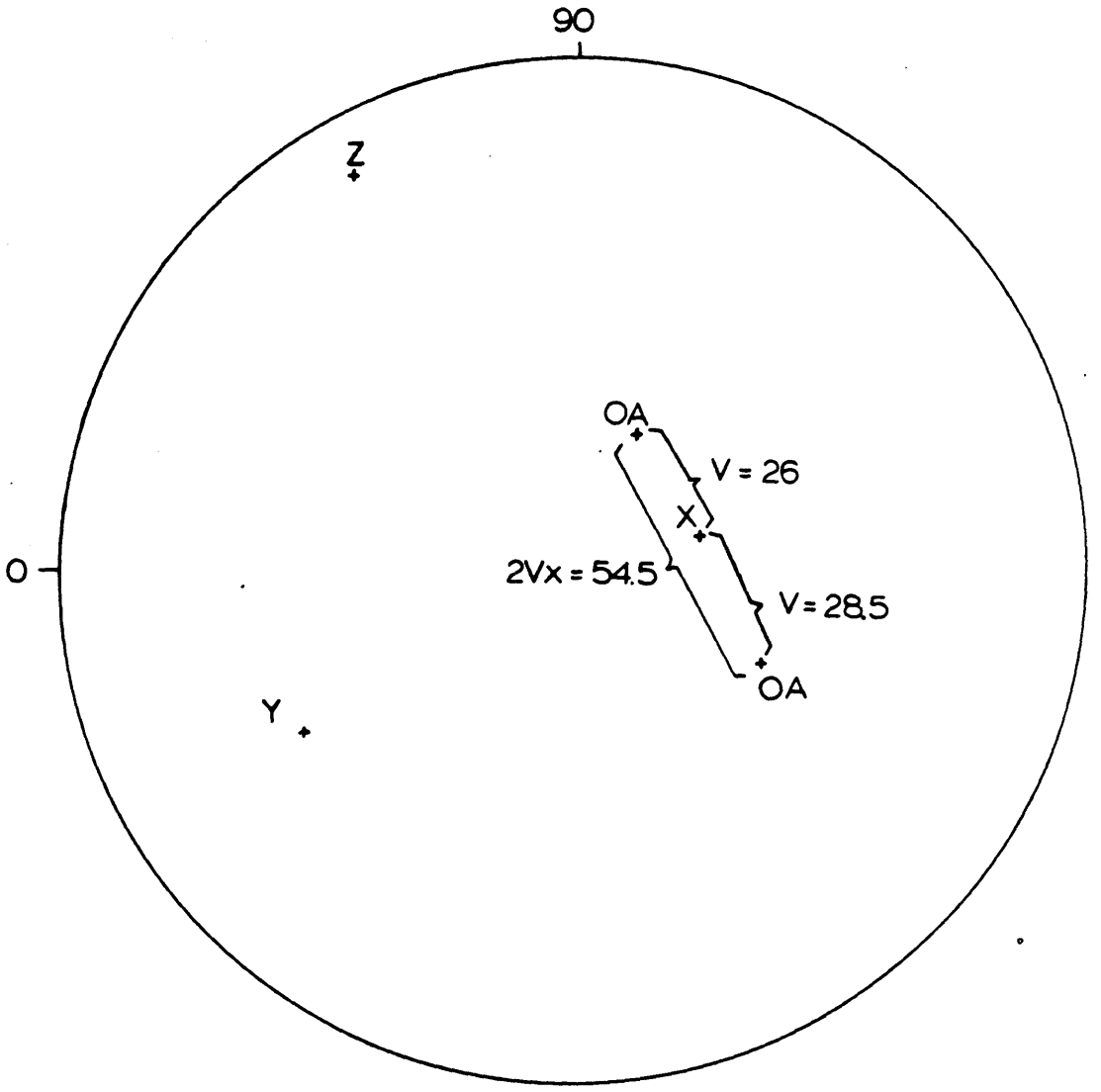

1987 DMC 0227

37

grain 3

iv arc oad

Y=320.5; ↦ 16; ↧ 23 core, ↧ 10.5 rim

Z=234; 18 ↤

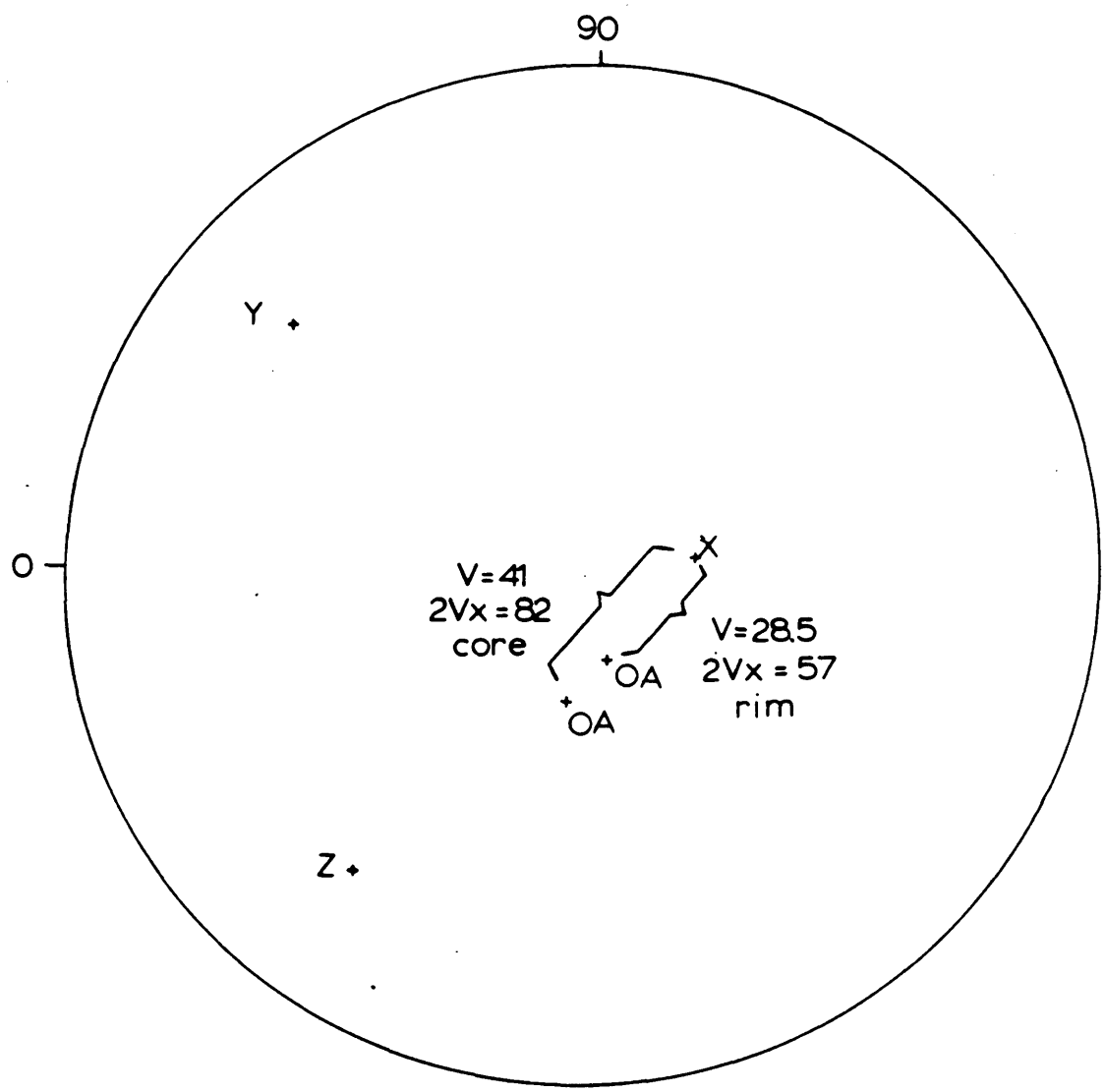

38

1987 DMC 0227

grain 4

| iv | arc | oad |
|---|---|---|

Y = 201 , ↦ 20 ; ↥ 32 and ↧ 22.5

Z = 295.5 ; ↦ 4

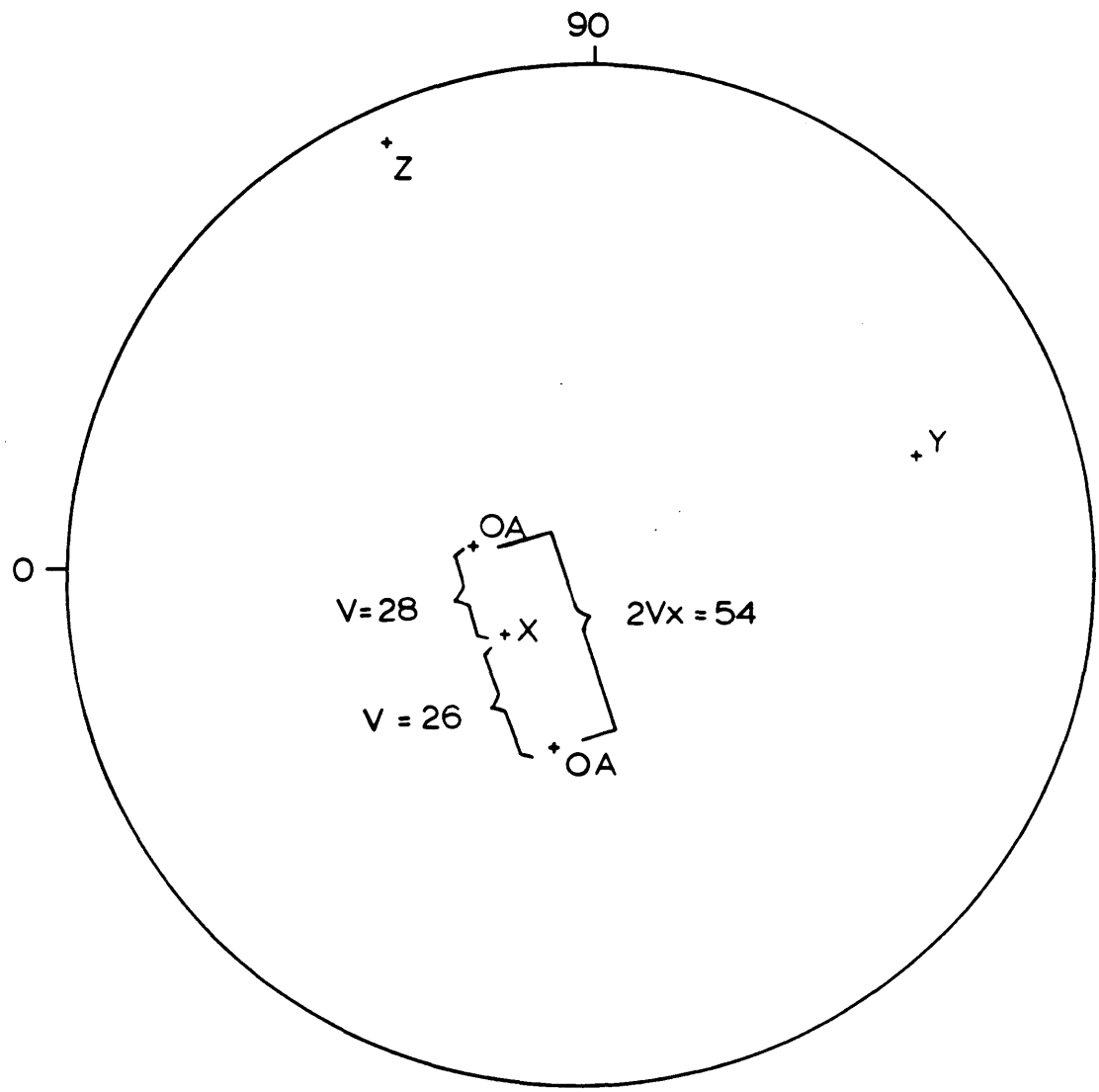

39

1987 DMC 0227

grain 5

| iv | arc | oad |
|---|---|---|

Y=214 ; ↔2.7 ; ↑4

Z=304 ; 38 ↔

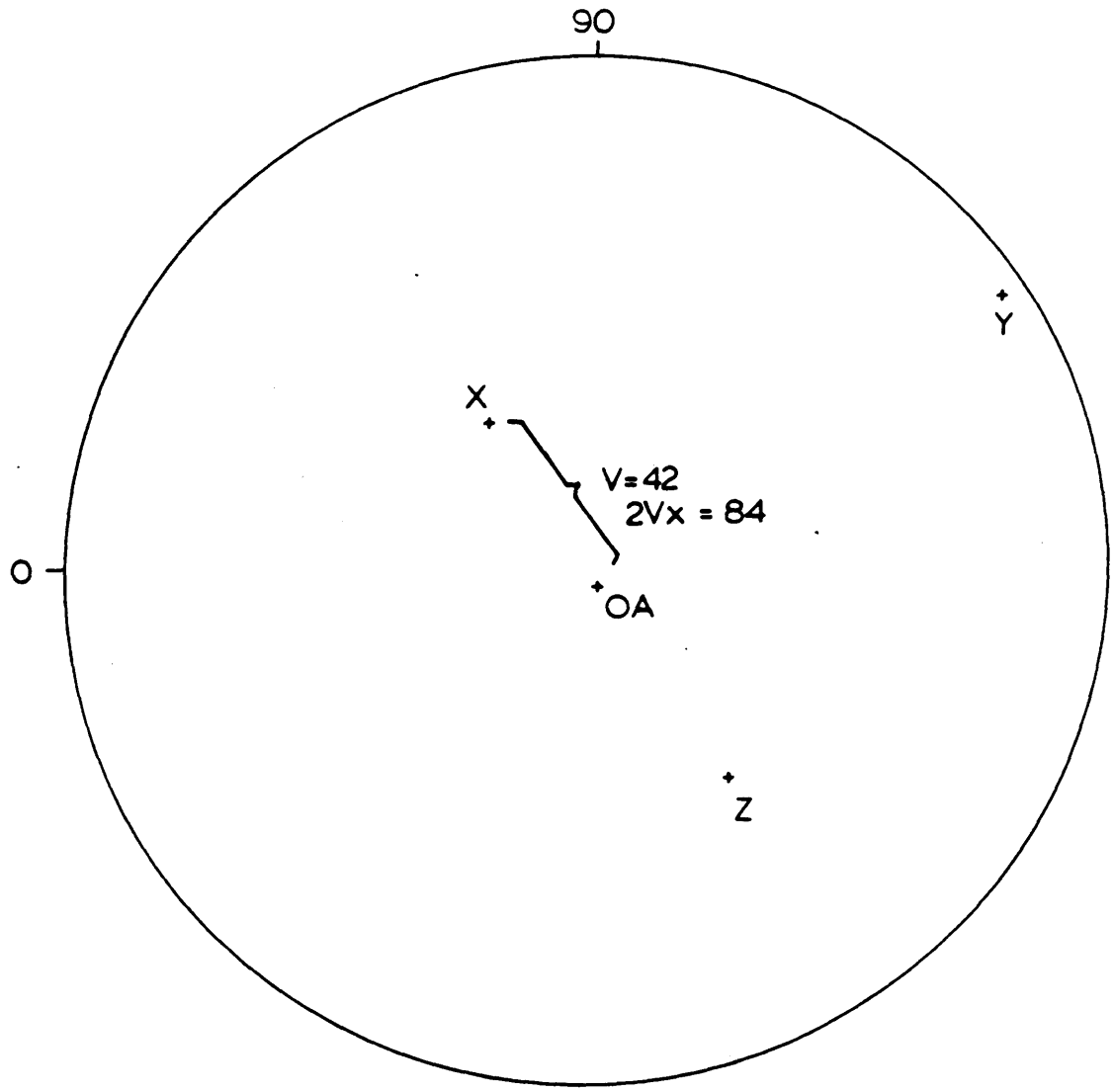

1987 DMC 0225

40

grain 1

| | iv | arc | oad |
|---|---|---|---|
| Y= | 329.5 ; | ⇾ 42 | ; ↥ 17.5 |
| X=040 ; | 19.7 ⇽ | | |

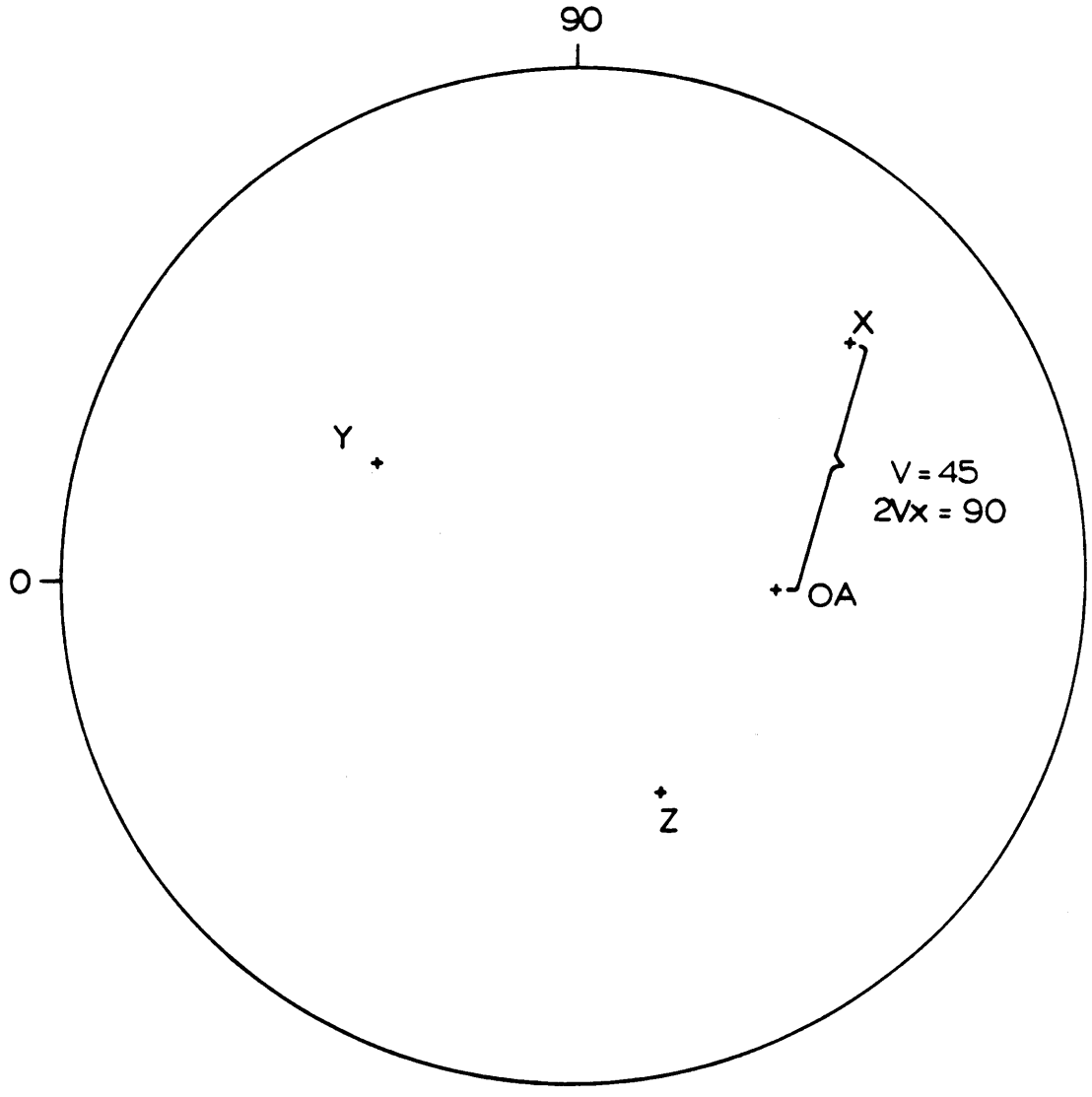

1987 DMC 0225

grain 2

41

| | iv | arc | oad |
|---|---|---|---|
| Y= | 289 ; | 12.5 ⇐ , | ↥ 30.5 |
| X= | 023.5 ; | 22 ⇐ | |

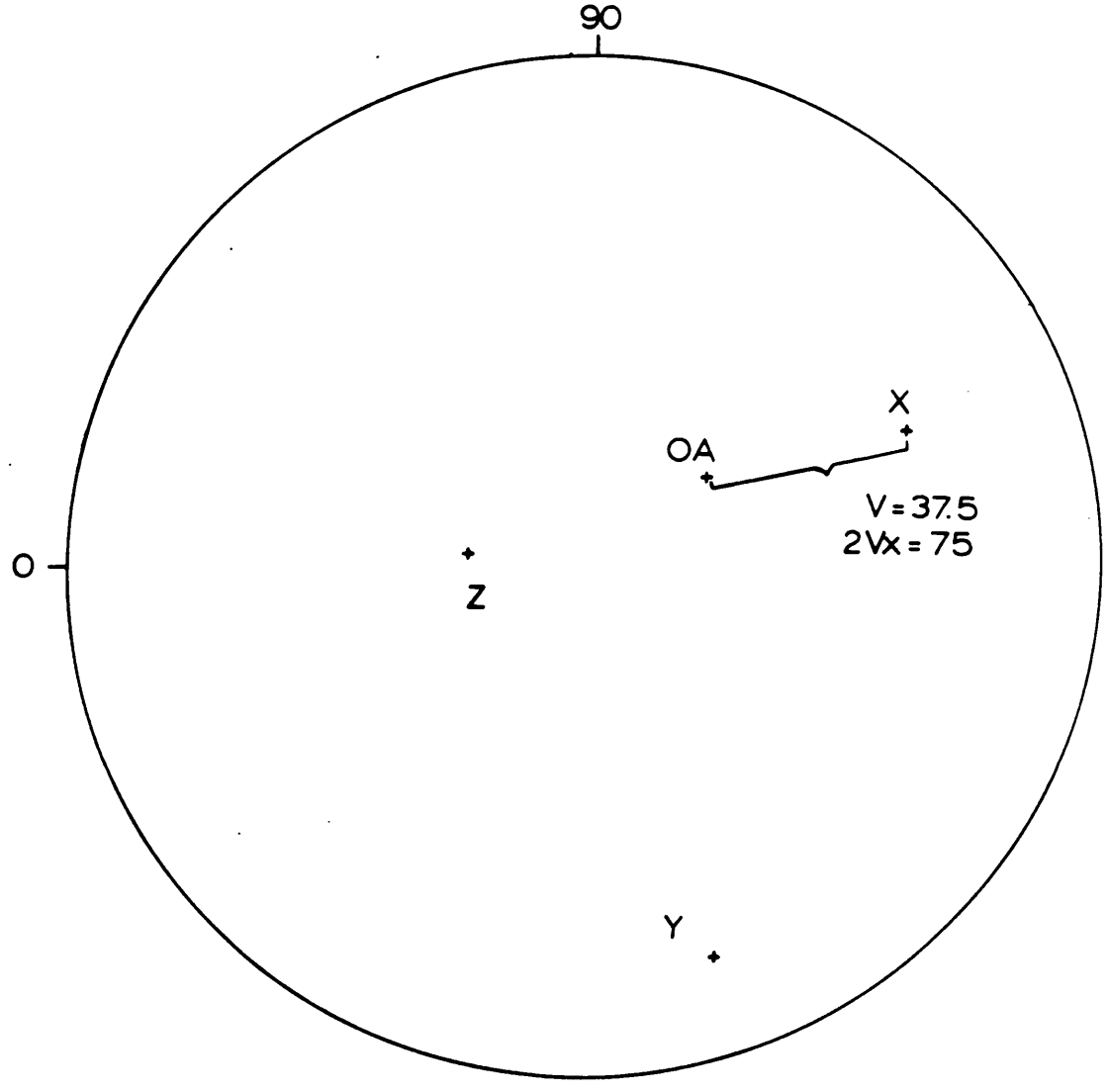

1987 DMC 0223

grain 1

42

| | iv | arc | oad |
|---|---|---|---|
| Y = | 343 ; | ↦ 36.5 ; | ↥ 20 |
| Z = | 058.7 ; | 18.5 ↤ | |

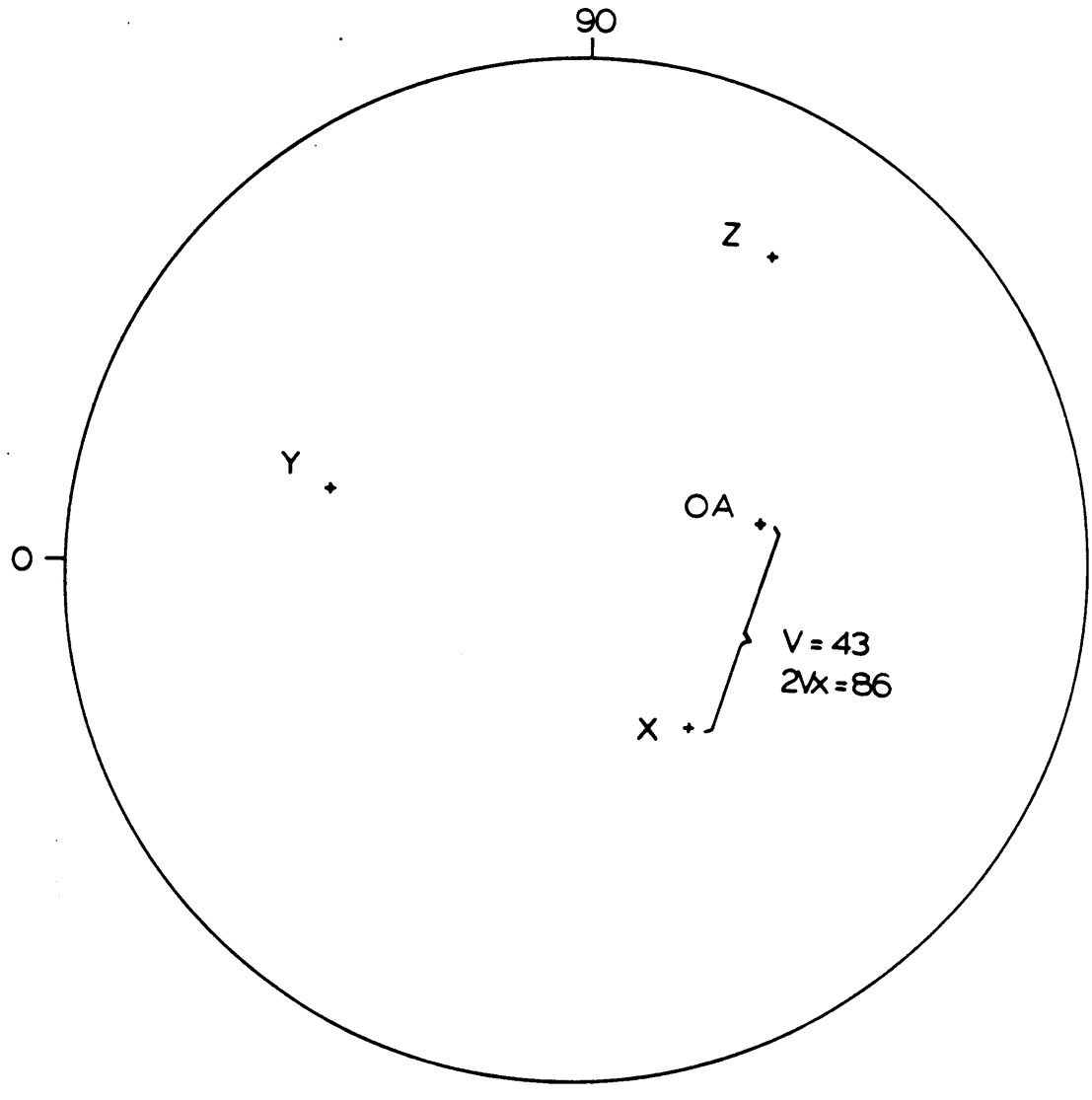

1987 DMC 0221

43

grain 1

| | iv | arc | oad |
|---|---|---|---|
| Y = | 264.5 | ; 0 | ; ↓ 20.5 |
| X = | 353.5 | ; → | 33.5 |

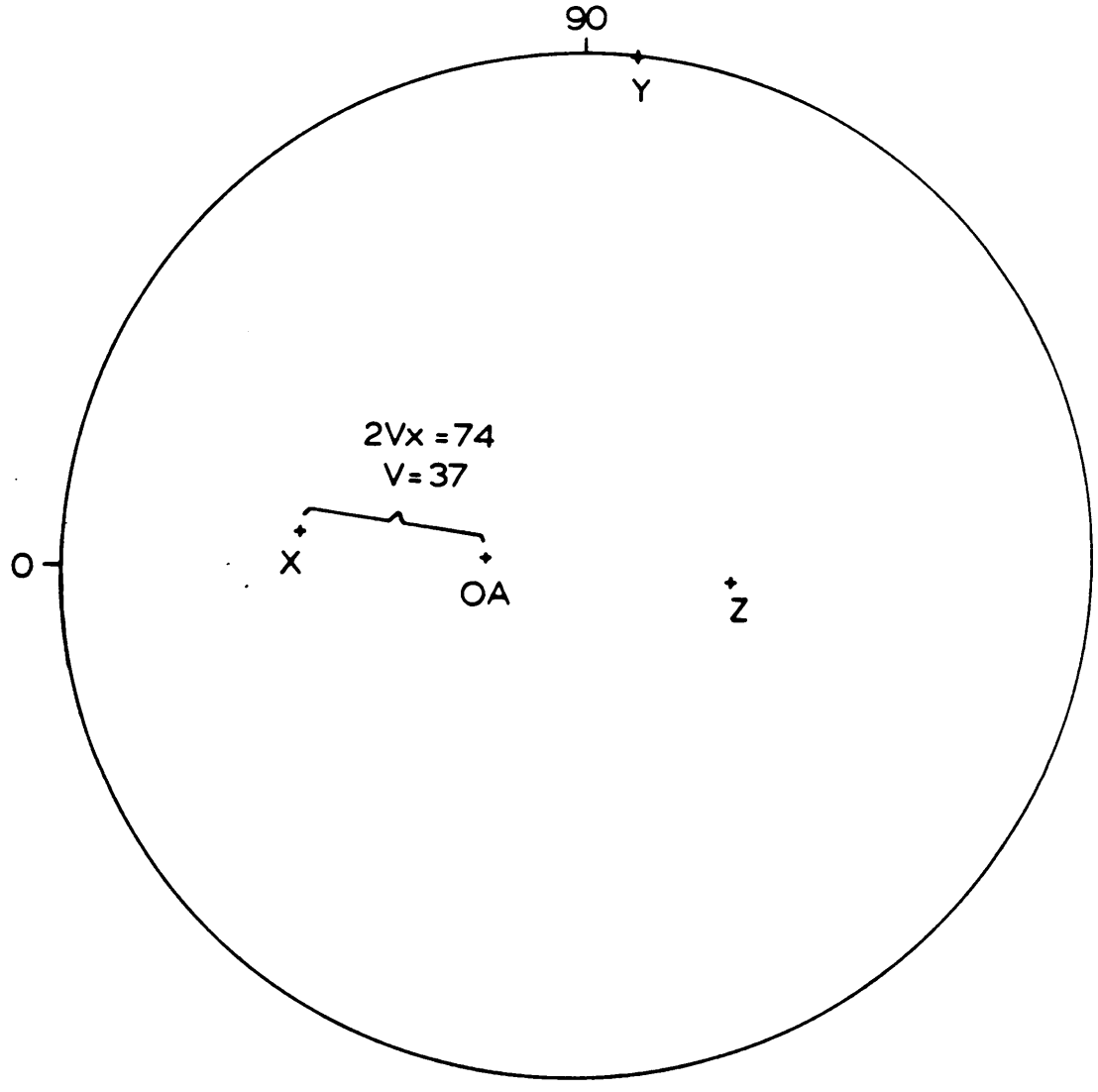

1987 DMC 0074

44

grain 1

| iv | arc | oad |
|---|---|---|

Y = 270 ; 23 ↔ ; ↓ 5.5 core and ↓ 17 rim

X = 335.5 ; ↦ 40.5

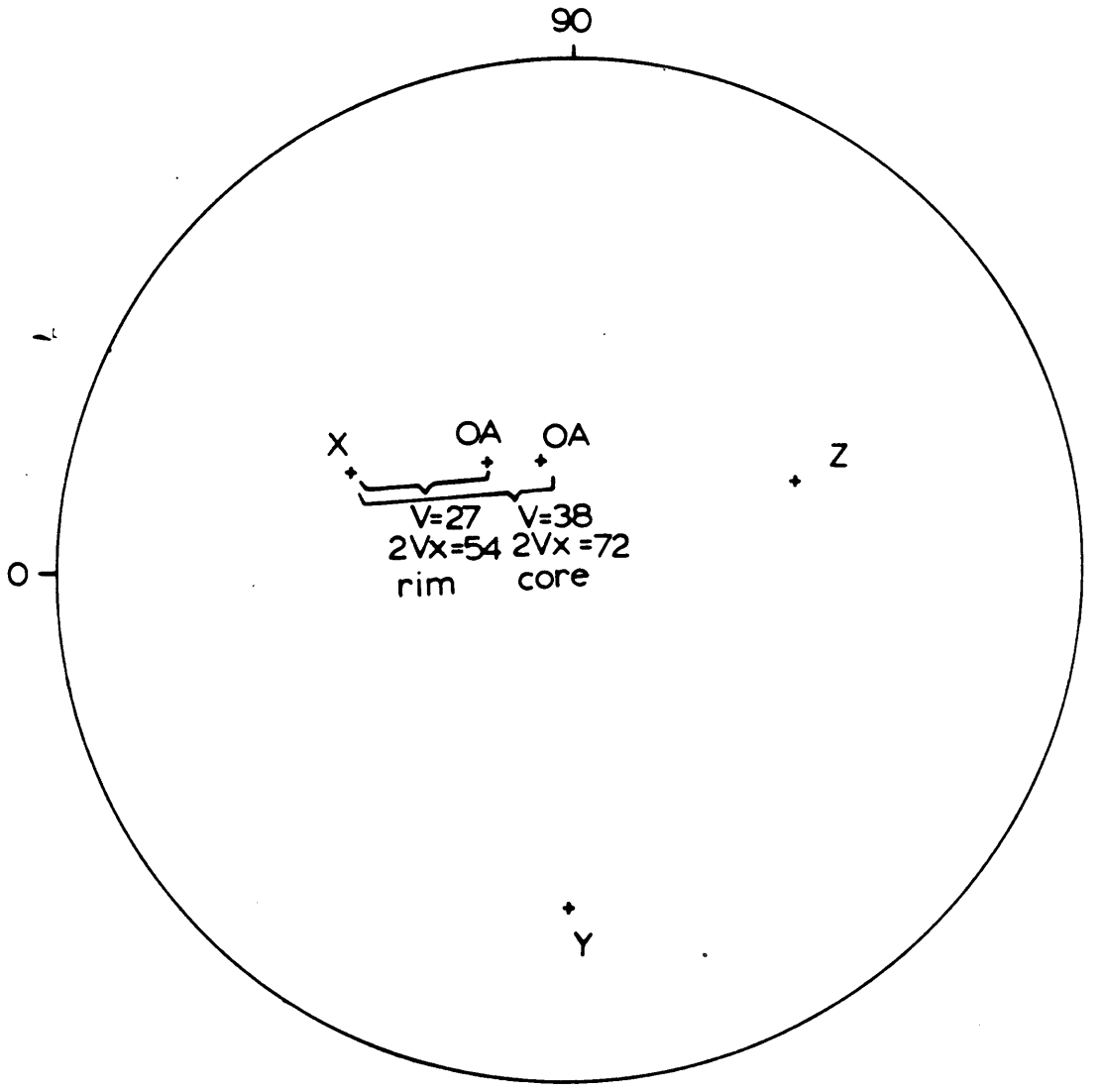

1987 DMC 0074

grain 2

45

iv arc oad

Y = 324 ; ↦ 10 ; ↥ 17 core and ↥ 6.5 rim

Z = 230 ; ↦ 21

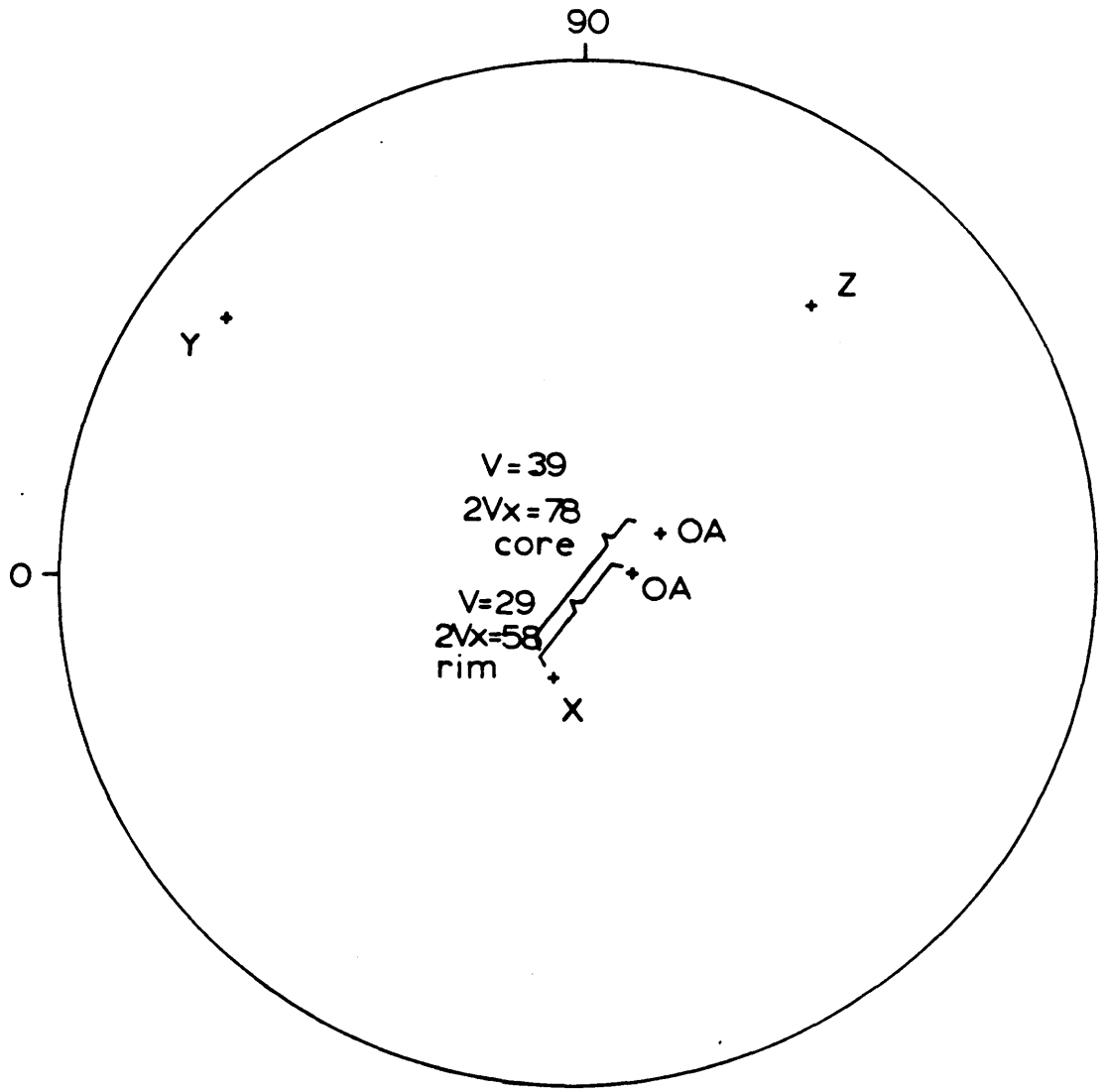

1987 DMC 0075

46

grain 1

| | iv | arc | oad |
|---|---|---|---|
| Y = | 079.5; | ⇾ 33.7; | ⇡ 21.5 |
| X = | 148 | , 29.5 | ⇽ |

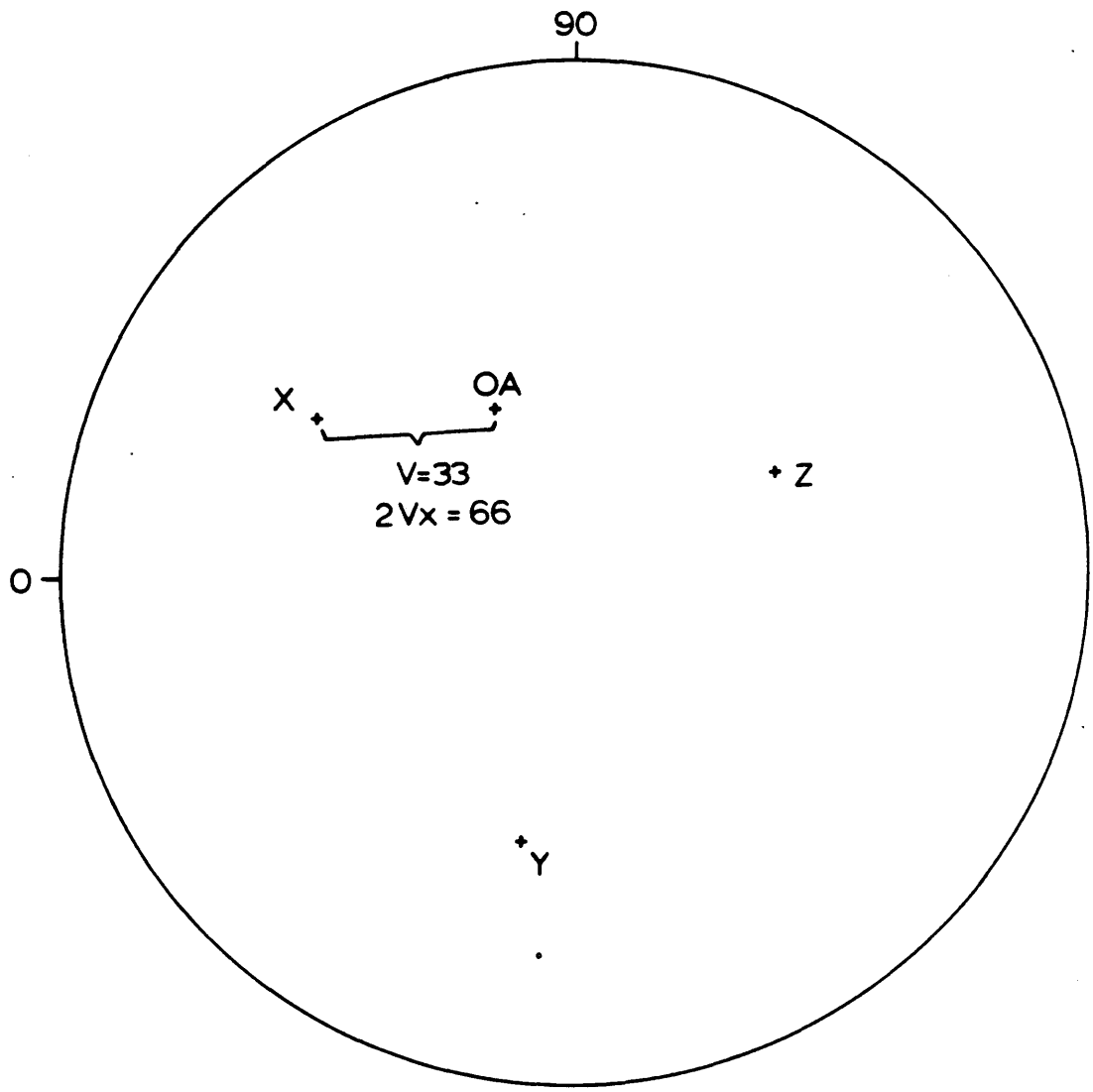


Photo 1. Hand specimen of varied texture gabbro.

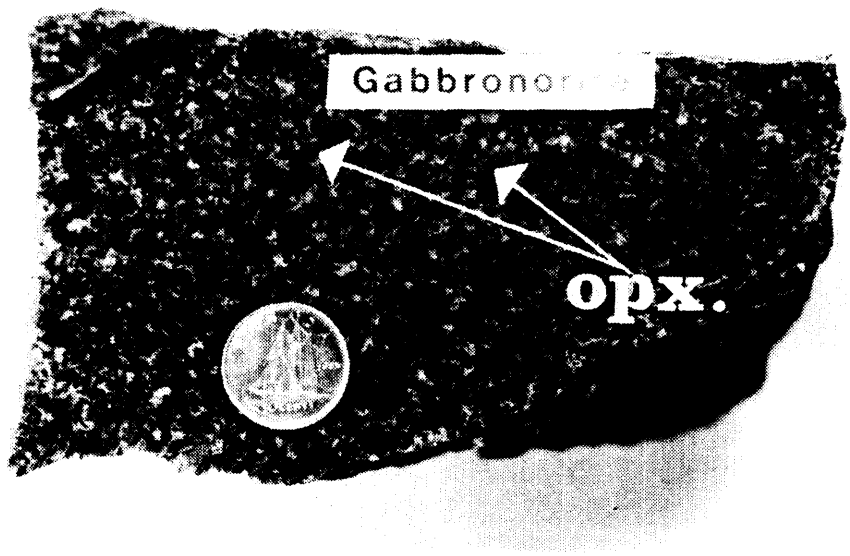


Photo 2. Hand specimen of Gabbronorite containing phenocrystic orthopyroxene.

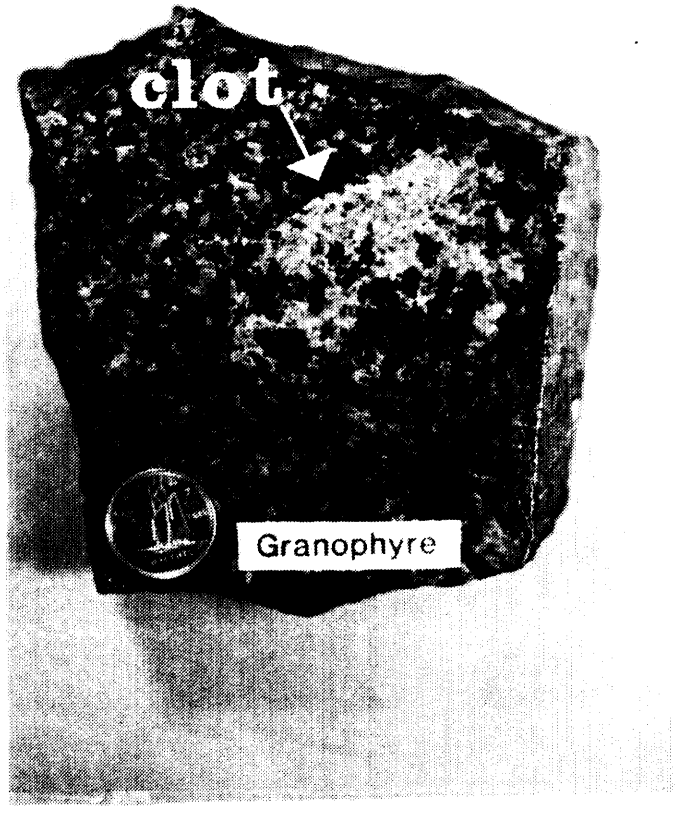


Photo 3. Feldspar clots within the Granophyric phase.


Photo 4. Vugs within the Granophyric Phase indicating a highly volatile environment at the time of crystallization.

Photo 5. Medium-grained, vuggy, granitic phase.

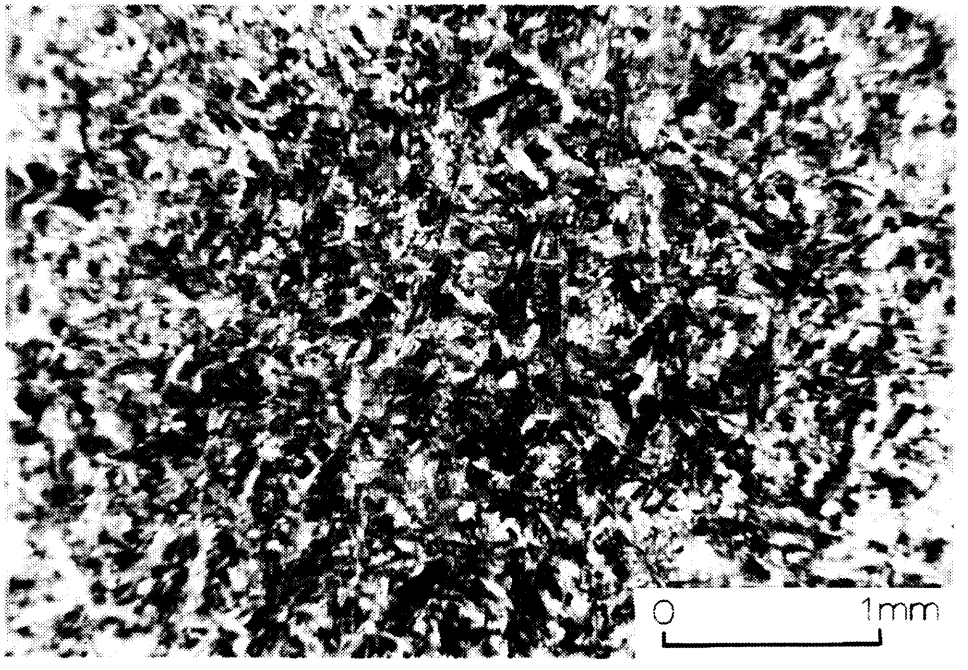


Photo 6. Radiating fan-like clusters of pyroxene and plagioclase crystals within the chilled magma.

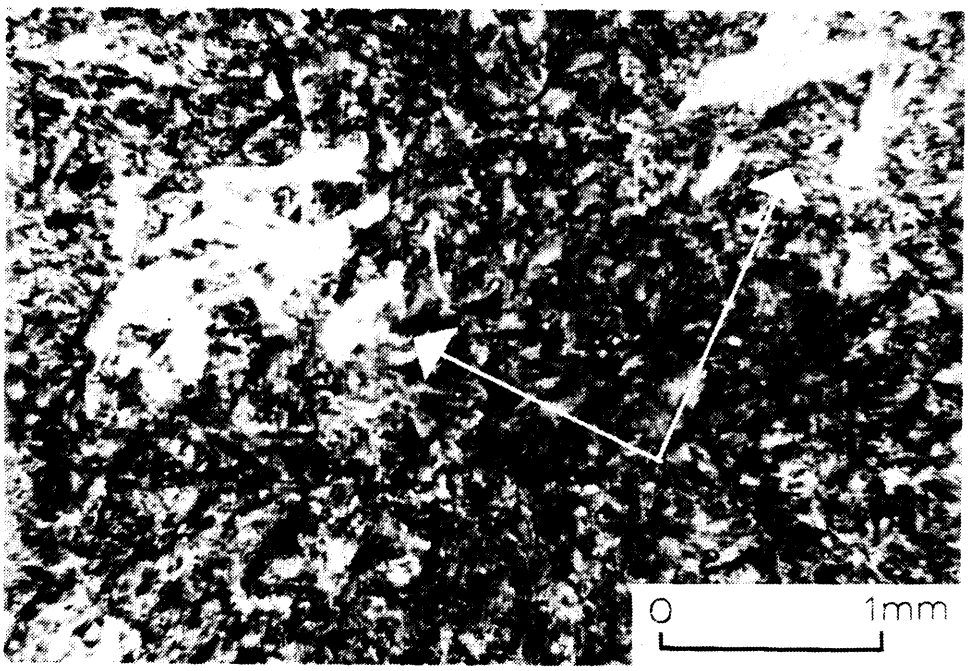


Photo 7. Glomeroporphyritic plagioclase within the chilled magma.

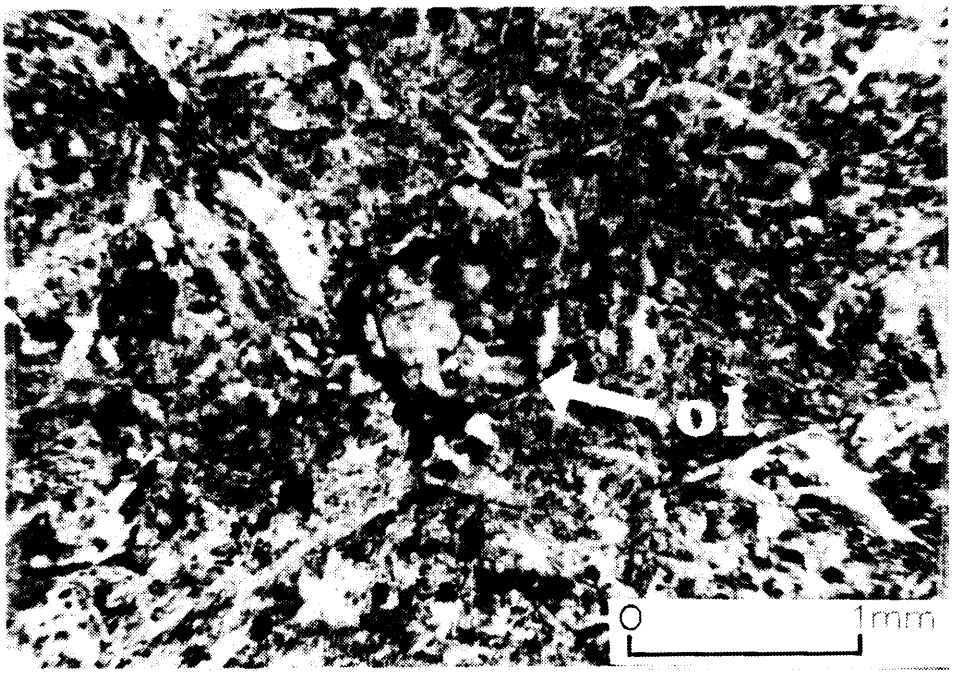


Photo 8. Olivine phenocrysts pseudomorphed by antigorite and talc within the chilled magma.


Photo 9. Inverted pigeonite molded onto and in crystal continuity with augite.

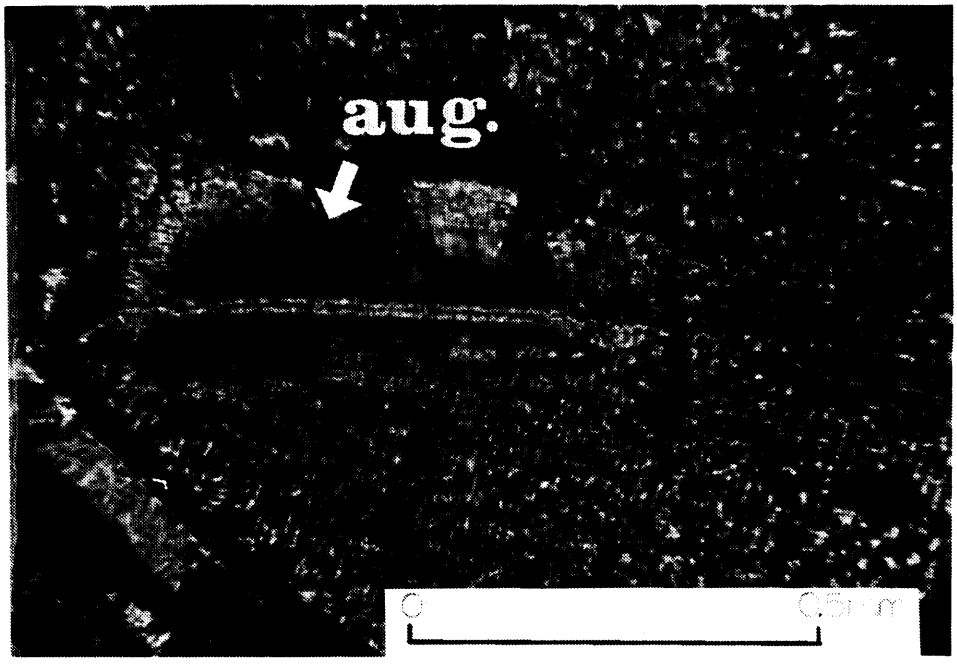


Photo 10. Herringbone exsolution lamellae of clinopyroxene in inverted pigeonite. Note the augite core.

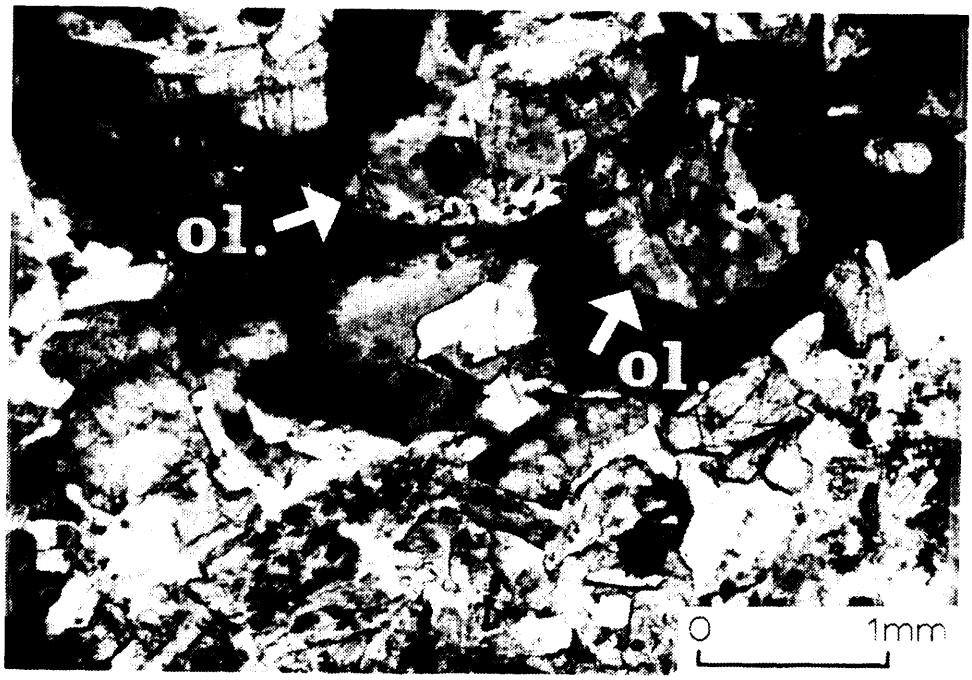


Photo 11. Partially resorbed olivine crystals surrounded by altered pigeonite.

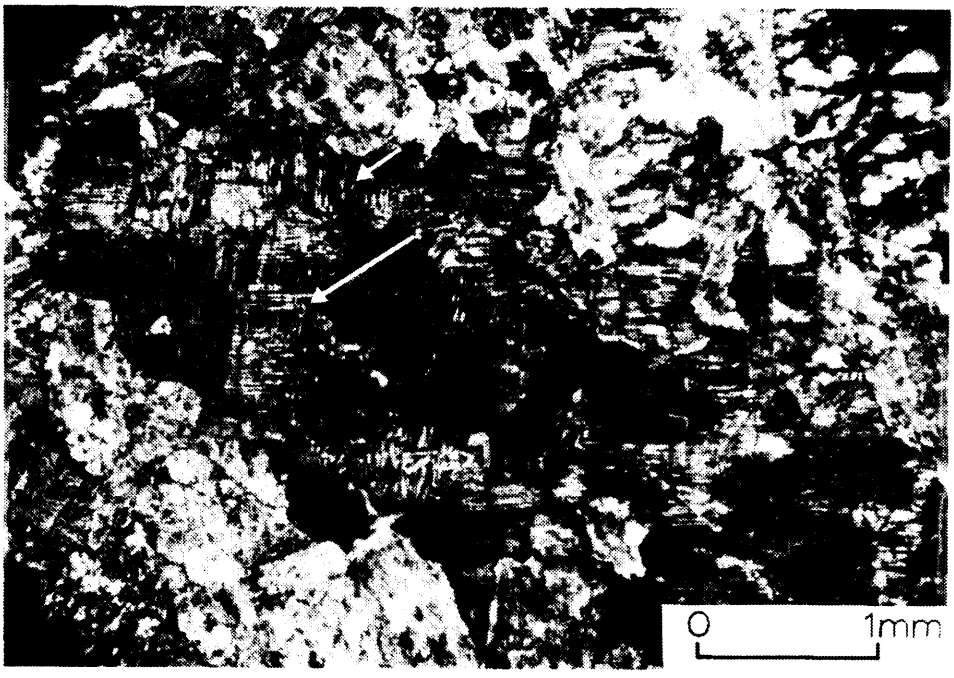


Photo 12. Clinopyroxene exsolving as plates along two crystallographic directions in the orthopyroxene.

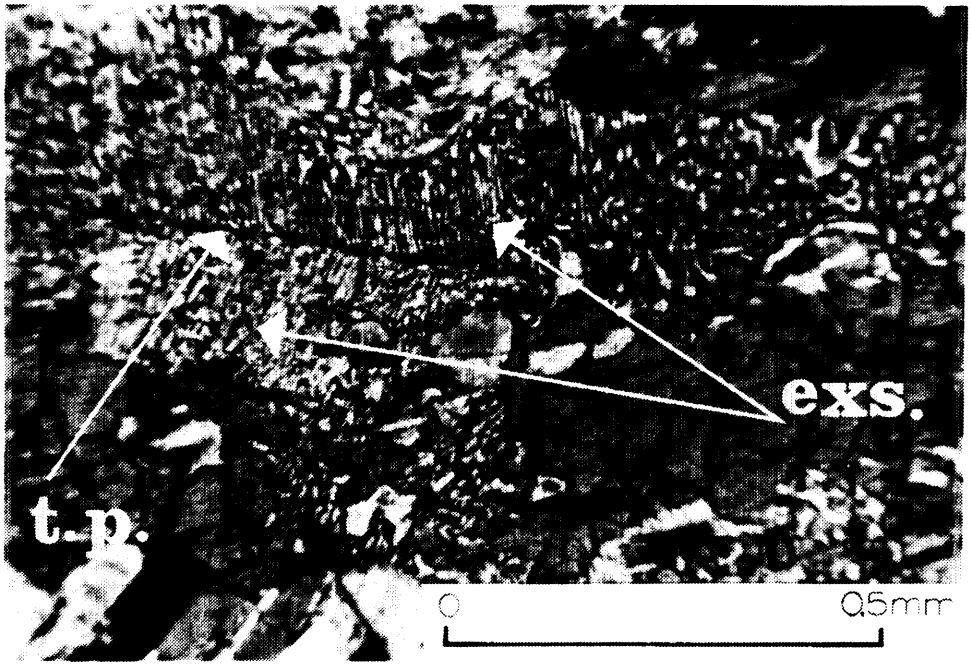


Photo 13. Blebby exsolution of clinopyroxene in the rim of an orthopyroxene crystal.

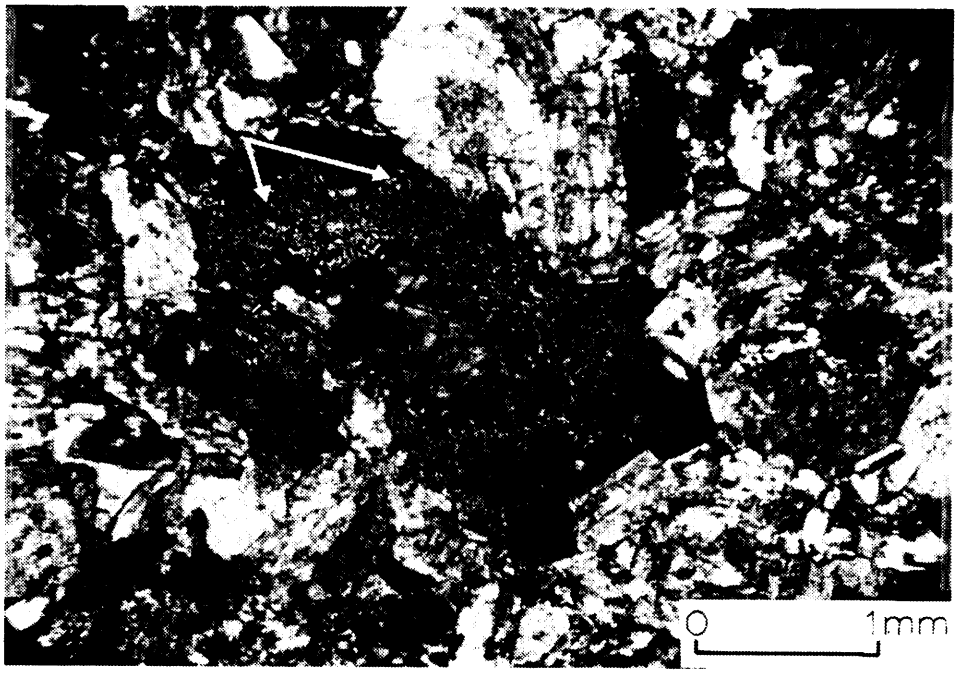


Photo 14. Remnant herringbone exsolution retained in the orthorhombic orthopyroxene (hypersthene).
"exs." exsolution plates of clinopyroxene
"t.p." remnant twin plane

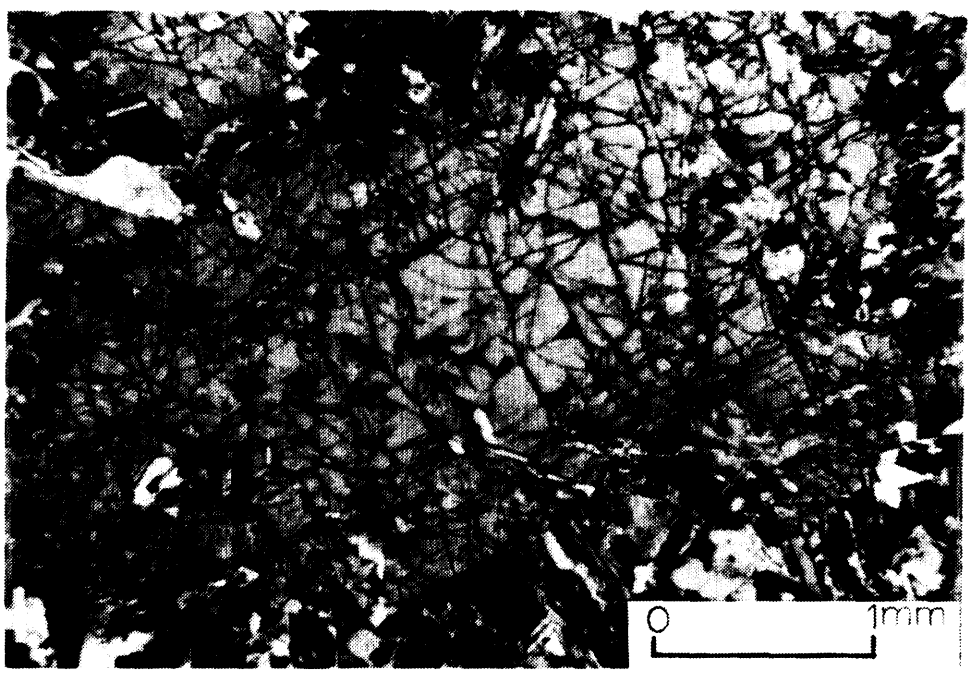


Photo 15. Phenocrystic orthopyroxene within gabbronorite.

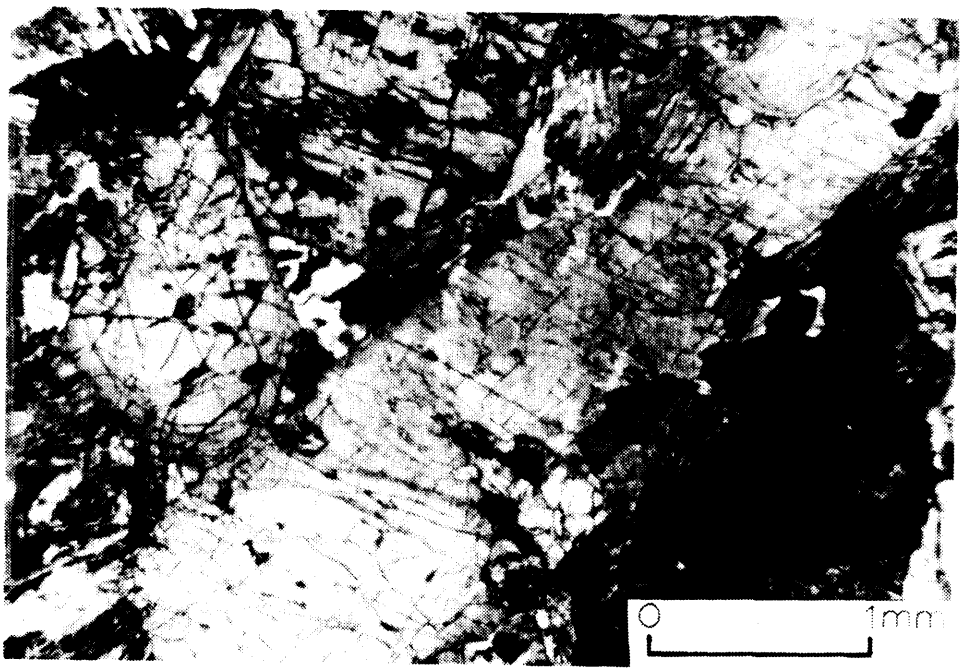


Photo 16. Cummulate orthopyroxene within gabbronorite.

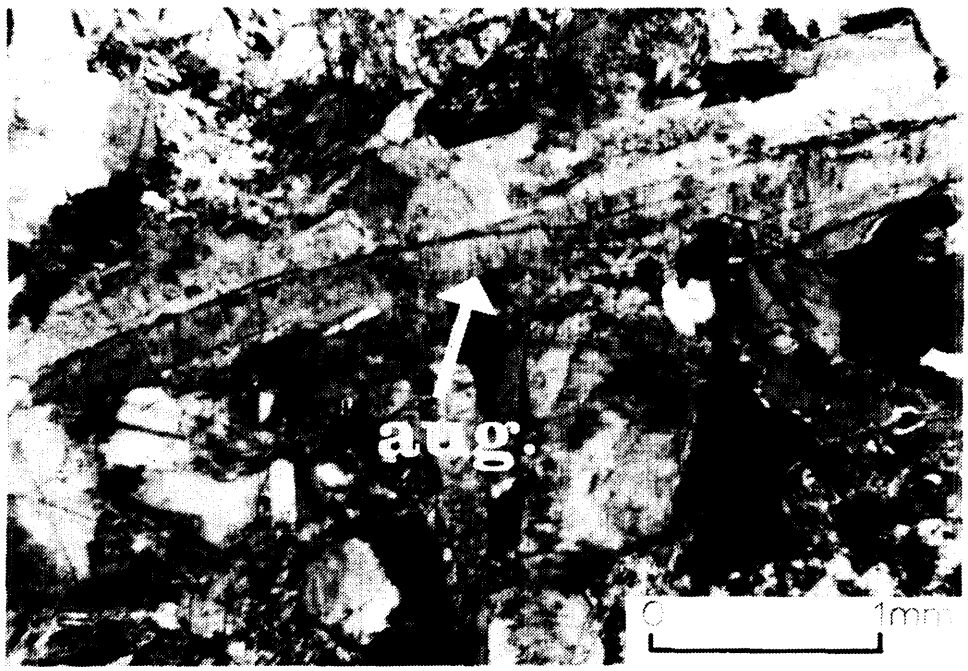


Photo 17. Phenocrystic augite within gabbronorite.

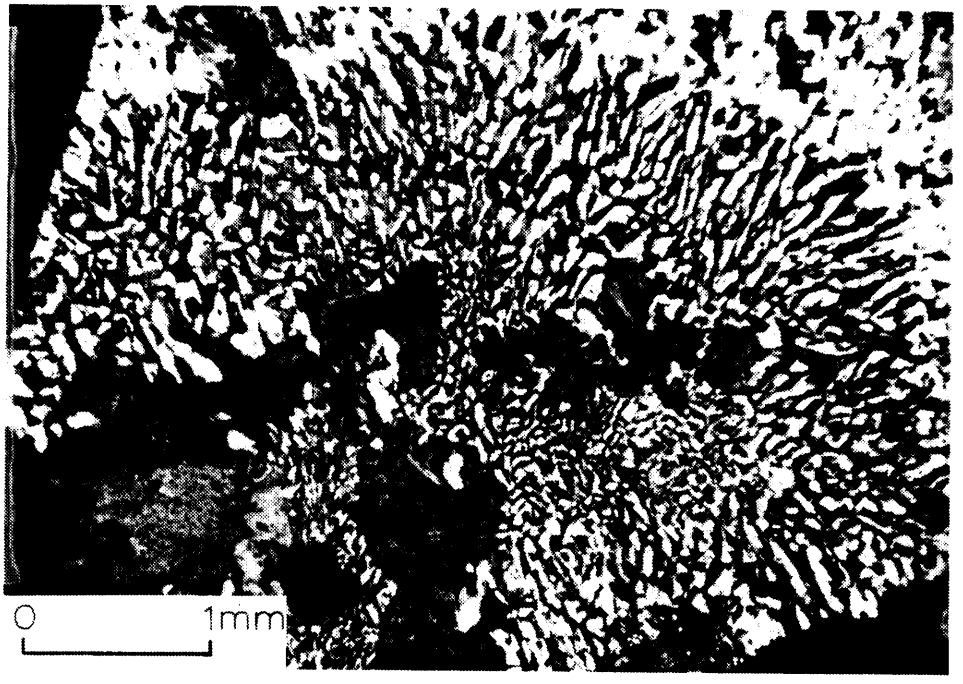


Photo 18. Eutectoid intergrowth of quartz and plagioclase within a granophyric phase.

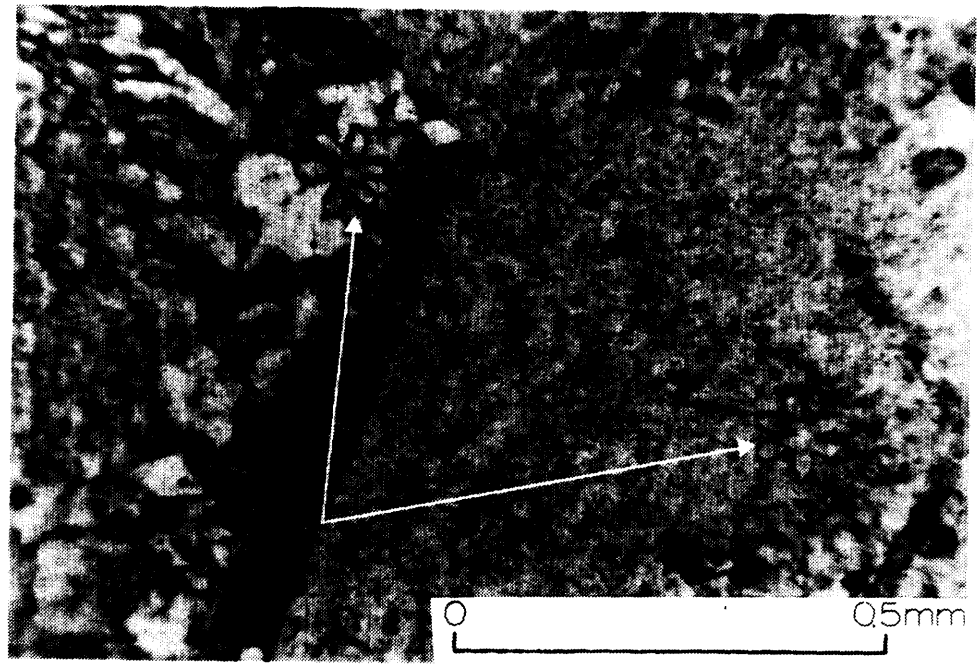


Photo 19. Skeletal apatite within the granophyric phase.

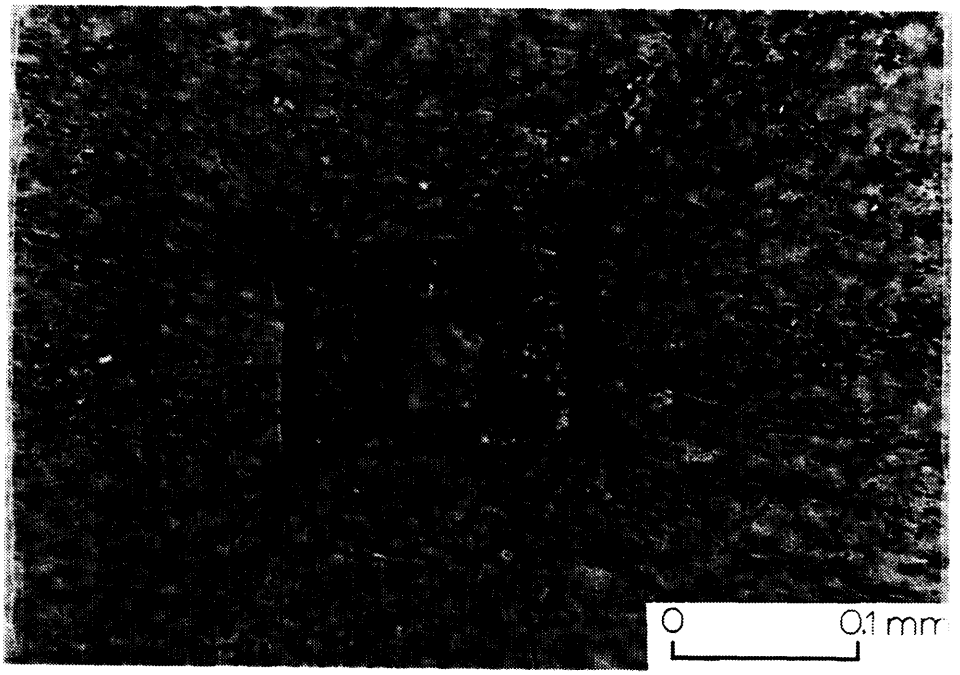


Photo 20a, 20b. Hollow, quenched zircons within the Bonanza Lake granodiorite.

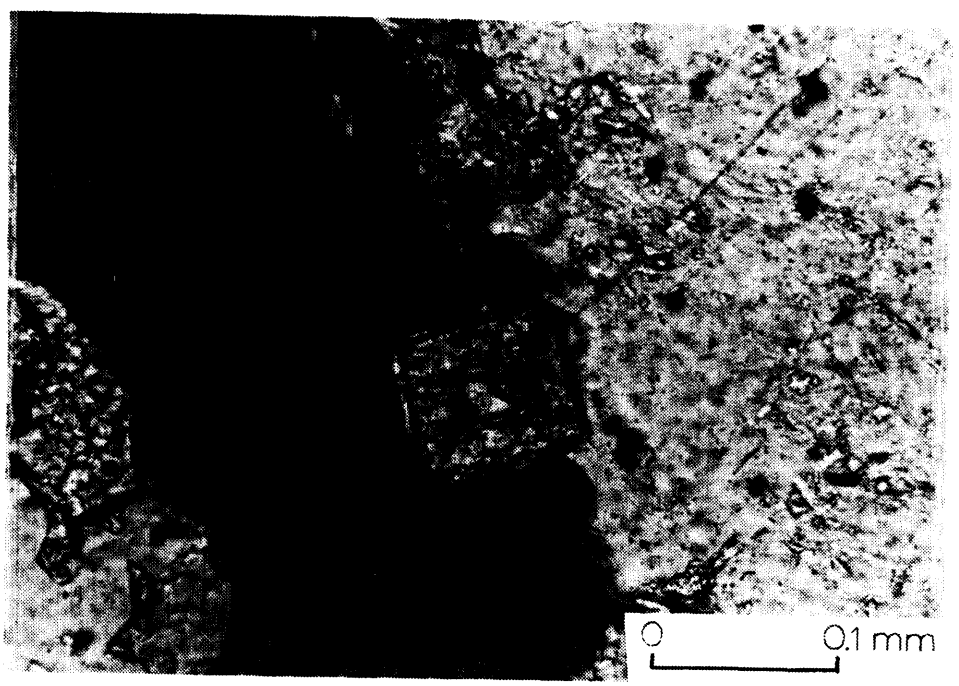

Table 1: Silver Production from the Mann Mine (McIlwaine, 1978)

| Year | Ounces of silver Produced |
|---|---|
| 1908-1920 | 98,822 |
| 1952 | 20,150 |
| 1968-1970 | 174,412 |
| 1984 | 30,000 |

Table 2: Ore Minerals Within the Gowganda Area Listed in Decreasing Abundance (Drake 1976)

| | | |
|---|---|---|
| Native Silver | Tetrahedrite | Galena |
| Lollingite | Smaltite | Niccolite |
| Skutteridite | Chloanthite | Breithauptite |
| Safflorite | Arsenopyrite | Chalcopyrite |
| Rammelsburgite | Cobaltite | Sphalerite |

Table 3: Production Figures for Castle Trethewey Mine

| Year | Ore and Conc shipped tons | Cobalt pounds | Silver ounces |
|---|---|---|---|
| 1920 | 45 | 254 | 48,373 |
| 1921 | 30 | - | 33,952 |
| 1922 | 9 | 1,530 | 40,098 |
| 1923 | 44 | 5,295 | 146,981 |
| 1924 | 163 | 15,994 | 544,575 |
| 1925 | 346 | 32,708 | 961,950 |
| 1926 | 313 | 32,443 | 979,890 |
| 1927 | 312 | 32,536 | 932,806 |
| 1928 | 310 | 33,557 | 800,968 |
| 1929 | 272 | 34,453 | 879,505 |
| 1930 | 238 | 47,125 | 723,226 |
| 1931 | 144 | 63,952 | 368,697 |
| 1979 to present | - | - | 2,800,000 |
| Total | - | 299,847 | 9,261,021 |

Table 4: Variation in Texture and Grain Size from the Chilled Magma to the Quartz Diabase

| Sample Number | Texture | Average clinopyroxene size (mm) |
|---|---|---|
| 0217 | quenched: (radiating Fan-like crystals of plagioclase and pyroxene) | 0.12 X 0.017 |
| 0067 | | 0.38 X 0.07 |
| 0099 and 0112 | quenched-diabase transition | 0.65 X 0.10 |
| | | 0.72 X 0.20 |
| 0069 | diabasic | 0.74 X 0.20 |
| 0072 | | |

Table 5: Modal Analyses Across the Milner Lake Intrusion

| Sample Number | 0067 | 0062 | 0103 | 0065 | 0064 | 0105 | 0106 | 0108 | 0101 | 0109 | 0100 | 0110 | 0112 |
|---|---|---|---|---|---|---|---|---|---|---|---|---|---|
| Quartz | 0.13 | 2.22 | 1.33 | 9.27 | 6.24 | 11.01 | 14.57 | 10.74 | 6.02 | 2.90 | 5.94 | 7.00 | 3.24 |
| Plagioclase | 35.13 | 53.57 | 43.14 | 29.7 | 50.46 | 38.99 | 44.90 | 51.96 | 56.94 | 53.65 | 45.97 | 41.76 | 30.61 |
| Clinopyroxene | 61.15 | 41.50 | 47.40 | 30.20 | 36.12 | 41.11 | 34.57 | 29.58 | 35.21 | 38.29 | 45.71 | 40.98 | 62.77 |
| Orthopyroxene | 0 | 0 | 0 | 0 | 0 | 0 | 0 | 0 | 0 | 0 | 0 | 0 | 0 |
| Olivine | 0.98 | 0 | 0 | 0 | 0 | 0 | 0 | 0 | 0 | 0 | 0 | 6.09 | 0.26 |
| Opaques | 2.70 | 2.46 | 7.06 | 6.62 | 4.65 | 5.84 | 4.90 | 6.40 | 1.70 | 2.14 | 2.11 | 3.12 | 2.46 |
| Chlorite* | 0 | 0 | 0 | 0 | 0 | 0 | 0.26 | 0.52 | 0.13 | 1.13 | 0 | 0.52 | 0 |
| Biotite* | 0 | 0 | 1.06 | 0 | 2.52 | 3.05 | 0.79 | 0.78 | 0 | 0.38 | 0.26 | 0.52 | 0.65 |
| Titanite | 0 | 0.25 | 0 | 0 | 0 | 0 | 0 | 0 | 0 | 1.51 | 0 | 0 | 0 |
| Potassic Feldspar | 0 | 0 | 0 | 24.2 | 0 | 0 | 0 | 0 | 0 | 0 | 0 | 0 | 0 |
| n | 780 | 812 | 751 | 755 | 753 | 754 | 755 | 764 | 764 | 794 | 757 | 771 | 771 |

All values are given in volume percent
The values include both the mineral and its alteration products
* Secondary biotite and chlorite for which the primary mineral is unknown

Table 6: Modal Analyses Across the Duncan Lake Intrusion

| Sample Number | 0069 | 0072 | 0073 | 0071 | 0074 | 0075 | 0076 | 0077 | 0079 | 0078 |
|---|---|---|---|---|---|---|---|---|---|---|
| Quartz | 3.56 | 4.61 | 2.10 | 1.45 | 3.78 | 2.59 | 7.71 | 10.64 | 7.62 | 11.37 |
| Plagioclase | 57.71 | 42.11 | 51.58 | 43.52 | 54.24 | 50.26 | 48.24 | 49.94 | 40.74 | 38.24 |
| Clinopyroxene | 37.29 | 46.71 | 42.76 | 47.49 | 23.21 | 24.35 | 36.99 | 34.50 | 46.65 | 45.35 |
| Orthopyroxene | 0 | 0 | 0.39 | 1.59 | 17.73 | 20.34 | 2.48 | 0 | 0 | 0 |
| Olivine | 0 | 2.5 | 0.13 | 0 | 0 | 0 | 0 | 0 | 0 | 0 |
| Hornblende | 0 | 0 | 0 | 0 | 0 | 0 | 0 | 1.29 | 0 | 0 |
| Opaques | 0.26 | 3.81 | 3.03 | 2.38 | 0.91 | 2.46 | 3.14 | 1.82 | 3.68 | 3.36 |
| Chlorite* | 0.53 | 0 | 0 | 0 | 0.13 | 0 | 1.44 | 0 | 0 | 0 |
| Biotite* | 0 | 0.26 | 0 | 0 | 0 | 0 | 0 | 1.82 | 0.66 | 1.68 |
| Titanite | 0.66 | 0 | 0 | 3.57 | 0 | 0 | 0 | 0 | 0.66 | 0 |
| n | 759 | 760 | 760 | 756 | 767 | 772 | 765 | 771 | 761 | 774 |

Table 7: Modal Analyses Across the Beaton Bay Intrusion

| Sample Number | 0099 | 0093 | 0098 | 0092 | 0097 | 0090 | 0096 | 0114 | 0113 | 0118 | 0117 |
|---|---|---|---|---|---|---|---|---|---|---|---|
| Quartz | 9.47 | 8.53 | 10.69 | 10.93 | 8.41 | 4.21 | 18.93 | 27.30 | 10.73 | 5.36 | 14.53 |
| Plagioclase | 29.34 | 52.10 | 48.24 | 48.53 | 47.17 | 49.34 | 38.80 | 31.56 | 48.48 | 39.22 | 52.93 |
| Clinopyroxene | 54.61 | 23.62 | 33.77 | 32.93 | 39.68 | 43.42 | 0 | 8.65 | 38.40 | 46.14 | 23.06 |
| Epidote | 0 | 0 | 0 | 0 | 0 | 0 | 0 | 0 | 0 | 1.70 | 0 |
| Opaques | 6.58 | 5.38 | 3.78 | 6.66 | 2.89 | 2.89 | 1.00 | 5.33 | 1.19 | 2.88 | 3.73 |
| Chlorite* | 0 | 0 | 2.99 | 0 | 1.84 | 0.13 | 12.93 | 2.93 | 0.93 | 0 | 0 |
| Biotite* | 0 | 8.27 | 0 | 0.66 | 0 | 0 | 0 | 0.53 | 0.26 | 4.71 | 0 |
| Hornblende | 0 | 1.44 | 0 | 0.28 | 0 | 0 | 0 | 0 | 0 | 0 | 0 |
| Titanite | 0 | 0 | 0.39 | 0 | 0 | 0 | 0 | 0 | 0 | 0 | 0 |
| Perthite | 0 | 0 | 0 | 0 | 0 | 0 | 28.27 | 19.71 | 0 | 0 | 4.67 |
| Apatite | 0 | 0 | 0 | 0 | 0 | 0 | tr | tr | 0 | 0 | 0 |
| calcite | 0 | 0.66 | 0 | 0 | 0 | 0 | 0 | 1.73 | 0 | 0 | 1.06 |
| n | 760 | 762 | 767 | 750 | 761 | 761 | 750 | 751 | 755 | 765 | 750 |

Table 8 Modal Analyses Across the Miller Lake Intrusion at the Castle Mine Site

| Sample Number | 0201 | 0202 | 0206 | 0208 | 0210 | 0211 | 0213 | 0242 | 0239 | 0235 | 0232 | 0231 |
|---|---|---|---|---|---|---|---|---|---|---|---|---|
| Quartz | 3.64 | 1.71 | 1.56 | 0.66 | 3.47 | 0.79 | 1.20 | 2.87 | 3.43 | 1.96 | 1.72 | 3.98 |
| Plagioclase | 49.02 | 45.85 | 45.63 | 54.43 | 44.09 | 46.56 | 40.61 | 39.37 | 48.88 | 48.30 | 58.20 | 46.35 |
| Clinopyroxene | 38.62 | 43.08 | 30.38 | 21.40 | 42.80 | 31.22 | 21.17 | 26.99 | 26.48 | 23.69 | 22.62 | 28.02 |
| Orthopyroxene | 4.94 | 3.69 | 20.73 | 21.27 | 8.23 | 21.03 | 36.09 | 20.38 | 18.71 | 25.26 | 16.67 | 20.32 |
| Olivine | 1.69 | 3.43 | 0.26 | 0.40 | 0.13 | 0.26 | 0.13 | 0 | 0 | 0 | 0 | 0 |
| Opaques | 2.08 | 1.84 | 1.30 | 1.71 | 1.02 | 0.13 | 0.80 | 0.39 | 1.71 | 0.78 | 0.79 | 1.06 |
| Chlorite* | 0 | 0.13 | 0.13 | 0.13 | 0.26 | 0 | 0 | 0 | 0.39 | 0 | 0 | 0 |
| Biotite* | 0 | 0.26 | 0 | 0 | 0 | 0 | 0 | 0 | 0.39 | 0 | 0 | 0 |
| Titanite | 0 | 0 | 0 | 0 | 0 | 0 | 0 | 0 | 0 | 0 | 0 | 0 |
| calcite | 0 | 0 | 0 | 0 | 0 | 0 | 0 | 0 | 0 | 0 | 0 | 0 |
| n(counts per slike) | 769 | 759 | 767 | 757 | 778 | 756 | 751 | 767 | 759 | 764 | 756 | 753 |

Table 9: $2V_X$ Angle Determinations in Orthopyroxene Across the Miller Lake Intrusion

| Sample Number | 2VX Grain 1 | Grain 2 | Grain 3 | Grain 4 | Grain 5 |
|---|---|---|---|---|---|
| 1987-DMC | | | | | |
| -0221 | 74 | | | | |
| -0223 | 86 | | | | |
| -0225 | 90 | 75 | | | |
| -0227 | 92 | 54.5 | 82core, 57 rim | 54 | 84 |
| -0229 | 77 | 79 | 78 | | |
| -0230 | 66 | | | | |
| -0232 | 70 | 69 | 64core, 50 rim | | |
| -0233 | 64 | 55 | 54 | | |
| -0235 | 68 | 75core, 56 rim | 66 | | |
| -0236 | 72 | 69core, 53 rim | | | |
| -0237 | 69* | 74 | 77 | 66 | |
| -0238 | 50 | 60 | | | |
| -0239 | 76 | | | | |
| -0241 | 93 | 84* | | | |
| -0242 | 68core, 50 rim | 82 | | | |
| -0213 | 80 | 86 | 68 | 56 | |
| -0211 | 68 | 76 | 84* | | |
| -0210 | 75.5* | | | | |
| -0209 | 79 | | | | |
| -0208 | 80* | | | | |
| -0206 | 86 | | | | |
| -0202 | 84 | 76 | | | |

- all values represent core measurements unless stated otherwise

* : 2V measurements determined by the direct conoscopic method

Table 10: Mg-Numbers of Orthopyroxene from the Miller Lake Intrusion

| Sample Number | Mg-number Grain 1 | Grain 2 | Grain 3 | Grain 4 | Grain 5 |
|---|---|---|---|---|---|
| 1987-DMC | | | | | |
| -0221 | 78.6 | | | | |
| -0223 | 85.5 | | | | |
| -0225 | 87.5 | 79.1 | | | |
| -0227 | 88.1 | 61.8 | 83.9core 65.2 rim | 61.1 | 84.5 |
| -0229 | 80.7 | 82.4 | 80.9 | | |
| -0230 | 73.5 | | | | |
| -0232 | 76 | 75.7 | 72 core, 54.5 rim | | |
| -0233 | 72 | 62.5 | 61.1 | | |
| -0235 | 75.2 | 79.1core 64.1 rim | 73.5 | | |
| -0236 | 77.6 | 75.7core, 60 rim | | | |
| -0237 | 75.9 | 78.6 | 80.7 | 73.5 | |
| -0238 | 54.5 | 68.2 | | | |
| -0239 | 79.8 | | | | |
| -0241 | 88.4 | 84.5 | | | |
| -0242 | 75.2core, 54.5 rim | 83.9 | | | |
| -0213 | 82.8 | 84.5 | | | |
| -0211 | 75.2 | 79.8 | 84.5 | | |
| -0210 | 81.1 | | | | |
| -0209 | 82.4 | | | | |
| -0208 | 82.8 | | | | |
| -0206 | 85.5 | | | | |
| -0202 | 84.5 | 79.8 | | | |

Table 11: $2V_X$ Angle Determinations of Orthopyroxene within the Duncan Lake Intrusion

| Sample Number | 2VX Grain 1 | Grain 2 |
|---|---|---|
| 1987-DMC-0075 | 66 | |
| -0074 | 72core, 54 rim | 78core, 58 rim |

Table 12: Mg-Numbers of Orthopyroxene within the Duncan Lake Intrusion

| Sample Number | Mg-number Grain 1 | Grain 2 |
|---|---|---|
| 1987-DMC-0075 | 73.5 | |
| -0074 | 77.6core, 61.1 rim | 81.5core, 58 rim |

Table 13a: Detection Limits and Precision for the Analyses of the Major Element Oxides

| Component | Fusion discs Range % | Precision % |
|---|---|---|
| $SiO_2$ | 30-80 | ±2.0 |
| $Al_2O_3$ | 0-20 | 0.4 |
| $Fe_2O_3$ | 0-15 | 0.6 |
| MgO | 0-20 | 0.3 |
| $Na_2O$ | 0-10 | 0.5 |
| $K_2O$ | 0-10 | 0.1 |
| CaO | 0-15 | 0.15 |
| $P_2O_5$ | 0-1 | 0.15 |
| $TiO_2$ | 0-3 | 0.16 |
| MnO | 0-1 | 0.015 |

Note: The precision quoted is the 95% confidence limit (2X the standard deviation (Ä)

Table 13b: Detection Limits and Precision for the Analyses of FeO, $CO_2$, S, $H_2O+$, $H_2O-$ and LOI

| Component | Method | Detection Limit(%) | Precision @ MRV(%) | MRV % |
|---|---|---|---|---|
| LOI | Gravimetric | 0.4 | ±0.4 | 4 |
| FeO | Volumetric | 0.2 | 0.2 | 5 |
| $CO_2$ (Total C) | IR | 0.05 | 0.06 | 2 |
| S | IR | 0.03 | 0.02 | 0.1 |
| $H_2O+$ | IR | 0.2 | 0.6 | 2 |
| $H_2O$ | Gravimetric | 0.05 | 0.1 | 0.5 |

Table 14: Detection Limits and Precision for the Analyses of the Trace Elements: Nb, Rb, Sr, Th, Y, and Zr

| Element | Method | Detection Limit (PPM) | Optimum Range (PPM) | Precision @10X Detection Limit |
|---|---|---|---|---|
| Nb | XRF | 5 | 5-1000 | 10 |
| Rb | XRF | 5 | 5-1000 | 5 |
| Sr | XRF | 5 | 5-1000 | 5 |
| Th | XRF | 10 | 10-5000 | 15 |
| Y | XRF | 5 | 5-1000 | 10 |
| Zr | XRF | 5 | 5-1000 | 10 |

Table 15: Major Element Concentrations Across the Duncan Lake Intrusion

| Sample No. | $SiO_2$ | $Al_2O_3$ | $Fe_2O_3$ | FeO | MgO | CaO | $Na_2O$ | $K_2O$ | $TiO_2$ | $P_2O_5$ | MnO | $CO_2$ | S | $H_2O^+$ | $H_2O^-$ | LOI | Total | Mg-No. (atomic) |
|---|---|---|---|---|---|---|---|---|---|---|---|---|---|---|---|---|---|---|
| 0078 | 52.1 | 13.9 | 3.27 | 8.85 | 6.15 | 7.60 | 2.47 | 1.57 | 1.04 | 0.07 | 0.22 | 0.23 | 0.10 | 2.23 | 0.00 | 1.7 | 99.8 | 0.553 |
| 0079 | 50.2 | 13.8 | 3.81 | 8.19 | 6.16 | 6.80 | 1.90 | 2.19 | 0.96 | 0.05 | 0.20 | 1.69 | 0.10 | 2.49 | 0.24 | 3.6 | 98.8 | 0.573 |
| 0077 | 53.6 | 12.7 | 4.40 | 10.8 | 3.56 | 5.30 | 4.18 | 0.99 | 1.65 | 0.17 | 0.26 | 0.27 | 0.06 | 2.08 | 0.00 | 1.4 | 10.00 | 0.370 |
| 0075 | 51.2 | 15.0 | 2.15 | 7.05 | 7.35 | 9.02 | 2.07 | 2.19 | 0.65 | 0.06 | 0.19 | 0.50 | 0.07 | 2.39 | 0.00 | 2.5 | 99.9 | 0.650 |
| 0074 | 51.5 | 16.0 | 1.84 | 6.66 | 7.06 | 9.92 | 2.12 | 1.75 | 0.63 | 0.04 | 0.16 | 0.15 | 0.07 | 1.87 | 0.05 | 1.5 | 99.7 | 0.654 |
| 0073 | 51.3 | 15.1 | 2.13 | 7.72 | 7.15 | 10.4 | 2.19 | 0.86 | 0.61 | 0.05 | 0.15 | 0.18 | 0.08 | 0.90 | 0.00 | 1.6 | 98.8 | 0.623 |
| 0072 | 51.0 | 14.3 | 2.37 | 8.58 | 7.34 | 9.07 | 2.18 | 1.60 | 0.74 | 0.04 | 0.18 | 0.25 | 0.10 | 2.11 | 0.00 | 1.6 | 99.8 | 0.604 |
| 0069 | 52.6 | 18.5 | 2.28 | 8.12 | 5.74 | 0.30 | 6.06 | 0.06 | 0.95 | 0.07 | 0.06 | 0.14 | 0.02 | 4.19 | 0.08 | 3.6 | 99.2 | 0.557 |

Table 16: Major Element Concentrations Across the Beaton Bay Intrusion

| Sample No. | $SiO_2$ | $Al_2O_3$ | $Fe_2O_3$ | FeO | MgO | CaO | $Na_2O$ | $K_2O$ | $TiO_2$ | $P_2O_5$ | MnO | $CO_2$ | S | $H_2O^+$ | $H_2O^-$ | LOI | Total | Mg-No. (atomic) |
|---|---|---|---|---|---|---|---|---|---|---|---|---|---|---|---|---|---|---|
| 0118 | 52.0 | 14.1 | 3.47 | 8.58 | 5.54 | 7.38 | 2.70 | 1.98 | 1.02 | 0.08 | 0.20 | 0.26 | 0.09 | 2.23 | 0.00 | 1.0 | 99.6 | 0.535 |
| 0116 | 50.1 | 13.1 | 3.80 | 9.33 | 5.15 | 5.24 | 2.96 | 1.52 | 1.02 | 0.11 | 0.21 | 2.85 | 0.11 | 3.40 | 0.40 | 5.0 | 99.3 | 0.496 |
| 0117 | 56.7 | 13.8 | 4.12 | 6.46 | 4.49 | 2.80 | 4.71 | 0.84 | 1.00 | 0.14 | 0.17 | 1.25 | 0.07 | 2.80 | 0.31 | 3.3 | 99.6 | 0.553 |
| 0113 | 51.6 | 14.2 | 3.01 | 8.45 | 5.81 | 7.75 | 3.23 | 1.61 | 0.65 | 0.06 | 0.21 | 0.53 | 0.08 | 2.74 | 0.00 | 2.5 | 99.9 | 0.551 |
| 0114 | 61.2 | 12.7 | 5.19 | 7.03 | 2.29 | 1.91 | 5.70 | 0.19 | 1.00 | 0.26 | 0.16 | 0.25 | 0.01 | 1.68 | 0.00 | 1.2 | 99.6 | 0.367 |
| 0094 | 51.7 | 14.1 | 4.32 | 8.98 | 5.46 | 3.70 | 4.13 | 0.92 | 1.16 | 0.12 | 0.25 | 0.31 | 0.11 | 3.24 | 0.27 | 2.7 | 98.8 | 0.520 |
| 0095 | 52.5 | 12.7 | 6.70 | 9.45 | 2.76 | 3.62 | 4.98 | 0.88 | 1.47 | 0.19 | 0.23 | 0.75 | 0.01 | 1.80 | 0.17 | 1.4 | 99.2 | 0.342 |
| 0096 | 63.6 | 14.2 | 2.97 | 5.52 | 1.65 | 0.76 | 5.33 | 1.88 | 0.88 | 0.20 | 0.05 | 0.44 | 0.01 | 2.00 | 0.00 | 1.6 | 99.5 | 0.348 |
| 0090 | 51.4 | 14.7 | 2.77 | 7.23 | 6.30 | 8.88 | 2.69 | 1.88 | 0.76 | 0.07 | 0.17 | 0.16 | 0.10 | 2.28 | 0.18 | 2.0 | 99.6 | 0.608 |
| 0091 | 52.4 | 13.7 | 3.10 | 10.2 | 4.76 | 7.61 | 3.01 | 1.38 | 0.99 | 0.09 | 0.18 | 0.11 | 0.10 | 2.47 | 0.00 | 1.6 | 100.0 | 0.454 |
| 0097 | 52.1 | 13.9 | 3.16 | 8.32 | 5.55 | 7.92 | 2.41 | 2.15 | 0.90 | 0.09 | 0.19 | 0.19 | 0.08 | 2.28 | 0.07 | 1.5 | 99.3 | 0.543 |
| 0092 | 52.9 | 13.6 | 4.10 | 9.78 | 4.03 | 6.13 | 3.39 | 1.60 | 1.23 | 0.12 | 0.24 | 0.08 | 0.14 | 2.20 | 0.00 | 1.7 | 99.5 | 0.423 |
| 0098 | 52.0 | 13.8 | 3.40 | 7.92 | 5.27 | 8.11 | 2.91 | 1.96 | 0.92 | 0.12 | 0.17 | 0.30 | 0.09 | 2.17 | 0.24 | 2.0 | 99.4 | 0.543 |
| 0093 | 54.4 | 12.7 | 5.40 | 9.25 | 3.30 | 3.94 | 5.05 | 1.00 | 1.37 | 0.14 | 0.31 | 0.42 | 0.16 | 1.91 | 0.21 | 1.4 | 99.6 | 0.389 |
| 0099 | 51.5 | 14.4 | 3.00 | 8.19 | 6.27 | 9.17 | 2.04 | 1.48 | 0.85 | 0.06 | 0.18 | 0.20 | 0.10 | 2.12 | 0.09 | 1.5 | 99.6 | 0.577 |

Table 17: Major Element Concentrations Across the Miller Lake Intrusion

| Sample No. | $SiO_2$ | $Al_2O_3$ | $Fe_2O_3$ | FeO | MgO | CaO | $Na_2O$ | $K_2O$ | $TiO_2$ | $P_2O_5$ | MnO | $CO_2$ | S | $H_2O^+$ | $H_2O^-$ | LOI | Total | Mg-No. (atomic) |
|---|---|---|---|---|---|---|---|---|---|---|---|---|---|---|---|---|---|---|
| 0217 | 51.9 | 14.7 | 2.77 | 7.05 | 6.73 | 7.48 | 3.45 | 1.42 | 0.65 | 0.06 | 0.31 | 0.09 | 0.07 | 2.58 | 0.15 | 1.9 | 99.4 | 0.630 |
| 0218 | 50.9 | 14.8 | 1.58 | 7.85 | 7.10 | 10.2 | 1.62 | 2.00 | 0.57 | 0.03 | 0.19 | 0.07 | 0.09 | 2.40 | 0.00 | 1.7 | 99.4 | 0.617 |
| 0220 | 50.2 | 14.6 | 1.56 | 7.59 | 8.20 | 10.1 | 1.99 | 1.27 | 0.52 | 0.02 | 0.21 | 0.09 | 0.07 | 3.24 | 0.00 | 2.5 | 99.6 | 0.651 |
| 0225 | 51.2 | 15.3 | 1.40 | 6.59 | 9.66 | 11.3 | 1.15 | 0.92 | 0.37 | 0.01 | 0.16 | 0.11 | 0.06 | 1.84 | 0.07 | 1.2 | 100.1 | 0.723 |
| 0228 | 52.2 | 15.8 | 1.68 | 7.85 | 6.18 | 10.7 | 2.19 | 0.70 | 0.52 | 0.03 | 0.18 | 0.06 | 0.10 | 1.70 | 0.00 | 1.1 | 99.9 | 0.584 |
| 0229 | 51.6 | 15.6 | 1.63 | 7.72 | 7.12 | 11.1 | 1.62 | 0.69 | 0.55 | 0.04 | 0.17 | 0.07 | 0.11 | 1.96 | 0.00 | 1.5 | 99.9 | 0.622 |
| 0230 | 51.5 | 15.5 | 1.71 | 8.45 | 7.25 | 11.2 | 1.75 | 0.42 | 0.47 | 0.03 | 0.20 | 0.05 | 0.11 | 1.33 | 0.06 | 0.8 | 100.0 | 0.605 |
| 0232 | 51.1 | 16.7 | 1.86 | 6.92 | 7.12 | 11.2 | 1.59 | 0.74 | 0.46 | 0.01 | 0.17 | 0.09 | 0.09 | 1.77 | 0.05 | 1.3 | 99.8 | 0.647 |
| 0236 | 50.1 | 15.5 | 1.75 | 6.32 | 9.19 | 9.28 | 1.22 | 2.73 | 0.35 | 0.01 | 0.16 | 0.83 | 0.06 | 2.38 | 0.00 | 2.8 | 99.9 | 0.722 |
| 0237 | 51.7 | 12.9 | 1.52 | 7.19 | 11.00 | 10.1 | 1.29 | 1.09 | 0.39 | 0.00 | 0.17 | 0.06 | 0.06 | 2.19 | 0.00 | 1.5 | 99.6 | 0.732 |
| 0238 | 45.3 | 14.8 | 1.67 | 6.79 | 6.76 | 10.5 | 1.84 | 2.03 | 0.43 | 0.02 | 0.18 | 5.25 | 0.04 | 3.33 | 0.00 | 6.0 | 98.9 | 0.640 |
| 0240 | 51.1 | 16.0 | 1.39 | 6.66 | 8.76 | 10.7 | 1.30 | 1.26 | 0.41 | 0.02 | 0.16 | 0.13 | 0.06 | 1.92 | 0.05 | 1.5 | 100.0 | |
| 0242 | 51.6 | 14.1 | 1.18 | 7.39 | 10.8 | 10.1 | 1.32 | 0.78 | 0.36 | 0.01 | 0.17 | 0.13 | 0.06 | 1.54 | 0.00 | 1.1 | 99.5 | 0.723 |
| 0216 | 48.0 | 14.1 | 1.30 | 7.19 | 11.4 | 8.23 | 1.94 | 1.38 | 0.34 | 0.03 | 0.22 | 1.10 | 0.04 | 4.22 | 0.18 | 4.5 | 99.7 | 0.739 |
| 0215 | 48.5 | 14.7 | 1.16 | 6.66 | 9.87 | 10.8 | 1.66 | 1.47 | 0.32 | 0.01 | 0.19 | 1.11 | 0.05 | 3.02 | 0.09 | 3.4 | 99.6 | 0.726 |
| 0214 | 43.9 | 15.8 | 1.12 | 5.46 | 7.38 | 13.2 | 2.97 | 10.5 | 0.38 | 0.03 | 0.27 | 5.31 | 0.04 | 3.01 | 0.07 | 7.8 | 99.9 | 0.707 |
| 0212 | 41.2 | 14.2 | 1.30 | 5.59 | 6.75 | 15.5 | 2.42 | 1.04 | 0.32 | 0.02 | 0.33 | 8.02 | 0.04 | 2.71 | 0.11 | 10.1 | 99.5 | 0.683 |
| 0210 | 50.9 | 15.7 | 0.96 | 6.66 | 8.42 | 11.6 | 1.84 | 0.67 | 0.32 | 0.01 | 0.15 | 0.14 | 0.07 | 2.11 | 0.05 | 1.6 | 99.6 | 0.693 |
| 0208 | 50.0 | 15.3 | 1.2 | 7.19 | 10.2 | 10.5 | 1.30 | 0.59 | 0.37 | 0.01 | 0.16 | 0.10 | 0.06 | 2.17 | 0.00 | 1.7 | 99.1 | 0.717 |
| 0206 | 50.8 | 14.0 | 1.31 | 7.65 | 10.5 | 9.47 | 1.46 | 1.42 | 0.45 | 0.03 | 0.17 | 0.08 | 0.07 | 2.10 | 0.10 | 1.6 | 99.6 | 0.710 |
| 0205 | 49.7 | 14.6 | 1.20 | 7.65 | 8.82 | 9.33 | 2.44 | 2.00 | 0.51 | 0.03 | 0.20 | 0.19 | 0.07 | 3.12 | 0.00 | 2.5 | 99.8 | 0.673 |
| 0203 | 50.1 | 14.5 | 2.37 | 7.32 | 7.65 | 9.73 | 1.94 | 1.87 | 0.62 | 0.03 | 0.18 | 0.12 | 0.09 | 2.66 | 0.06 | 2.2 | 99.2 | 0.651 |
| 0202 | 50.4 | 14.7 | 1.58 | 8.12 | 8.69 | 9.78 | 1.56 | 1.87 | 0.55 | 0.03 | 0.18 | 0.09 | 0.06 | 2.09 | 0.00 | 1.4 | 99.7 | 0.656 |
| 0201 | 50.6 | 15.0 | 2.67 | 7.59 | 7.76 | 8.78 | 1.64 | 2.26 | 0.64 | 0.04 | 0.29 | 0.30 | 0.08 | 2.21 | 0.00 | 1.9 | 99.8 | 0.646 |

Table 18: Major Element Concentrations Across the Milner Lake Intrusion

| Sample No. | $SiO_2$ | $Al_2O_3$ | $Fe_2O_3$ | FeO | MgO | CaO | $Na_2O$ | $K_2O$ | $TiO_2$ | $P_2O_5$ | MnO | $CO_2$ | S | $H_2O^+$ | $H_2O^-$ | LOI | Total | Mg-No. (atomic) |
|---|---|---|---|---|---|---|---|---|---|---|---|---|---|---|---|---|---|---|
| 0112 | 51.2 | 14.3 | 2.65 | 8.78 | 6.79 | 9.29 | 1.86 | 0.89 | 0.72 | 0.05 | 0.22 | 0.42 | 0.08 | 2.40 | 0.15 | 2.0 | 99.8 | 0.580 |
| 0110 | 5.04 | 2.81 | 8.72 | 8.72 | 7.99 | 8.32 | 1.86 | 1.45 | 0.81 | 0.05 | 0.18 | 0.28 | 0.06 | 2.70 | 0.00 | 2.1 | 99.6 | 0.620 |
| 0109 | 51.1 | 14.3 | 3.70 | 9.98 | 4.09 | 6.26 | 3.68 | 2.06 | 1.27 | 0.09 | 0.18 | 0.36 | 0.19 | 2.34 | 0.12 | 1.7 | 99.7 | 0.422 |
| 0106 | 53.3 | 12.2 | 4.40 | 12.0 | 2.70 | 4.52 | 3.94 | 1.67 | 1.74 | 0.15 | 0.24 | 0.61 | 0.13 | 1.95 | 0.00 | 1.7 | 99.5 | 0.286 |
| 0105 | 52.3 | 11.9 | 4.50 | 13.0 | 2.44 | 6.12 | 2.95 | 1.70 | 1.99 | 0.15 | 0.27 | 0.18 | 0.08 | 2.26 | 0.00 | 1.1 | 99.8 | 0.051 |
| 0065 | 55.0 | 12.4 | 5.60 | 10.2 | 2.84 | 3.03 | 4.73 | 1.61 | 1.53 | 0.21 | 0.21 | 0.15 | 0.06 | 1.78 | 0.22 | 1.2 | 99.6 | 0.332 |
| 0063 | 54.6 | 12.5 | 5.10 | 10.0 | 3.16 | 4.66 | 4.34 | 1.21 | 1.34 | 0.16 | 0.25 | 0.24 | 0.05 | 2.09 | 0.18 | 1.3 | 99.9 | 0.360 |
| 0062 | 50.1 | 13.8 | 2.40 | 9.18 | 6.94 | 7.81 | 3.38 | 1.17 | 0.88 | 0.08 | 0.20 | 0.08 | 0.10 | 2.61 | 0.14 | 2.2 | 98.9 | 0.574 |
| 0100 | 50.7 | 16.1 | 1.93 | 7.72 | 6.16 | 9.96 | 2.42 | 1.41 | 0.89 | 0.05 | 0.16 | 0.60 | 0.06 | 2.06 | 0.07 | 2.0 | 100.0 | 0.587 |
| 0101 | 51.0 | 16.4 | 2.04 | 712 | 5.75 | 10.3 | 2.14 | 1.14 | 0.68 | 0.05 | 0.15 | 0.40 | 0.07 | 2.21 | 0.14 | 1.7 | 99.6 | 0.590 |
| 0103 | 49.8 | 12.6 | 5.20 | 12.3 | 3.56 | 5.40 | 3.84 | 1.24 | 1.84 | 0.12 | 0.38 | 0.20 | 0.16 | 2.55 | 0.17 | 1.6 | 99.3 | 0.340 |
| 0104 | 53.4 | 12.4 | 5.97 | 8.58 | 3.32 | 4.13 | 5.93 | 0.73 | 1.52 | 0.14 | 0.34 | 0.42 | 0.14 | 1.59 | 0.00 | 1.6 | 98.6 | 0.408 |
| 0067 | 50.1 | 14.1 | 3.43 | 7.72 | 6.87 | 7.96 | 3.01 | 1.45 | 0.87 | 0.05 | 0.23 | 1.01 | 0.12 | 2.31 | 0.06 | 2.4 | 99.3 | 0.613 |

Table 19: The Mg-numbers of chilled Nipissing phase from the Gowganda, Cobalt, and Temagami

| Intrusion | Chill | | Mg# | Area |
|---|---|---|---|---|
| | Upper | Lower | | |
| Milner Lake | x | | 0.580 | } |
| Milner Lake | | x | 0.613 | } |
| Beaton Bay | | x | 0.577 | } * |
| Duncan Lake | x | | 0.553 | }Gowganda |
| Duncan Lake | | x | 0.557 | } |
| Miller Lake | x | | 0.630 | } |
| Portage Bay | x | | 0.536 | } ** |
| Portage Bay | | x | 0.550 | }Cobalt |
| Temagami | | x | 0.66 | } |
| Temagami | | x | 0.68 | } *** |
| Temagami | | x | 0.64 | } |
| Temagami | | x | 0.70 | }Temagami |
| Temagami | | x | 0.60 | } |

* data from the present study
** data from Conrod (1988)
*** data from Lightfoot et al. (1987)

Table 20: Trace Element Concentration Across the Duncan Lake Intrusion

| Sample Number | Nb | Rb | Sr | Y | Zr | Th |
|---|---|---|---|---|---|---|
| 0078 | -5 | 68 | 150 | 21 | 103 | 12 |
| 0079 | -5 | 91 | 130 | 17 | 89 | 12 |
| 0077 | -5 | 43 | 147 | 33 | 154 | -10 |
| 0076 | -5 | 45 | 204 | 16 | 93 | -10 |
| 0075 | -5 | 80 | 191 | 13 | 78 | -10 |
| 0074 | -5 | 65 | 202 | 12 | 78 | -10 |
| 0071 | -5 | 98 | 177 | 18 | 93 | -10 |
| 0073 | -5 | 39 | 199 | 17 | 84 | -10 |
| 0072 | -5 | 66 | 169 | 14 | 80 | 11 |
| 0069 | -5 | -5 | 22 | 18 | 86 | -10 |

Note:

The negative values indicate that the concentration of that particular element is below the detection limit for the method of analyses

Table 21: Trace Element Concentration Across the Beaton Bay Intrusion

| Sample Number | Nb | Rb | Sr | Y | Zr | Th |
|---|---|---|---|---|---|---|
| 0117 | -5 | 31 | 103 | 31 | 147 | 13 |
| 0116 | -5 | 65 | 129 | 24 | 118 | -10 |
| 0113 | -5 | 63 | 145 | 17 | 88 | -10 |
| 0118 | -5 | 89 | 156 | 20 | 118 | -10 |
| 0114 | 8 | -5 | 48 | 53 | 239 | 14 |
| 0094 | -5 | 36 | 163 | 27 | 133 | 10 |
| 0095 | -5 | 36 | 120 | 37 | 164 | -10 |
| 0096 | 6 | 27 | 23 | 25 | 159 | 15 |
| 0090 | -5 | 81 | 190 | 16 | 105 | -10 |
| 0091 | -5 | 63 | 196 | 22 | 117 | -10 |
| 0097 | -5 | 95 | 152 | 20 | 114 | 13 |
| 0092 | -5 | 75 | 201 | 28 | 145 | 12 |
| 0098 | -5 | 84 | 139 | 22 | 111 | 10 |
| 0093 | -5 | 46 | 132 | 37 | 159 | -10 |
| 0099 | -5 | 58 | 194 | 19 | 91 | -10 |

Table 22: Trace Element Concentration Across the Milner Lake Intrusion

| Sample Number | Nb | Rb | Sr | Y | Zr | Th |
|---|---|---|---|---|---|---|
| 0112 | -5 | 40 | 150 | 19 | 85 | -10 |
| 0111 | -5 | 61 | 153 | 17 | 84 | -10 |
| 0110 | -5 | 61 | 157 | 18 | 83 | -10 |
| 0100 | -5 | 61 | 194 | 13 | 84 | -10 |
| 0109 | 8 | 87 | 145 | 21 | 115 | -10 |
| 0101 | -5 | 48 | 205 | 13 | 82 | -10 |
| 0108 | -5 | 57 | 129 | 36 | 156 | 12 |
| 0107 | 5 | 68 | 145 | 37 | 164 | -10 |
| 0106 | 6 | 65 | 140 | 37 | 167 | -10 |
| 0105 | -5 | 52 | 192 | 37 | 169 | 10 |
| 0064 | 5 | 79 | 132 | 37 | 169 | 10 |
| 0102 | -5 | 36 | 159 | 27 | 119 | -10 |
| 0065 | -5 | 42 | 93 | 39 | 174 | 12 |
| 0104 | -5 | 29 | 89 | 35 | 158 | -10 |
| 0103 | +5 | 50 | 134 | 32 | 148 | 11 |
| 0063 | -5 | 66 | 116 | 34 | 162 | -10 |
| 0062 | -5 | 48 | 171 | 18 | 99 | -10 |
| 0067 | -5 | 62 | 143 | 17 | 85 | -10 |

Table 23: Trace Element Concentration Across the Milner Lake Intrusion

| Sample Number | Nb | Rb | Sr | Y | Zr | Th |
|---|---|---|---|---|---|---|
| 0236 | -5 | 94 | 94 | -5 | 47 | -10 |
| 0237 | -5 | 44 | 90 | 9 | 50 | -10 |
| 0238 | -5 | 85 | 82 | 14 | 55 | 11 |
| 0239 | -5 | 55 | 116 | 12 | 61 | -10 |
| 0240 | -5 | 48 | 121 | 9 | 58 | -10 |
| 0241 | -5 | 31 | 120 | 12 | 58 | -10 |
| 0242 | -5 | 32 | 123 | 11 | 55 | -10 |
| 0216 | -5 | 51 | 66 | 10 | 47 | -10 |
| 0215 | -5 | 58 | 97 | 10 | 49 | -10 |
| 0214 | -5 | 45 | 100 | 13 | 51 | -10 |
| 0213 | -5 | 37 | 111 | 9 | 55 | -10 |
| 0212 | -5 | 46 | 97 | 25 | 51 | -10 |
| 0211 | -5 | 21 | 116 | 14 | 57 | -10 |
| 0210 | -5 | 29 | 116 | 9 | 53 | -10 |
| 0209 | -5 | 33 | 123 | 13 | 64 | -10 |
| 0208 | -5 | 22 | 128 | 11 | 57 | 12 |
| 0297 | -5 | 56 | 112 | 9 | 61 | -10 |
| 0217 | -5 | 41 | 127 | 22 | 80 | -10 |
| 0218 | 5 | 80 | 130 | 16 | 72 | -10 |
| 0219 | -5 | 64 | 144 | 16 | 72 | -10 |
| 0220 | -5 | 49 | 142 | 15 | 67 | 11 |
| 0221 | -5 | 50 | 126 | 13 | 64 | -10 |
| 0223 | -5 | 52 | 126 | 11 | 61 | 11 |
| 0224 | -5 | 47 | 117 | 12 | 58 | -10 |
| 0225 | -5 | 33 | 129 | 10 | 54 | -10 |
| 0226 | -5 | 23 | 131 | 13 | 63 | -10 |
| 0227 | -5 | 16 | 118 | 15 | 65 | -10 |
| 0228 | -5 | 31 | 137 | 16 | 71 | -10 |
| 0230 | -5 | 15 | 134 | 12 | 60 | -10 |
| 0231 | -5 | 23 | 123 | 15 | 67 | -10 |
| 0232 | -5 | 33 | 136 | 14 | 61 | -10 |
| 0233 | -5 | 48 | 128 | 14 | 61 | -10 |
| 0235 | -5 | 45 | 114 | 11 | 57 | -10 |
| 0206 | -5 | 52 | 119 | 10 | 63 | -10 |
| 0205 | -5 | 79 | 116 | 12 | 63 | 12 |
| 0204 | -5 | 100 | 142 | 12 | 70 | -10 |
| 0203 | -5 | 72 | 131 | 13 | 77 | -10 |
| 0202 | -5 | 71 | 137 | 14 | 70 | -10 |
| 0201 | -5 | 88 | 151 | 15 | 75 | 10 |

Table 24: Zr, Y and $TiO_2$ Contents of Chilled Nipissing Phases from the Cobalt, Gowganda and Temagami Areas

| Sample Number | Intrusion | Area | Upper Contact | Lower Contact | (ppm) | Zr (ppm) | Y | Zr/Y (wt%) | $TiO_2$ | |
|---|---|---|---|---|---|---|---|---|---|---|
| PB-951 | Portage Bay | Cobalt | X | | | | 60.32 | 15.73 | 3.83 | 0.77 |
| PB-747 | Portage Bay | Cobalt | | | X | | 72.26 | 17.43 | 4.15 | 0.80 |
| TM-86/148 | N.W. Lake Temagami | Temagami | | X | | 61.00 | 17.00 | 3.59 | 0.61 | |
| TM-86/141 | E. Lake Temagami | Temagami | | | X | | 60.00 | 16.00 | 3.75 | 0.63 |
| TM-86/136 | SW Lake Temagami | Temagami | | | X | | 70.00 | 17.00 | 4.12 | 0.72 |
| ML-0217 | Miller Lake | Gowganda | X | | | | 66.00 | 18.00 | 3.67 | 0.66 |
| MR-0112 | Milner Lake | Gowganda | X | | | | 80.00 | 22.00 | 4.54 | 0.65 |
| MR-0067 | Milner Lake | Gowganda | | | X | | 85.00 | 19.00 | 4.47 | 0.72 |
| DL-0072 | Duncan Lake | Gowganda | | | X | | 85.00 | 17.00 | 5.00 | 0.87 |
| DL-0078 | Duncan Lake | Gowganda | X | | | | 103.0 | 21.00 | 4.90 | 1.04 |
| BB-0099 | Beaton Bay | Gowganda | | X | | 91.00 | 19 | 4.79 | 0.85 | |

Table 25: Preliminary Results of the U-Pb Age Determination on the Bonanza Lake Granodiorite

| Sample Number | Number of grains used in the analyses | $Pb^{207}/Pb^{206}$ age (m.y.) | Percent discordant (percent of common Pb lost) |
|---|---|---|---|
| WL 636 | 4 | 2210 | 1.2% |
| WL 182 | 6 | 2214 | 2.3% |

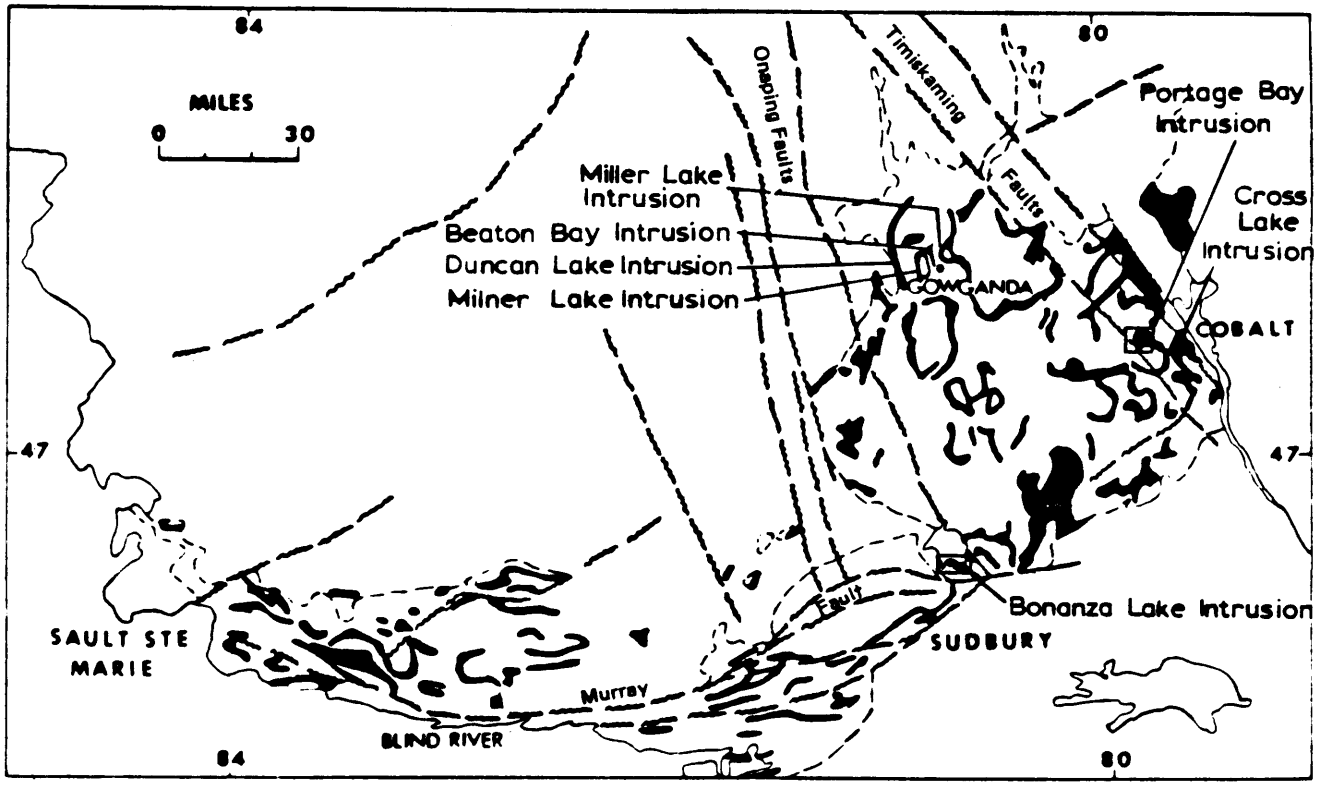


Figure 1. Distribution of Nipissing Intrusions across northern Ontario.

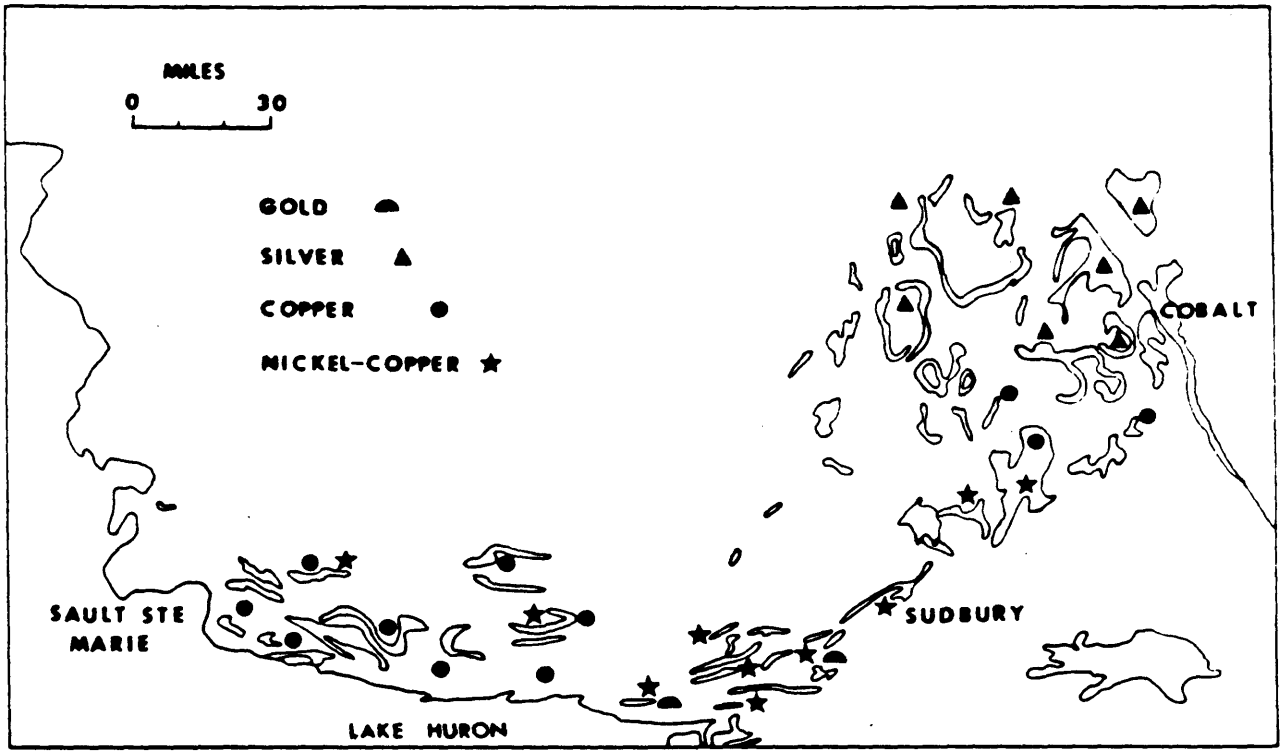


Figure 2. Variation in the type of mineralization spatially associated with Nipissing Intrusions across northern Ontario.

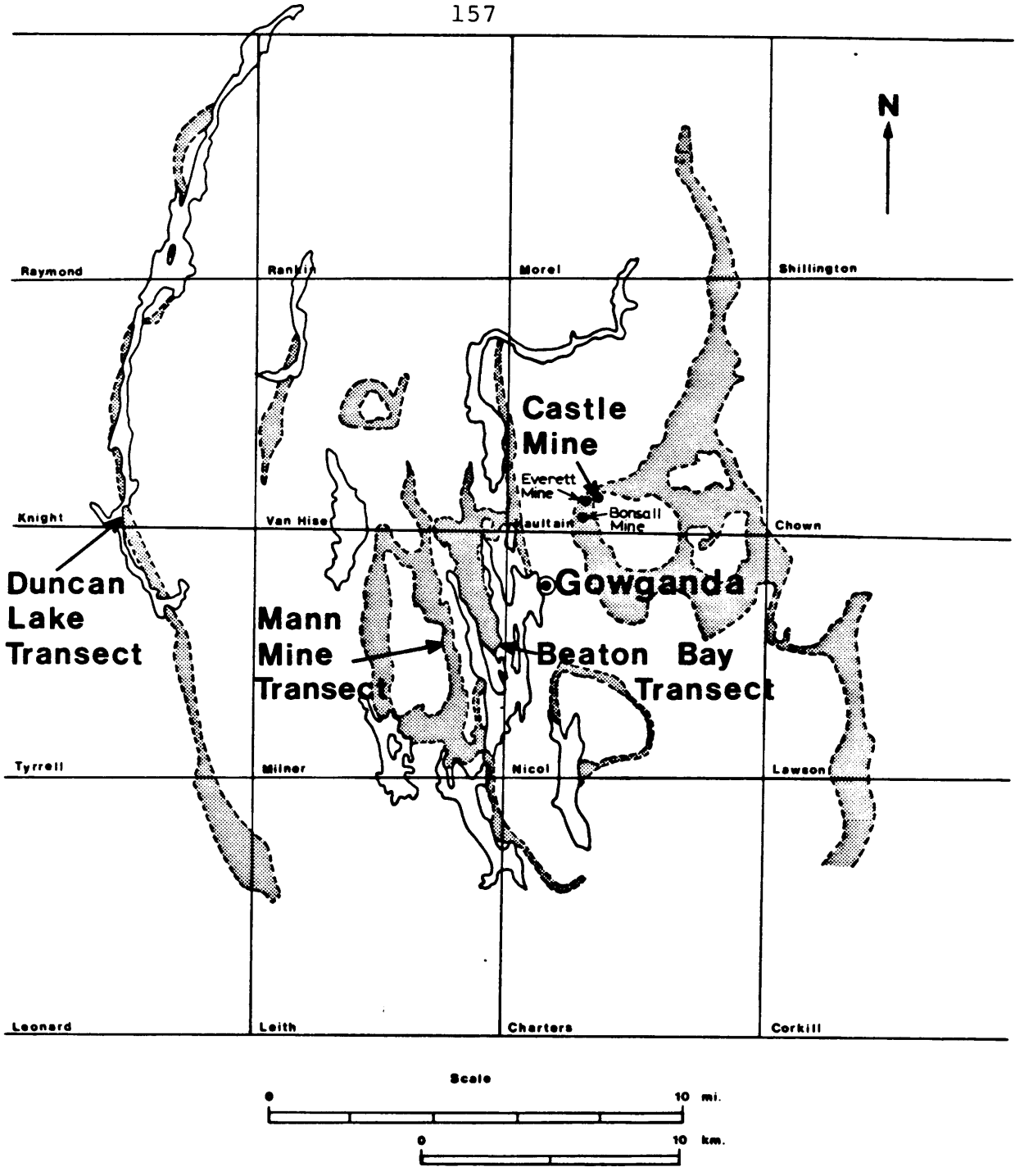


Figure 3. Location of the Duncan Lake, Milner Lake, Beaton Bay, and Miller Lake Nipissing intrusions.

Figure 4. Sample collection sites across the Duncan Lake Intrusion.

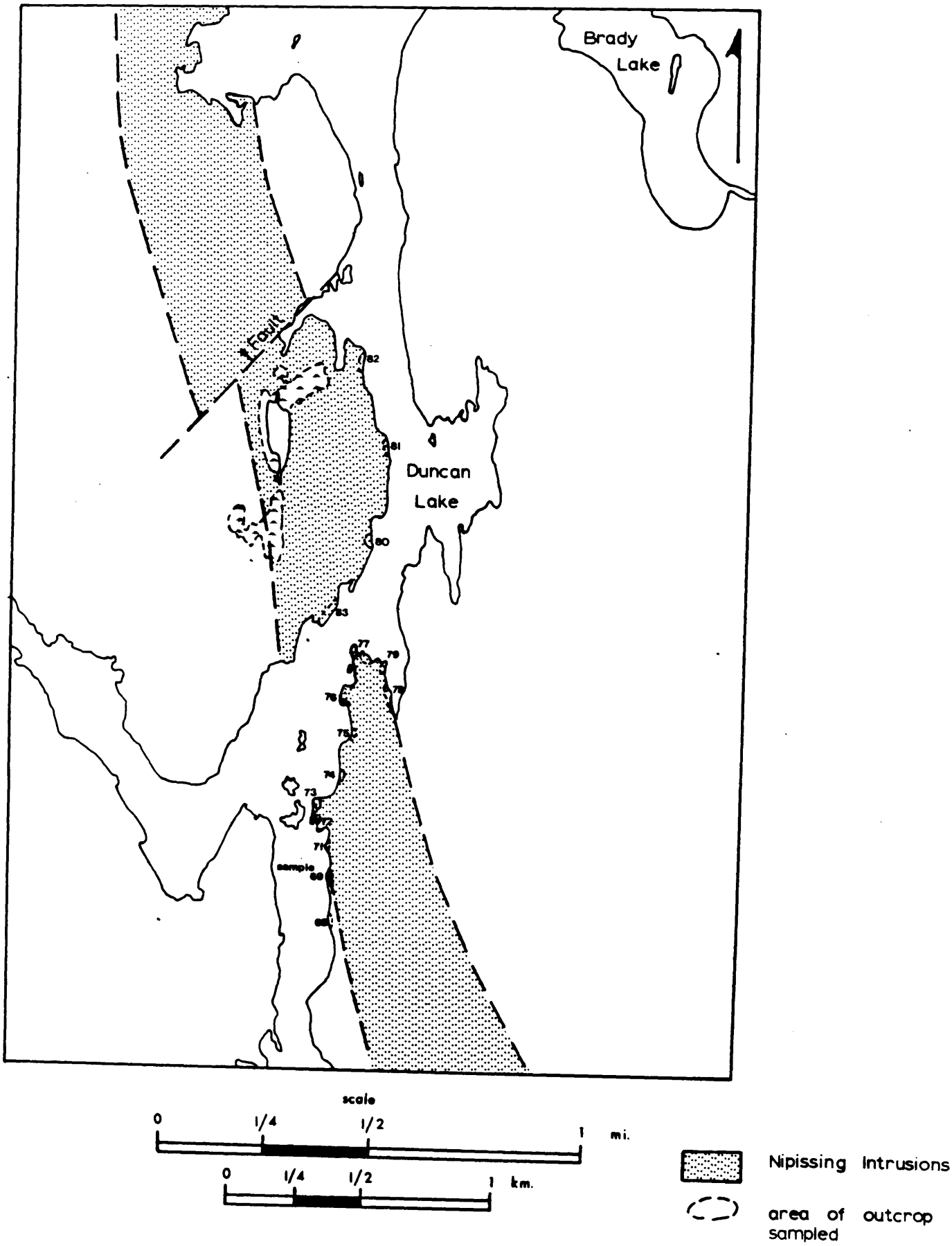

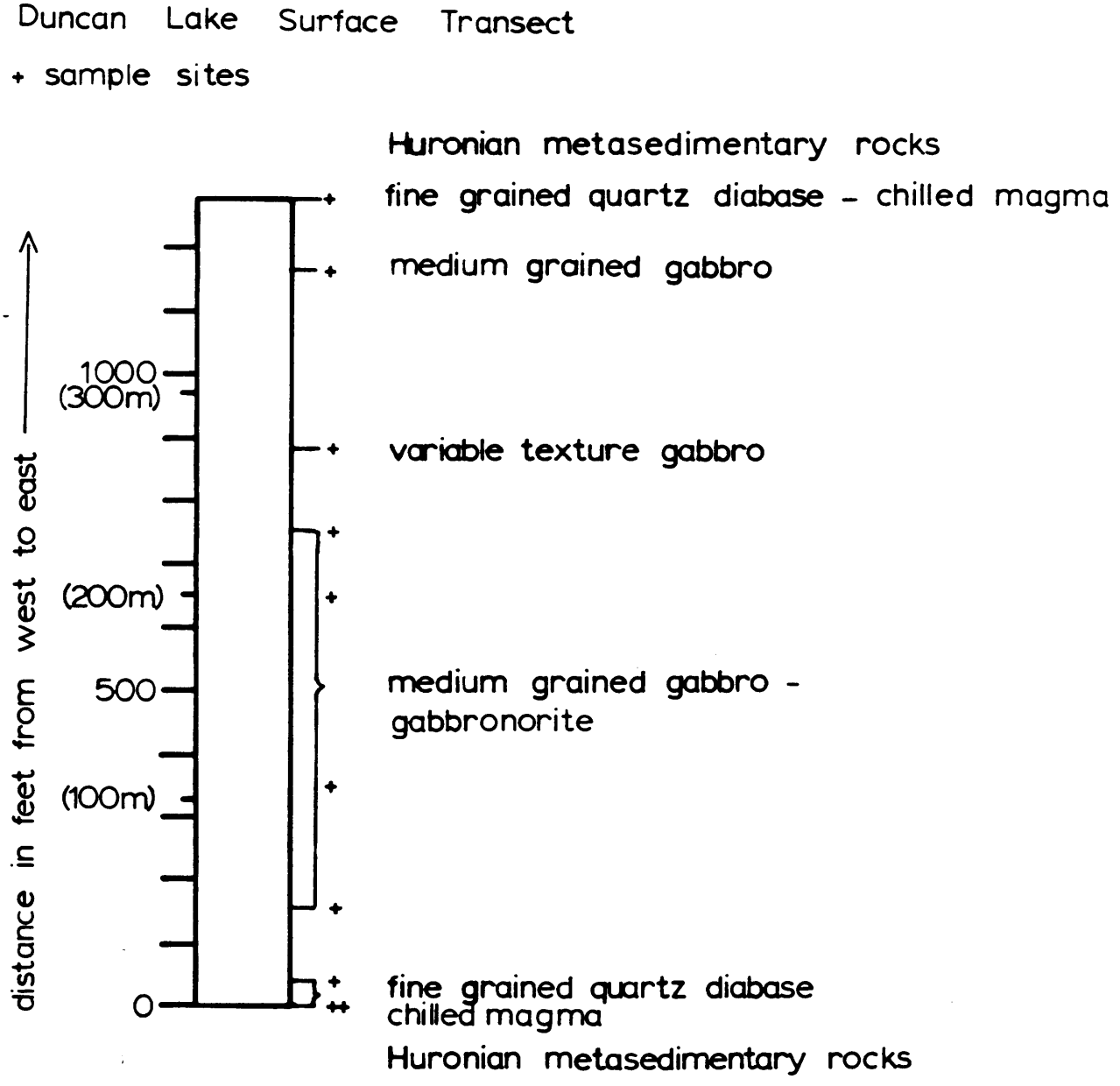


Figure 5. Lithologic surface transect across the Duncan Lake Intrusion.

Lithologic Section Through the Duncan Lake Intrusion

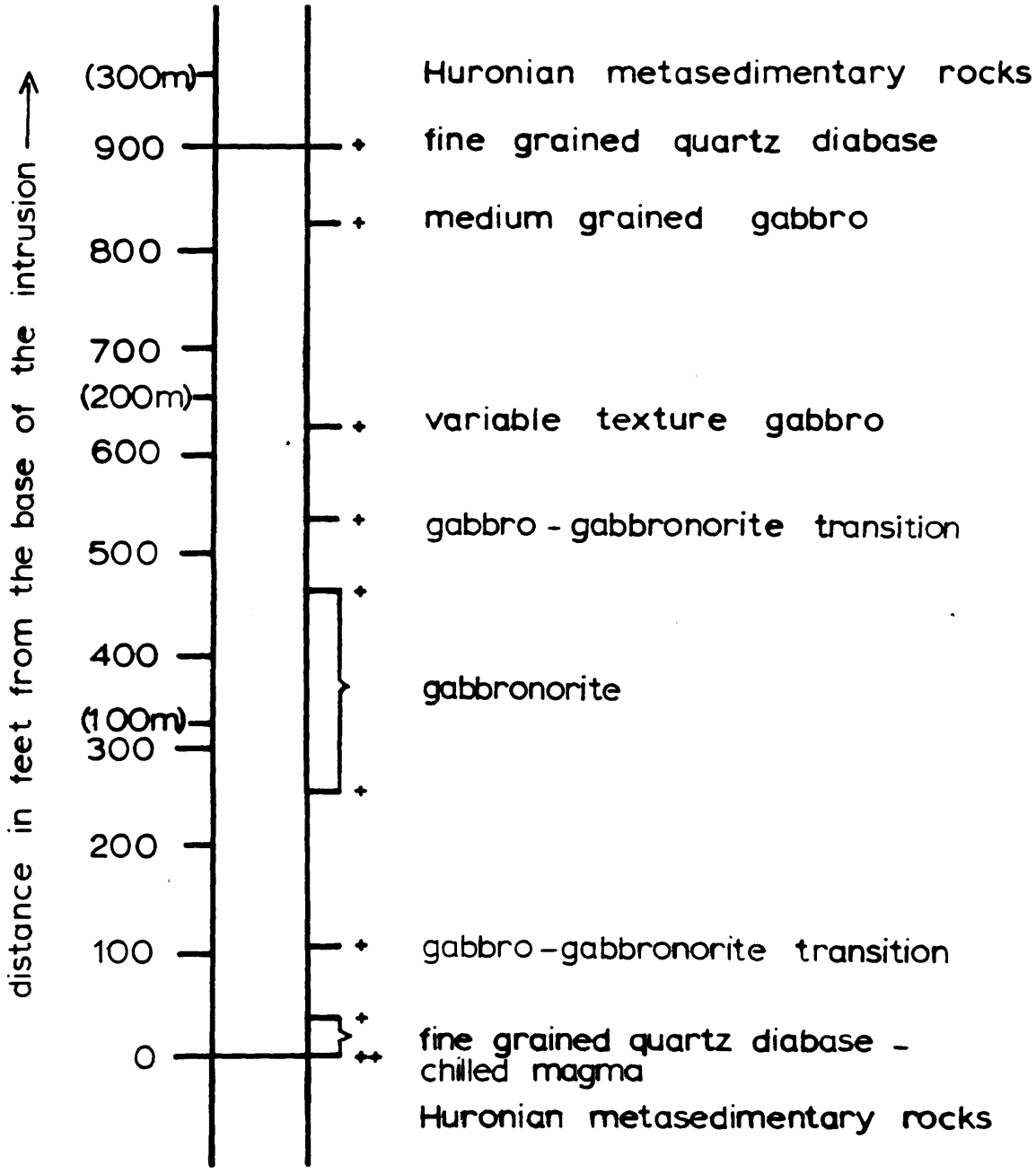


Figure 6. Lithologic section through the Duncan Lake Intrusion.

Figure 7. Sample collection sites across the Beaton Bay Intrusion.

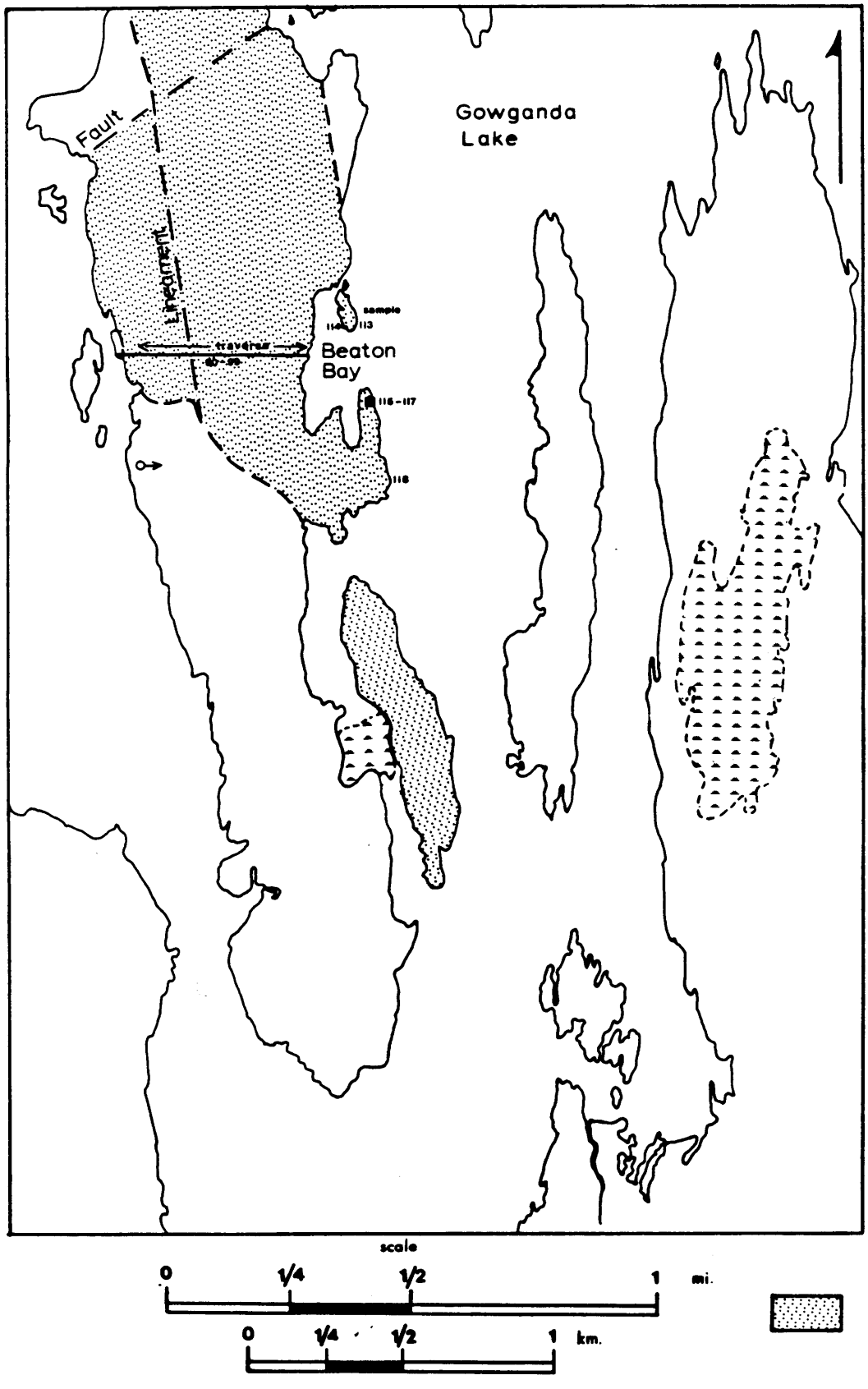

Beaton Bay Surface Transect

• sample sites

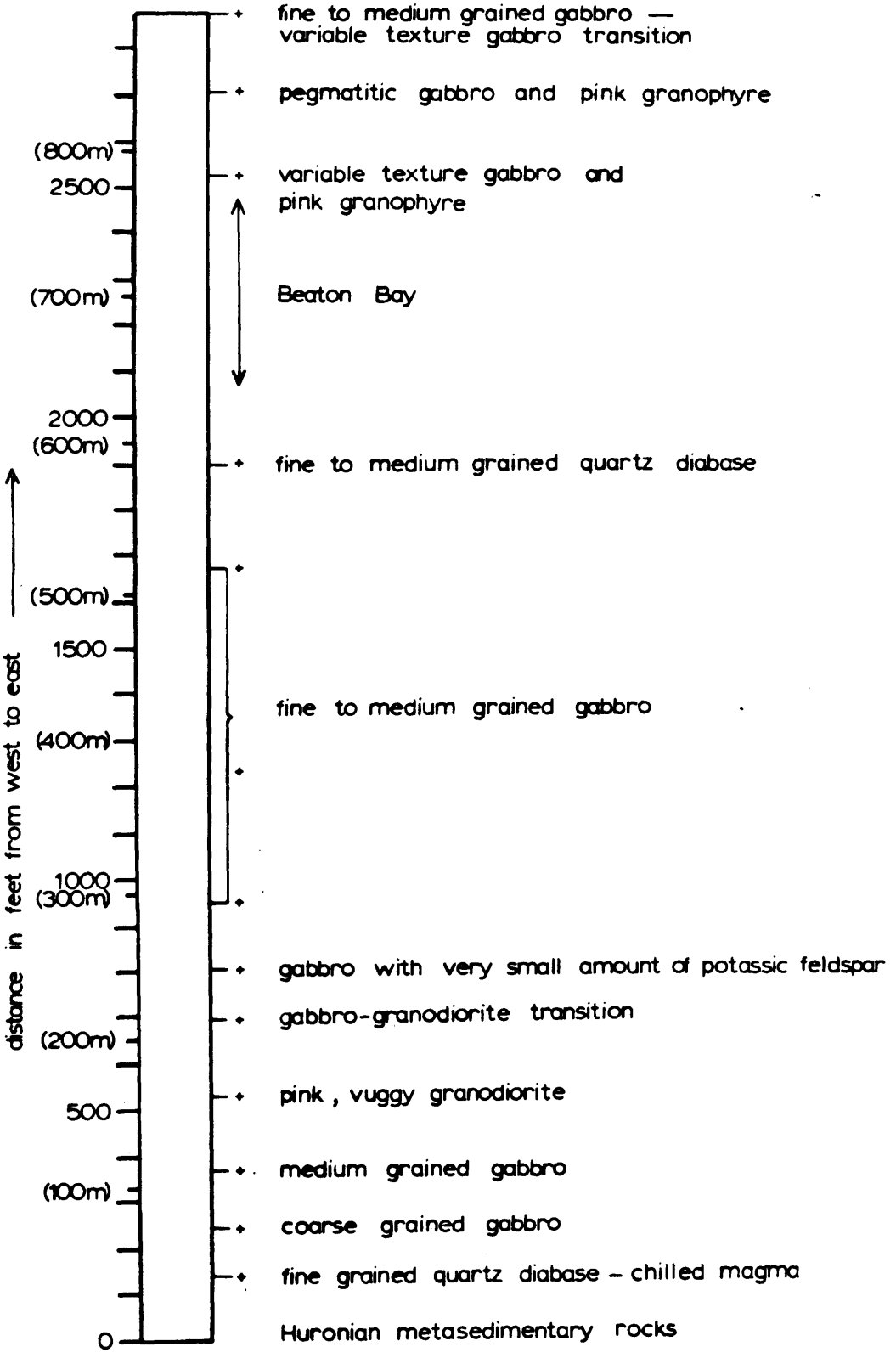


Figure 8. Lithologic section through the Beaton Bay Intrusion.

Figure 9. Reconstruction of the Lithologic Section Through the Beaton Bay Intrusion

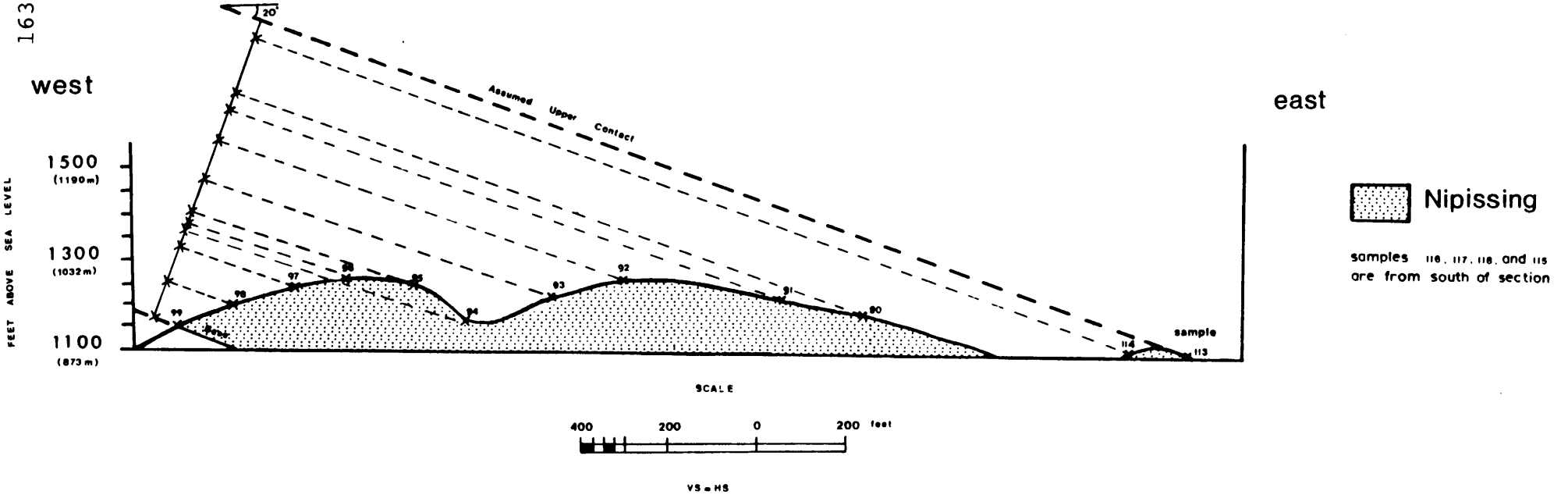

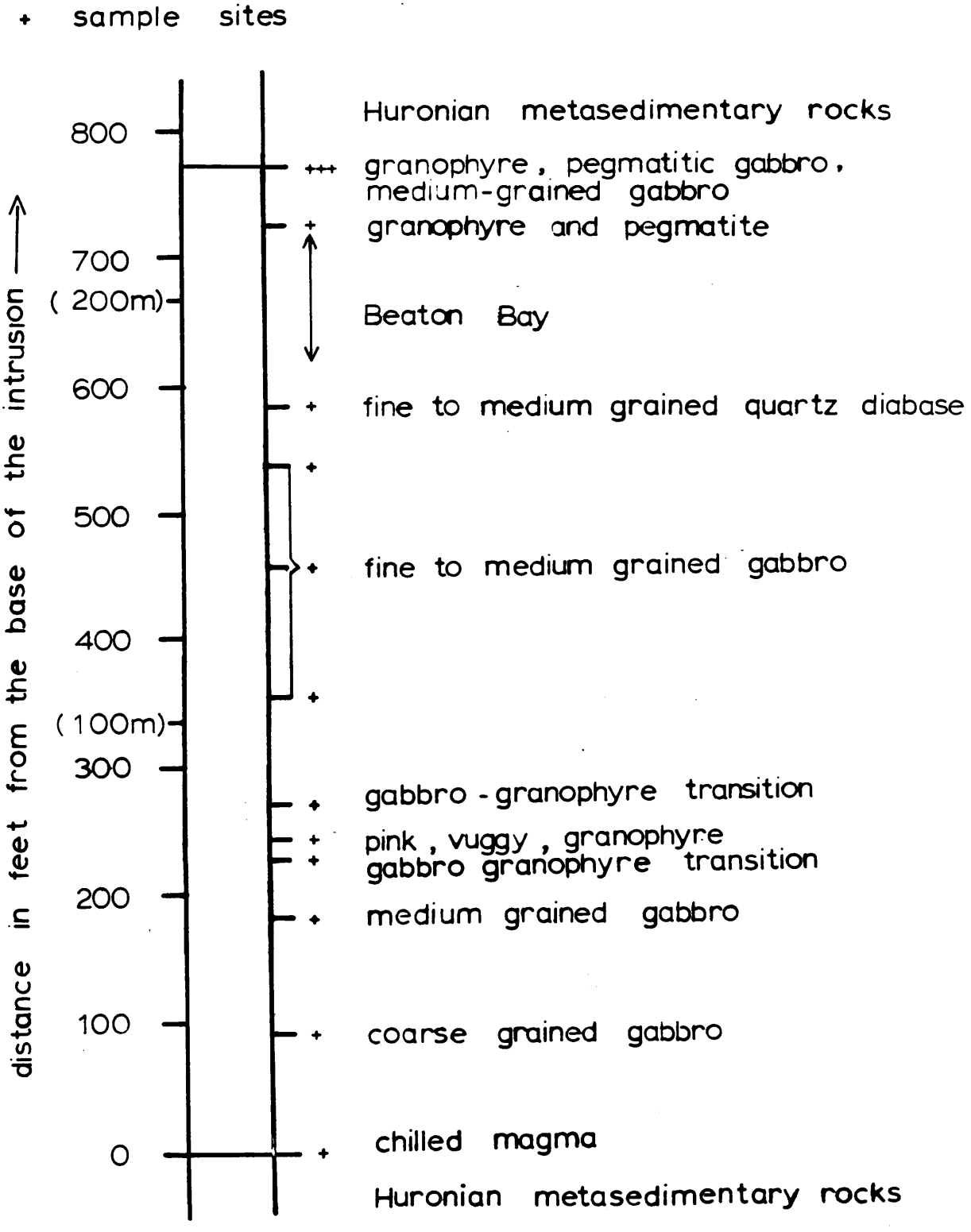


Figure 10. Corrected lithologic section through the Beaton Bay Intrusion.

Figure 12. Sample collection sites across the Milner Lake Intrusion at the Mann Mine site.

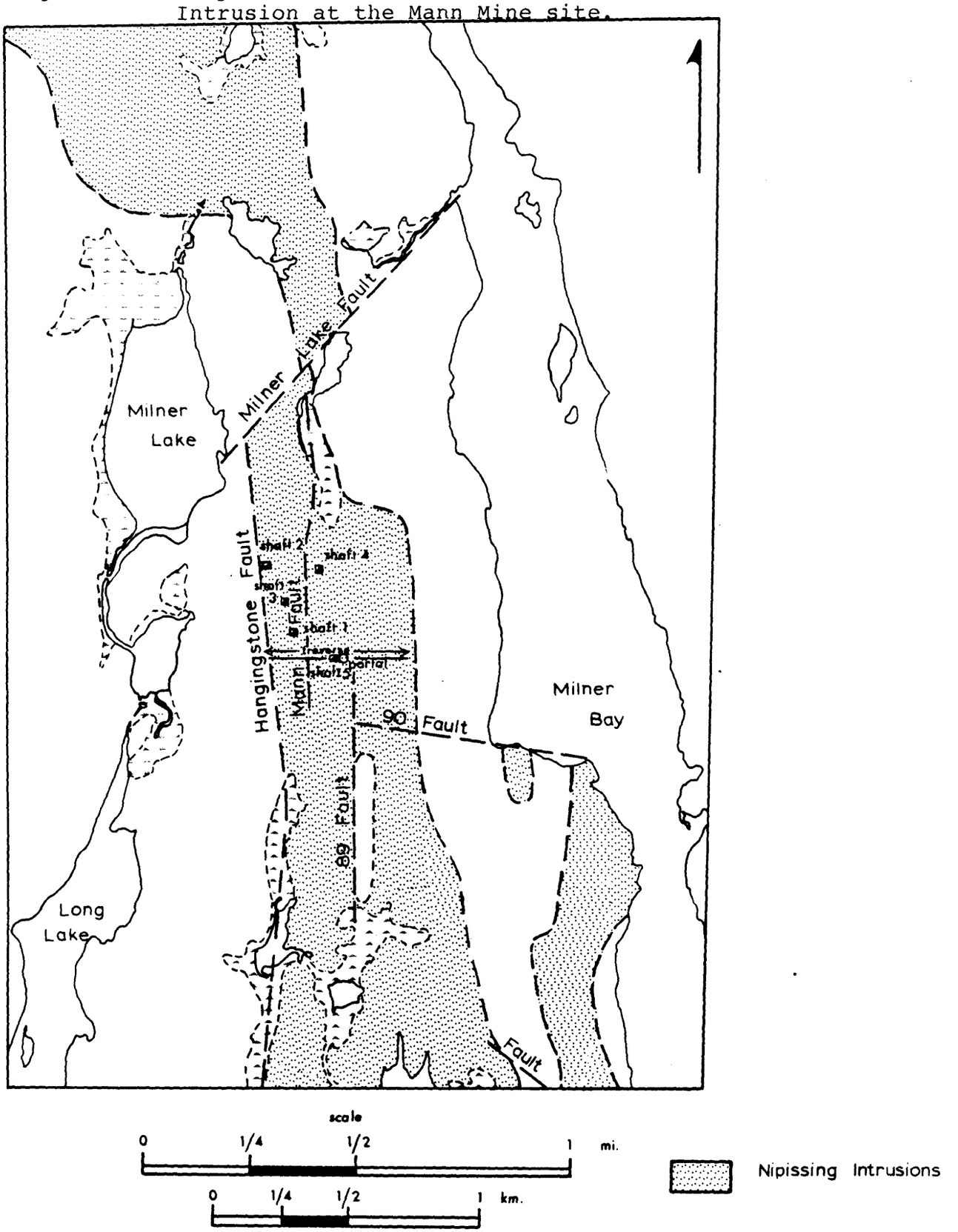

Figure 13. Lithologic surface transect across the Milner Lake Intrusion.

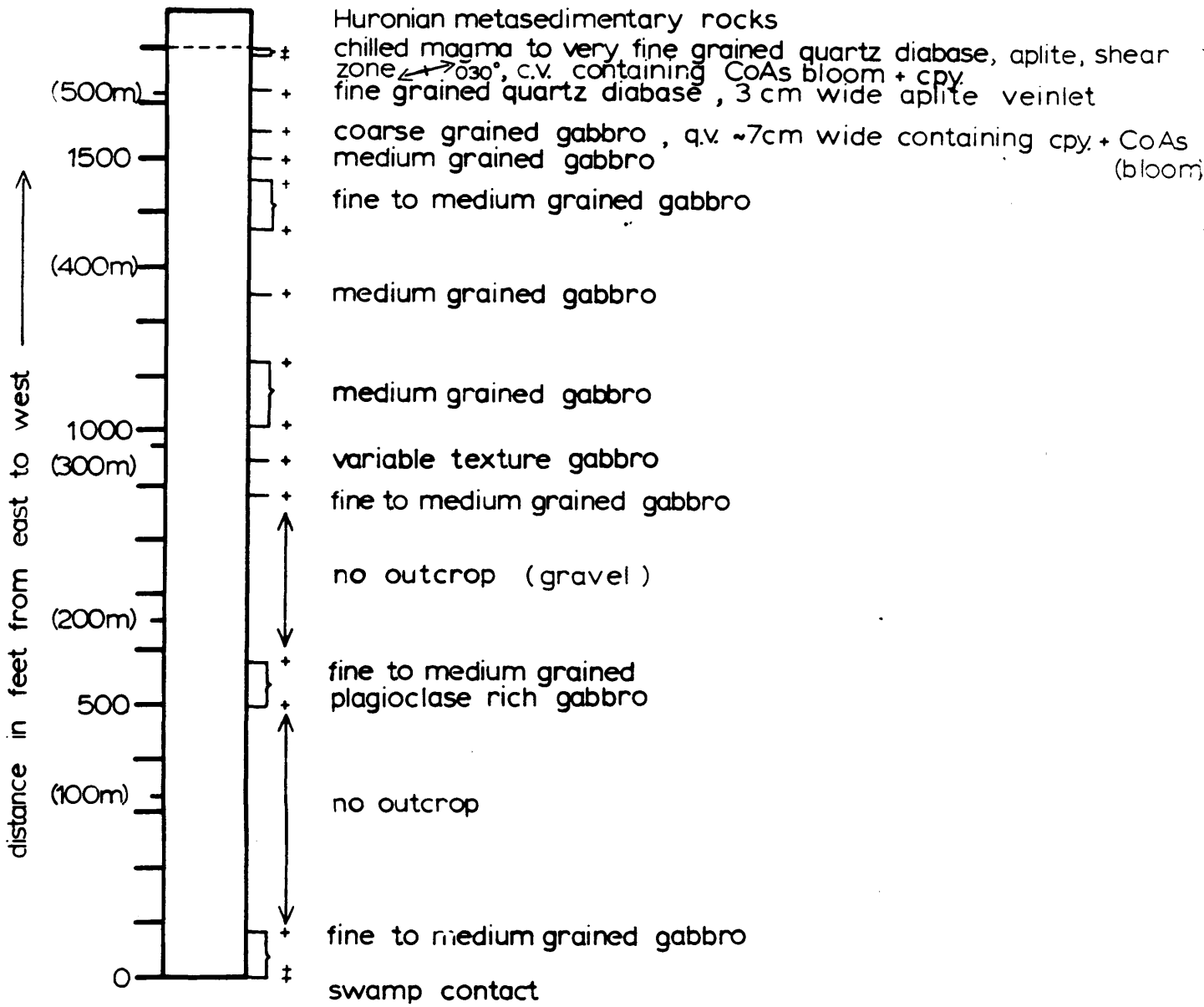

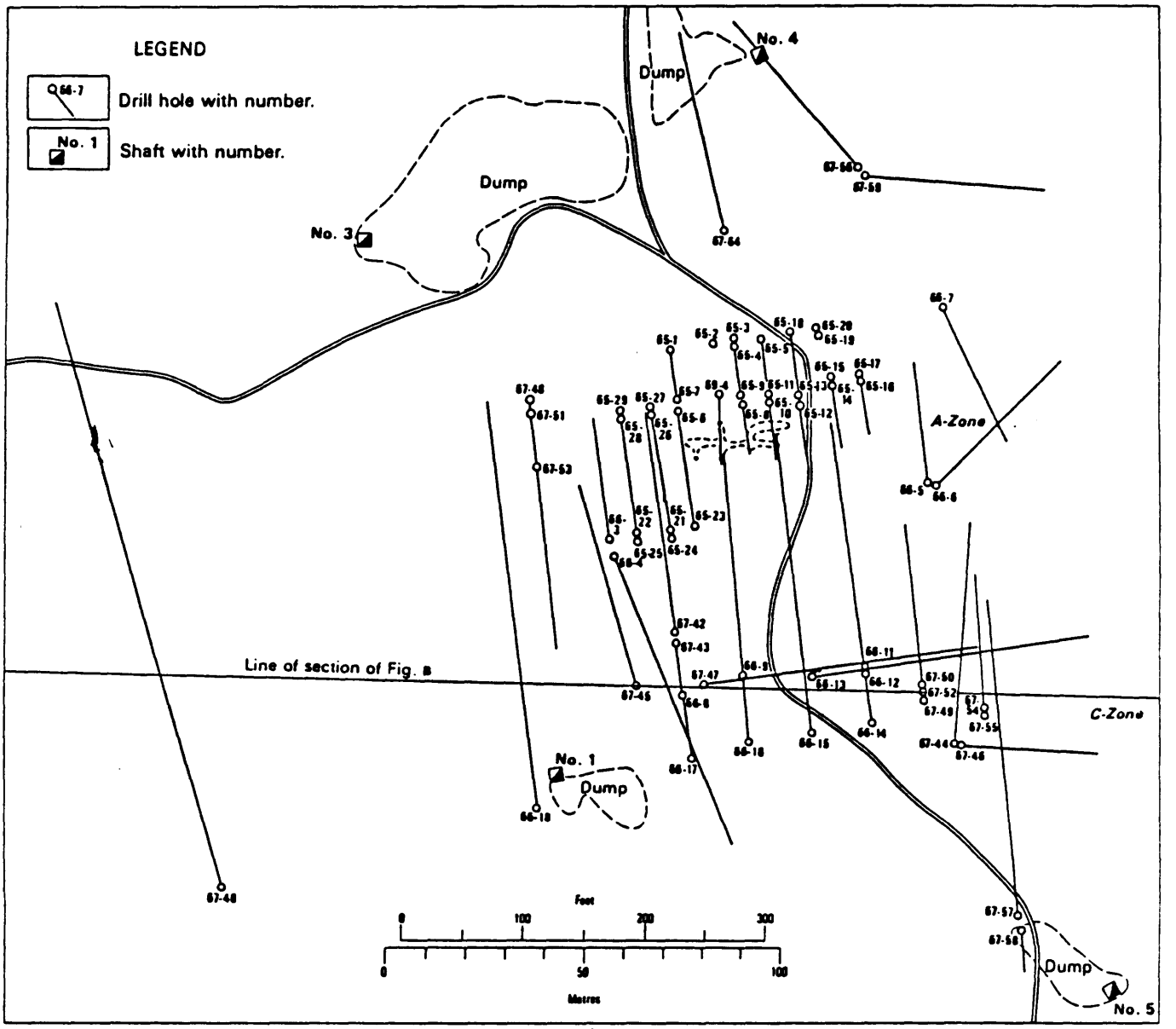


Figure 14a. Surface plan and cross section of the Milner Lake Intrusion at the Mann Mine site.

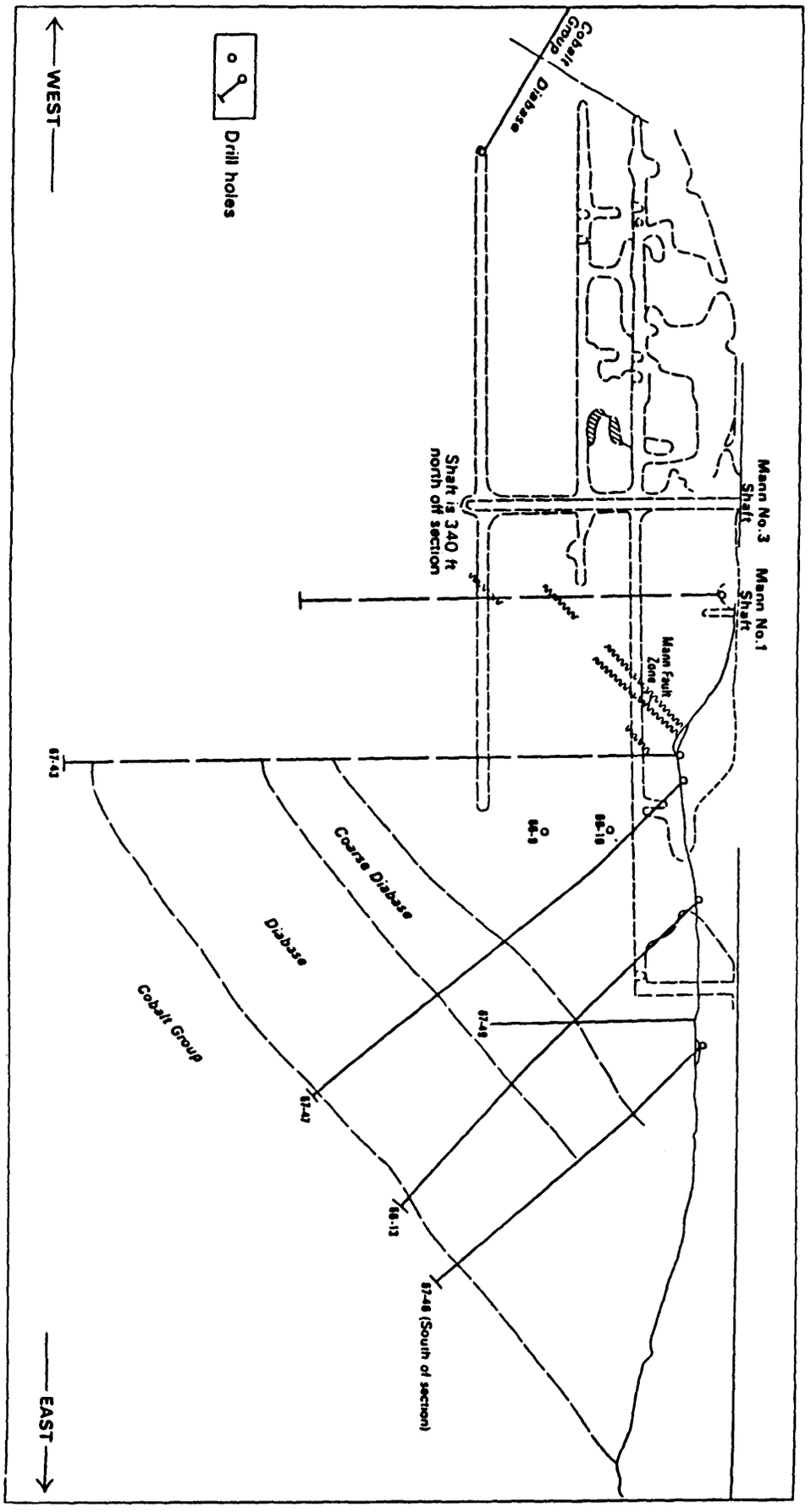


Figure 14b. Surface plan and cross section of the Milner Lake Intrusion at the Mann Mine site.

Figure 15. Reconstruction of the Lithologic Section Through the Milner Lake Intrusion at the Mann Mine Site

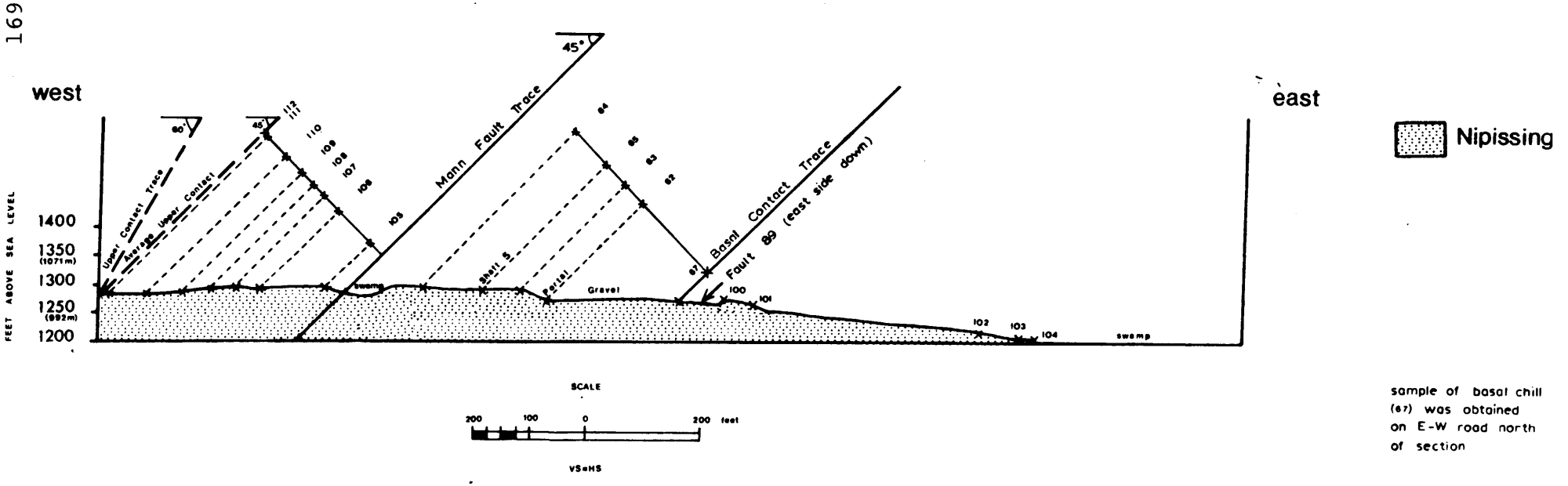

Figure 16.
Lithologic Section Through the Milner Lake Intrusion at the Mann Mine Site

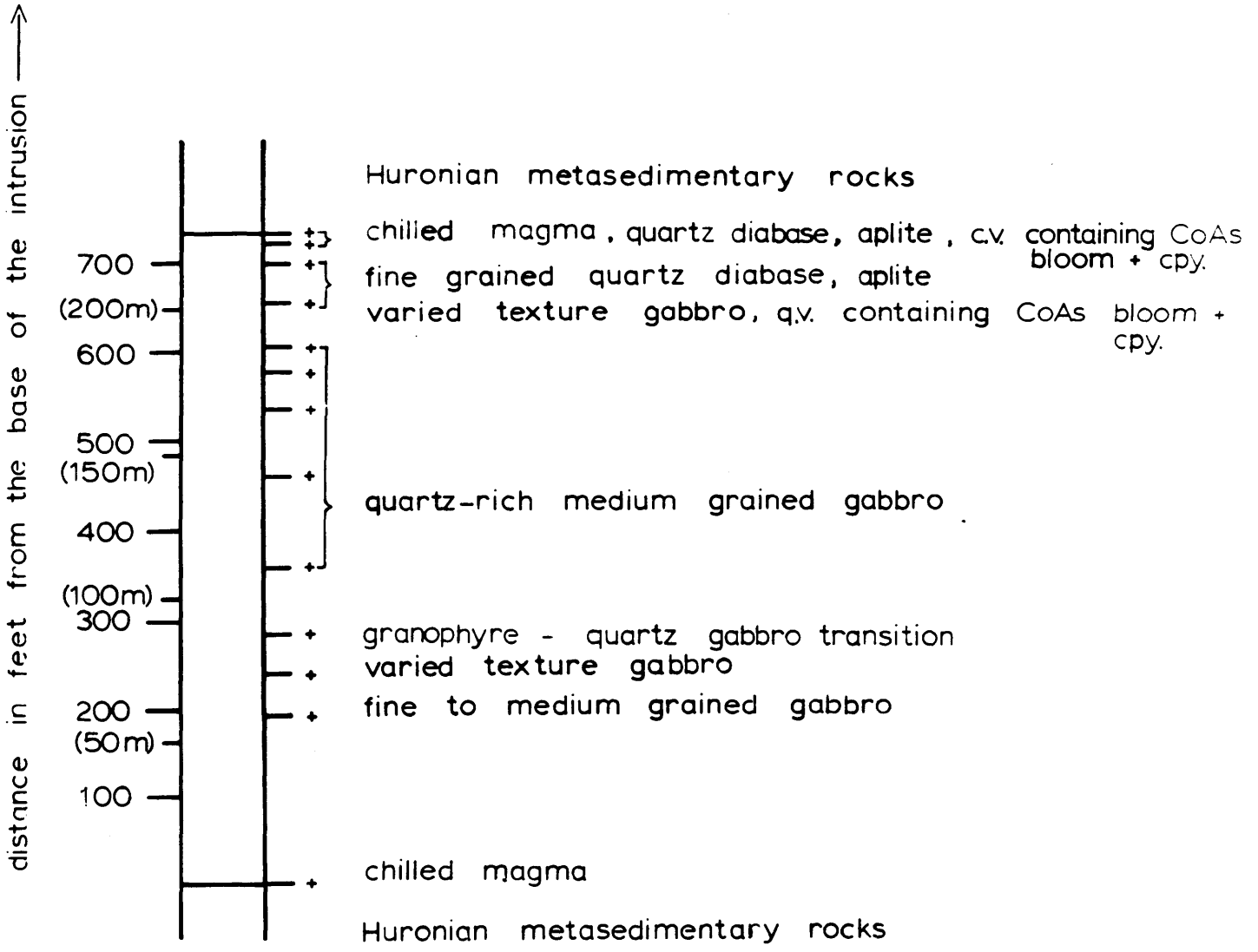

Figure 19a.

Lithologic section through the Miller Lake Intrusion at the Castle Mine site.

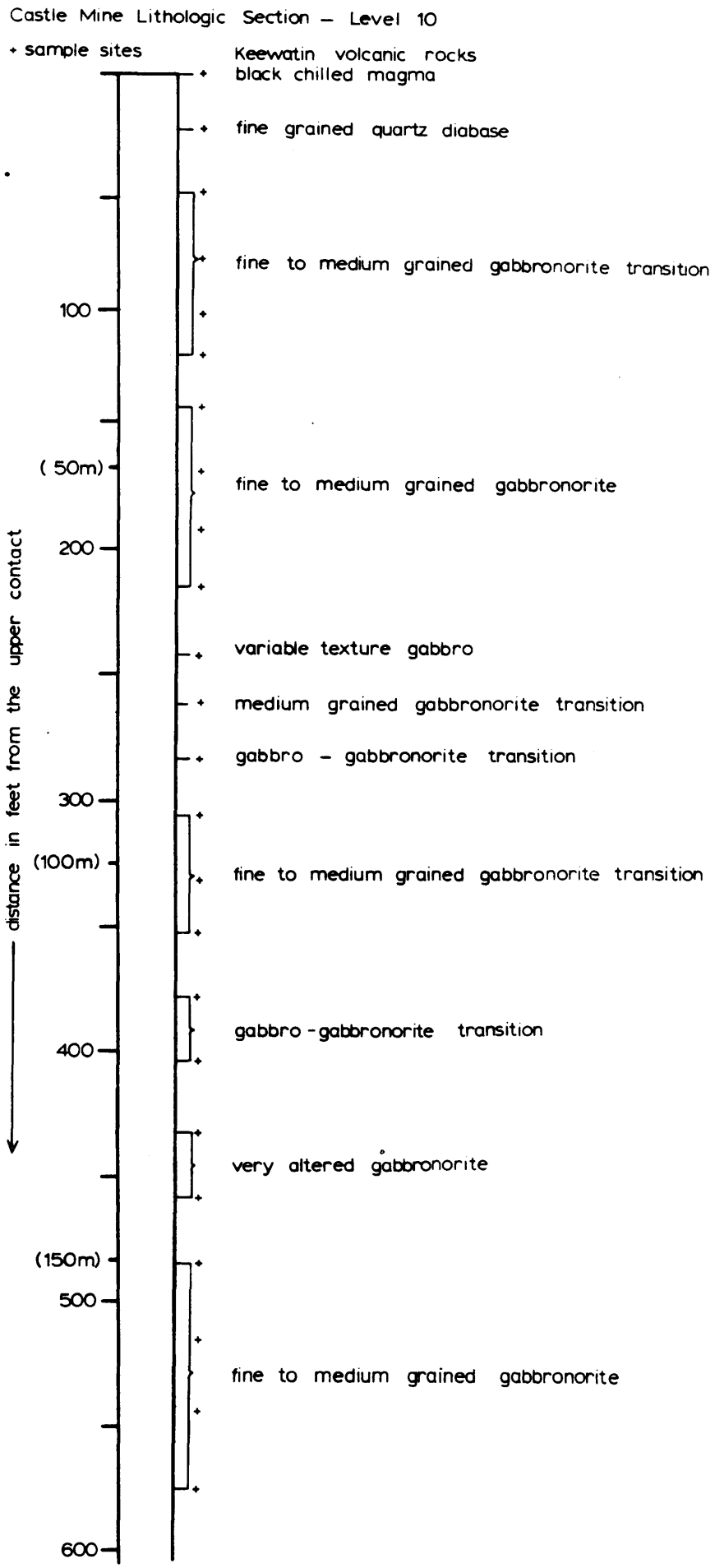

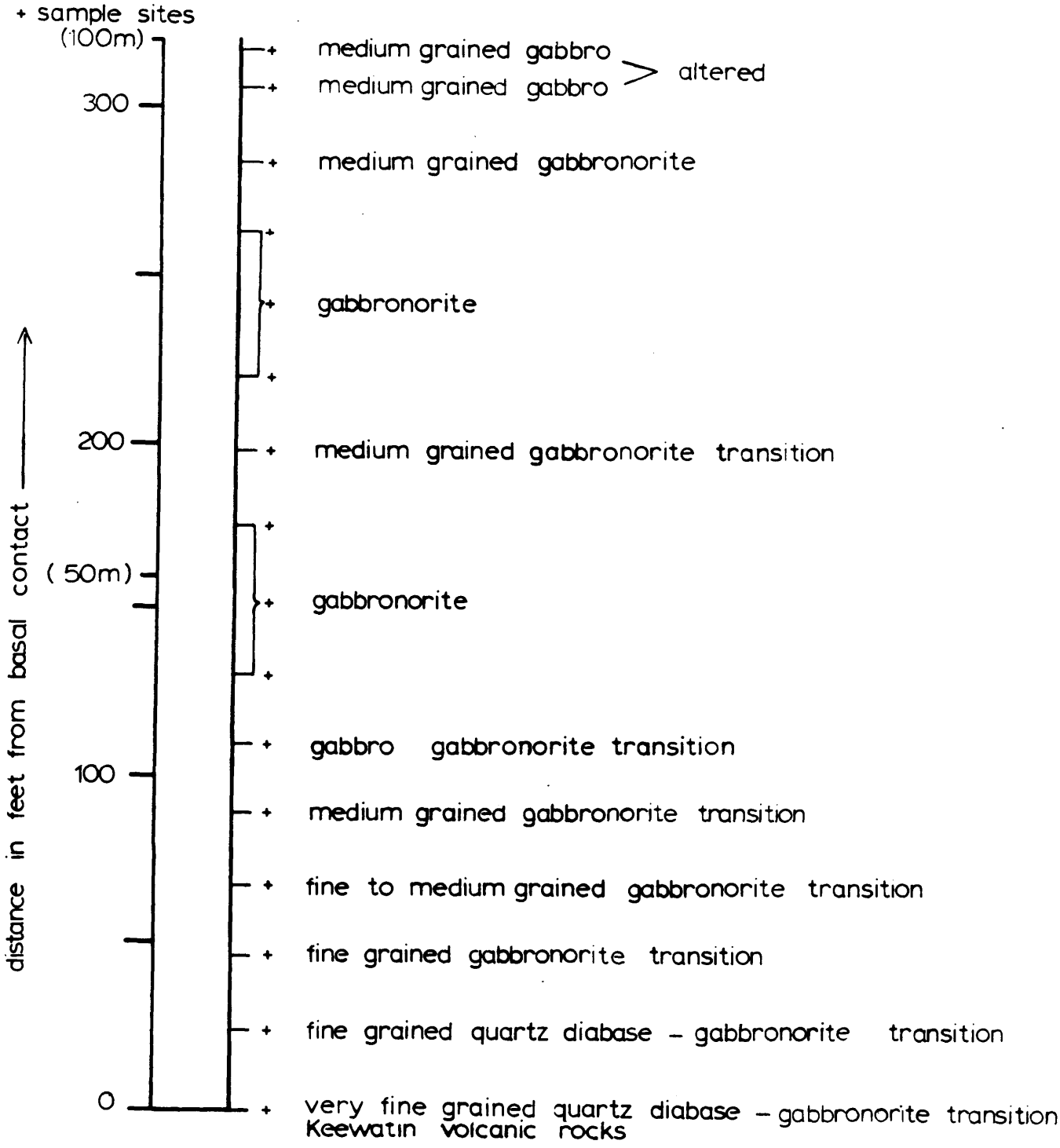


Figure 19b. Lithologic section through the Miller Lake Intrusion at the Castle Mine site.

Figure 20. Distribution of Nipissing lithologies throughout a hypothetical undulating sheet and the location of the four sections under examination.

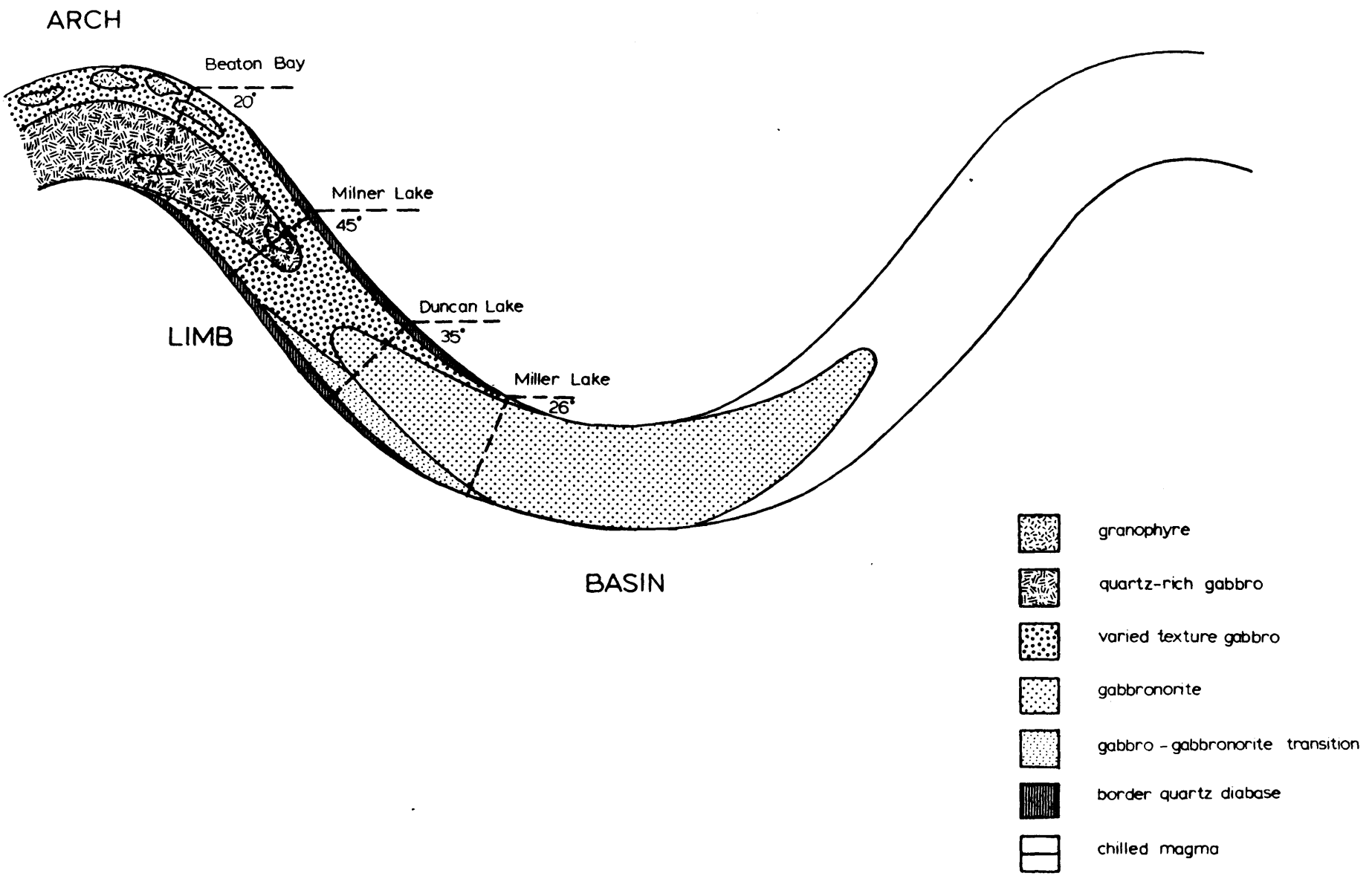

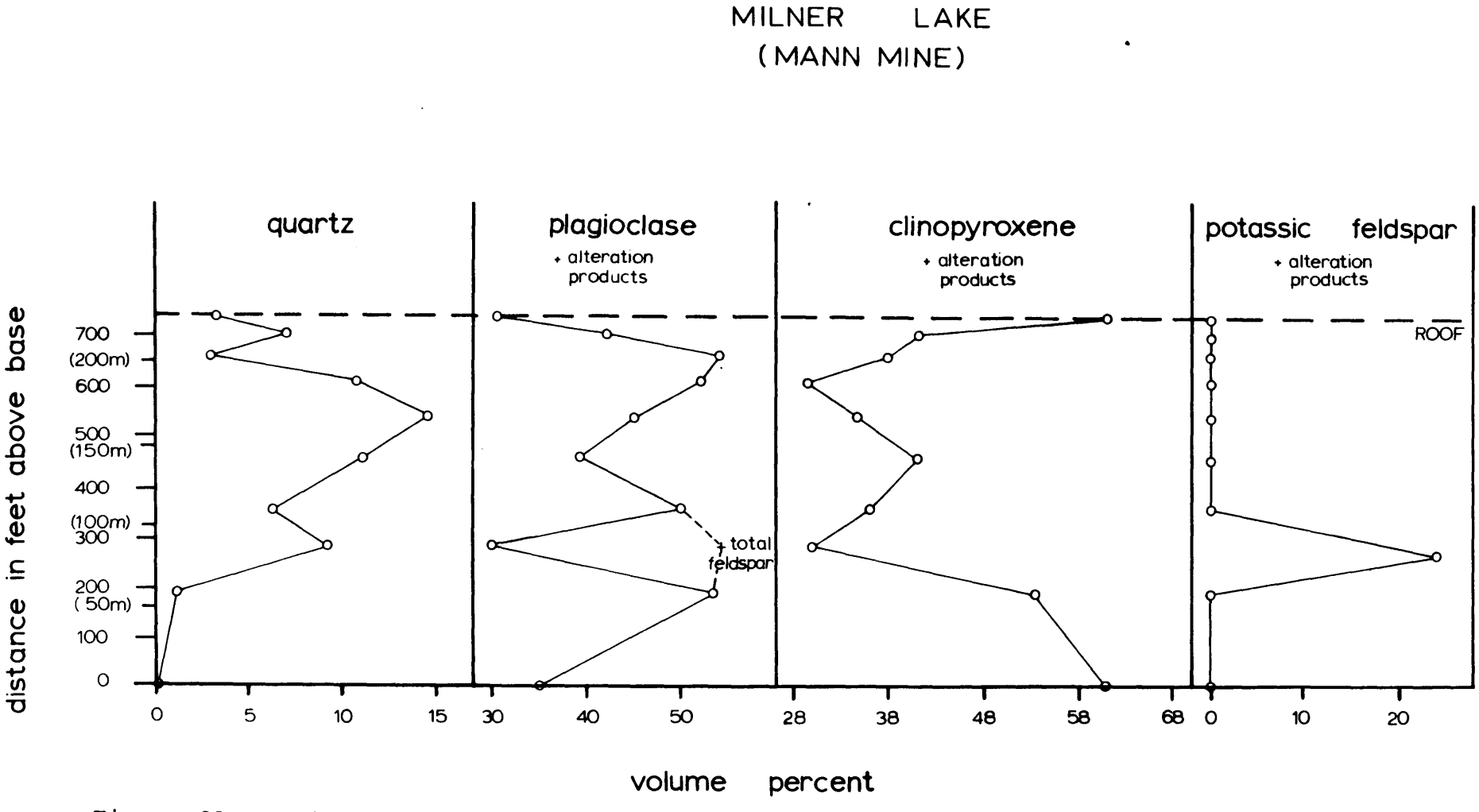


Figure 21. Modal analyses across the Milner Lake limb.

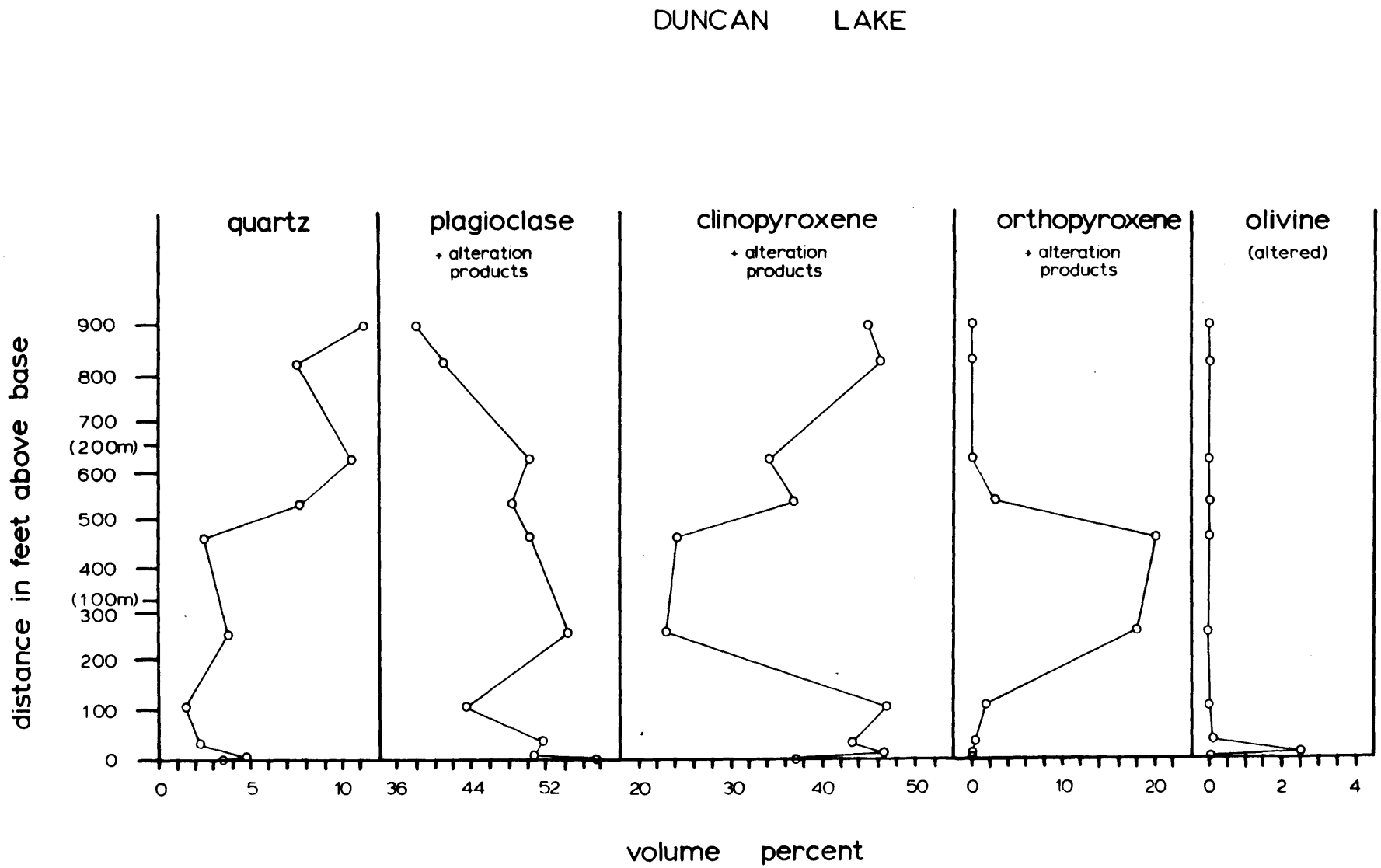


Figure 22. Modal analyses across the Duncan Lake Intrusion.

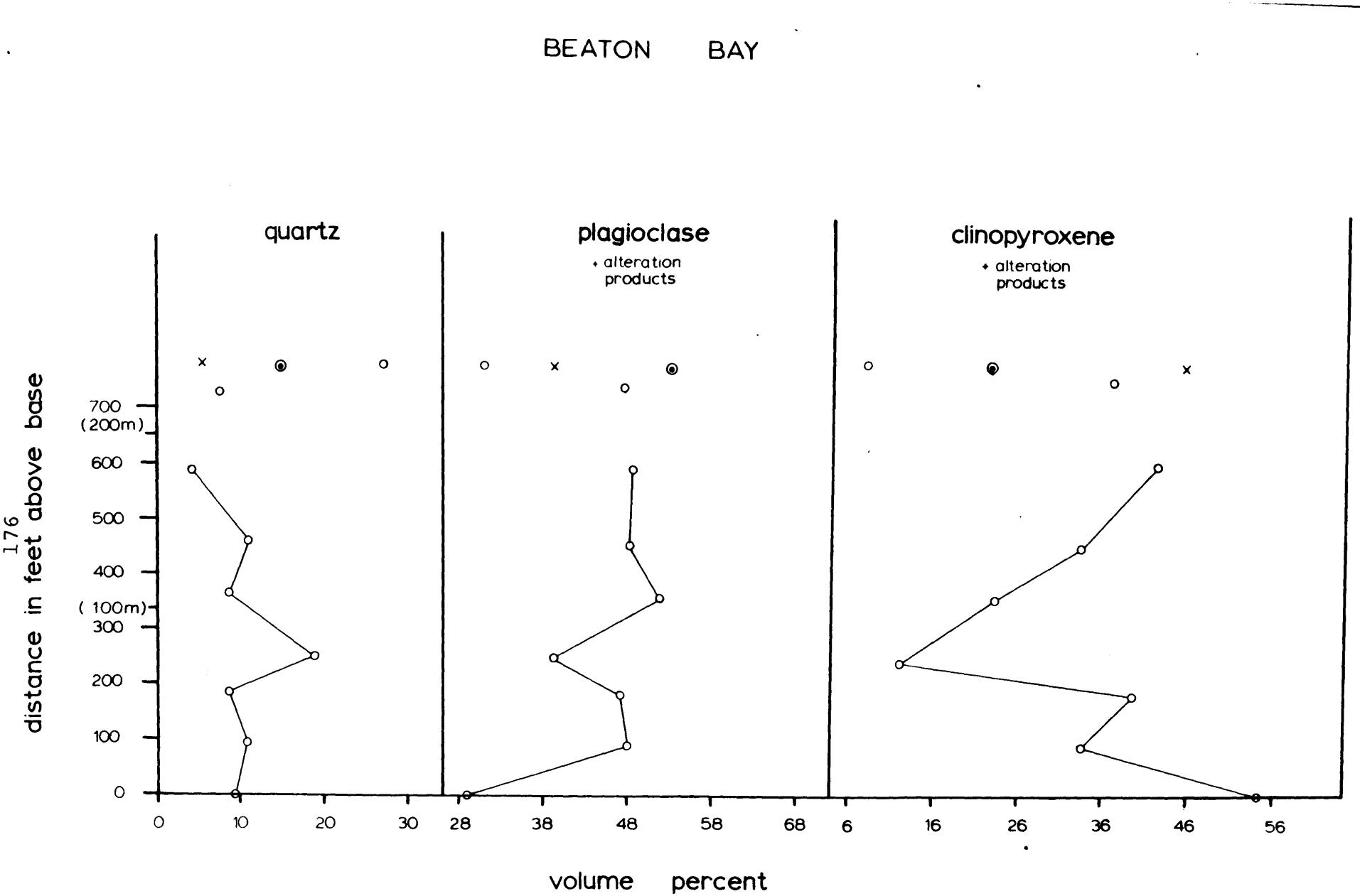


Figure 23. Modal analyses across the Beaton Bay Intrusion.

samples 117(◉), and 118(x) have been projected onto the section.

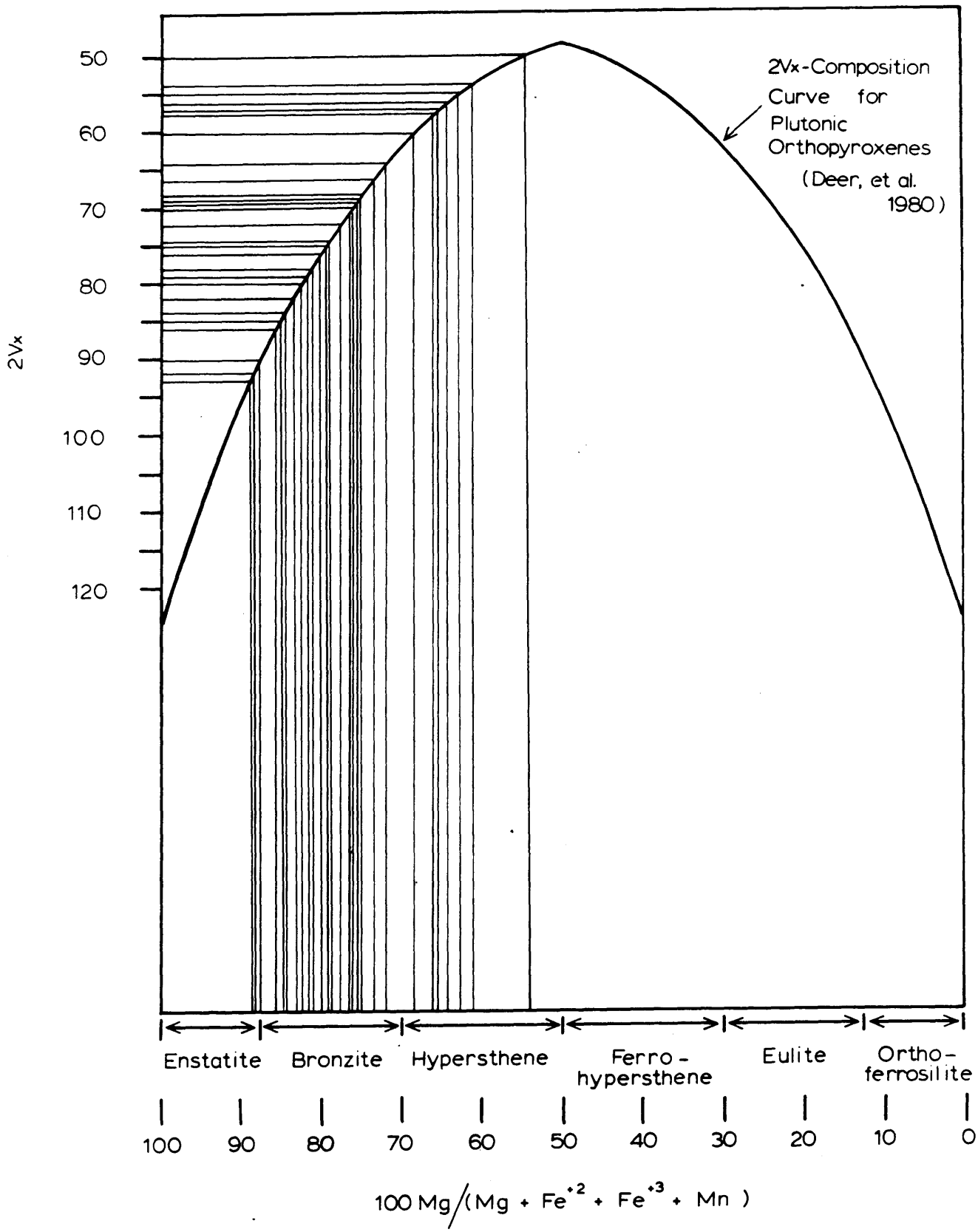


Figure 25. 2V angles and the Mg-numbers of orthopyroxene from the Miller Lake and Duncan Lake intrusions plotted onto the 2V-composition curves of Deer et al. (1980).

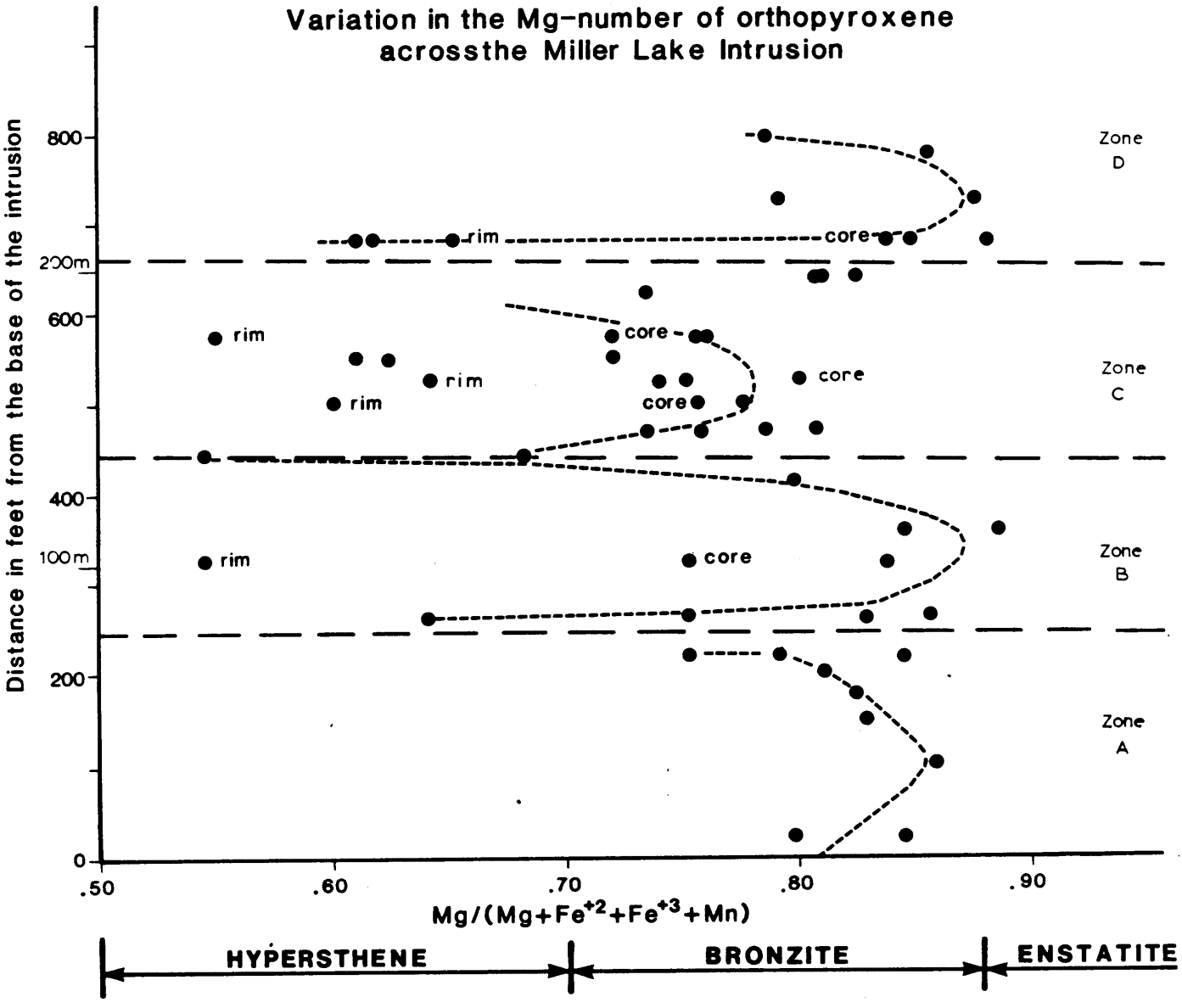


Figure 26. Variation in the Mg-number of orthopyroxene across the Miller Lake Intrusion.

Figure 27. **Variation in the whole rock Mg-number across the Duncan Lake Intrusion**

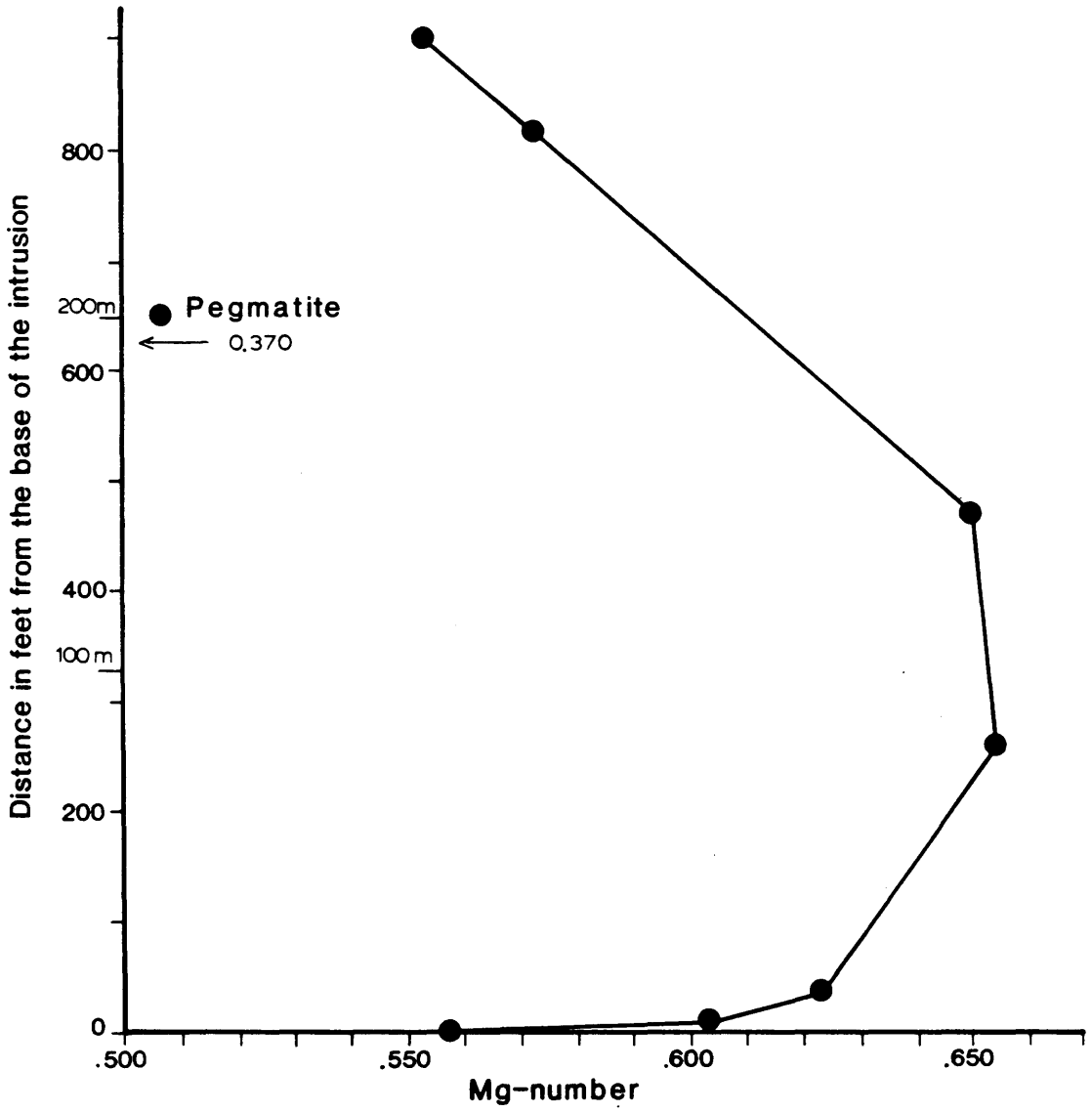

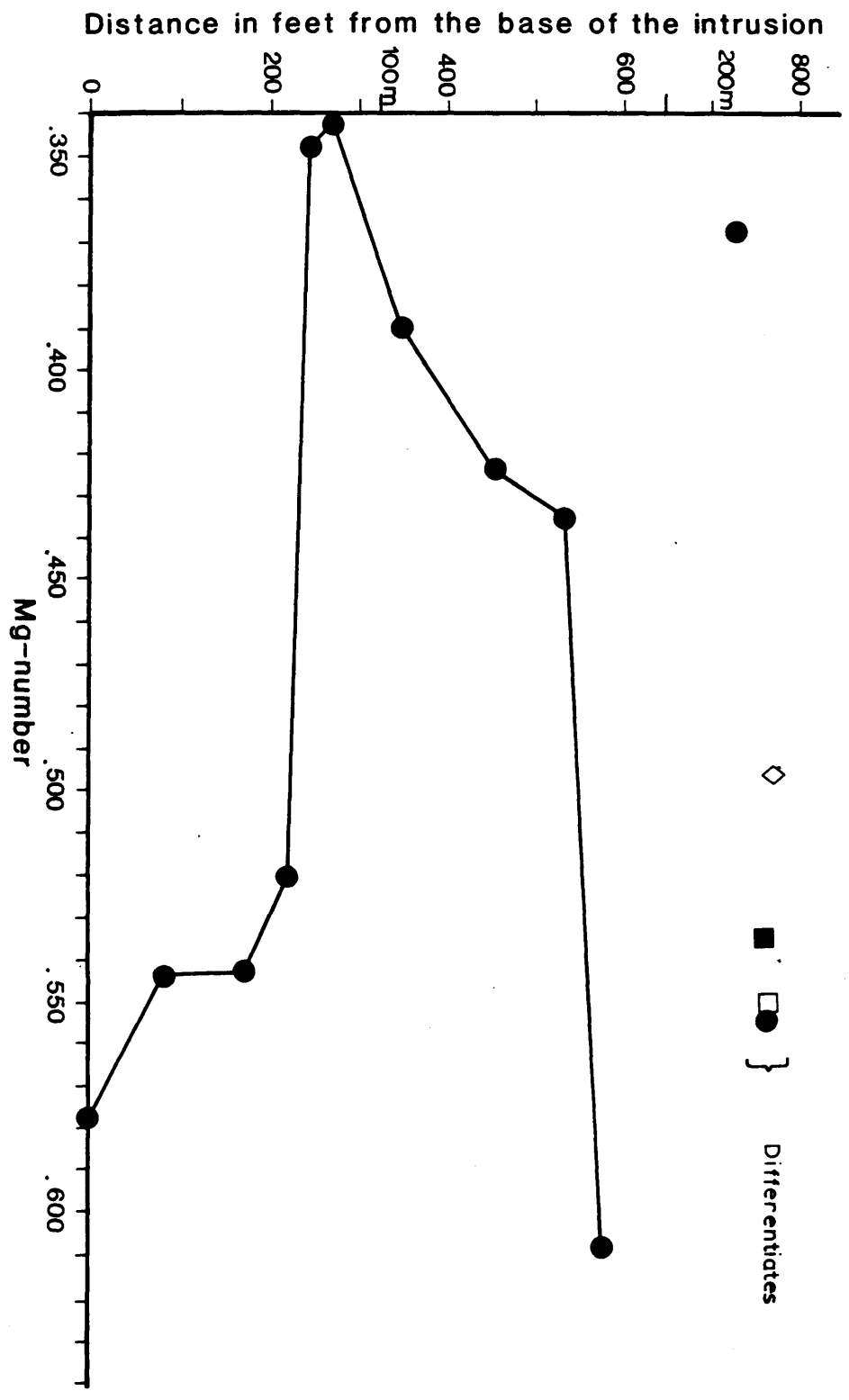
Variation in the whole rock Mg-number
across the Beaton Bay Intrusion
Distance in feet from the base of the intrusion
0
200
100m
400
600
200m
800
.350
.400
.450
.500
.550
.600
Mg-number
Differentiates

Figure 28.

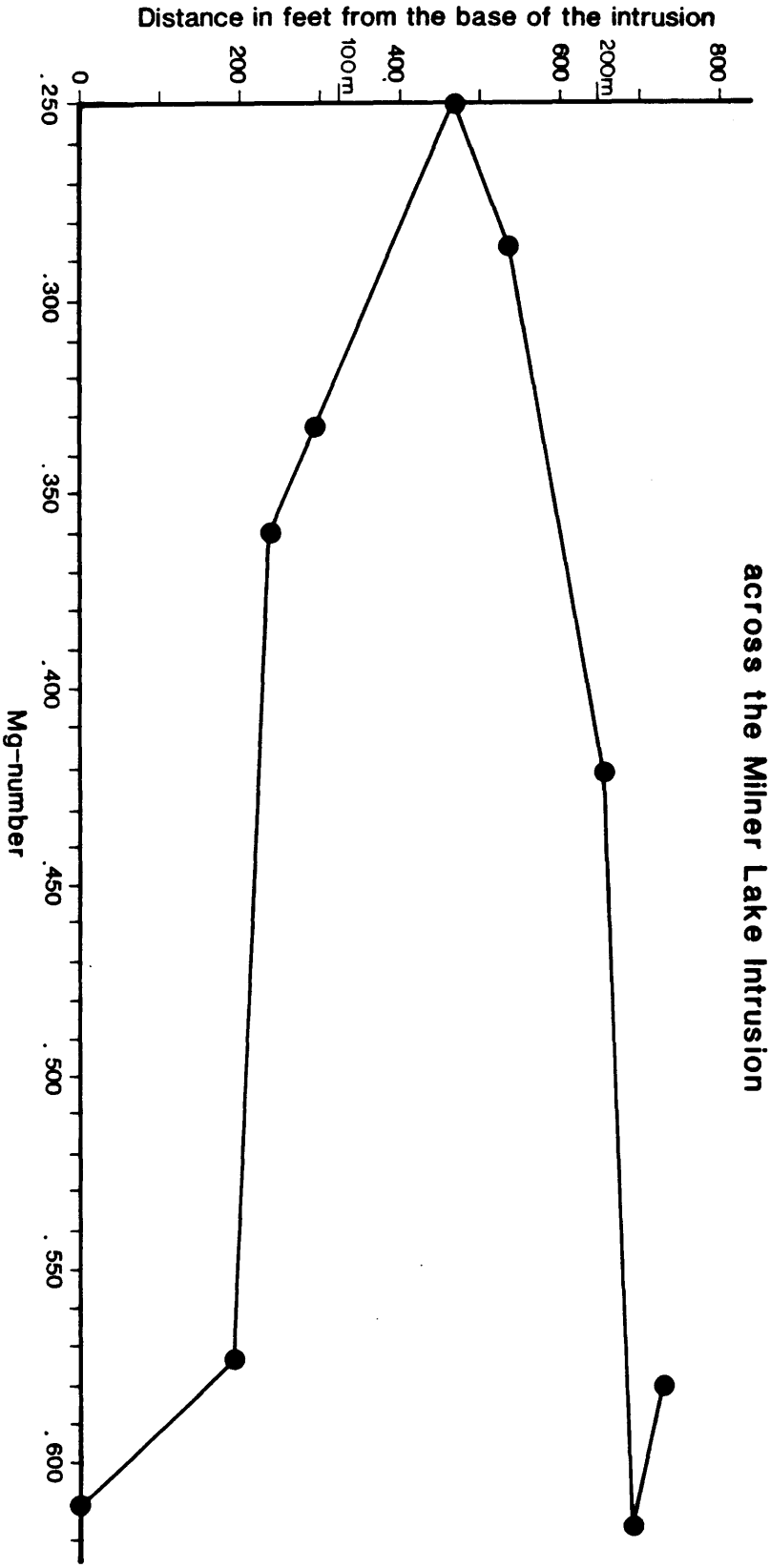


Figure 29. Variation in the whole rock Mg-number across the Milner Lake Intrusion

Figure 30. **Variation in the whole rock Mg-number across the Miller Lake Intrusion**

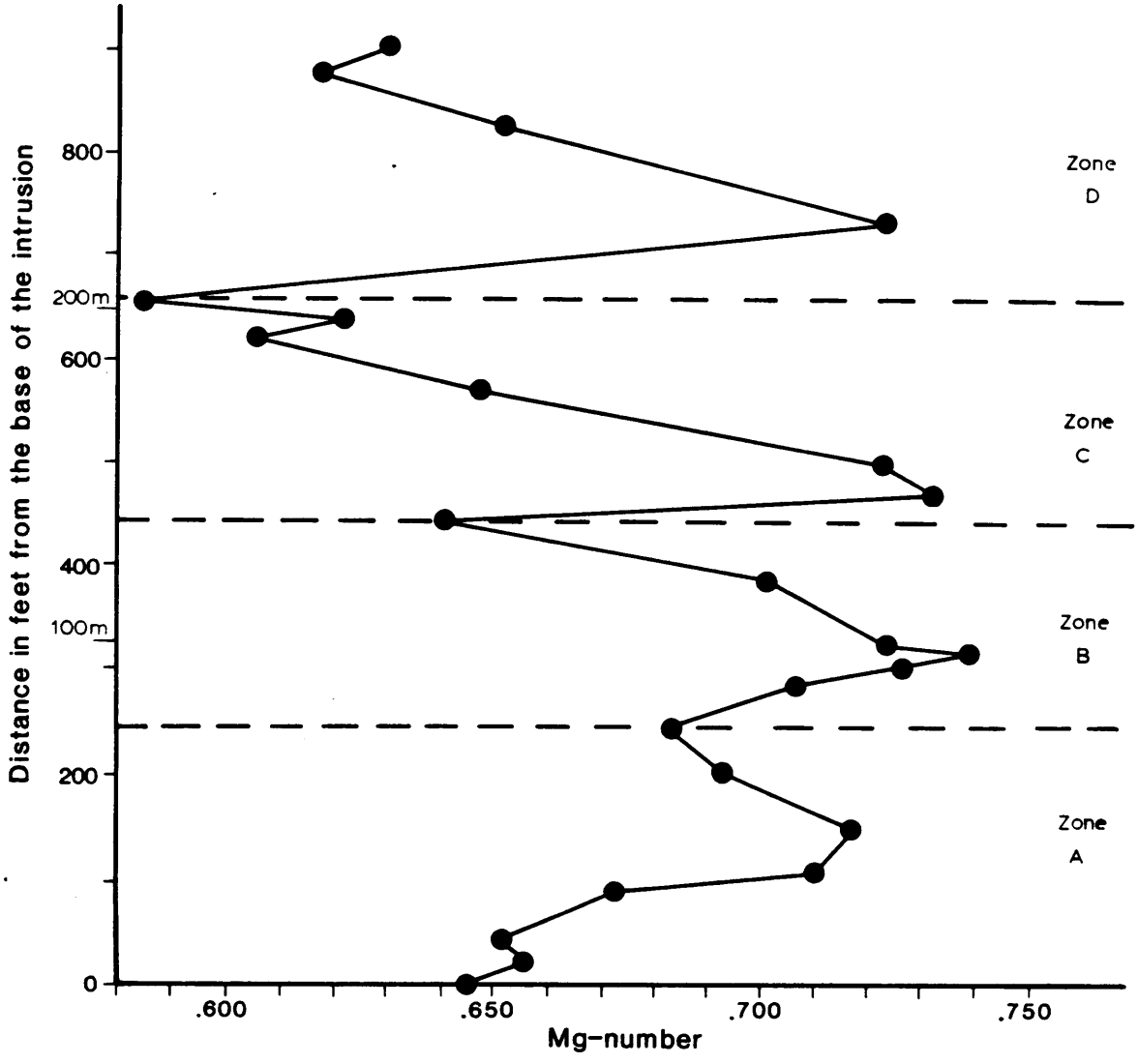

# Cross Lake Intrusion , Cobalt

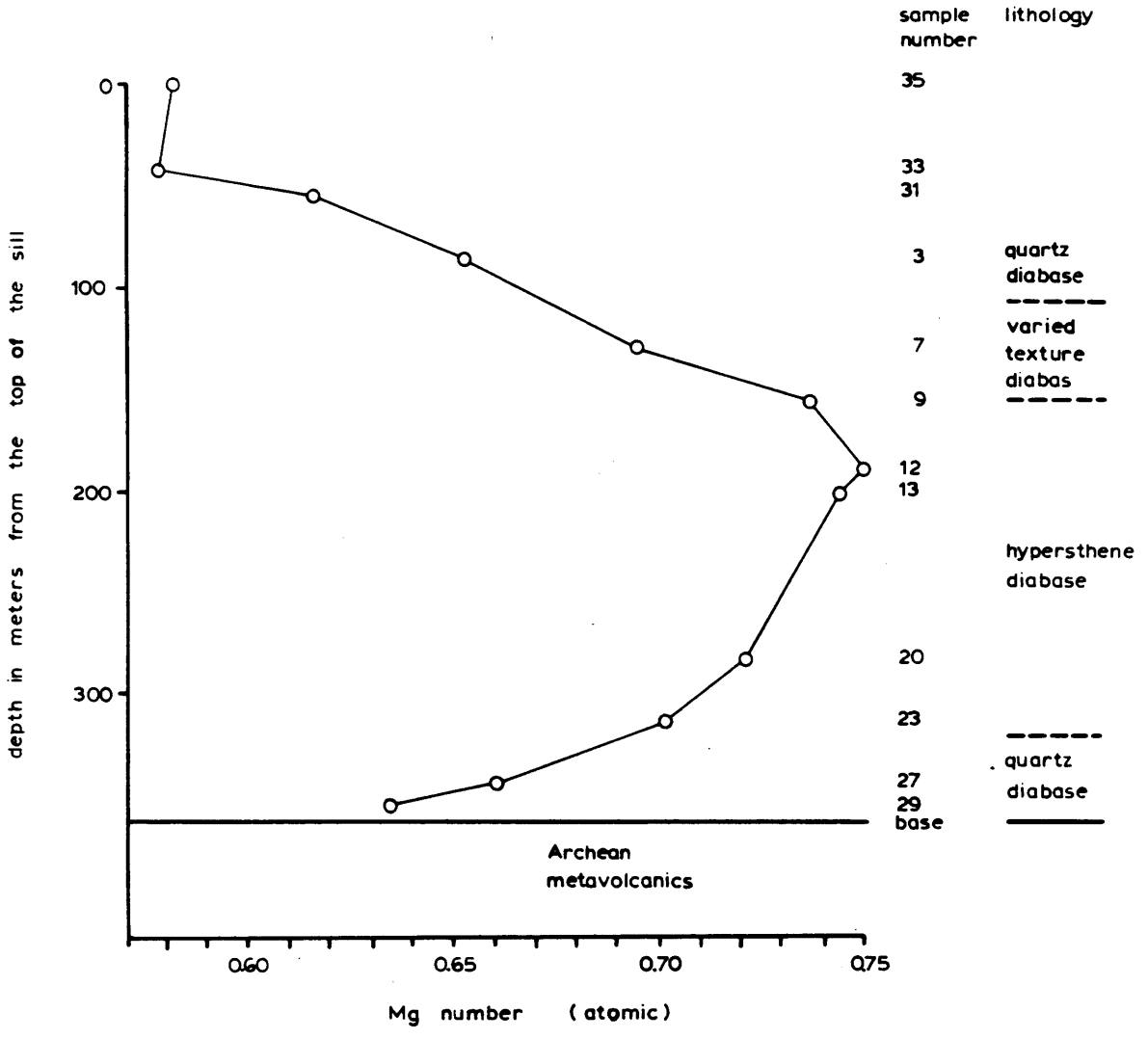


Figure 31. Variation in whole rock Mg-number across the Cross Lake Intrusion.

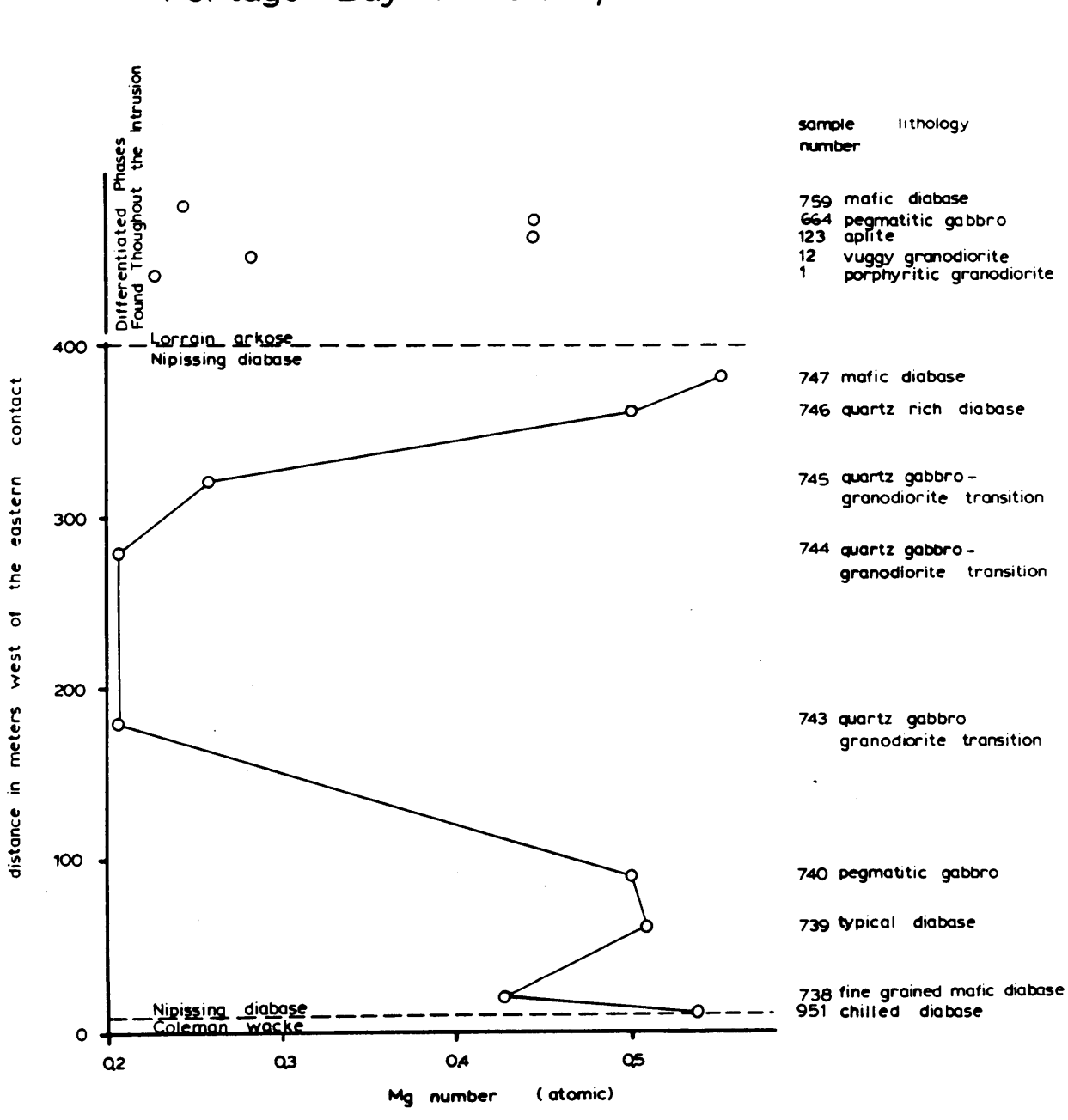


Figure 32. Variation in whole rock Mg-number across the Portage Bay Intrusion.

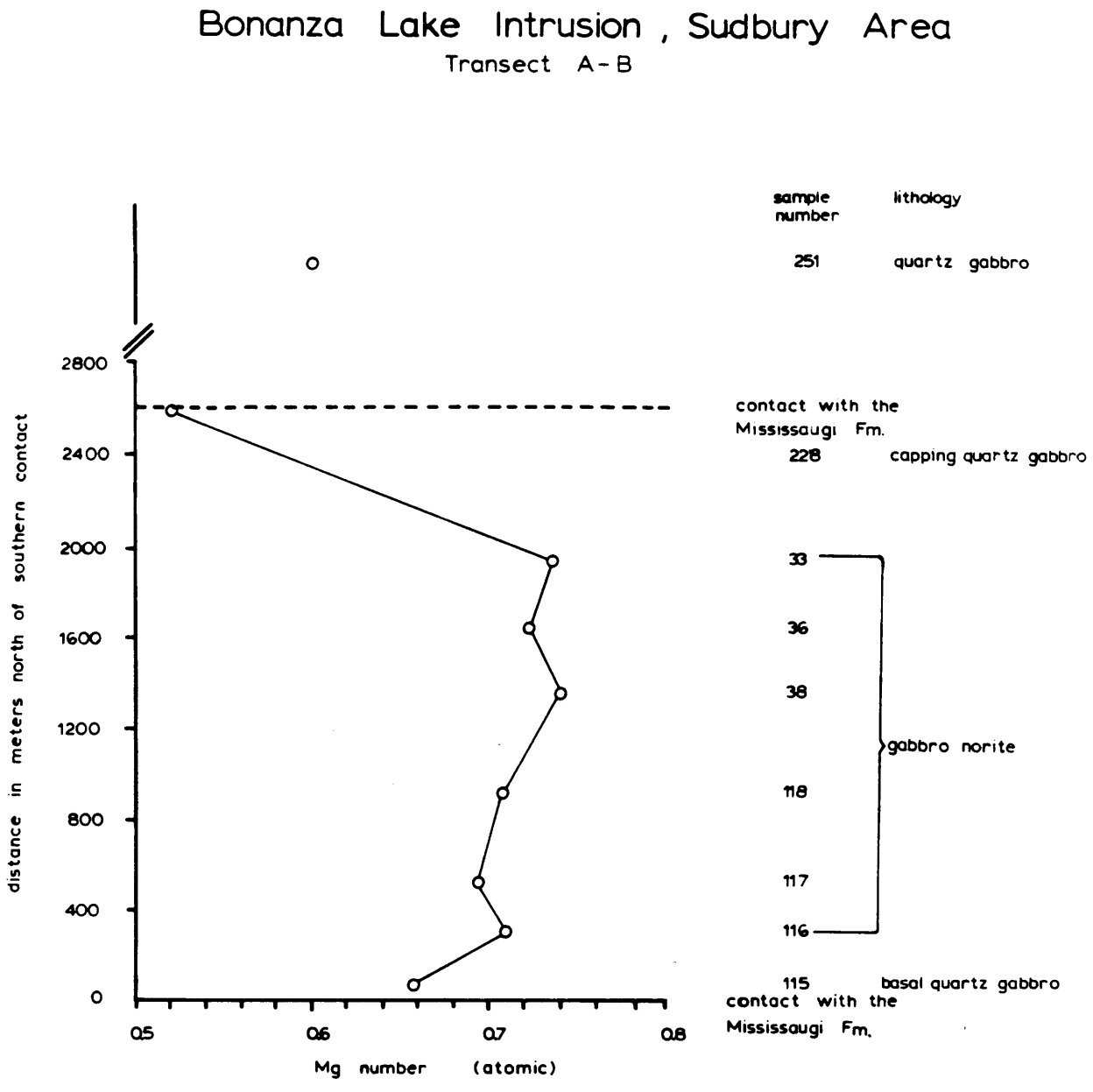


Figure 33. Variation in whole rock Mg-number across the Bonanza Lake Intrusion.

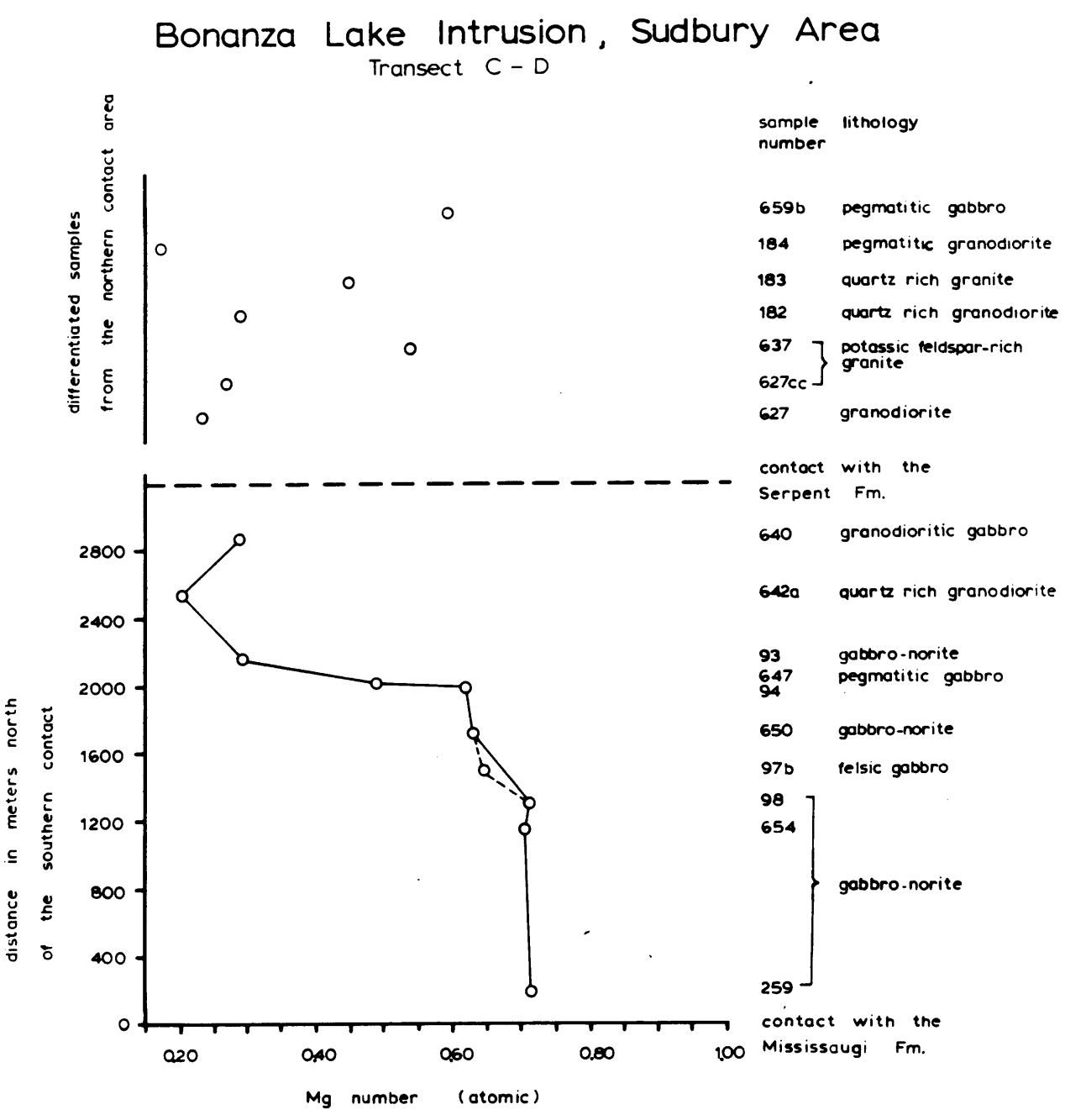


Figure 34. Variation in whole rock Mg-number across the Bonanza Lake Intrusion.

Figure 35. Cobalt and Temagami area Nipissing chilled margin samples plotted on a Th/Yb versus Ta/Yb plot (Pearce 1984).

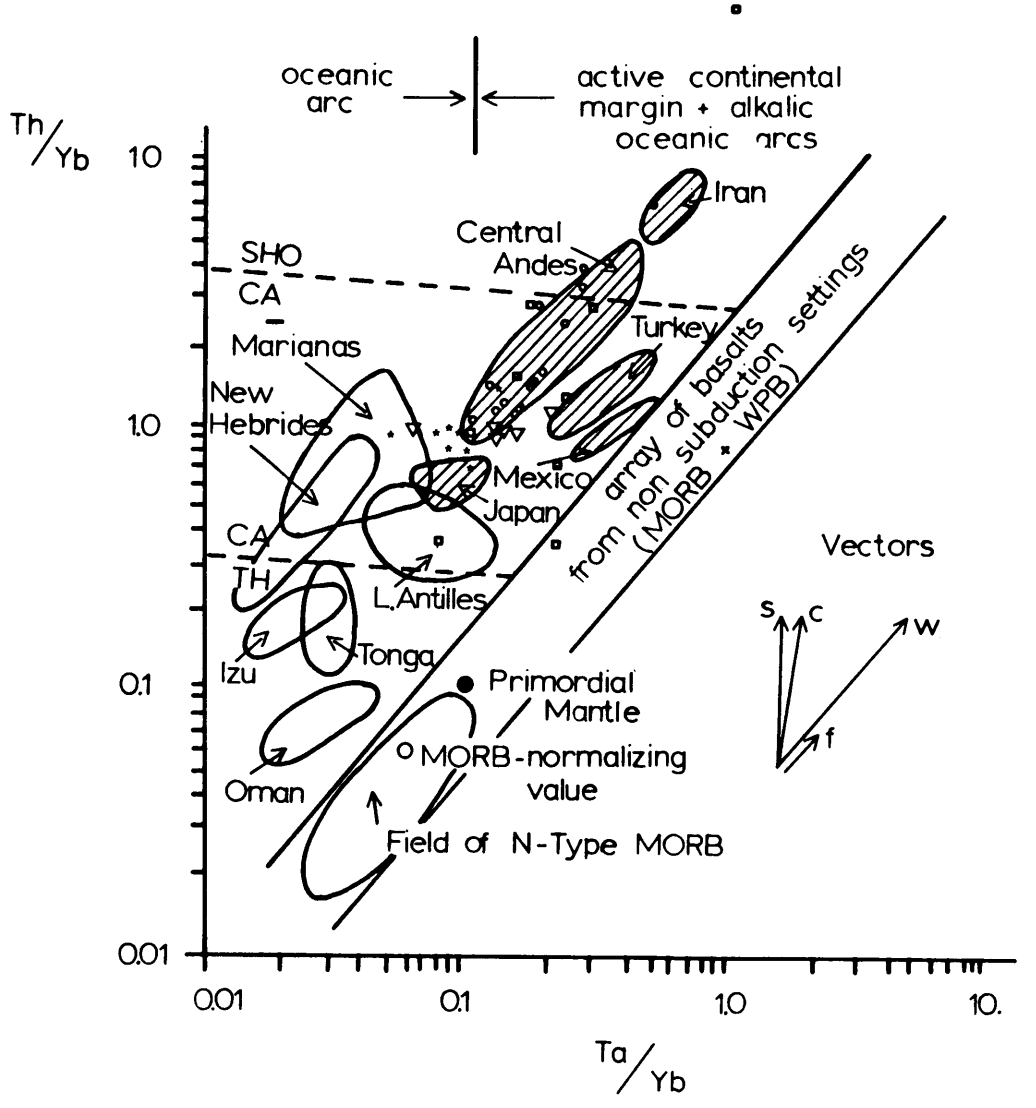


LEGEND

NIPISSING INTRUSIONS

- • Portage Bay Intrusion
- ▪ Bonanza Lake Intrusion
- * Cross Lake Intrusion
- ▿ Cobalt and Temagami Area Chills

- s Subduction Zone Enrichment
- c Crustal Contamination
- w Within Plate Enrichment
- f Fractional Crystallization (for F= 0.5)

SHO-Shoshonitic

TH –Tholeiitic

CA-Calc Alkaline

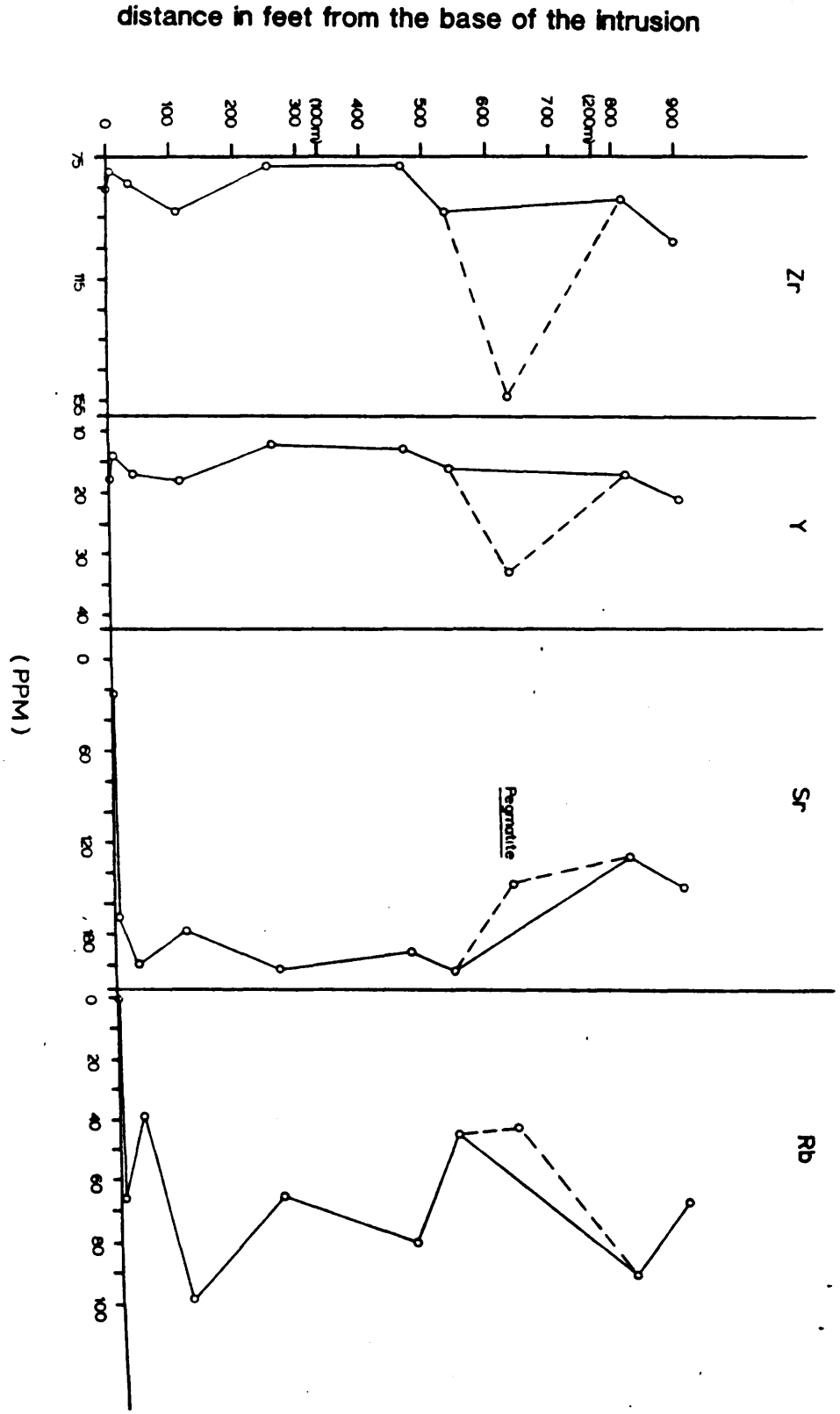


Figure 36. Variation in Zr, Y, Sr, and Rb across the Duncan Lake Intrusion.

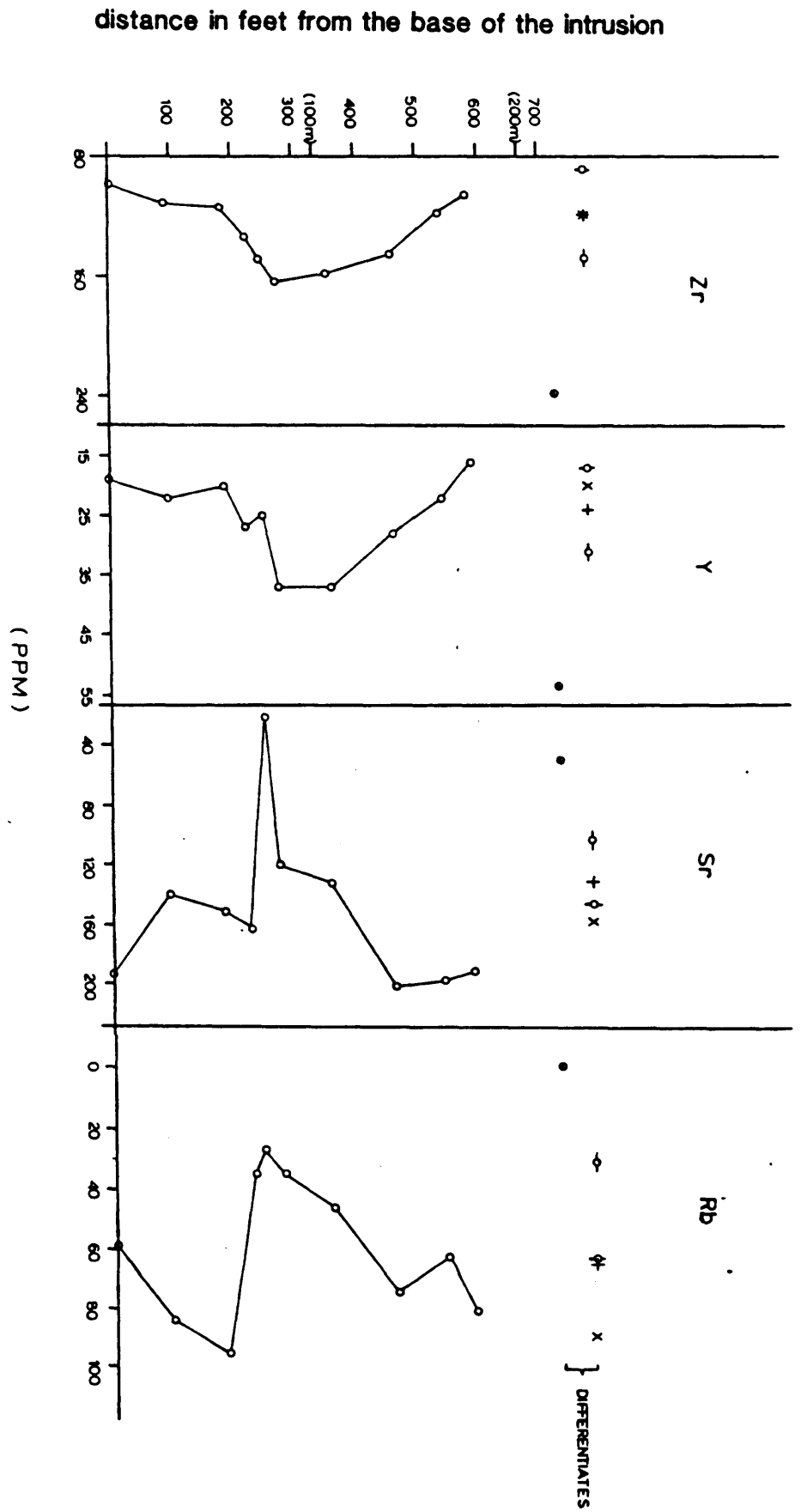


Figure 37. Variation in Zr, Y, Sr, and Rb across the Beaton Bay Intrusion.

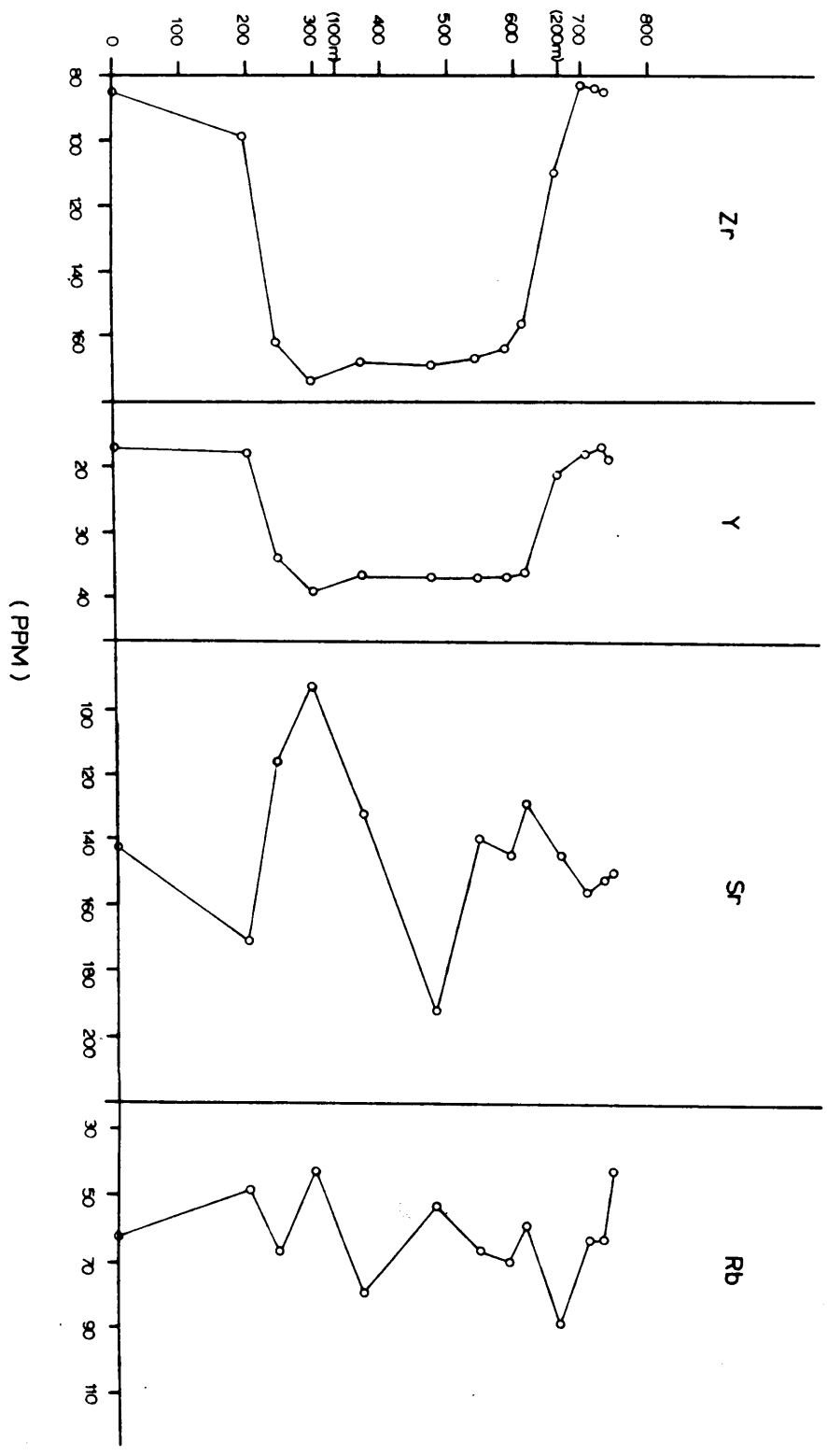


Figure 38. Variation in Zr, Y, Sr, and Rb across the Milner Lake Intrusion.

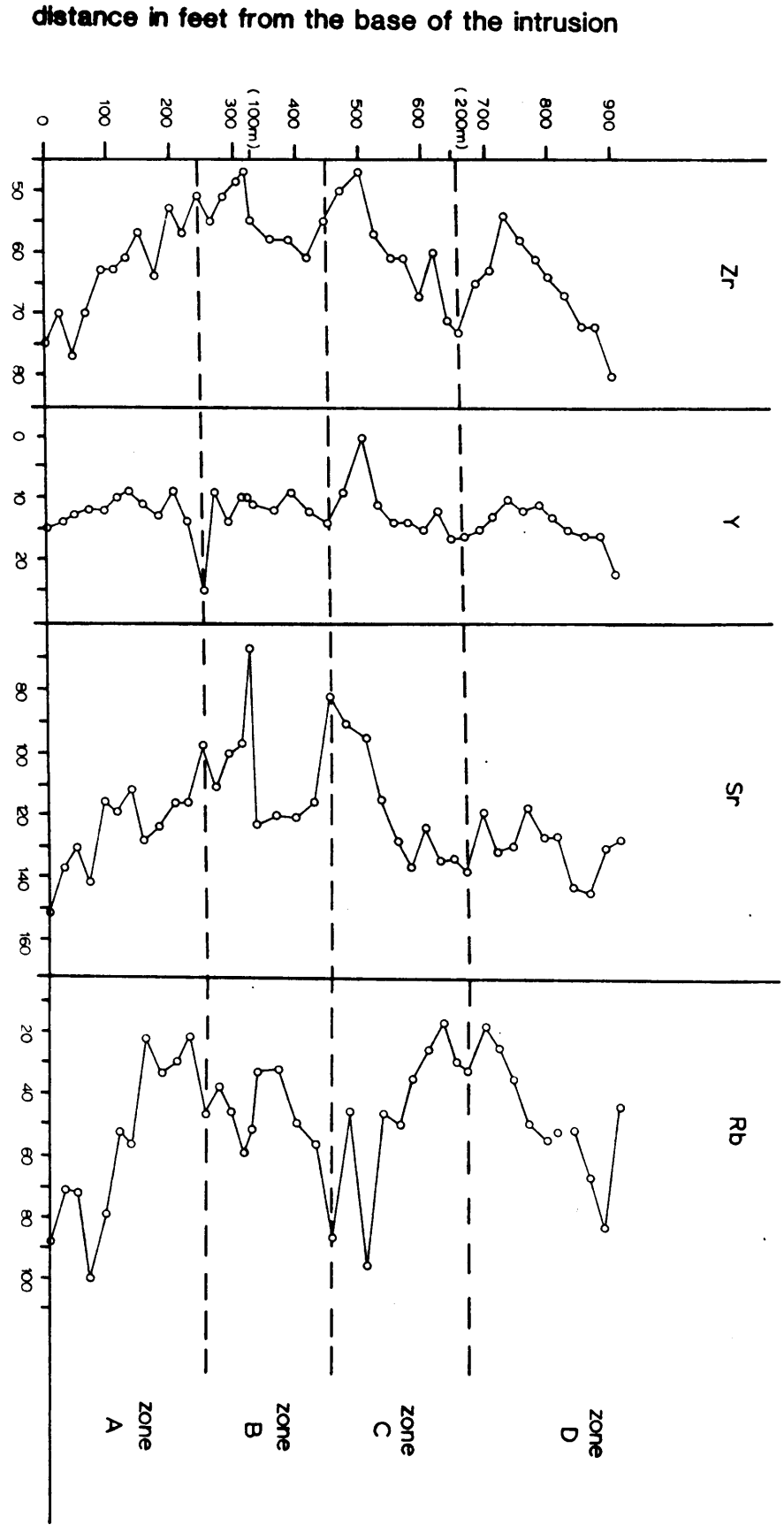


Figure 39. Variation in Zr, Y, Sr, and Rb across the Miller Lake Intrusion.

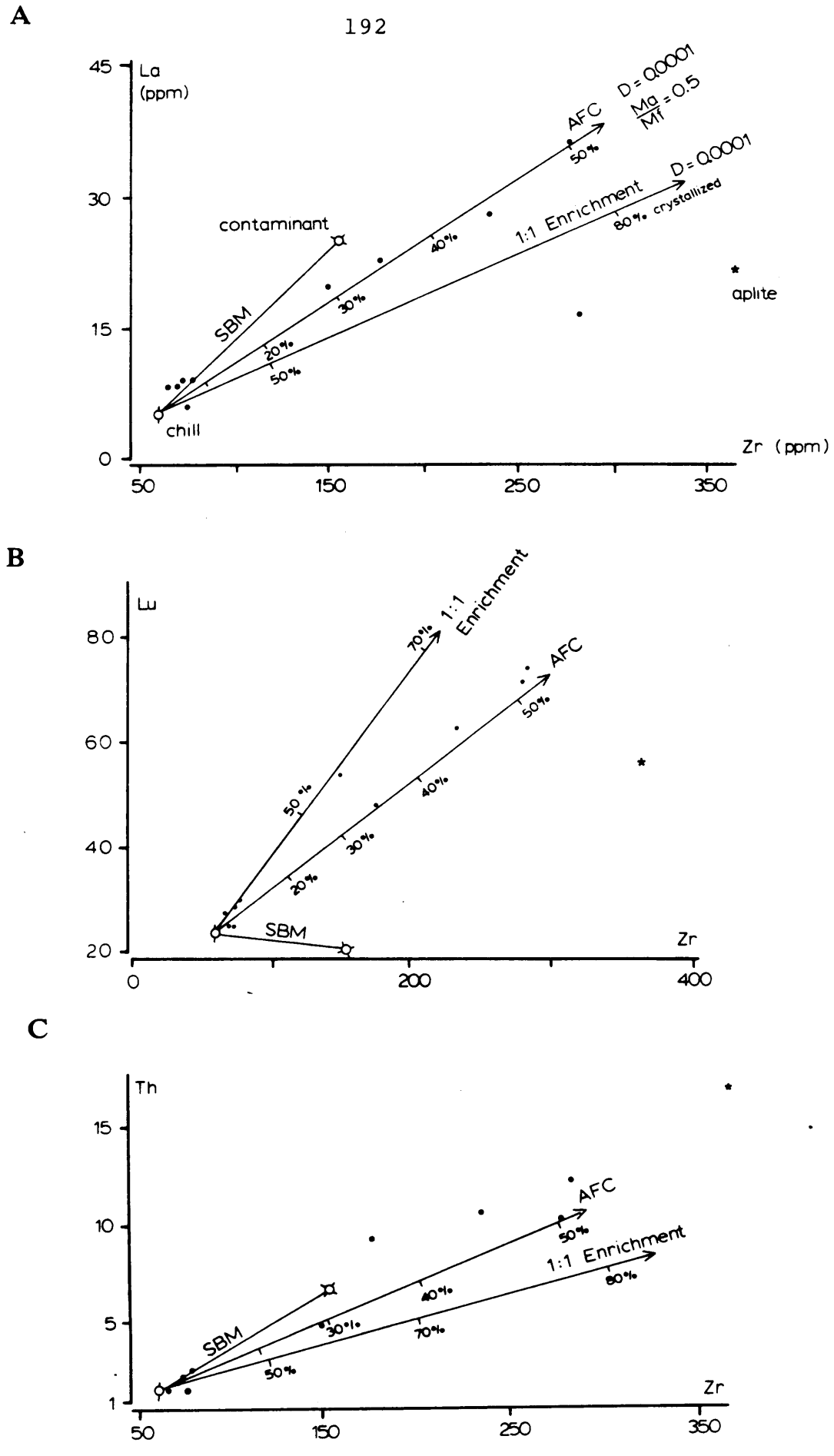


Figure 40. Quantitative modelling of the Portage Bay Intrusion.

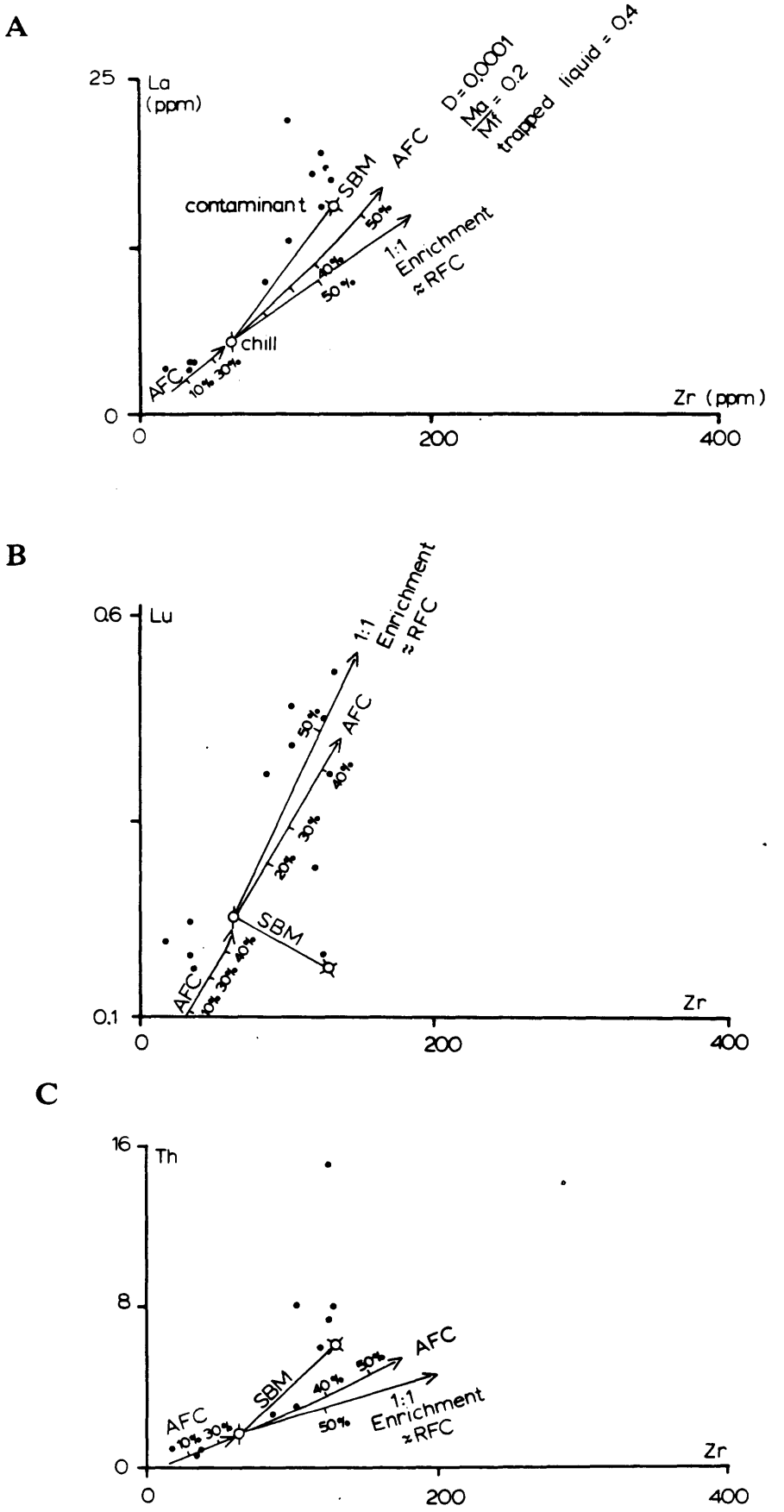


Figure 41. Quantitative modelling of the Bonanza Lake Intrusion.

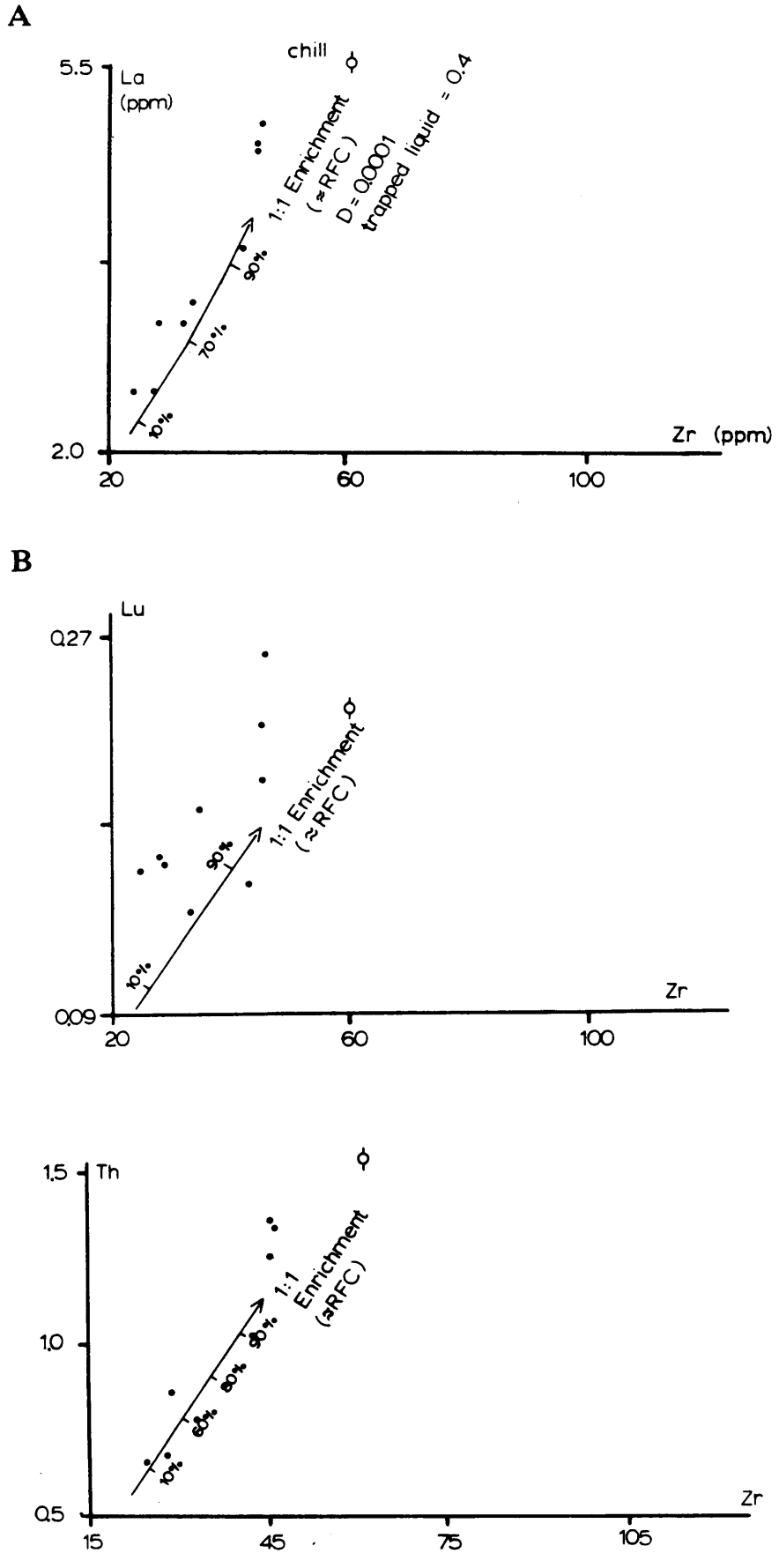


Figure 42. Quantitative modelling of the Cross Lake Intrusion.

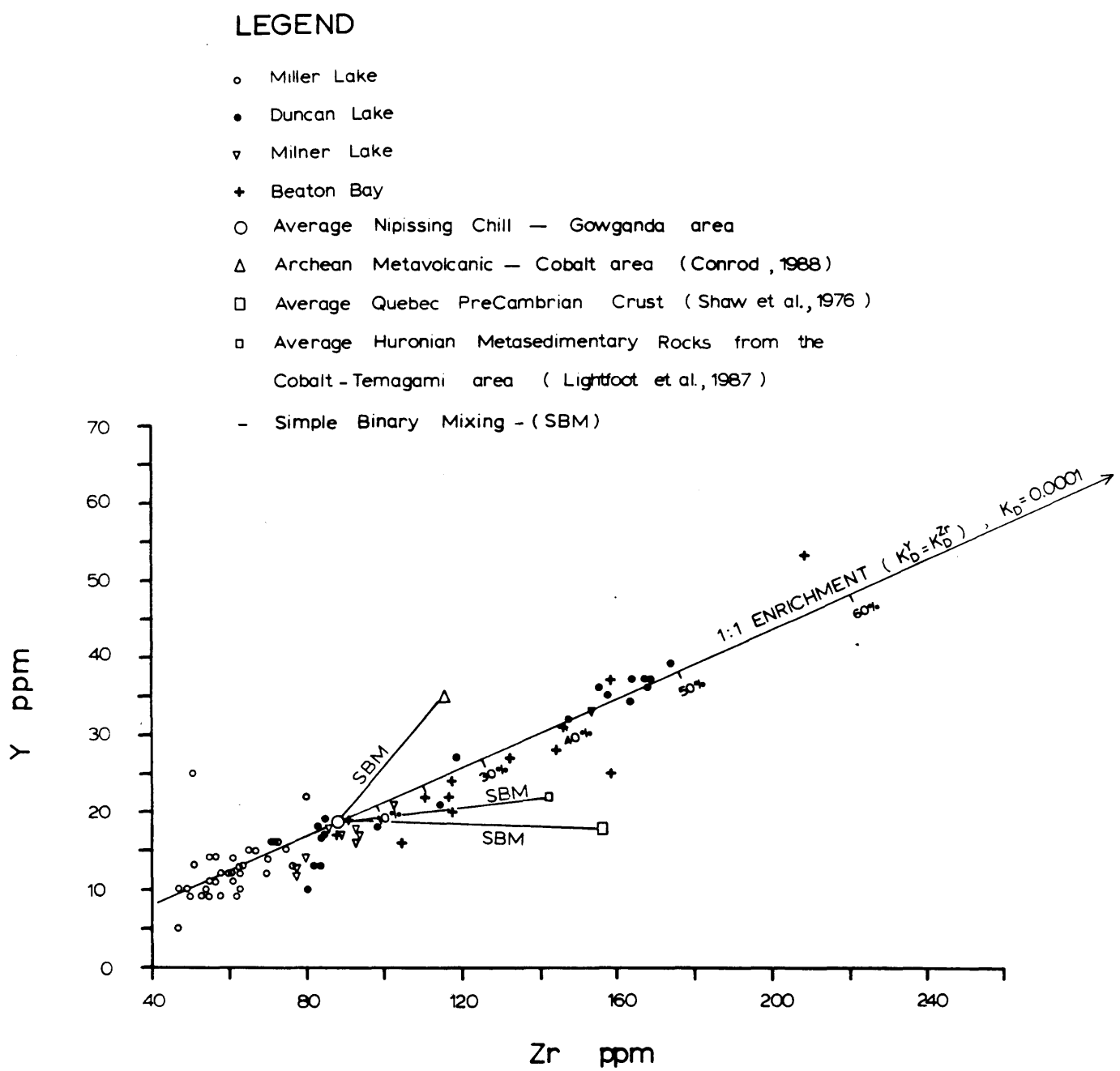


Figure 43. Gowganda area Nipissing intrusion lithologies plotted on a Y versus Zr plot.

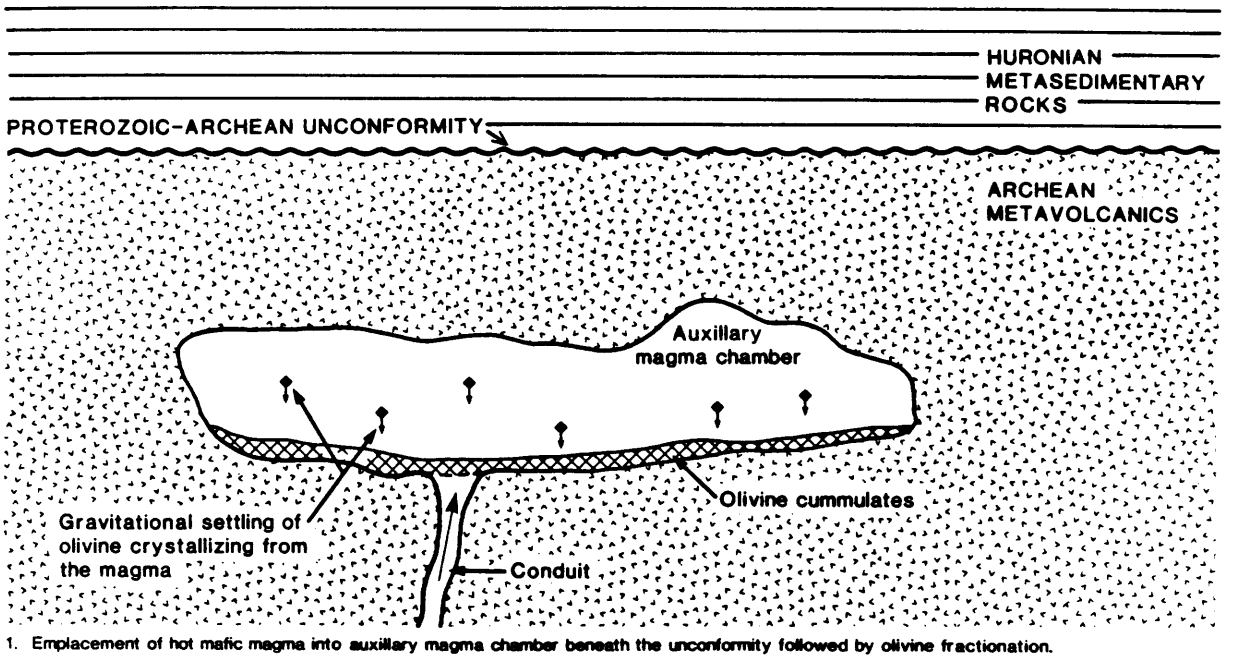


1. Emplacement of hot mafic magma into auxillary magma chamber beneath the unconformity followed by olivine fractionation.

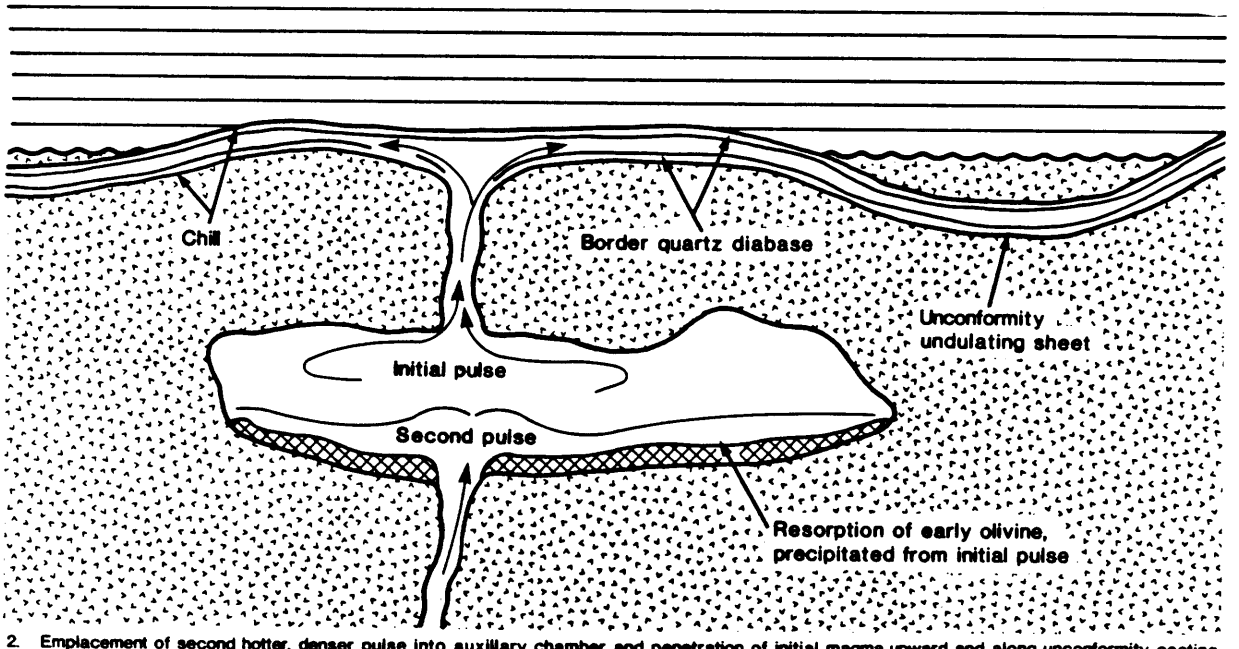


2. Emplacement of second hotter, denser pulse into auxillary chamber and penetration of initial magma upward and along unconformity coating the upper and lower contacts with magma of the same composition. Resorption of some of the olivine occurs within the auxillary chamber.

Figure 44. Model for the emplacement and crystallization of the Gowganda area Nipissing magmas.

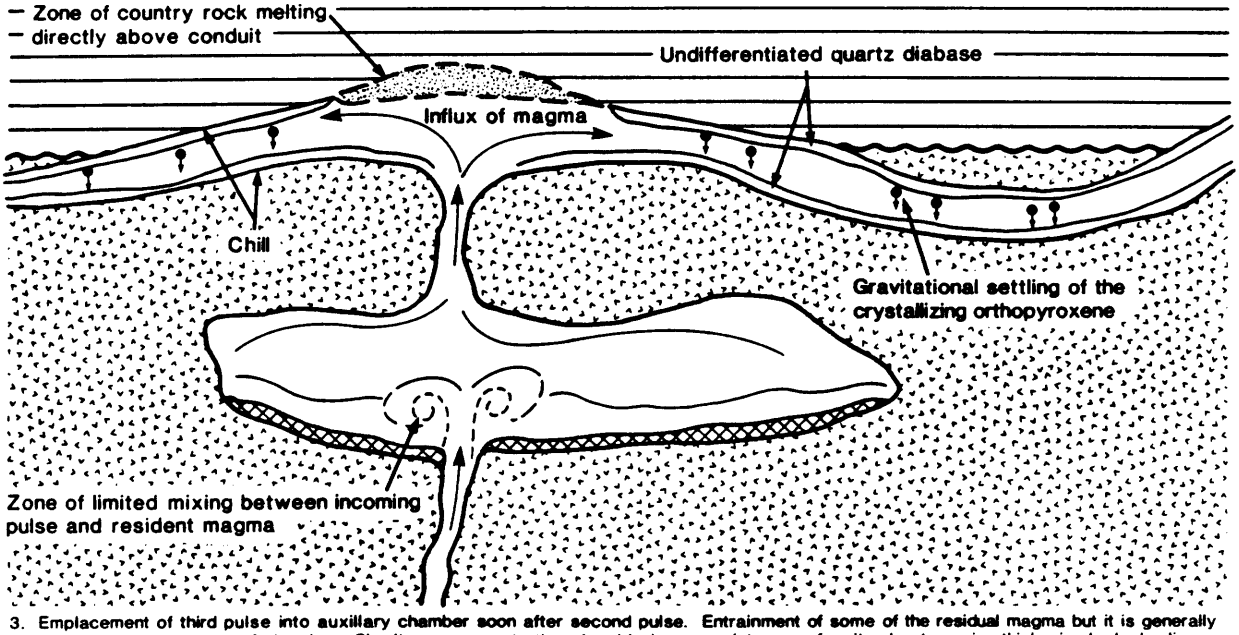


3. Emplacement of third pulse into auxillary chamber soon after second pulse. Entrainment of some of the residual magma but it is generally restricted to lower part of chamber. Simultaneous penetration of residual magma into unconformity sheet causing thickening by hydraulic jacking of the overlying Huronian sedimentary rocks. Continued absorption of crystal mush from floor of auxillary chamber. A zone of wall rock melting develops above the conduit.

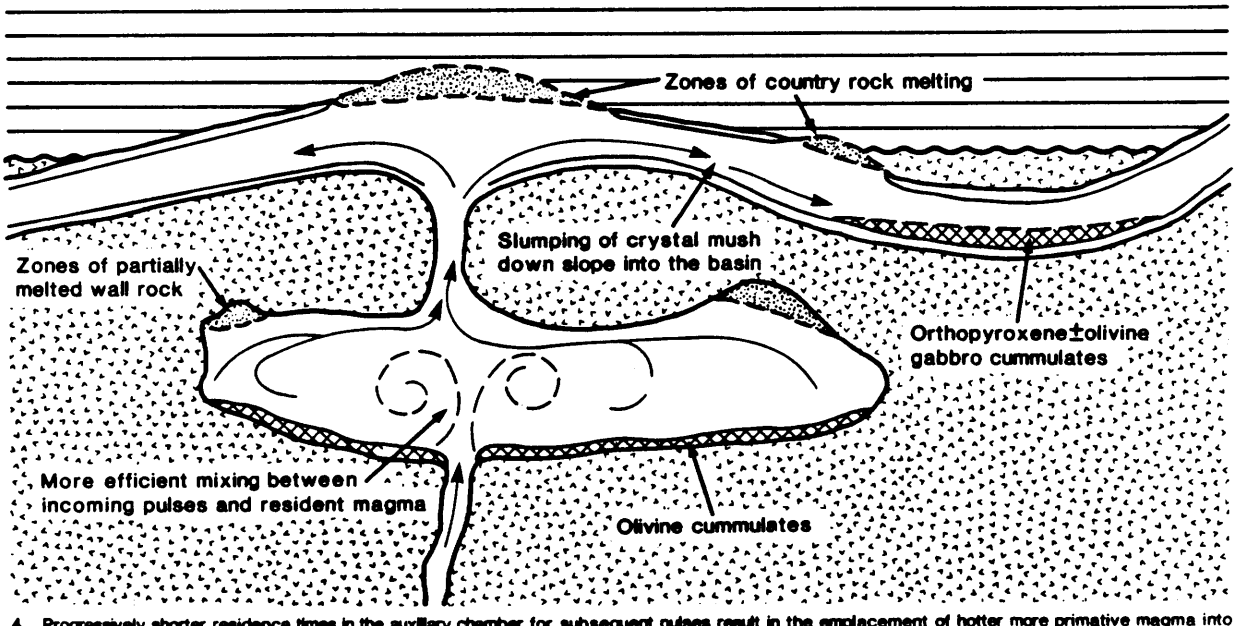


4. Progressively shorter residence times in the auxiliary chamber for subsequent pulses result in the emplacement of hotter more primative magma into the unconformity sheet. Any crystal mush beginning to accummulate on the floors of the arches are washed down slope by the incoming pulses or simply slump under the infuence of gravity. Patches of wall rock melting begin around the auxillary chamber but remain isolated from the mafic magma due to its bouyant nature. Accumulation of bronzite and hypersthene gabbros occur within the basins of the undulating unconformity sheet.

Figure 44 (con'd). Model for the emplacement and crystallization of the Gowganda area Nipissing magmas.

E

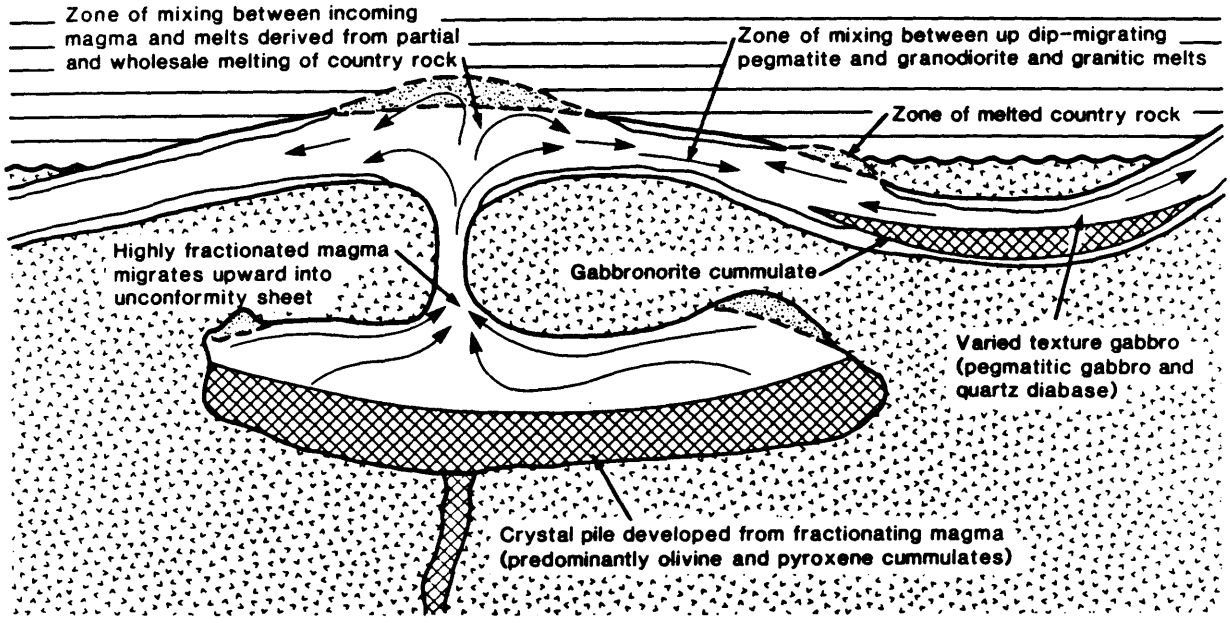


5. In the latest stages of magmatism a longer residence time in the auxillary chamber allows the last pulses to fractionate and to mix with the pockets of partially melted country rock before emplacement into the unconformity sheet. Once emplaced this magma mixes with partially melted Huronian rocks above the conduit and along the limbs. This bouyant viscous magma tends to remain in the arch an central portions of the limbs. Filter pressing within the gabbronorite pile in the basins causes the migration of volatile material upward through the crystal pile to form the varied texture pegmatitic gabbro above the gabbronorites. Some of this volatile material moves upward and mixes with the granodioritic and granitic magmas in the limbs and arches. Aplites lacking chills most likely represent the last magma differentiates coming from the auxillary chamber or remobilized melted country rock.

Figure 44 (con'd). Model for the emplacement and crystallization of the Gowganda area Nipissing magmas.

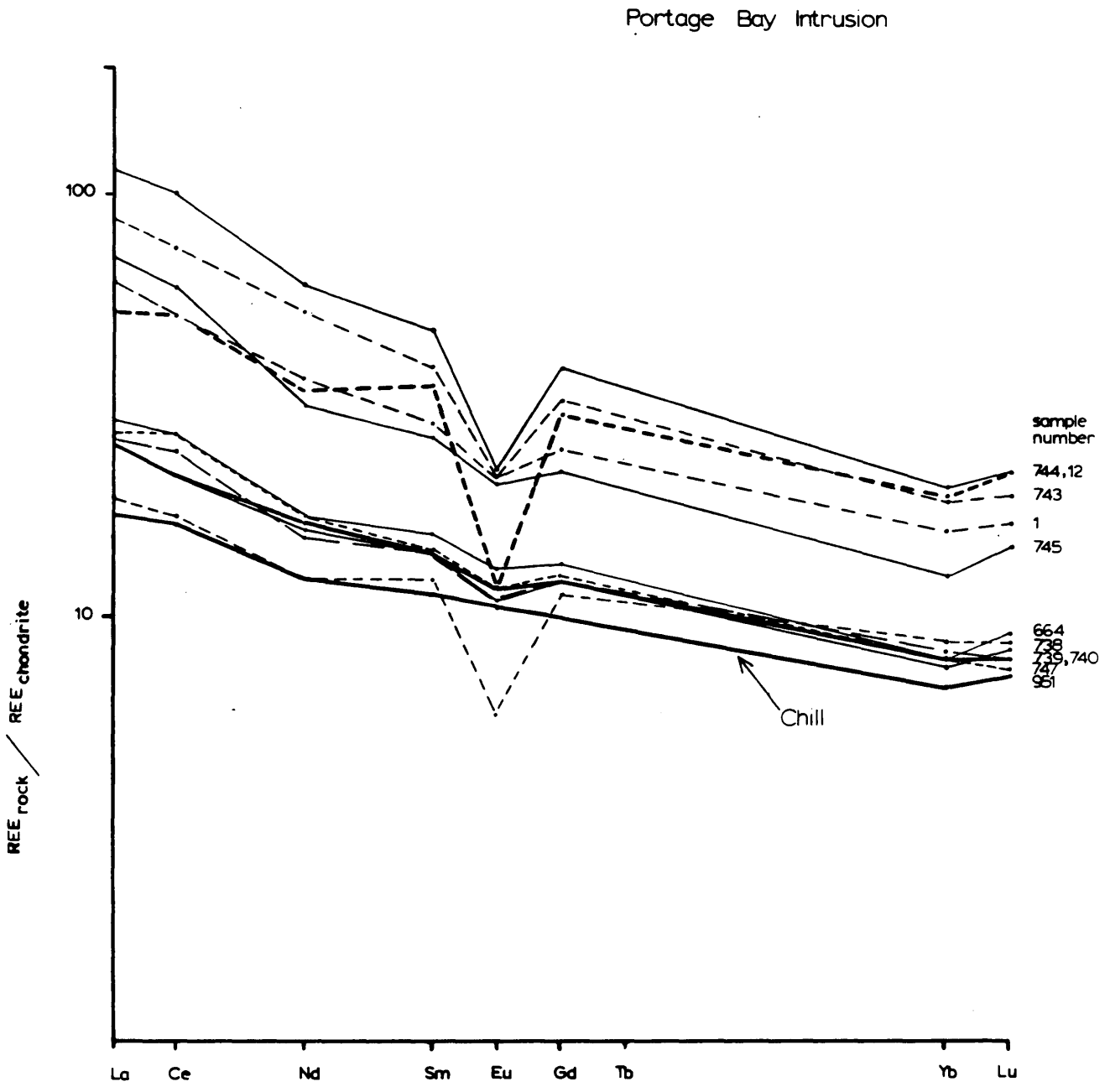


Figure 45. Chondrite-normalized Rare Earth Element (REE) plot of the lithologies comprising the Portage Bay Intrusion.

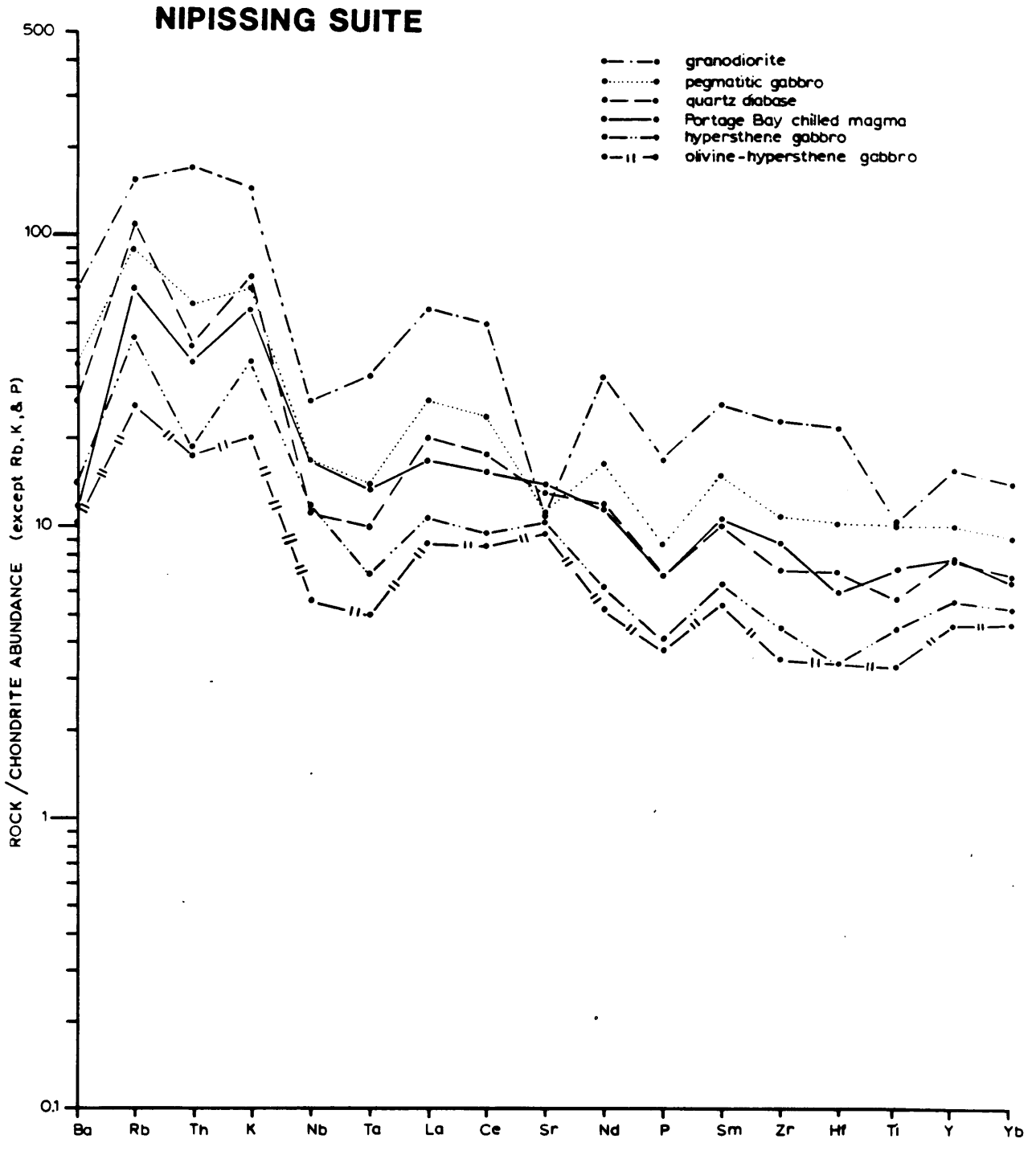


Figure 46. Chondrite-normalized spidergram of the lithologies comprising the Nipissing Suite.

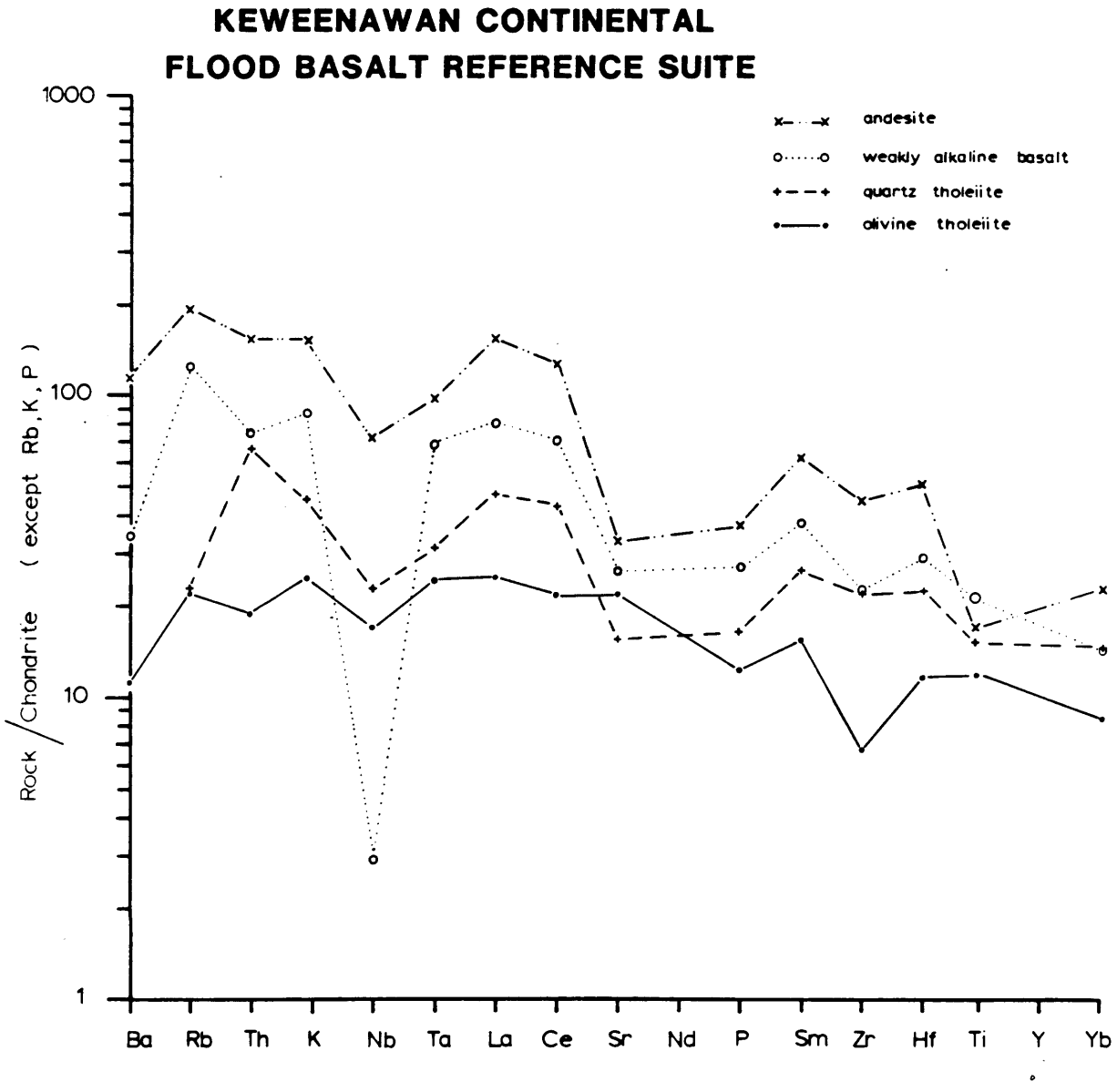


Figure 47. Chondrite-normalized spidergram of the lithologies comprising the Keweenawan Reference Suite.

Figure 48. Chondrite-normalized spidergram of pelite-contaminated dolerite sills.

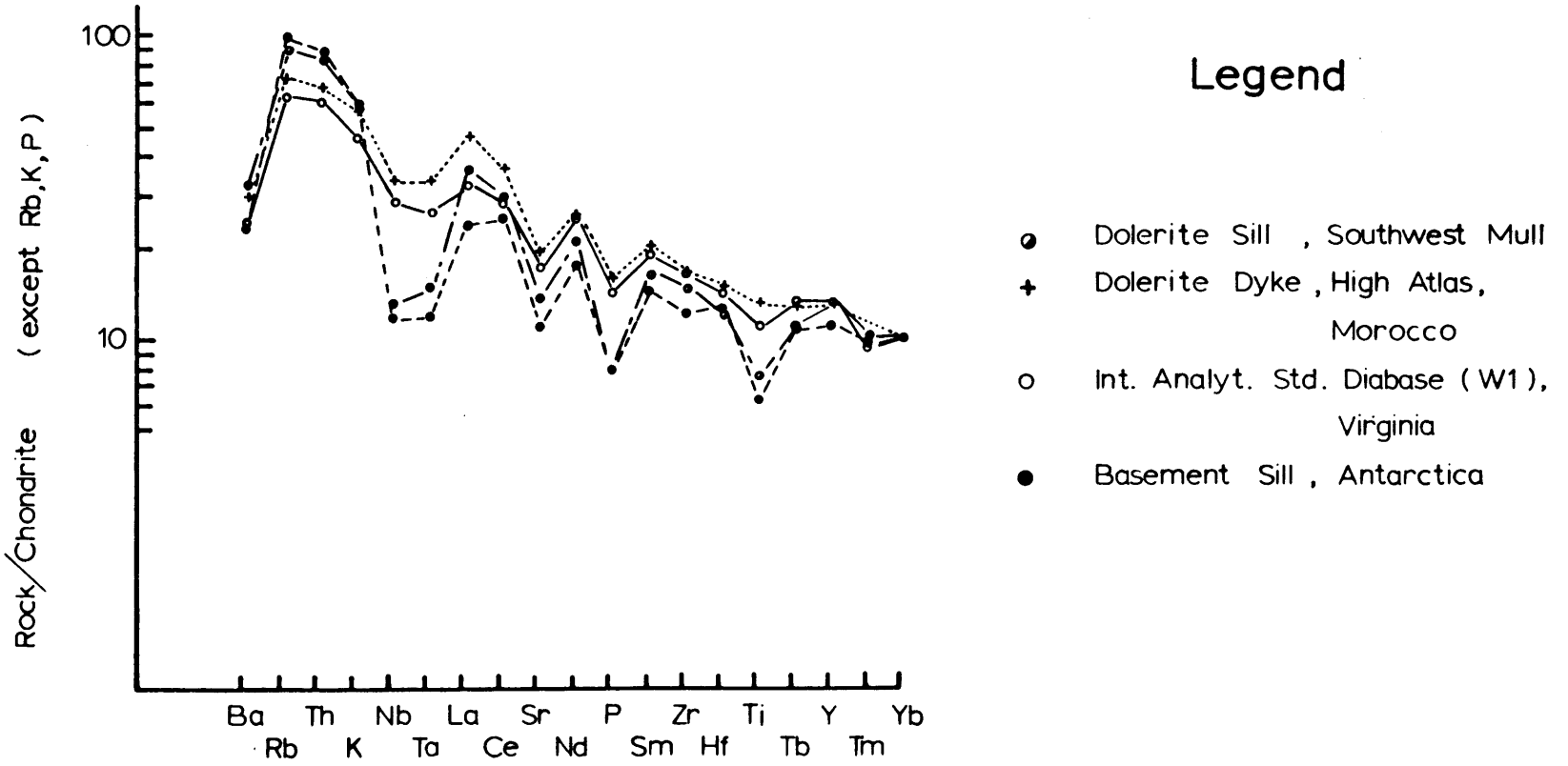

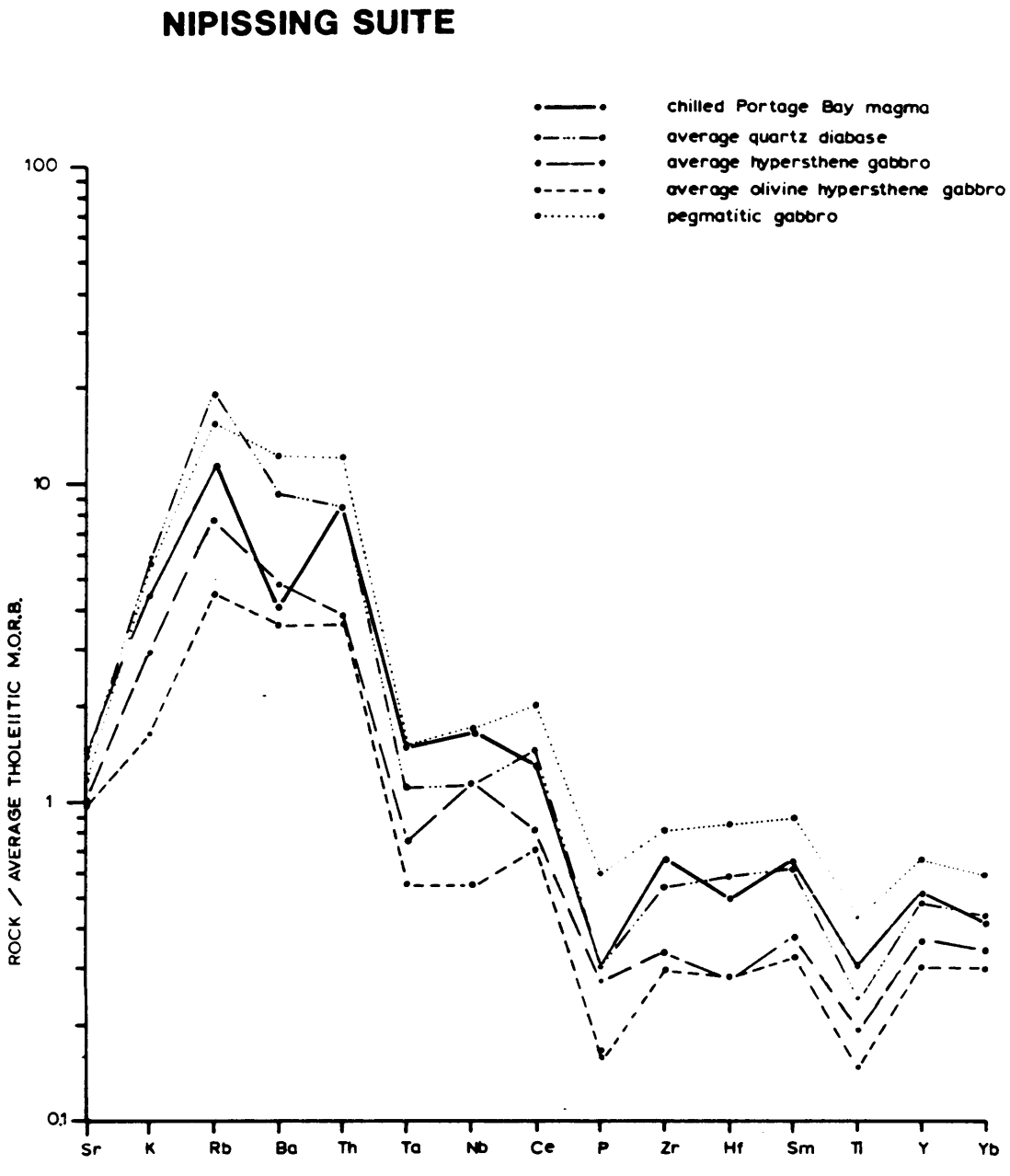


Figure 49a. MORB-normalized spidergram of the lithologies comprising the Nipissing Suite.

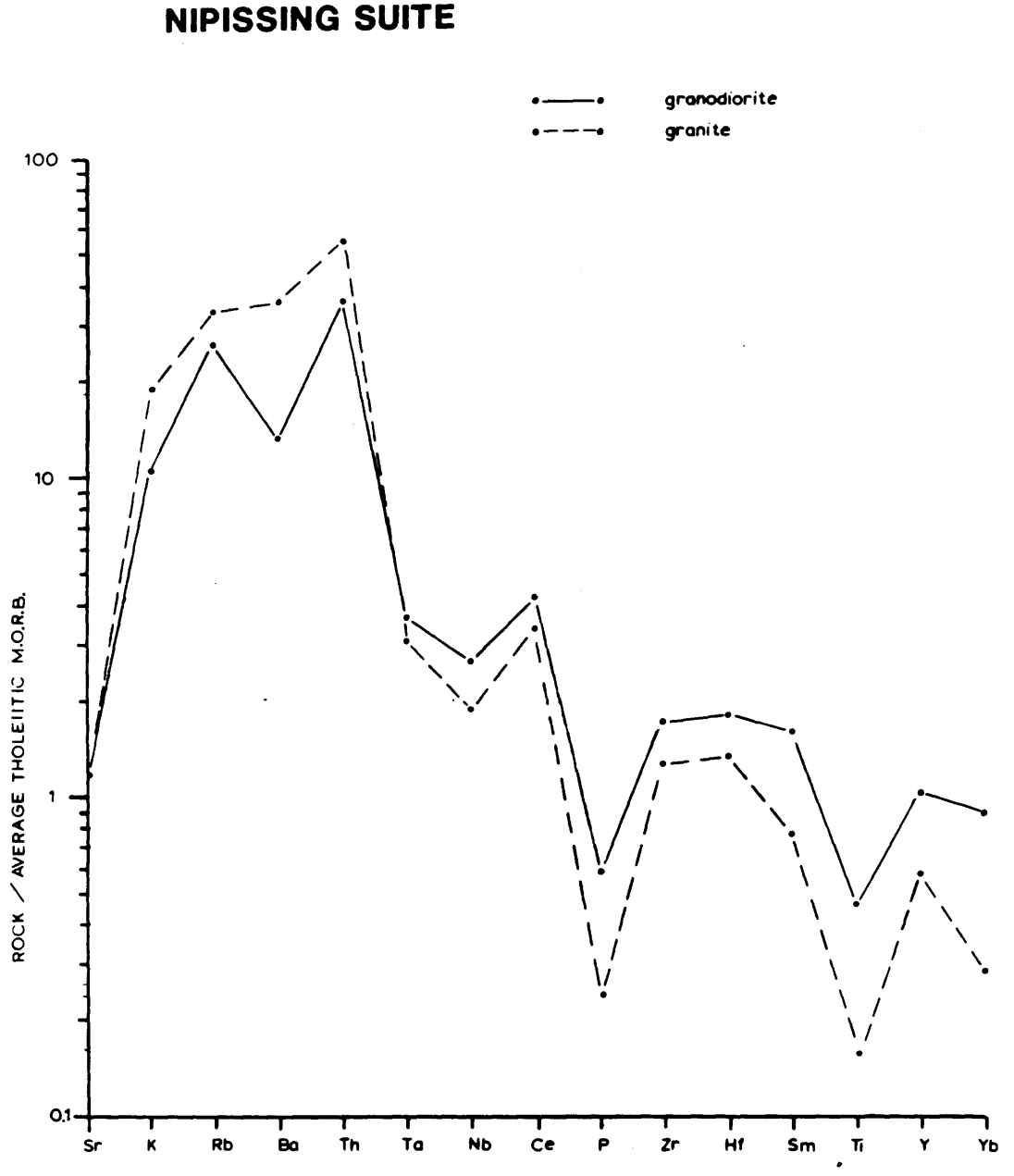


Figure 49b. MORB-normalized spidergram of the lithologies comprising the Nipissing Suite.

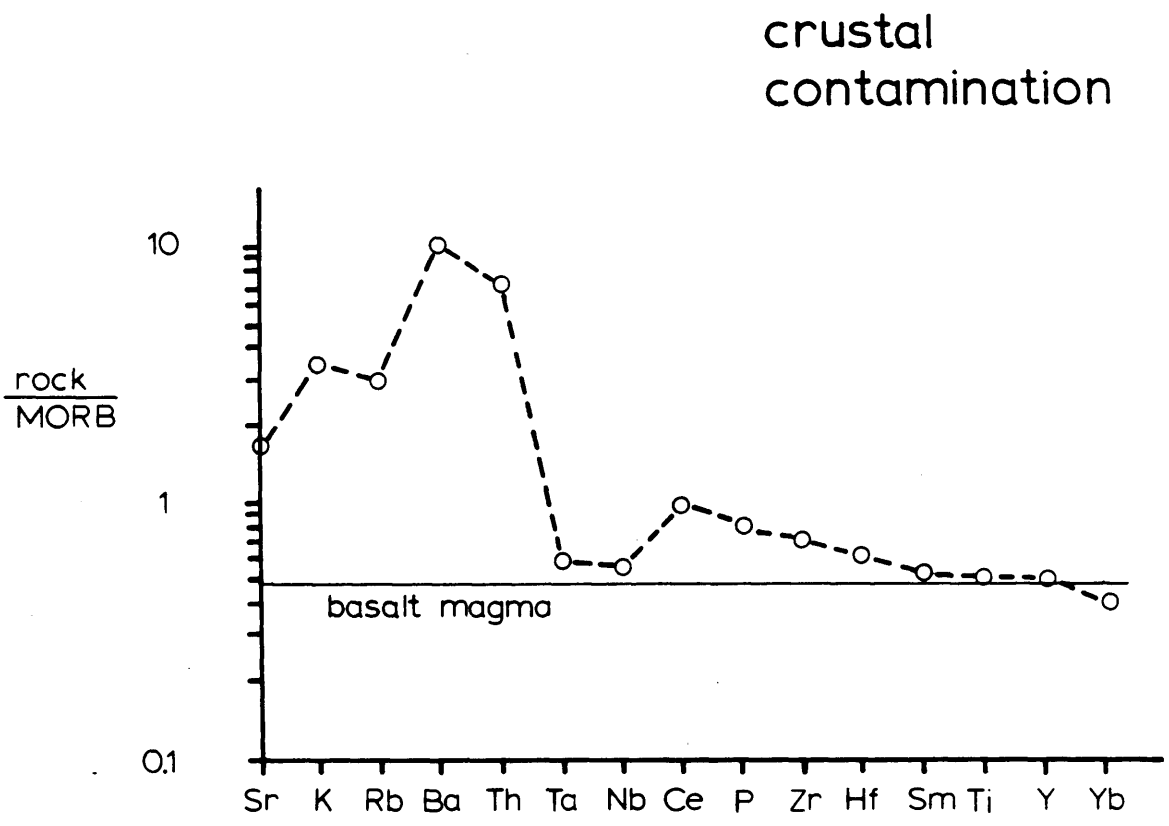


Figure 50. MORB-normalized spidergram of primitive basalt which has undergone crustal contamination.

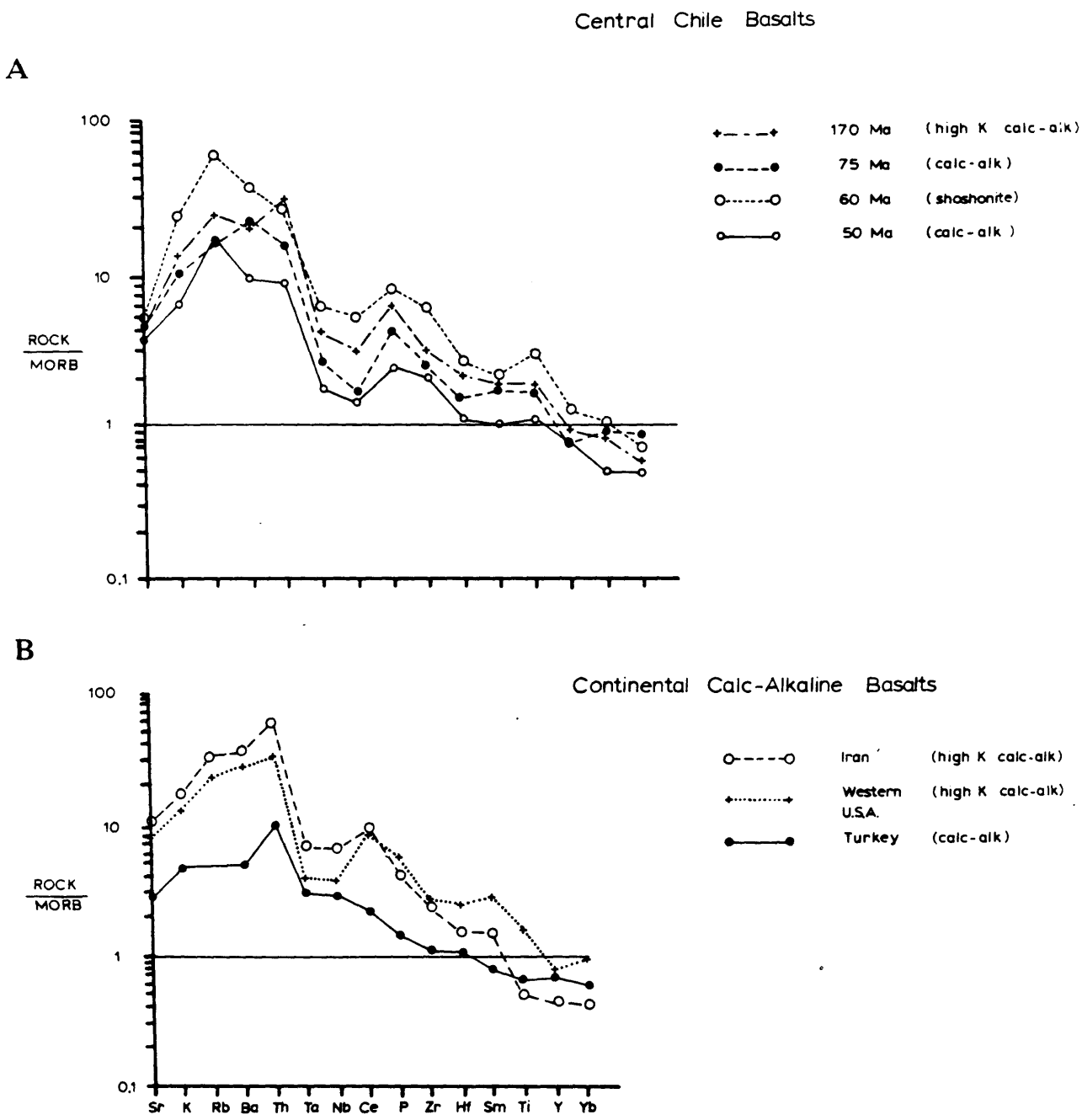


Figure 51. MORB-normalized spidergram of Chilean calc-alkalic and continental calc-alkalic basalts.

Figure 52. Nipissing Suite plotted on the Th-Hf-Ta discrimination plot of Wood (1980).

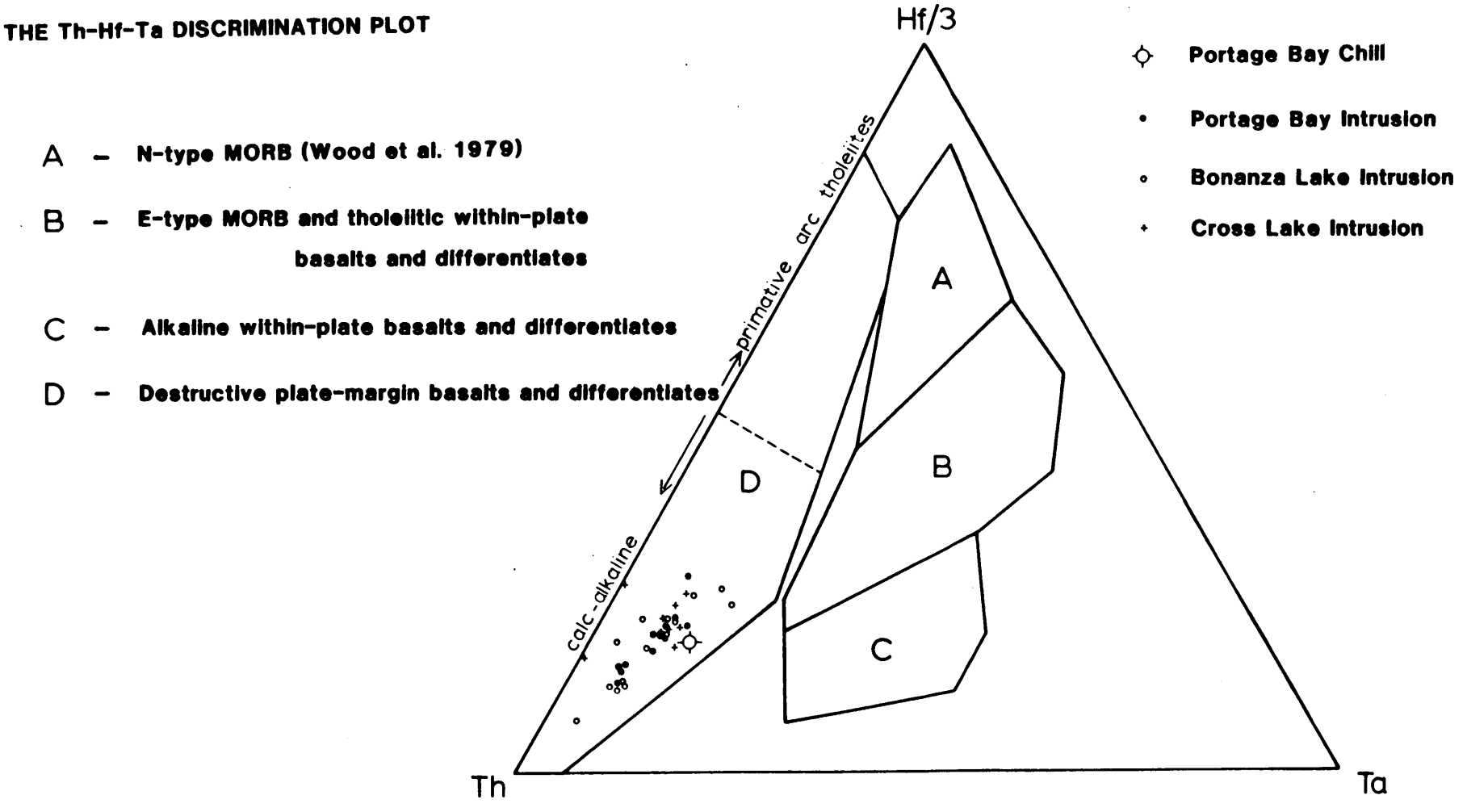

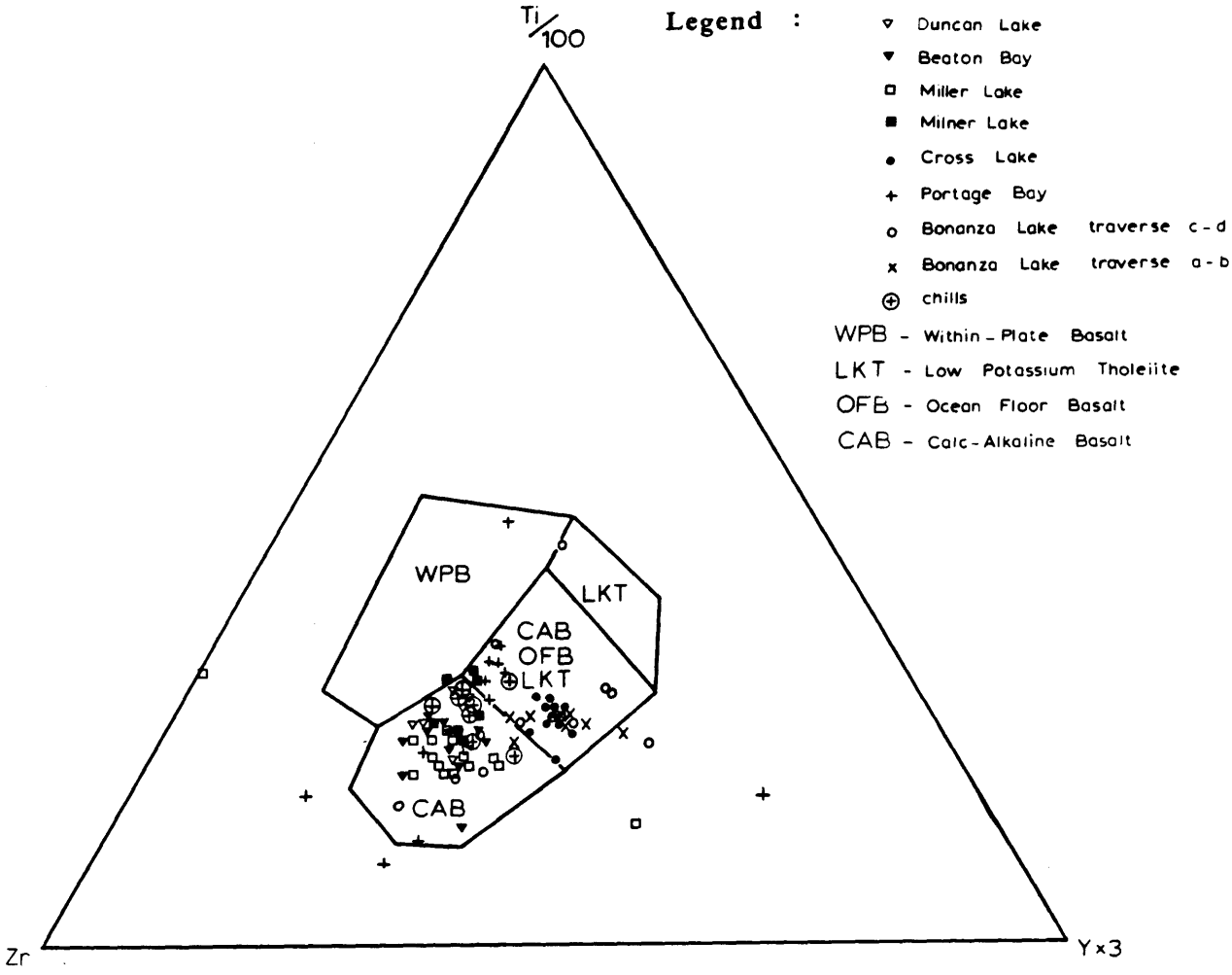


Figure 53. Nipissing Suite plotted on the Zr-Ti-Y discrimination plot of Pearce and Cann (1973).

Figure 54. Chilled Nipissing magmas from the Gowganda, Cobalt, and Temagami areas plotted on the Zr/Y versus Zr discrimination plot of Pearce and Norry (1979).

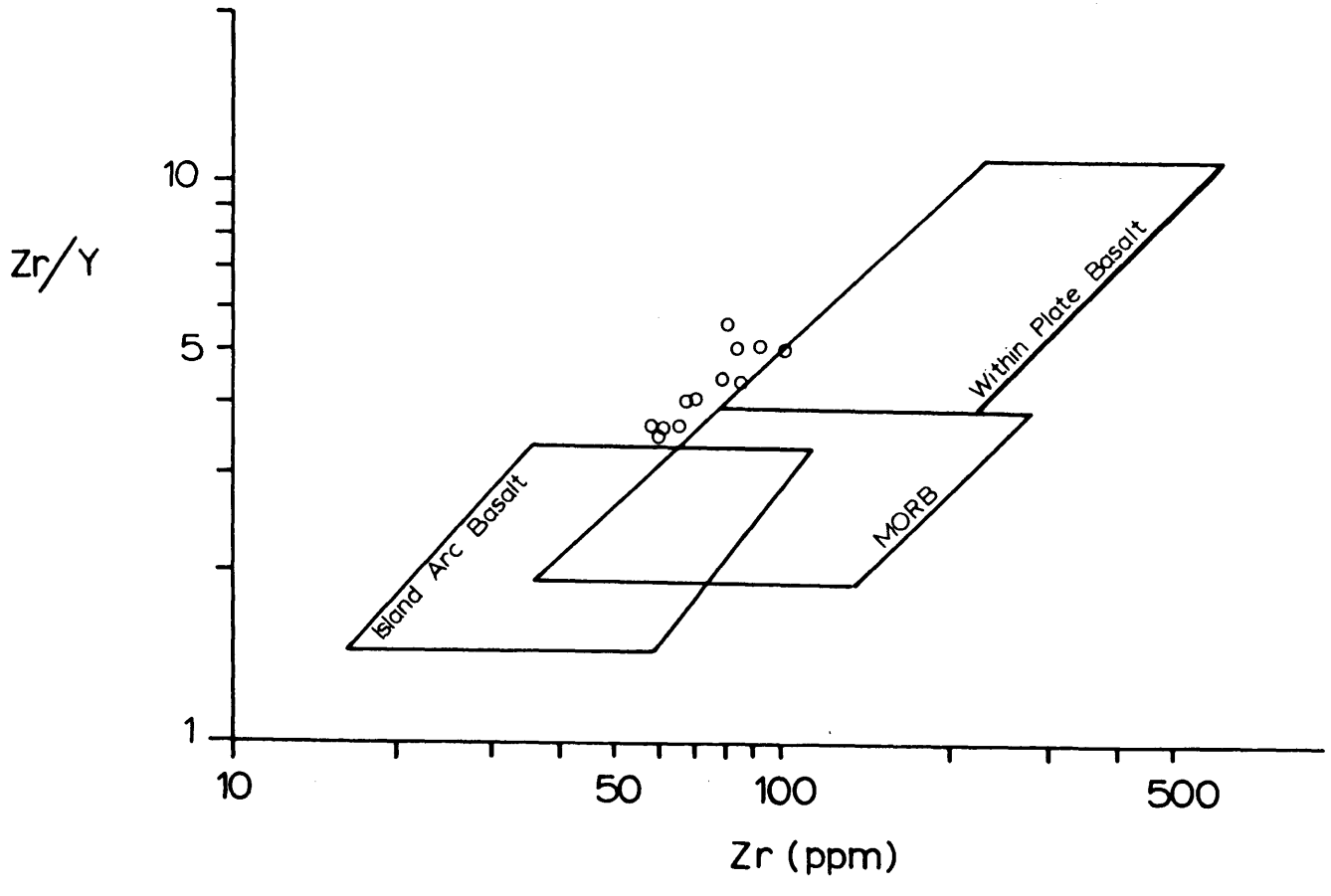

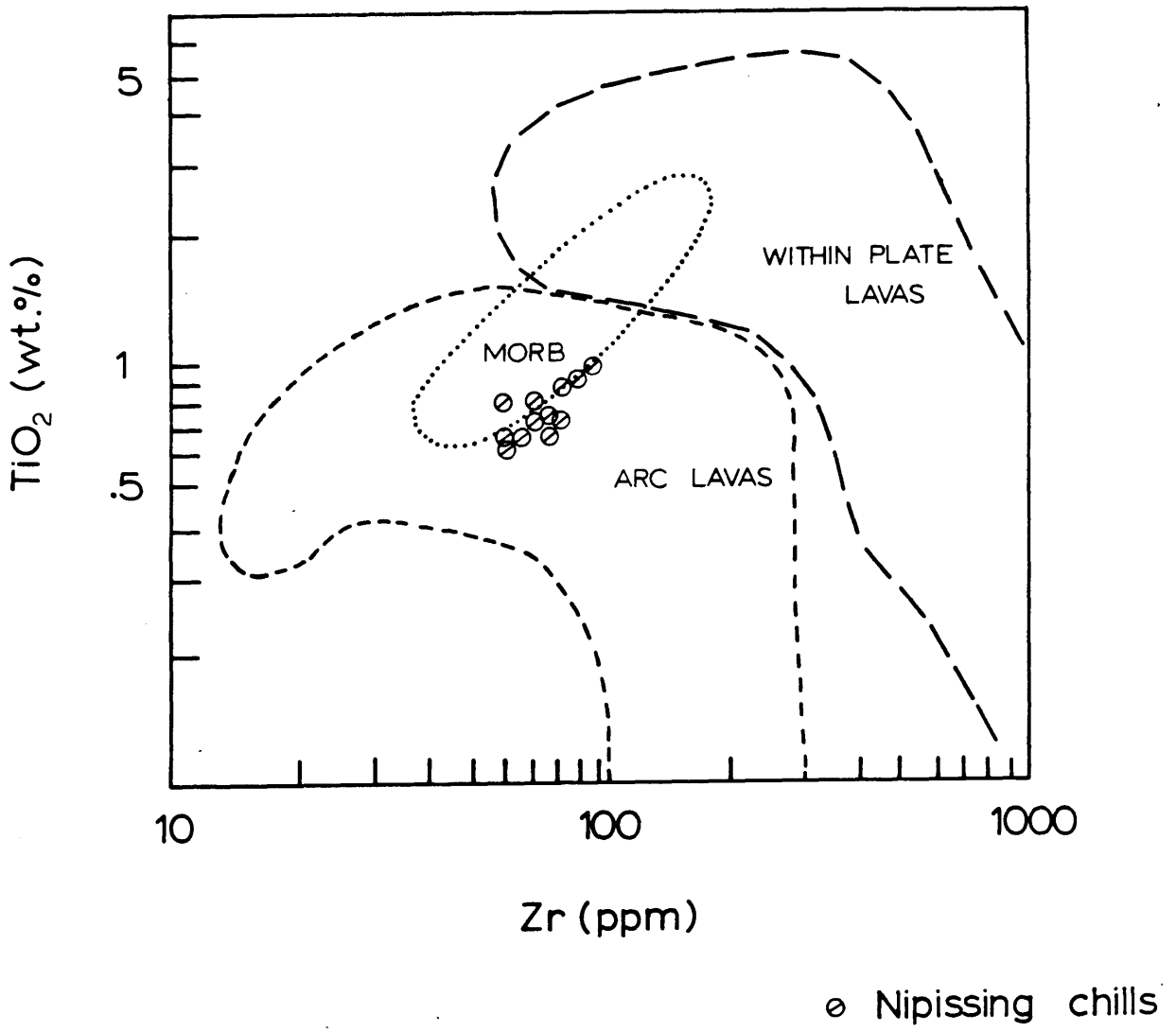


Figure 55. Chilled Nipissing magmas plotted on the Zr versus $TiO_2$ discrimination plot of Pearce (1980).

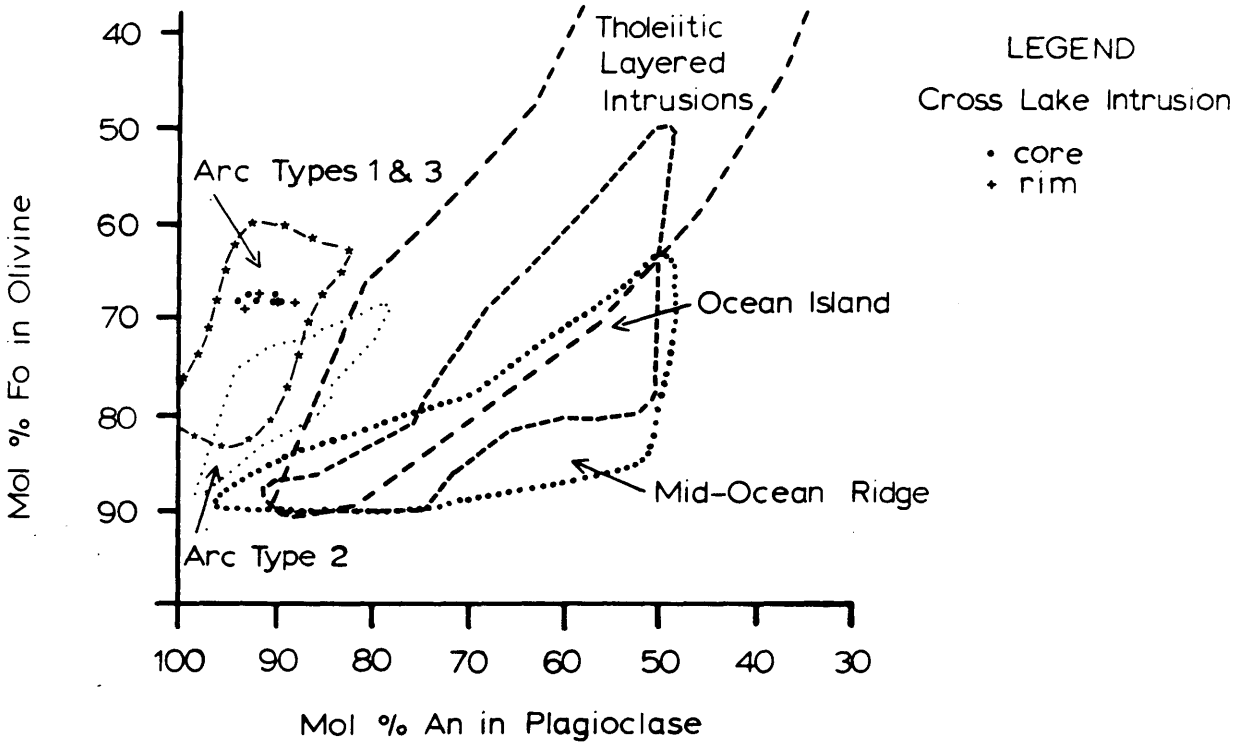


Figure 56 Cross Lake Nipissing intrusion plotted on the plagioclase versus olivine discrimination plot of Beard (1986).

# Plan of Underground Workings, Portal, and Ramp

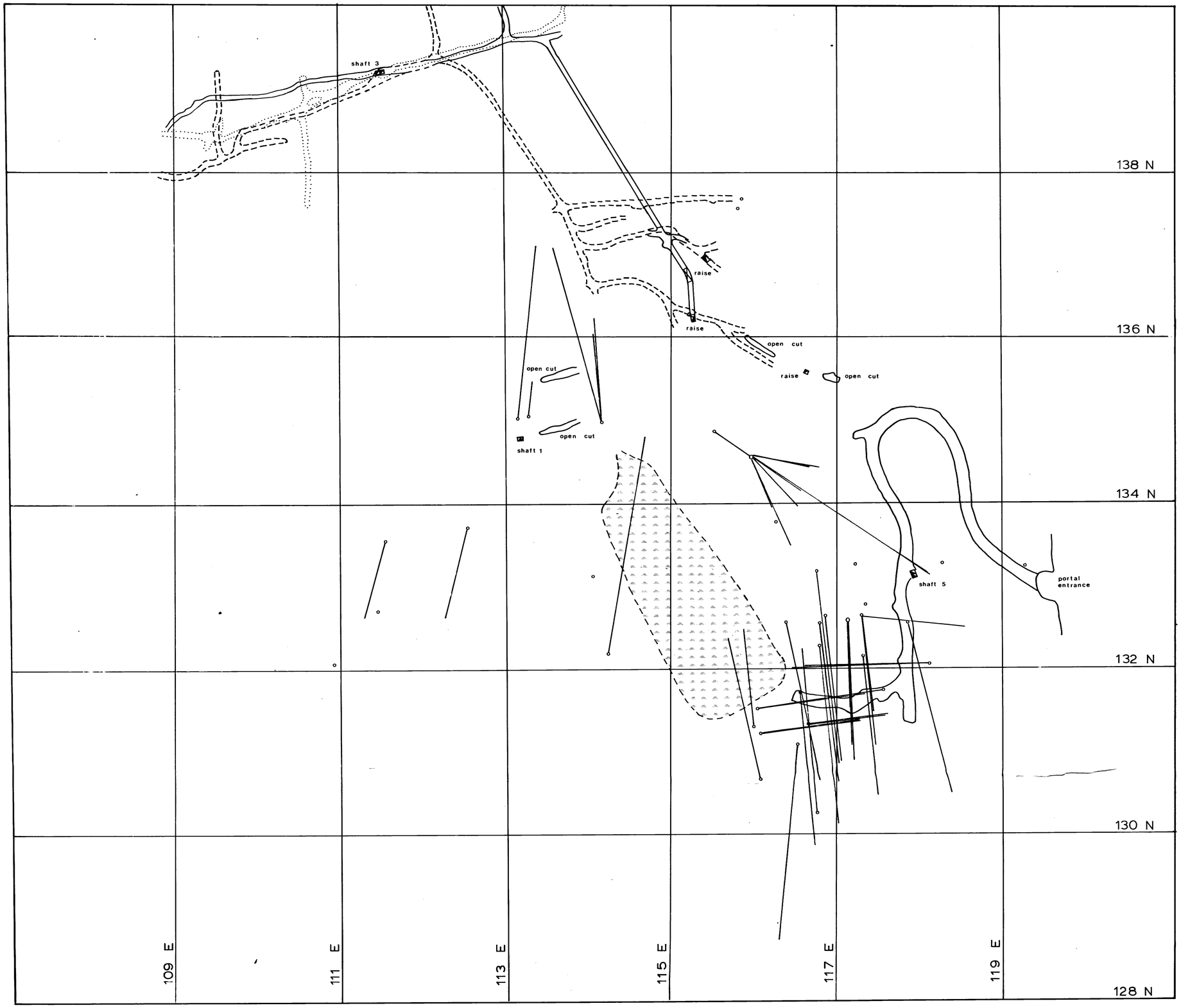


1st level
2nd level
3rd level

Scale

200 100 0 100 200

100 50 0 100

reduce to 30%

Figure 14c CONTOUR 1:045 CV

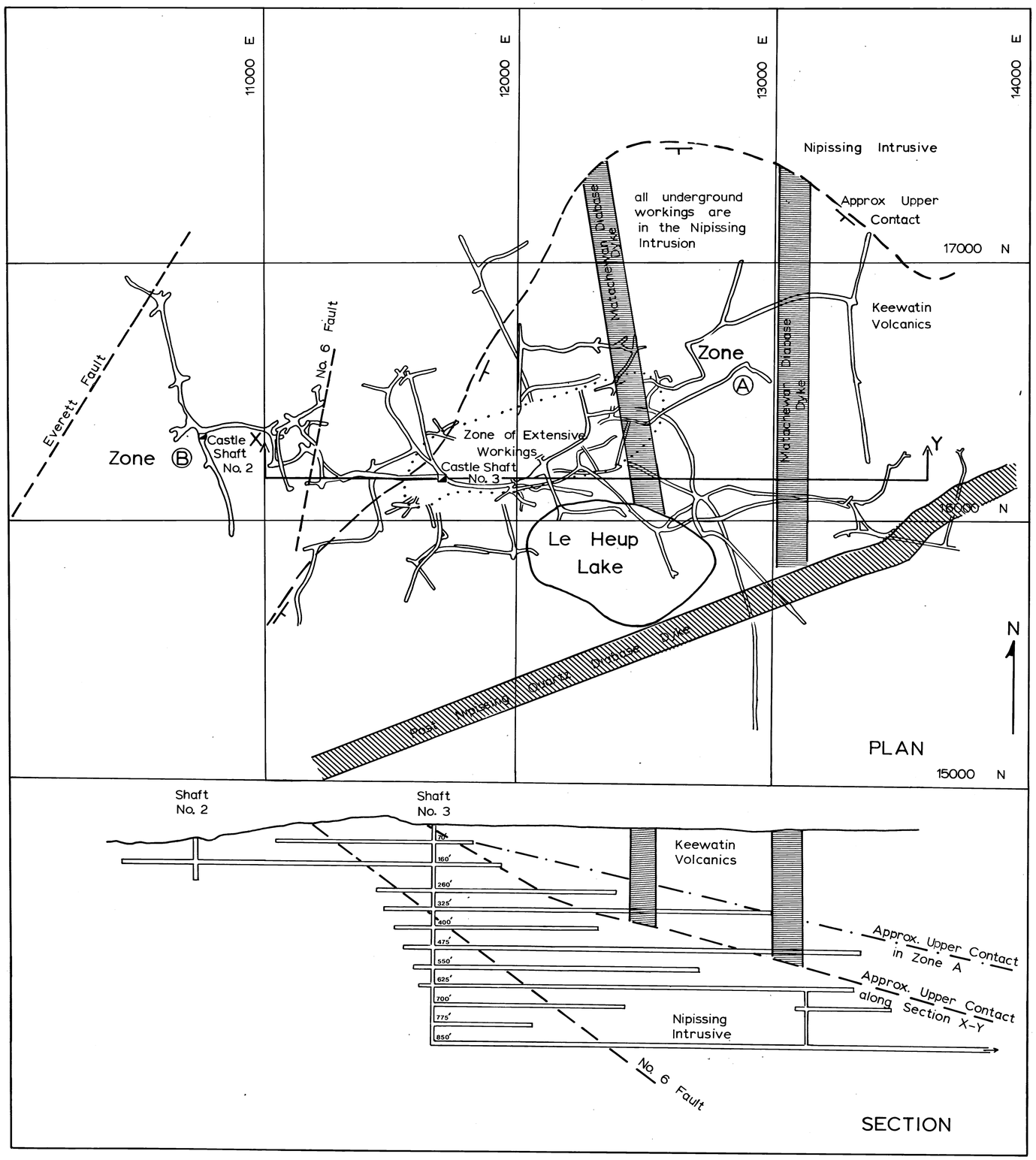


# PLAN AND SECTION
# CASTLE TRETHEWEY MINE
# SHAFT No. 3 AREA

Scale

400 0 200 400 feet

100 0 100 meters

reduce to 30%

FIGURE 11 CONROD 87-045 CO

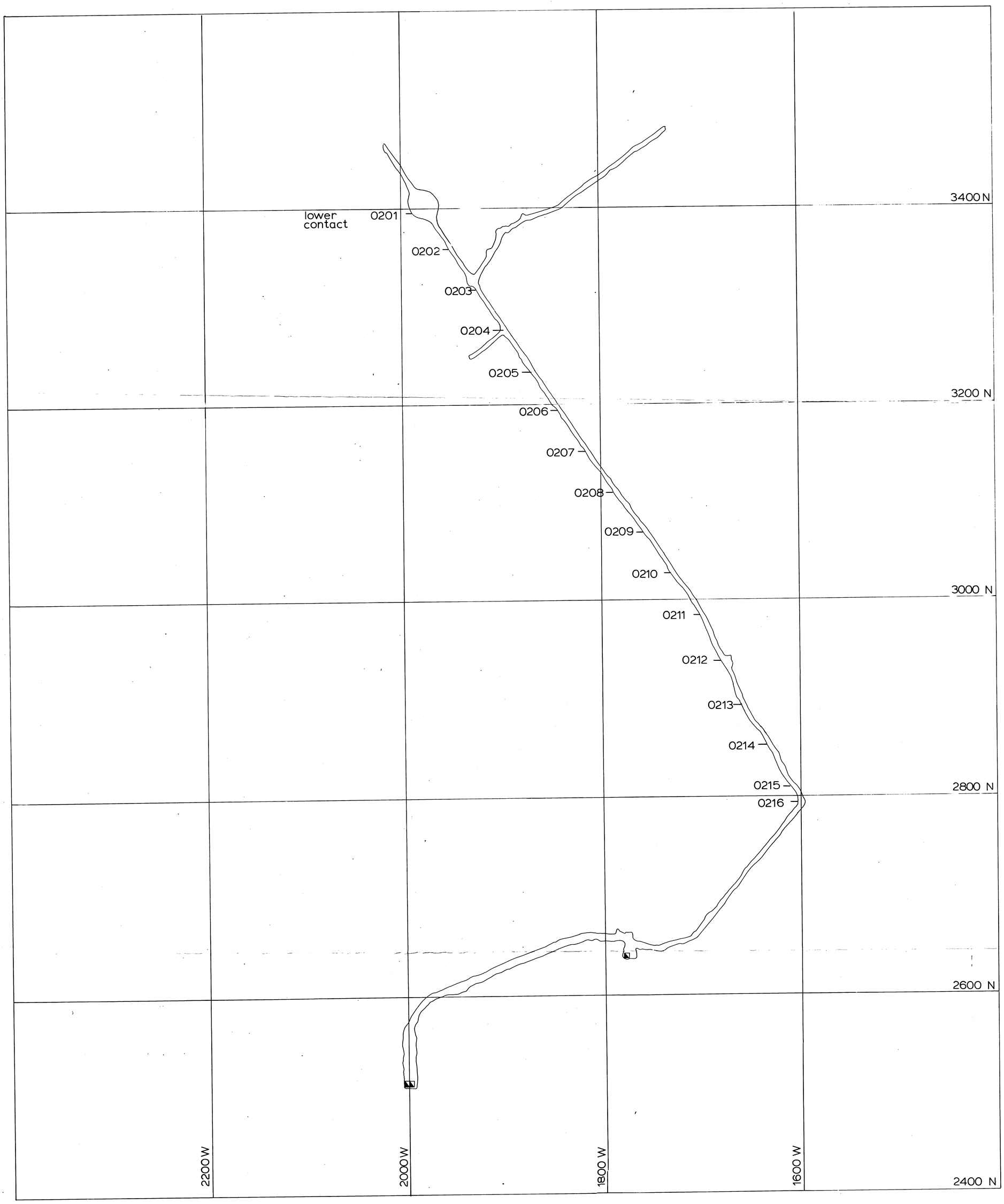


# CASTLE MINE
# 10th LEVEL PLAN

Scale

100 50 0 100 feet

0201, 0202, etc. – sample sites

MILLER LAKE
(CASTLE MINE)

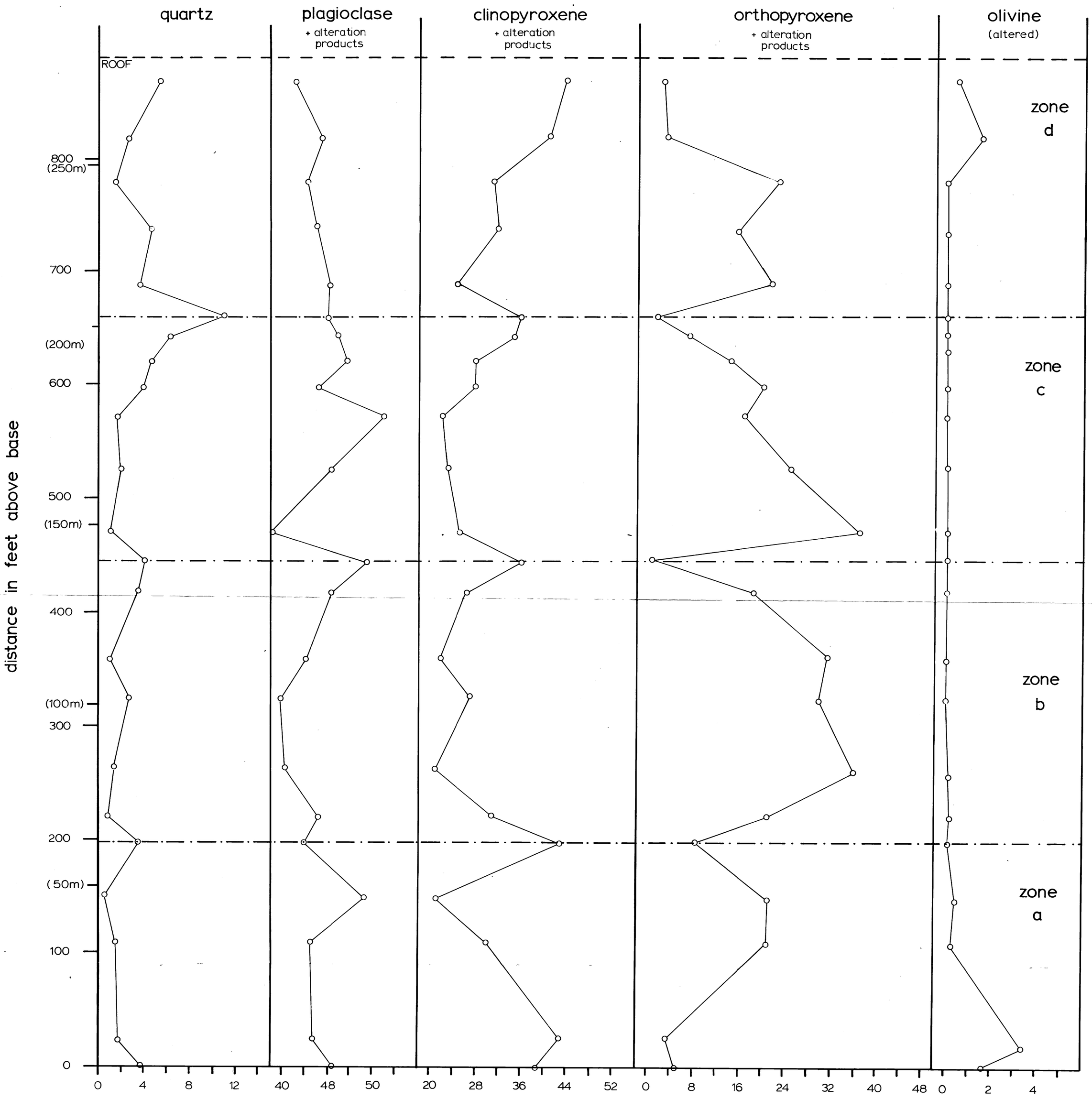


FIGURE 24 CANADA 87-045

reduce to 30%

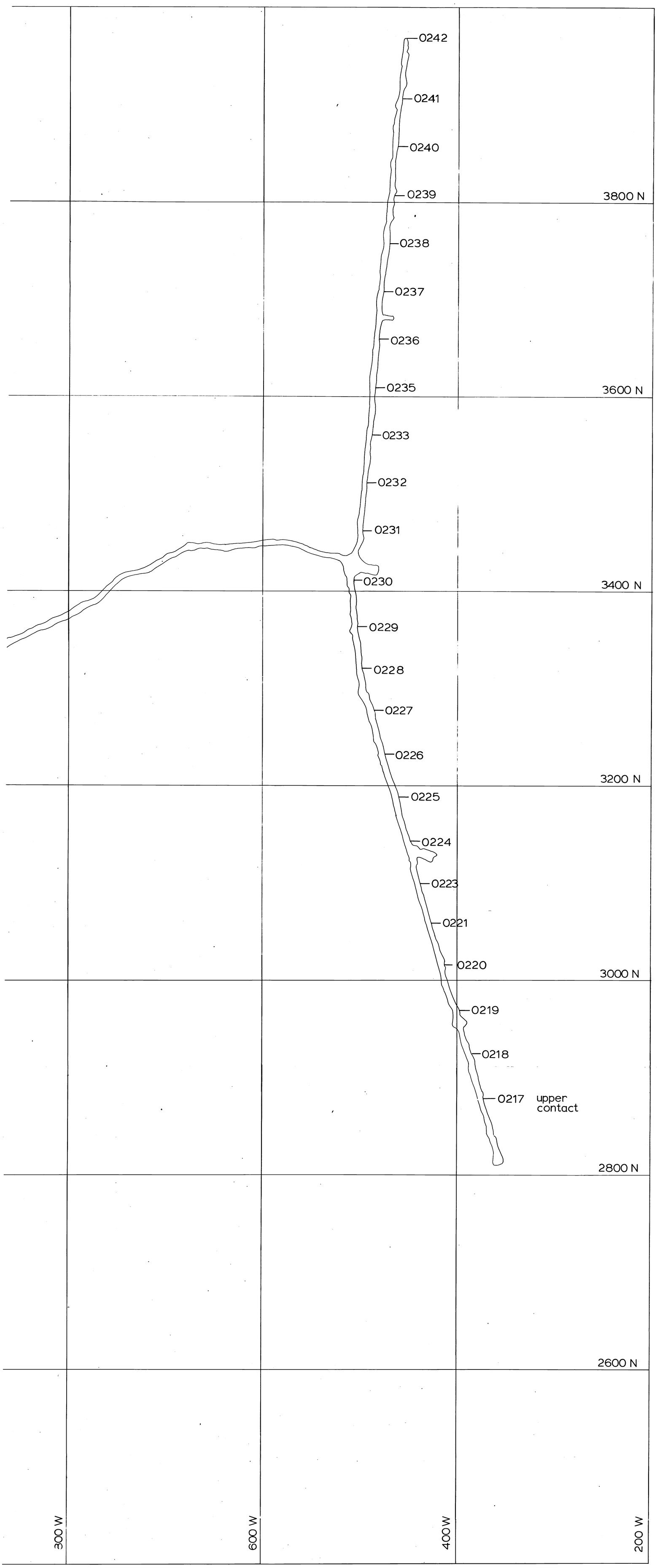


# CASTLE MINE
# 6th LEVEL PLAN

Scale

100 50 0 100 feet

0217, 0218, etc. — sample sites


1200W
1000W


Varied Texture Gabbro

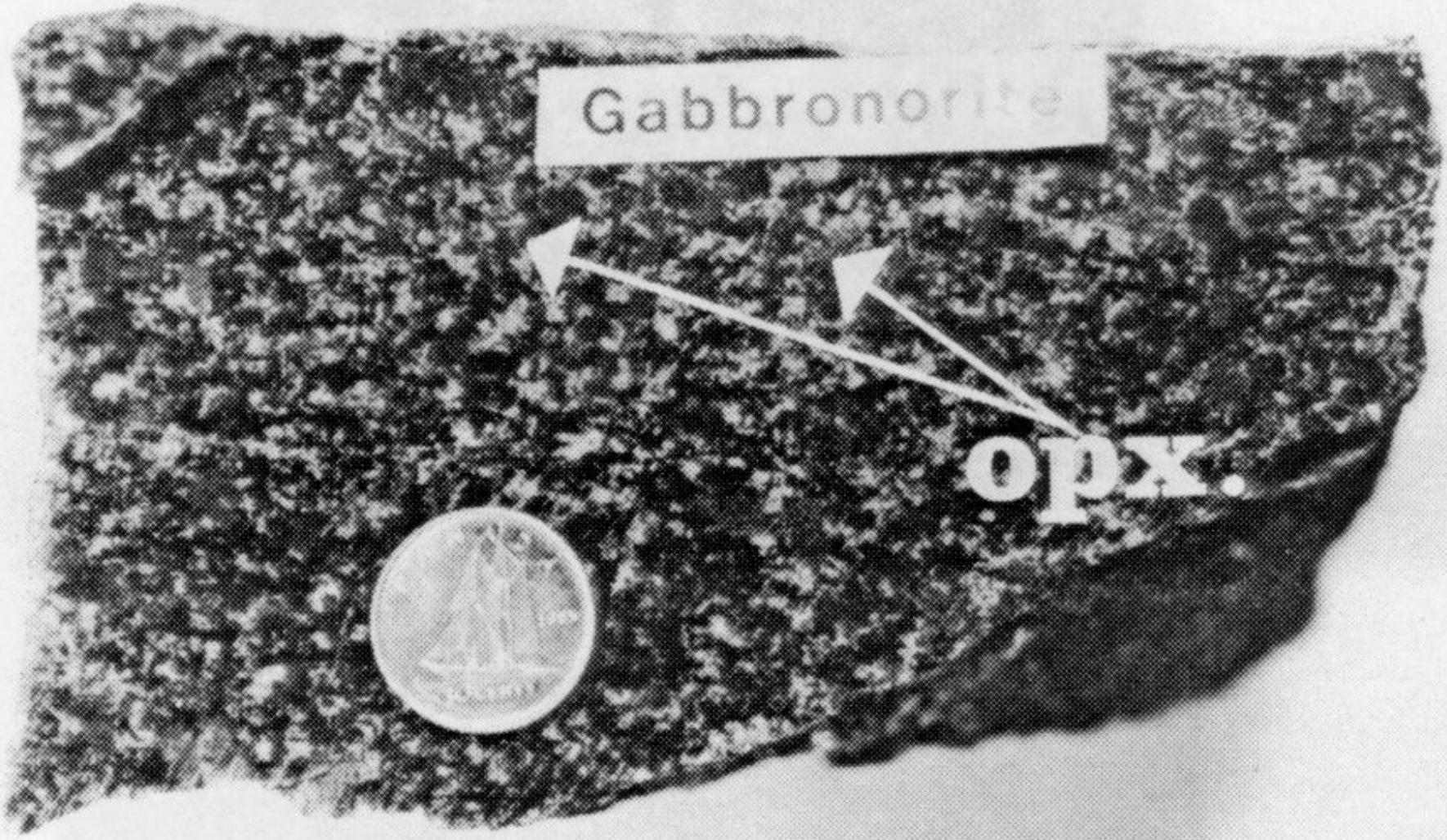
Gabbronorite
opx.


clot
Granophyre

vug

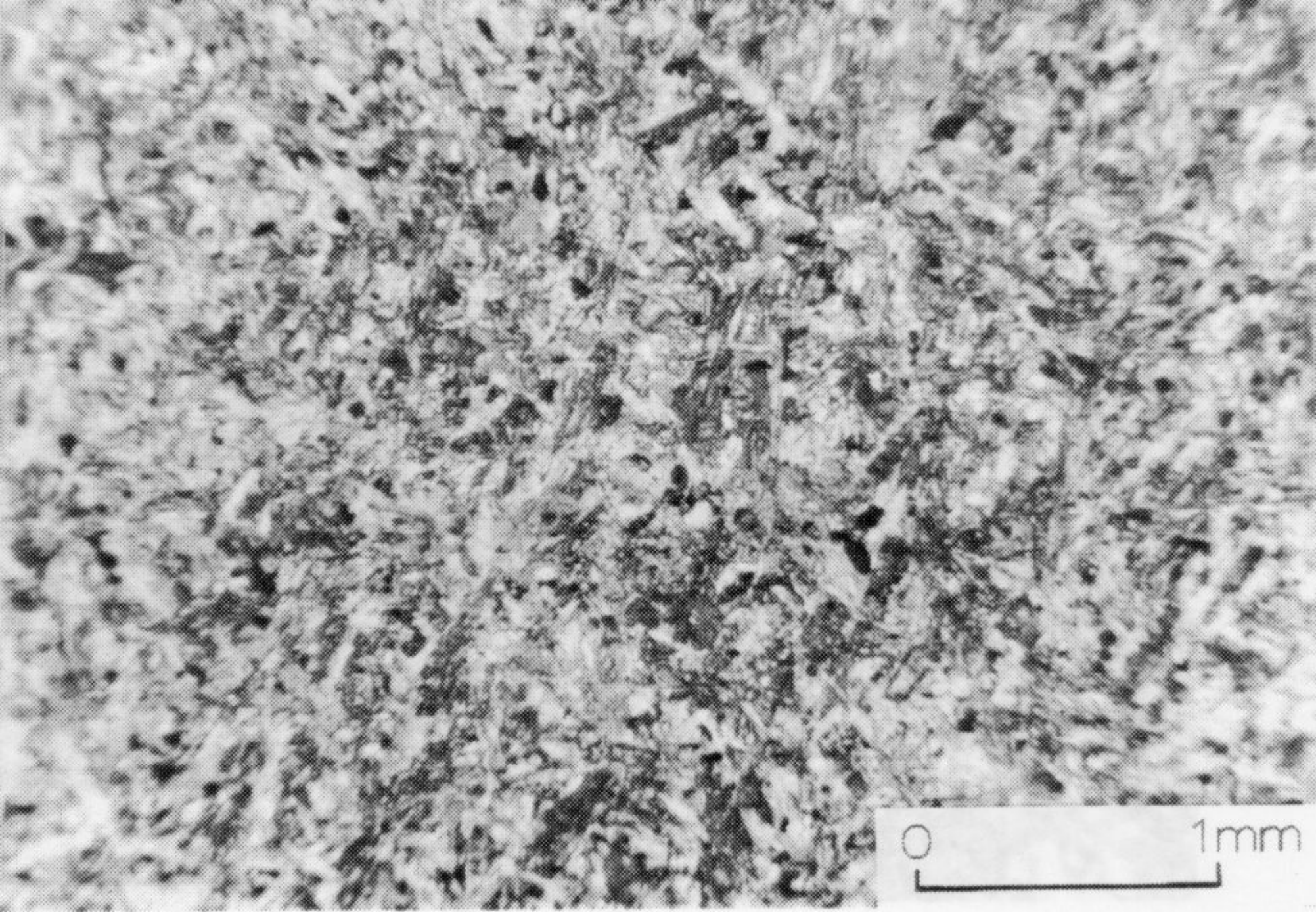
0
1mm

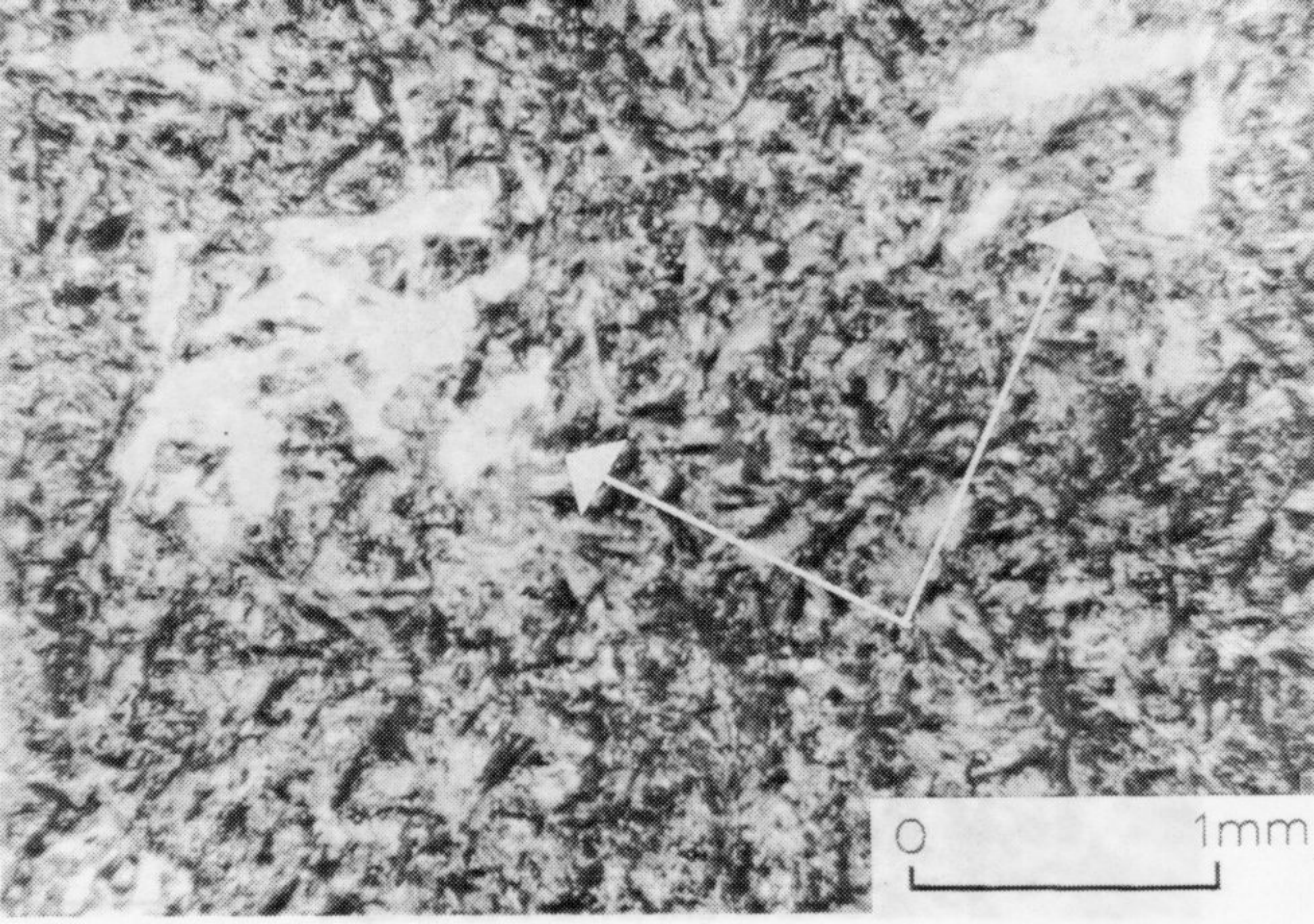
0
1mm

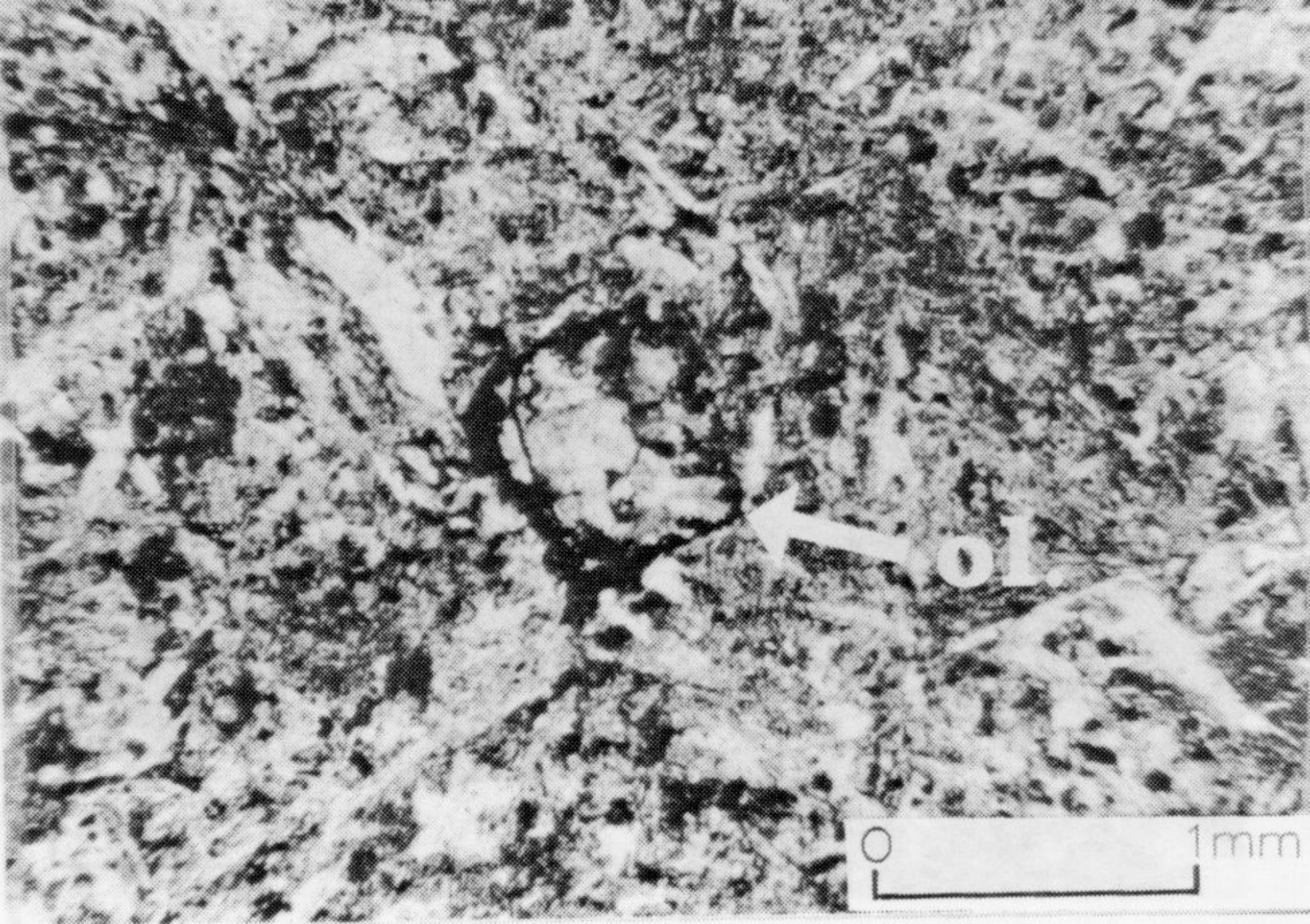
ol
0
1mm

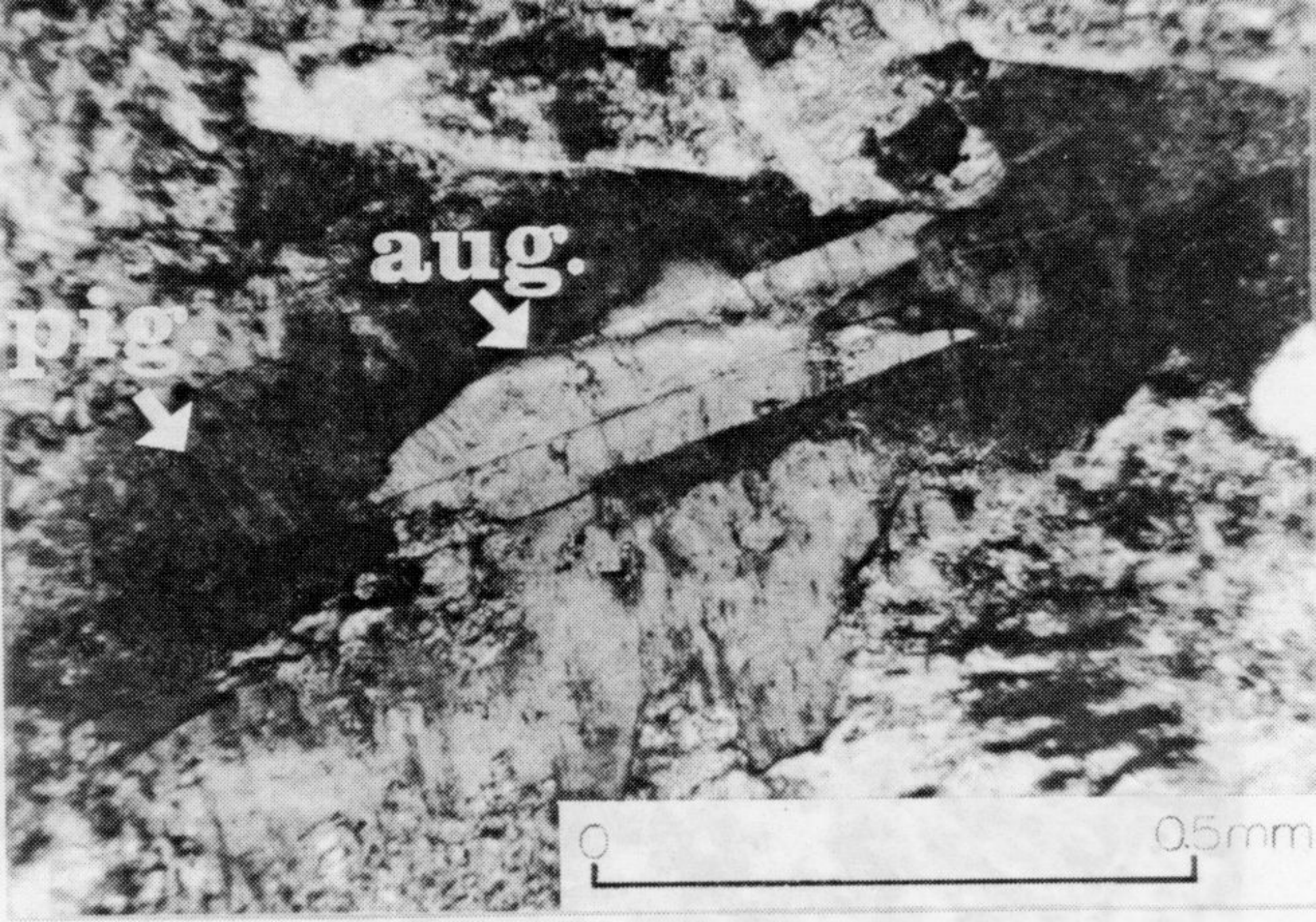
aug.
plg.
0
0.5mm


aug.
0
0.5mm

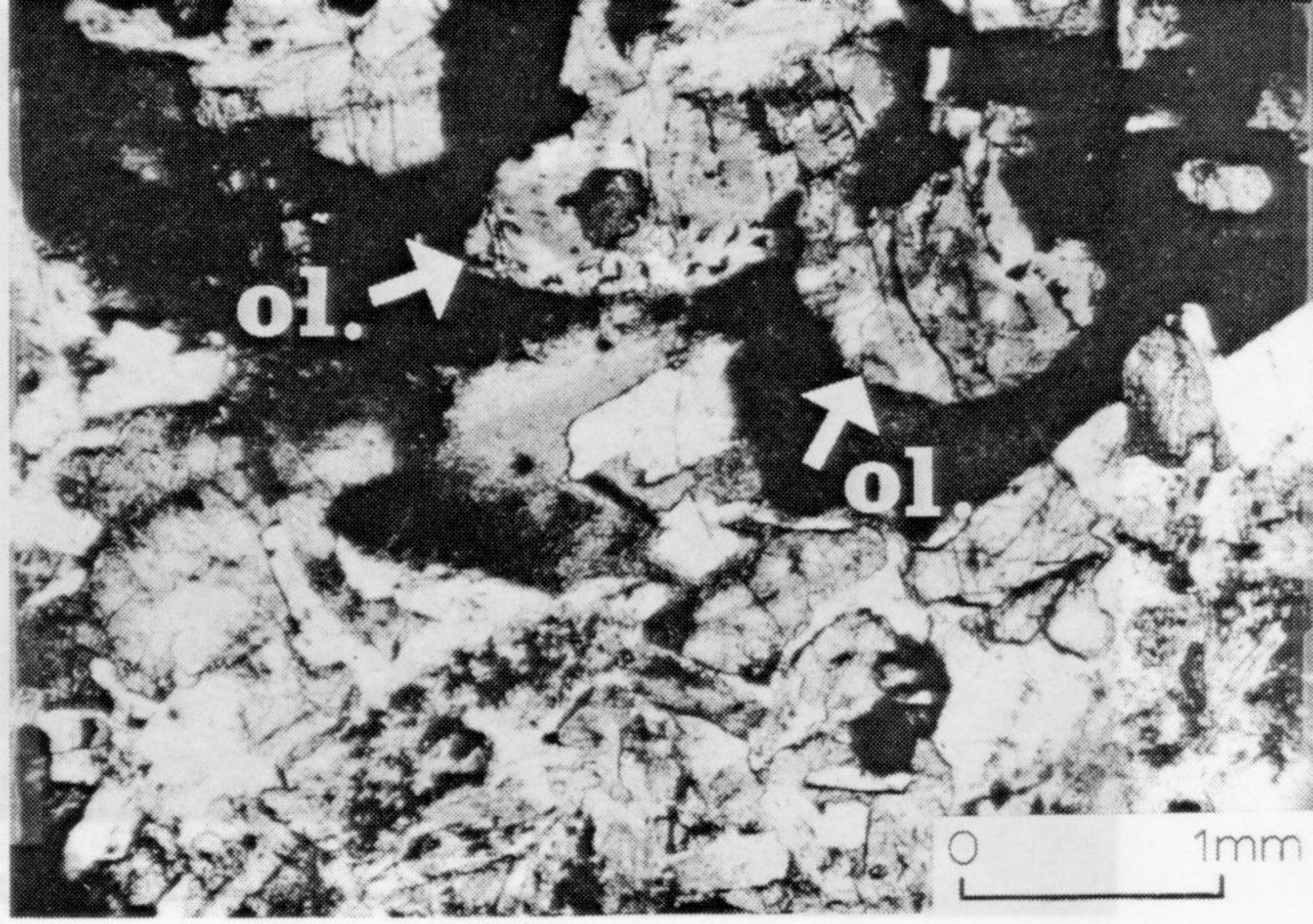
ol.
ol
0
1mm

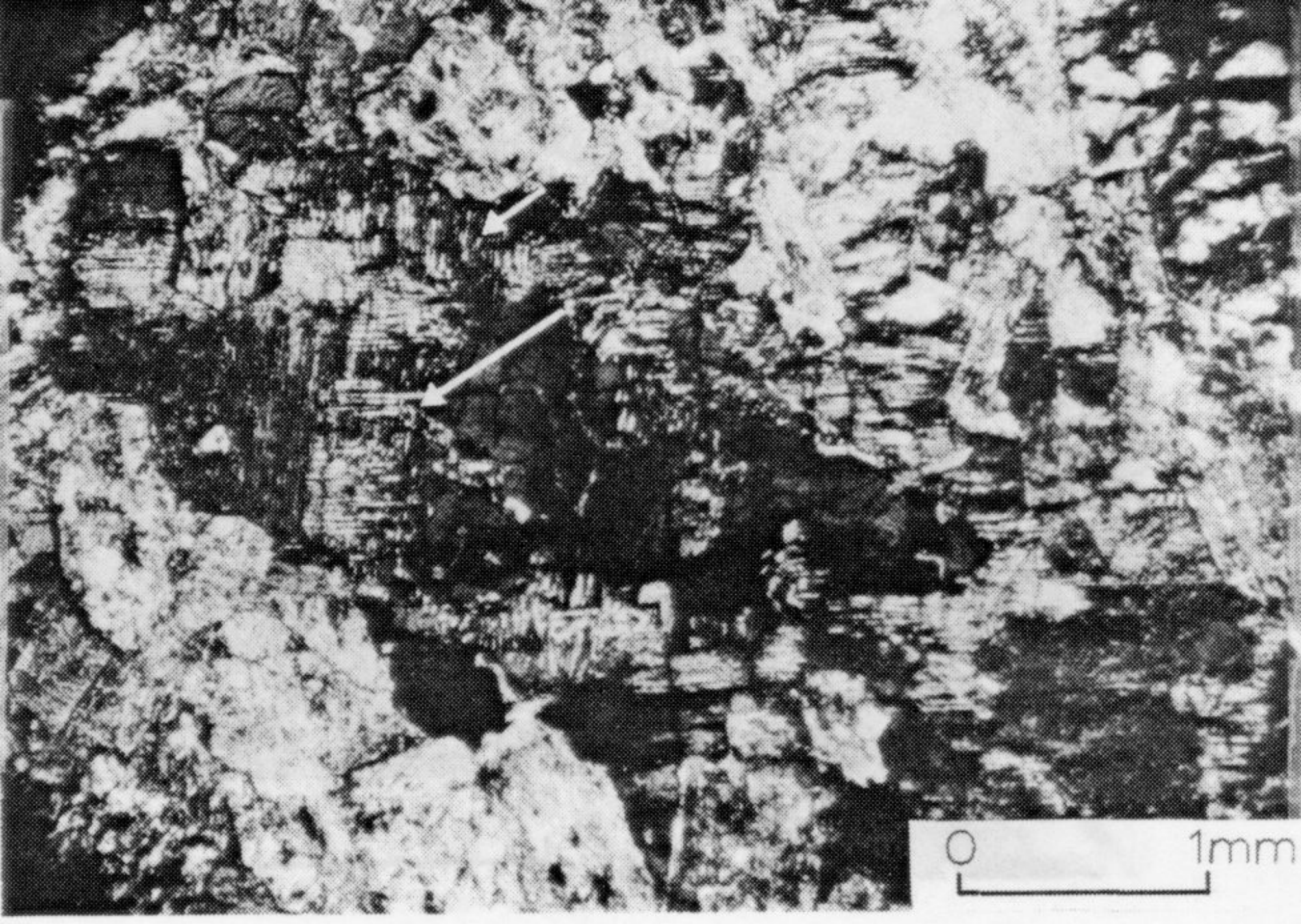
0
1mm


exs.
t.p.
0
0.5mm

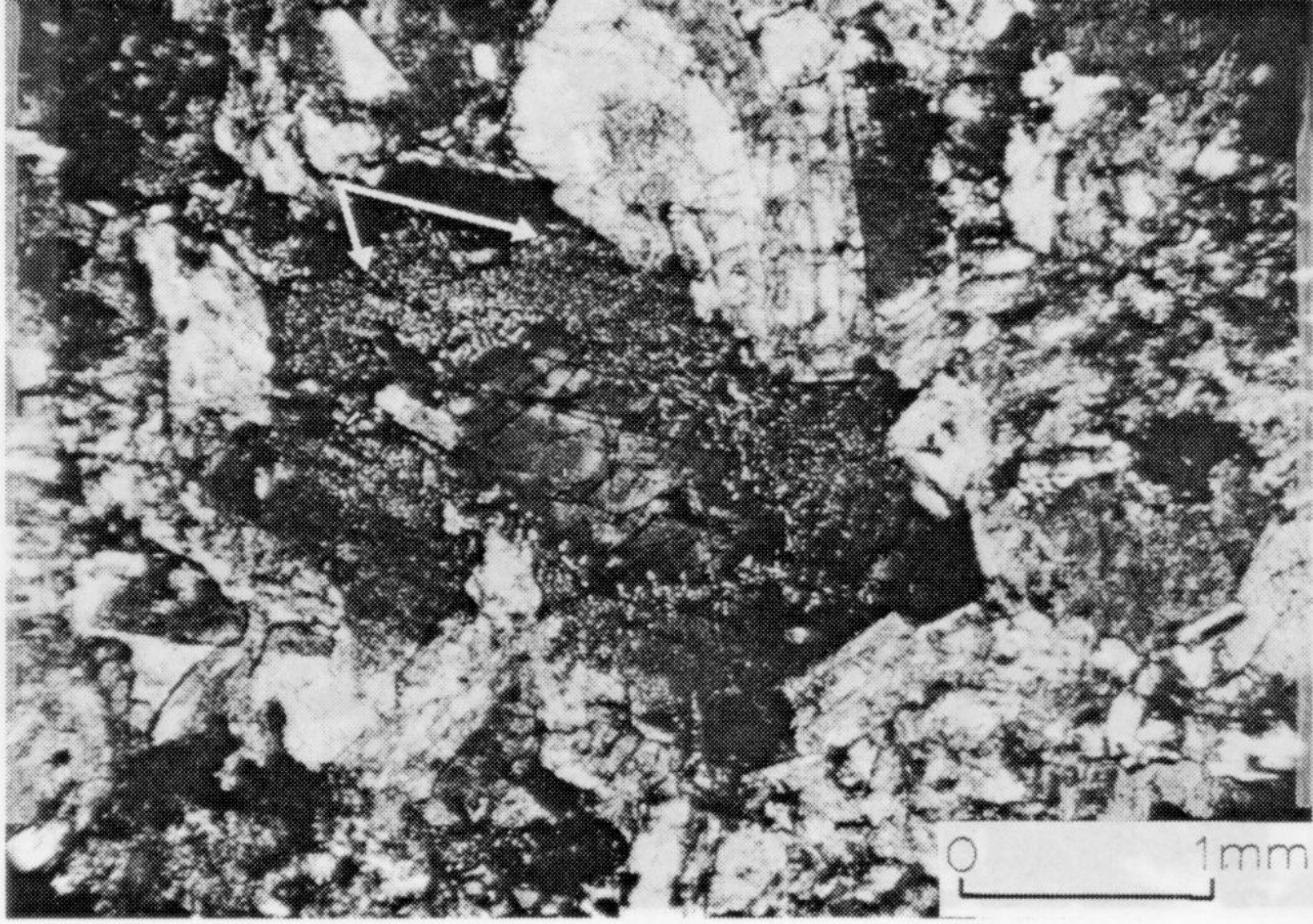
0
1mm

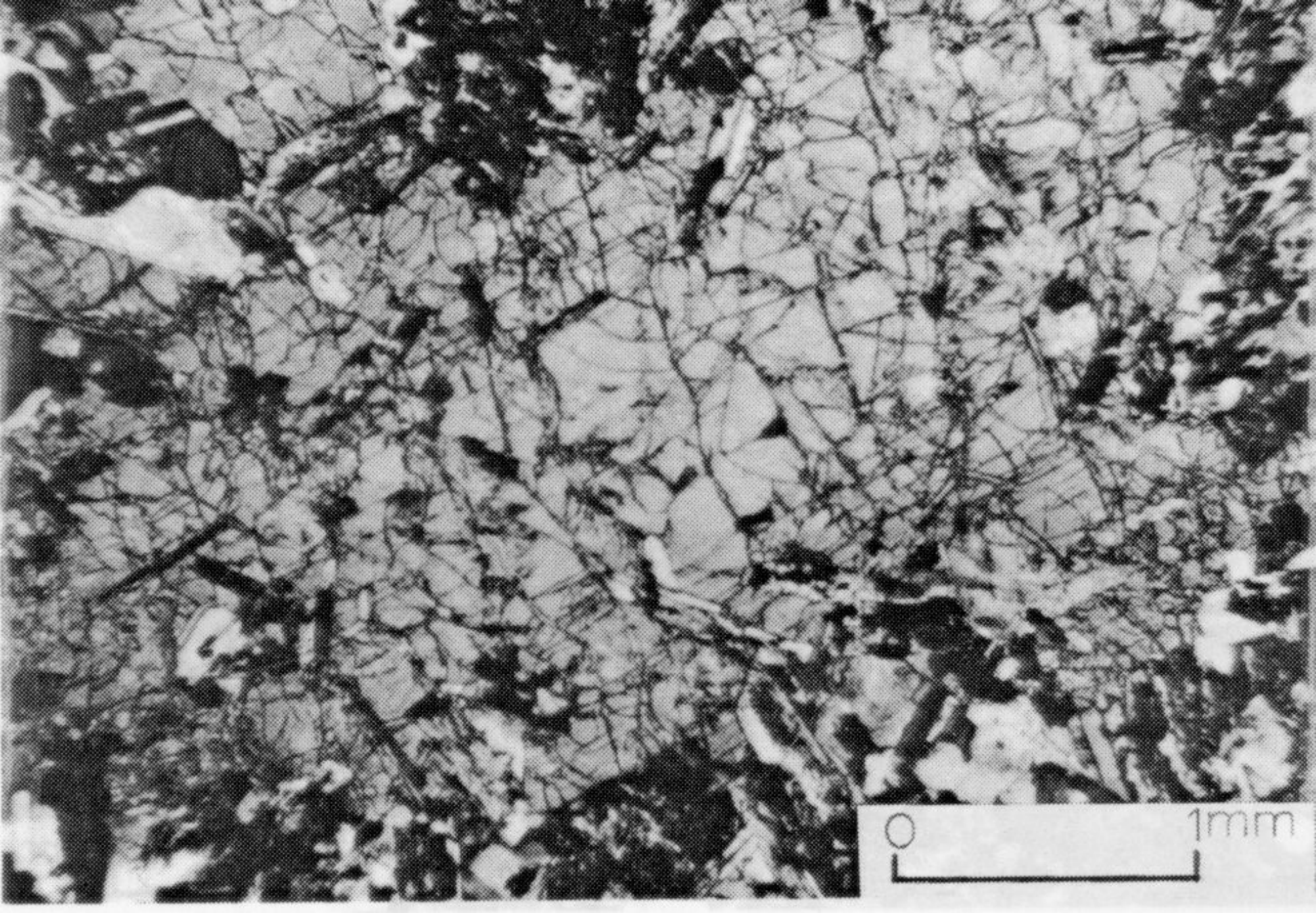
0
1mm

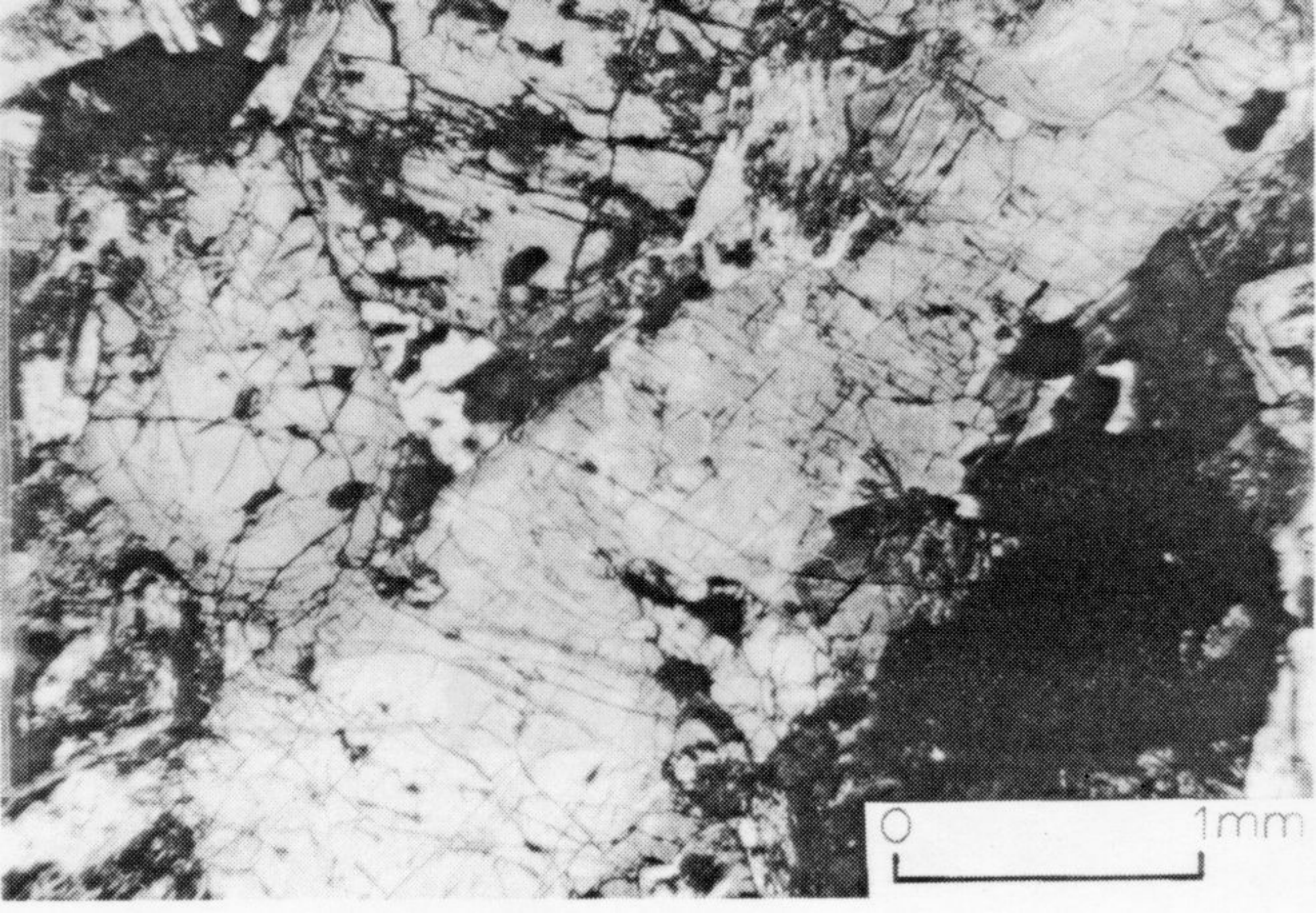
1mm


a.g.
0
1mm

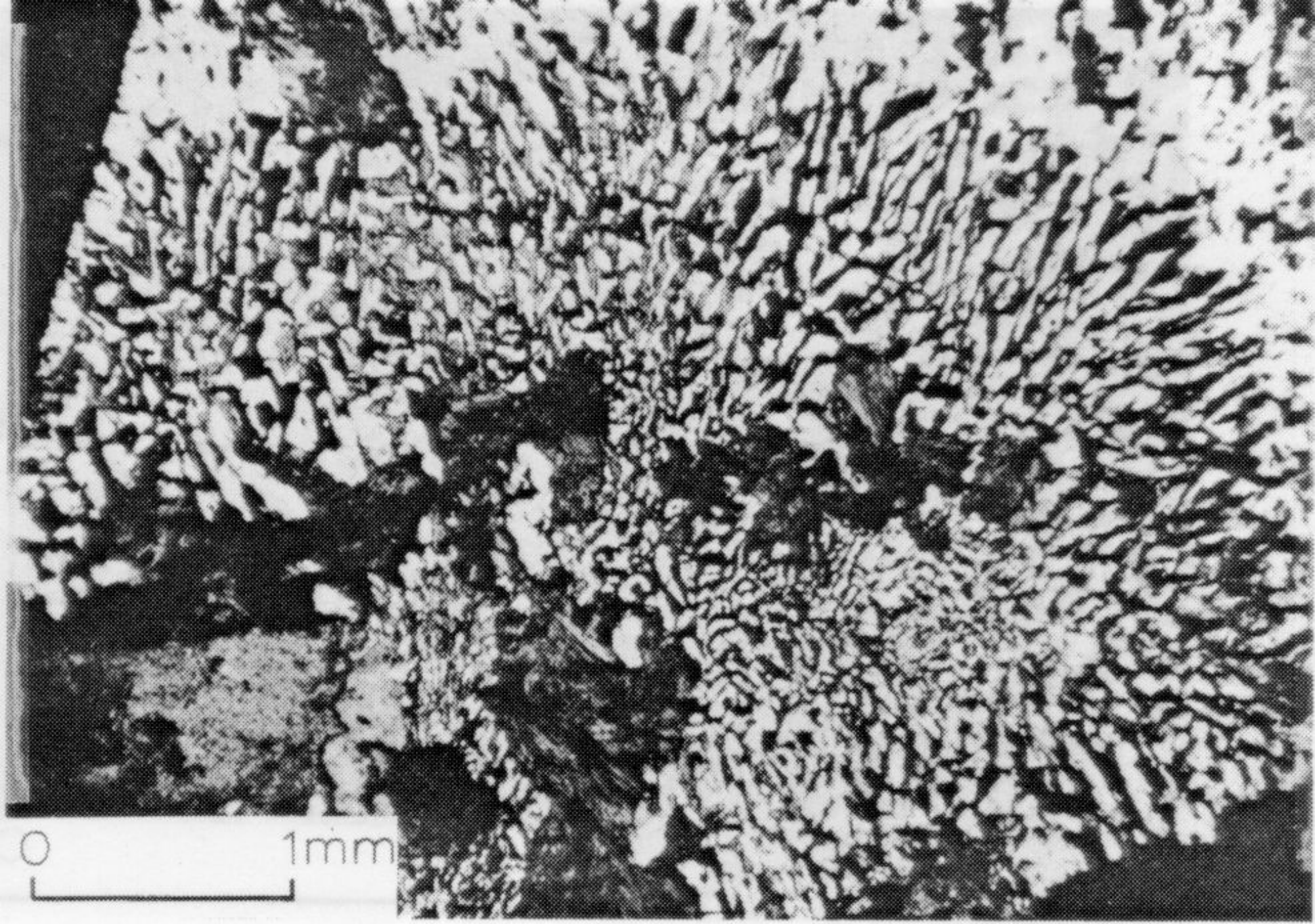
0
1mm

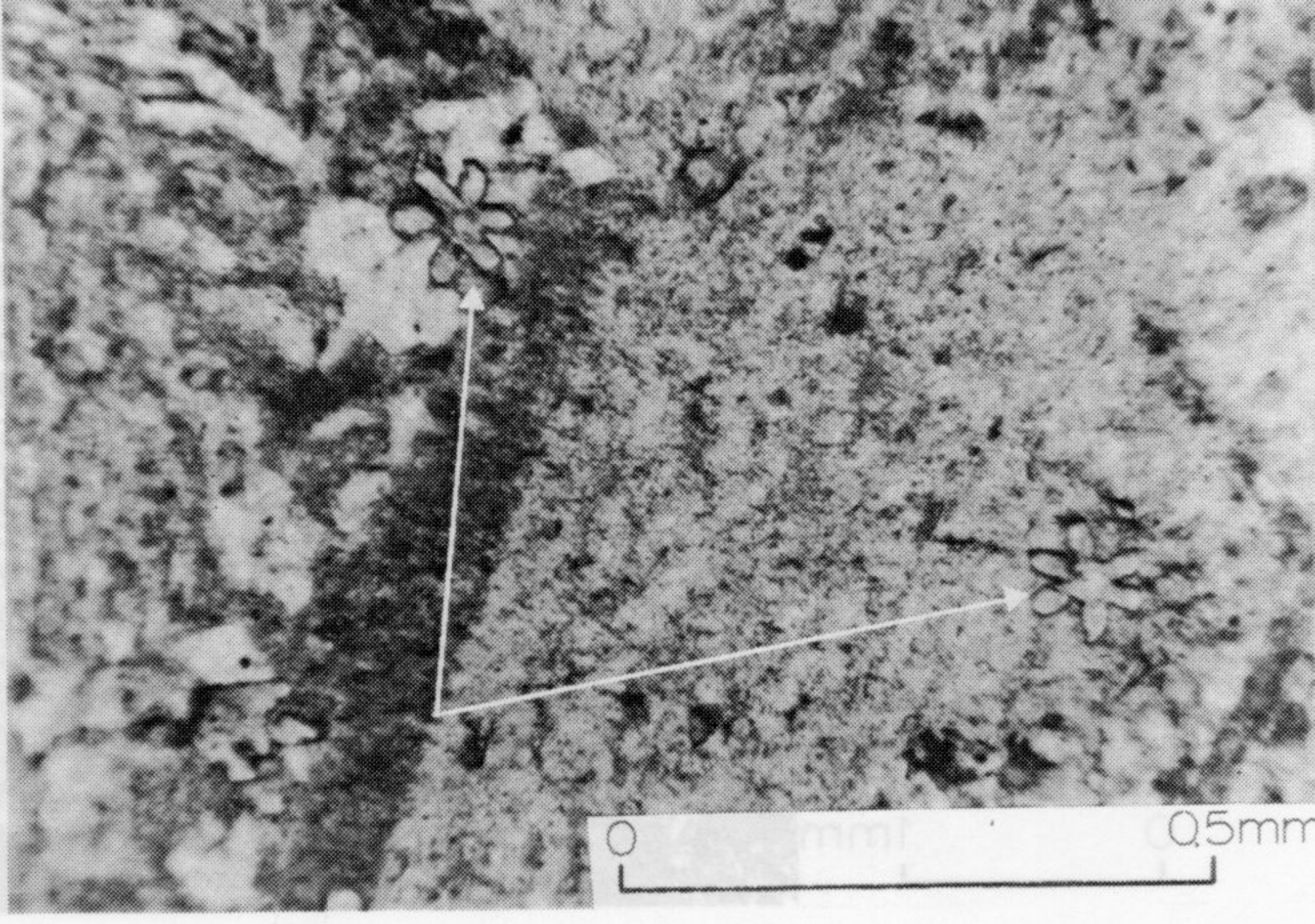
0
0.5mm

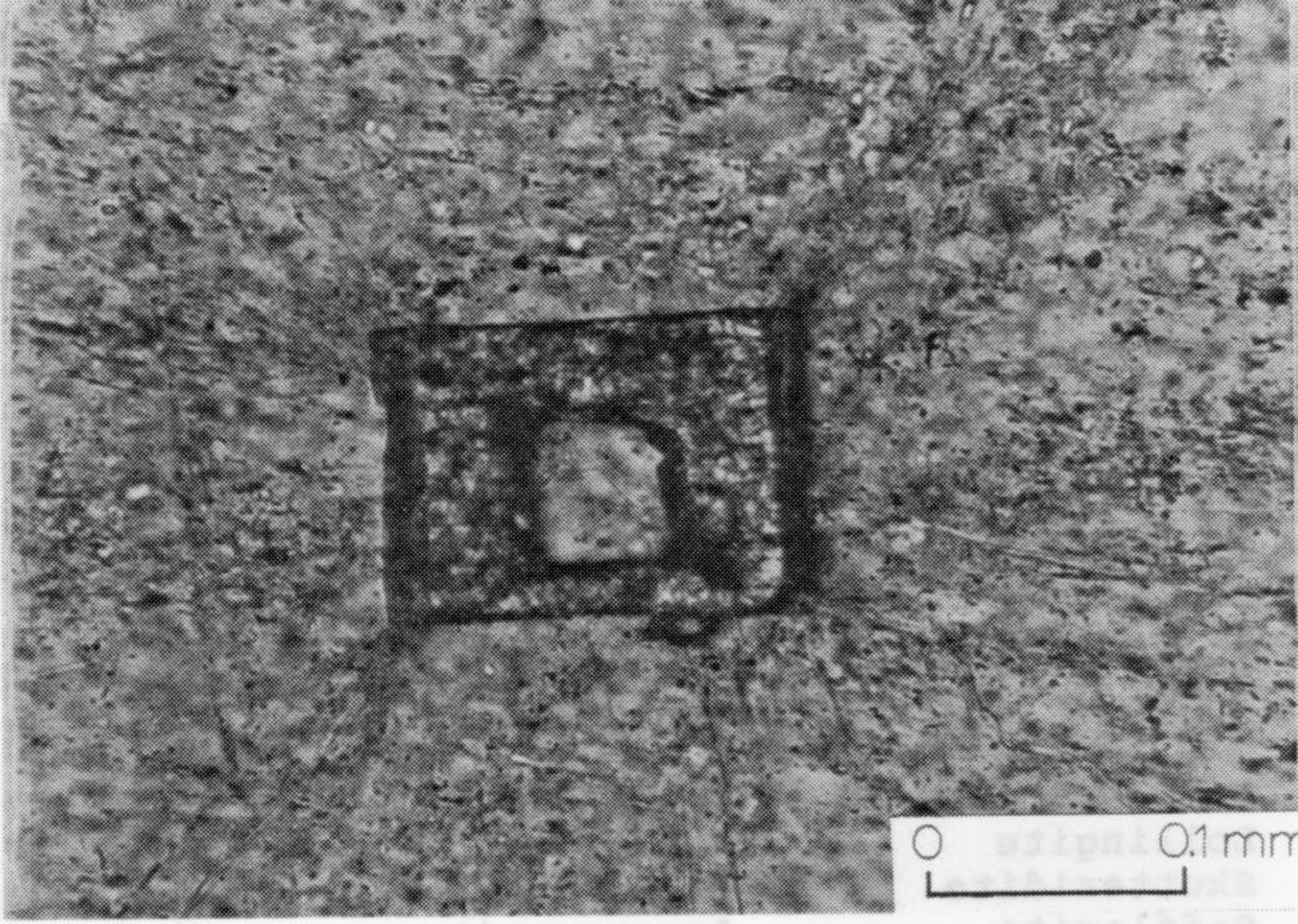
0
0.1 mm

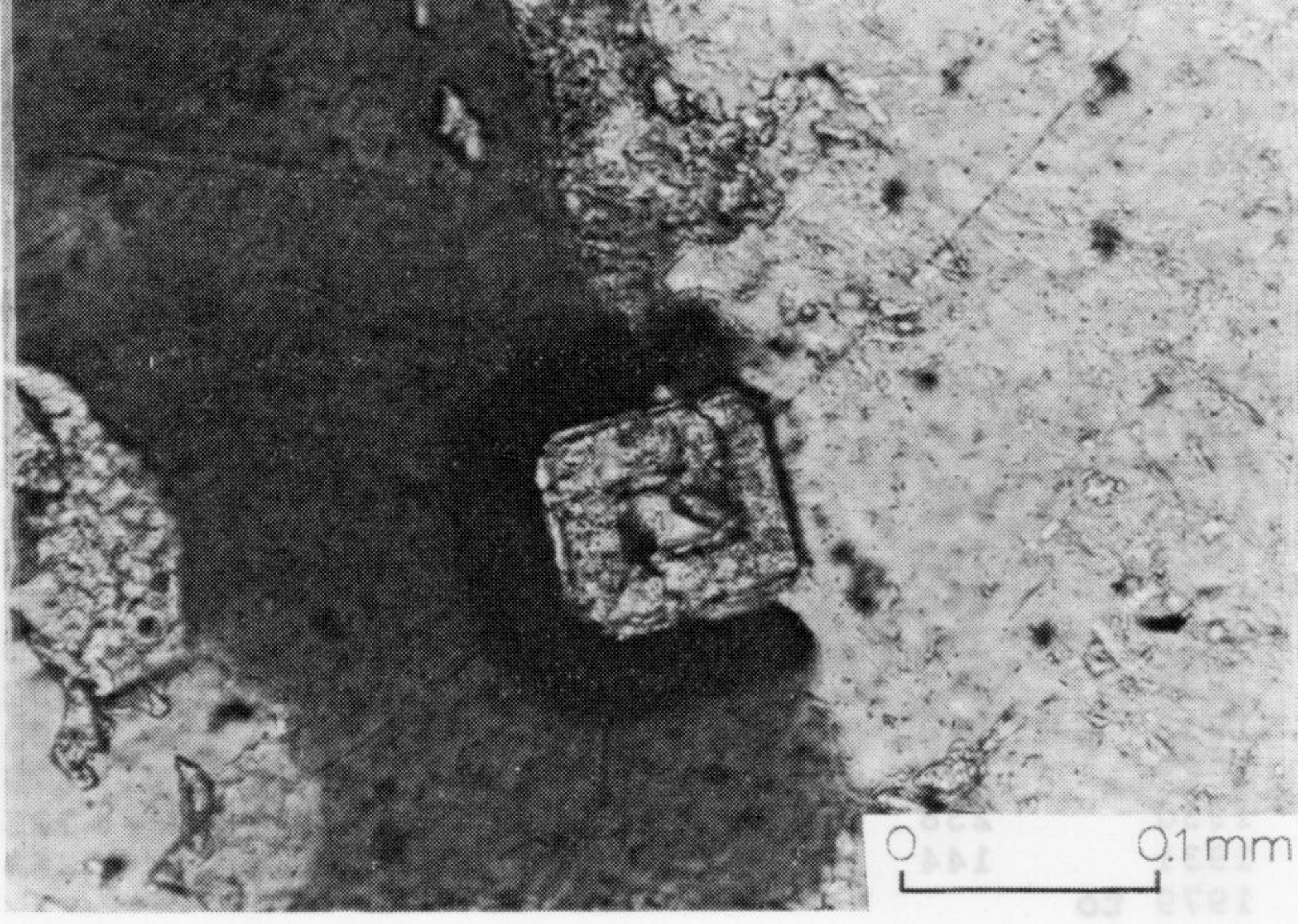
0
0.1 mm